Imperial College London

Department of Immunology and Inflammation

Antibody-mediated activation of Vδ1 γδ T-cells for cancer immunotherapy

Author:
Shefali A. Bhumbra

Imperial College Supervisor:
Dr Jessica Strid

Takeda Supervisors:
Dr Robert Good
Dr Andrew Hutton

Submitted in fulfillment of the requirements for a Doctorate of Philosophy from Imperial College London

August 2025

Statement of Originality and Copyright

I hereby declare that this thesis, the work and ideas presented are my own, unless appropriately referenced.

Signature: Shefali Bhumbra

Date: August 2025

The copyright of this thesis rests with the author. Unless otherwise indicated, its contents are licensed under a Creative Commons Attribution-Non Commercial 4.0 International Licence (CC BY-NC). Under this licence, you may copy and redistribute the material in any medium or format. You may also create and distribute modified versions of the work. This is on the condition that: you credit the author and do not use it, or any derivative works, for a commercial purpose. When reusing or sharing this work, ensure you make the licence terms clear to others by naming the licence and linking to the licence text. Where a work has been adapted, you should indicate that the work has been changed and describe those changes. Please seek permission from the copyright holder for uses of this work that are not included in this licence or permitted under UK Copyright Law.

Acknowledgements

First, to my Imperial and Takeda supervisors, Jessica, Rob, Andy, Antara, Kathy, David Thomas and Robert Snelgrove. Thank you for your invaluable guidance and support over the last few years, I will carry the knowledge and experience I gained whilst working with you throughout my career and beyond.

For making this project possible, and constant generosity throughout, I express my sincere appreciation to the Royal Commission for the Exhibition of 1851. Your Industrial Fellowship program provided an invaluable structure to the project, as well as a network of support through the networking and public engagement opportunities (which I thoroughly enjoyed taking part in!).

This journey would not have been possible without the teams at Legacy-Adaptate and Takeda. With special mention to Caitlin, Nikitas, Shauna, Julie, Georgia, Josh, Ellie, Luke, Tyreese, Tanguy, Aneesha, Aoife, Sarah, Adrianna, Erica, Andrea, Mauro, Izzy, Dan A, Sam, Dan F, and Oxana, your constant intellectual and emotional support carried me throughout these years. I am also immensely grateful to Mark for making this program possible, as well as to Natalie, Mihri, Stewart, Craig, Jose, and Jem for your support, expertise, and your role in the creation and development of Adaptate.

To Jessica's lab, especially Christina, I truly appreciate you welcoming me into your group at each BSI conference and your support during my visits from across the road and my viva!

And finally to Jaana, Shobita, Magson, Ethel, Terry, Charlie, Nonans, Shub, Rosa, Tim, Ashley, Mum, Dad and Caitlin again. Thank you for all of your love, kindness and encouragement. I would not have survived everything that happened inside and out of this project without you ♡ .

Abstract

Cancer remains a global leading cause of death as current treatments are often ineffective and present with high relapse-rates and severe adverse reactions. Vδ1 $\gamma\delta$ T-cells are gaining interest as promising onco-immunotherapeutic targets due to their association with favourable prognoses in a myriad of malignancies. This thesis explores whether Vδ1-targeting bispecific engagers can improve immune responses against CD19$^+$ haematological malignancies. Initial experiments investigated four Vδ1/CD19 bispecific engager formats, where only the BiTE format successfully enhanced Vδ1 function. The Vδ1/CD19 BiTE demonstrated specific binding to both Vδ1 TCR$^+$ and CD19$^+$ cells, resulting in TCR-downregulation, upregulation of T-cell activation markers 41BB, CD25 and CD107a, and enhanced cytotoxicity against CD19$^+$ cell lines. Vδ1/CD19-treatment also increased PBMC cytotoxicity against CD19$^+$ MEC-1 and primary CLL B-cells. To investigate mechanisms of healthy cell discrimination, differentially expressed ligands were identified from primary healthy B-cells, CLL B-cells and CD19$^+$ cancer cell lines by RNA-analysis. Corresponding co-receptors to such ligands were identified using the literature. Following Vδ1/CD19 engager-treatment, naive PBMC-based Vδ1 T-cells increased expression of co-receptors NKG2D, CD96, DNAM-1, CD2, ICOS and PD-1 alongside CTLA-4 downregulation. Co-culture with MEC-1 cells enhanced granzyme B expression in PBMC-based Vδ1 T-cells and promoted effector-memory phenotypes. Blocking MEC-1 stress ligands reduced engager-treated Vδ1 cytotoxicity, though only under conditions of combined ligand-blockade, suggesting reduced susceptibility of these cells to immune evasion via downregulation of individual stress ligands. Engager treatment may prime *naive* Vδ1 T-cells for cytotoxicity by TCR-engagement but only engager-treated *effector* Vδ1 T-cells elicited a cytotoxic response when stimulated by plate-bound recombinant ligands, highlighting a potential lower threshold of activation for effector, over naive, Vδ1 T-cells. Findings also suggest effector Vδ1 T-cells modulate cytotoxicity through co-receptor signalling to discriminate between healthy and cancerous cells. Overall, the work presented in this thesis supports the continued investigation of Vδ1-targeting engagers as potential treatments for cancer.

Contents

1 Introduction **19**

1.1 Cancer . . . 19

1.1.1 Cancer formation . . . 19

1.1.2 Traditional Cancer Therapies . . . 20

1.1.3 Cancer and the Immune System . . . 21

1.1.4 Onco-Immunotherapy . . . 24

1.2 Human $\gamma\delta$ T-cells . . . 26

1.2.1 $\gamma\delta$ T-cell Activation . . . 28

1.2.1.1 $\gamma\delta$ TCR recognition . . . 28

1.2.1.2 $\gamma\delta$ Costimulation . . . 31

1.2.2 $\gamma\delta$ Cytotoxic Responses . . . 34

1.3 Vδ1 $\gamma\delta$ T-cells . . . 36

1.3.1 Vδ1 characterisation . . . 37

1.3.2 Blood vs tissue Vδ1 T-cells . . . 38

1.4 Vδ1 T-cells as an onco-therapeutic target . . . 39

1.4.1 Bispecific Antibodies for Vδ1-directed therapy . . . 40

1.4.2 $CD19^{+}$ cancers as a target for a Vδ1-directed engager . . . 42

1.5 Summary . . . 43

2 Hypothesis and Aims **44**

2.1 Hypothesis . . . 44

2.2 Aims . . . 44

3 Methods **45**

3.1 Antibody Design . . . 45

3.2 Antibody Production . . . 51

3.3 High Performance Liquid Chromatography (HPLC) . . . 51

3.4 Cell Lines . . . 51
3.5 Primary tissue collection . . . 51
3.6 Whole Blood processing . . . 52
3.7 Vδ1 expansion from skin . . . 52
3.8 Vδ1 expansion from blood . . . 53
3.9 Binding Assay . . . 53
3.10 Cell Trace Violet (CTV) Staining . . . 53
3.11 Primary B-cell isolation . . . 53
3.12 Activation and Cytotoxicity assays with expanded Vδ1 T-cells . . . 54
3.13 Vδ1 proliferation from PBMCs . . . 54
3.14 Vδ1 cytotoxicity from PBMCs . . . 54
3.15 RNA expression analysis . . . 54
3.16 B-cell Phenotyping . . . 55
3.17 Vδ1 phenotyping assay . . . 55
3.18 Cytokine Analysis . . . 55
3.19 Cytotoxicity Blockade . . . 55
3.20 Magnetic-Activated Cell Sorting (MACS) . . . 56
3.21 Vδ1 T-cell isolation . . . 57
3.22 Plate-bound recombinant ligand activation assay . . . 57
3.23 Flow Cytometry . . . 57
3.24 Statistical Analysis . . . 57
3.24.1 Flow Panels . . . 59
3.24.1.1 Binding assay . . . 59
3.24.1.2 Activation with expanded Vδ1 T-cells assay . . . 60
3.24.1.3 Activation and cytotoxicity with expanded Vδ1 T-cells assay . . . 61
3.24.1.4 Vδ1 proliferation assay . . . 61
3.24.1.5 PBMC Cytotoxicity assay . . . 62
3.24.1.6 B-cell Phenotyping . . . 62
3.24.1.7 Vδ1 Phenotyping . . . 65
3.24.1.8 Cytotoxicity Blockade assay . . . 70
3.24.1.9 Plate-bound recombinant ligand activation assay . . . 71

4 Results **72**

4.1 V$\boldsymbol{\delta}$1/CD19 Antibody Design and Selection . . . 72
4.1.1 Antibody Design . . . 72

4.1.2 Antibody Validation . . . 72
4.1.3 Vδ1 engager function . . . 79
4.1.3.1 TCR Downregulation . . . 79
4.1.3.2 T-cell activation . . . 81
4.1.3.3 Cytotoxicity . . . 86
4.1.3.4 Proliferation . . . 91
4.1.4 Summary . . . 93
4.2 Selected Vδ1/CD19 Engager Evaluation . . . 94
4.2.1 Binding . . . 94
4.2.2 Engager-mediated Vδ1 activation and cytotoxicity . . . 95
4.2.3 Engager-mediated Vδ1 proliferation . . . 98
4.2.4 Engager-mediated PBMC-based Vδ1 cytotoxicity . . . 99
4.2.5 Summary . . . 104
4.3 Identification of Vδ1 receptors involved in cancer cell recognition . . . 105
4.3.1 Target cell phenotyping . . . 105
4.3.2 Vδ1 T-cell models . . . 113
4.3.3 Summary . . . 115
4.4 Engager-mediated Vδ1 Cytotoxicity . . . 115
4.4.1 Engager-mediated Vδ1 phenotype . . . 115
4.4.2 Co-receptor role in engager-mediated Vδ1 function . . . 121
4.4.2.1 Proliferation . . . 121
4.4.2.2 Cytotoxicity . . . 124
4.4.2.3 Activation . . . 127
4.4.3 Summary . . . 128

5 Discussion **130**
5.1 Study Design Limitations . . . 130
5.2 Considerations for Vδ1 engagers as a therapy . . . 132
5.2.1 Engager Format . . . 132
5.2.2 Implications of co-receptors for Vδ1-based therapies . . . 134
5.2.3 Therapy for cancer . . . 137
5.2.4 Therapy for other indications . . . 140
5.3 Summary . . . 141

6 Concluding Remarks **142**

7 References **144**

8 Appendices **168**

8.1 Appendix 1 168

8.2 Appendix 2 169

8.3 Appendix 3 170

8.4 Appendix 4 171

8.5 Appendix 5 172

8.6 Appendix 6 173

8.7 Appendix 7 174

8.8 Appendix 8 175

8.9 Appendix 9 176

8.10 Appendix 10 177

8.11 Appendix 11 178

List of Figures

1.1 Tumour Heterogeneity 20
1.2 Cancer Immunoediting 23
1.3 Immunotherapy Landscape 25
1.4 Somatic Recombination 27
1.5 $\gamma\delta$ T-cell Activation 29
1.6 $\gamma\delta$ T-cell Co-receptors 31
1.7 Structure of a T-cell Immunological Synapse 35
1.8 T-cell characterisation 38
1.9 IgG Antibody Structure 40
1.10 Bispecific Formats 41

3.1 Bispecific engager sequence format 46

4.1 Design of Vδ1/CD19 bispecific engagers 73
4.2 Vδ1/CD19 engager stability 74
4.3 Vδ1 T-cell purity following isolation protocols 75
4.4 Representative histograms of Vδ1/CD19 engager binding 76
4.5 Vδ1/CD19 engager binding 78
4.6 Vδ1/CD19 antibody-mediated TCR Downregulation 79
4.7 Representative histograms of Vδ1/CD19 antibody-mediated TCR Downregulation 80
4.8 Vδ1/CD19 antibody-mediated 41BB upregulation 82
4.9 Representative histograms of Vδ1/CD19 antibody-mediated 41BB upregulation . 83
4.10 Vδ1/CD19 antibody-mediated CD25 upregulation 84
4.11 Representative histograms of Vδ1/CD19 antibody-mediated CD25 upregulation . 85
4.12 Vδ1/CD19 antibody-mediated CD107a upregulation 87
4.13 Representative histograms of Vδ1/CD19 antibody-mediated CD107a upregulation 88
4.14 Vδ1/CD19 engager-mediated enhanced Vδ1 cytotoxicity 89

4.15 Representative flow plots of Vδ1/CD19 engager-mediated enhanced Vδ1 cytotoxicity 90
4.16 Vδ1/CD19 engager-mediated Vδ1 proliferation 91
4.17 Representative flow plots of Vδ1/CD19 engager-mediated Vδ1 proliferation . . . 92
4.18 Selected Vδ1/CD19 engager specifically binds to Vδ1 and B-cells in PBMCs . . . 95
4.19 Cell line CD19 expression 96
4.20 Selected Vδ1/CD19 engager activates and enhances cytotoxicity of Vδ1 T-cells . 97
4.21 Selected Vδ1/CD19 engager induces proliferation of Vδ1 T-cells 98
4.22 Vδ1/CD19-mediated Vδ1 proliferation correlates to basal CD27 expression 99
4.23 Vδ1/CD19 engager treatment enhances PBMC cytotoxicity against CLL cancer cells 100
4.24 Vδ1/CD19 treatment does not induce MEC-1 cell death without Vδ1 T-cell presence 101
4.25 Vδ1/CD19 treatment enhances cytotoxicity comparably to CD3/CD19 when normalised to effector cell numbers 102
4.26 Vδ1/CD19 engager treatment targets Vδ1 T-cells allowing for controlled cytotoxic and proliferative response 103
4.27 CLL B-cells are more susceptible than healthy B-cells to Vδ1 cytotoxicity when treated with Vδ1/CD19 106
4.28 Healthy and CLL B cells differentially express membrane-expressed and apoptotic-associated genes 107
4.29 Cancer B-cell lines and primary B cells differentially express genes encoding for membrane-bound and costimulatory-associated proteins 109
4.30 Identified co-receptors and corresponding ligands potentially capable of regulating the Vδ1 cytotoxic response 111
4.31 $CD19^+$ cell line protein expression validation of ligands potentially capable of initiating Vδ1 cytotoxic response 112
4.32 $CD19^+$ cell line susceptibility Vδ1 cytotoxic response 113
4.33 Protein expression by PBMC-based, blood or skin-derived Vδ1 T-cell populations 114
4.34 Engager-mediated PBMC cytotoxicity using different bispecific formats 117
4.35 Vδ1/CD19 engager treatment affects Vδ1 T-cell phenotype. 118
4.36 Representative histograms of affected Vδ1 T-cell phenotype following Vδ1/CD19 engager treatment. 119
4.37 Vδ1/CD19 engager treatment promotes granzyme B upregulation only in a cancerous context 120
4.38 CD27 expression on Vδ1 T-cells with Vδ1/CD19 engager treatment 120

4.39 CD45RA expression on Vδ1 T-cells with Vδ1/CD19 engager treatment 121
4.40 Vδ1 T-cells proliferate to different extents depending on the co-culture 122
4.41 CD44 and ICAM-3 expression on MEC-1, Nalm-6 and healthy B-cells 122
4.42 Neutralising CD44 reduces engager-mediated Vδ1 proliferation 123
4.43 MEC-1 cell cytotoxicity following blockade of cancer-associated ligands 124
4.44 MEC-1 cell death reduced by blockade of a combination of cancer-associated ligands 125
4.45 Engager-treated Vδ1 T-cell cytotoxicity reduces with combined blockade of MEC-1 ligands 126
4.46 Engager-treated Vδ1 T-cells upregulate activation receptors in response to a combination of plate-bound ligands 127
4.47 Diagram to illustrate the current model of enhanced Vδ1 activation following Vδ1/CD19 engager treatment 129

8.1 Antibody-mediated CD25 upregulation on skin-derived Vδ1 T-cells over time . . 168
8.2 Differential TCR downregulation 169
8.3 Target cells cultured alone with Vδ1/CD19 antibodies 170
8.4 Control Gene Transcripts 171
8.5 Target cell viability 172
8.6 Representative histogram plots of co-receptor expression from Vδ1 T-cells from untreated PBMCs 173
8.7 Engager- and target cell-mediated Vδ1 T-cell phenotypic changes 174
8.8 Vδ1 Fas-L expression from culture with ligand-blocked MEC-1 cells 175
8.9 Vδ1 CD107a expression from culture with ligand-blocked MEC-1 cells 176
8.10 Engager-treated Vδ1 T-cells response to plate-bound ligands 177
8.11 Skin derived-Vδ1 T-cell cytotoxicity may be dependent on target cell associated LFA-3 178

List of Tables

3.1 Variable chain sequences used in Figure 3.1 47
3.2 BiTE-specific sequences used in Figure 3.1 48
3.3 KIH-specific sequences used in Figure 3.1 49
3.4 MB-specific sequences used in Figure 3.1 50
3.5 MACS depletion antibody conditions 56
3.6 MACS depletion microbead conditions 56
3.7 PBMC Binding flow panel 59
3.8 Cell line and Isolated Vδ1 T-cell Binding flow panel 59
3.9 4hr Activation with expanded Vδ1 T-cells flow panel 60
3.10 24hr activation and cytotoxicity with expanded Vδ1 T-cells flow panel 61
3.11 Vδ1 Proliferation flow panel 61
3.12 PBMC cytotoxicity flow panel 62
3.13 B-cell phenotyping flow panel 1 62
3.14 B-cell phenotyping flow panel 2 63
3.15 B-cell phenotyping flow panel 3 63
3.16 B-cell phenotyping flow panel 4 64
3.17 B-cell phenotyping flow panel 5 64
3.18 B-cell phenotyping flow panel 6 64
3.19 Vδ1 phenotyping flow panel 1 65
3.20 Vδ1 phenotyping flow panel 2 66
3.21 Vδ1 phenotyping flow panel 3 67
3.22 Vδ1 phenotyping flow panel 4 68
3.23 Vδ1 phenotyping flow panel 5 69
3.24 Vδ1 phenotyping flow panel 6 70
3.25 Cytotoxicity blockade flow panel 70
3.26 Plate-bound recombinant activation flow panel 71

4.1 Identified co-receptors that may affect Vδ1 cytotoxicity 116

Abbreviations

ADCC Antibody-Dependent Cellular Cytotoxicity

AF Alexa Fluor

ALL Acute Lymphocytic Leukaemia

ANG Angiogenin

APC Allophycocyanin

APC Antigen Presenting Cell

AXNA Annexin A

B-LCL B-Lymphoblastoid

BCR B-cell Receptor

BiKE Bispecific Killer Cell Engagers

BiTE Bispecific T-cell Engagers

BSA Bovine Serum Albumin

BTLA B- and T-Lymphocyte Attenuator

BTNL Butyrophilin-Like

BTN Butyrophilin

BV Brilliant Violet

CAF Cancer-Associated Fibroblast

CAR Chimeric Antigen Receptor

CCR C-C chemokine receptor

CDC Cellular-Dependent Cytotoxicity

CDR Complementarity Determining Region

CD Cluster of Differentiation

CLL Chronic Lymphocytic Leukaemia

CMV Cytomegalovirus

COX Cyclooxygenase-2

CRC Colorectal Cancer

CRS Cytokine Release Syndrome

CTLA-4 Cytotoxic T-Lymphocyte Antigen 4

CTV Cell Trace Violet

CXCR CXC Chemokine Receptors

DAP DNAX-Activating Protein

DART Dual Affinity Retargeting Antibodies

DNAM DNAX Accessory Molecule

DOT Delta one T-cells

Ecto-CRT Surface-Exposed Calreticulin

EDTA Ethylenediaminetetraacetic Acid

EGFR Epidermal Growth Factor Receptor

EGF Epidermal Growth Factor

EphA2 Ephrin Type-A Receptor 2

F-actin Filamentous Actin

Fab Antibody Fragment

FADD Fas-Associated Death Domain

FcR Fc Receptor

FCS Fetal Calf Serum

FITC Fluorescein

Fox-P3 Forkhead Box Protein P3

GM-CSF Granulocyte-Macrophage Colony-Stimulating Factor

GZM Granzyme

HBV Hepatitis B Virus

HCV Hepatitis B Virus

HER Human Epidermal Growth Factor Receptor

His Histidine

HIV Human Immunodeficiency Virus

HLA Human Leukocyte Antigen

HPLC High Performance Liquid Chromatography

IBD Irritable Bowel Disease

ICAM Intercellular Cell Adhesion Molecule

ICOS Inducible T-Cell Costimulator

IDO Indoleamine 2, 3-Dioxygenase

IGF Insulin-Like Growth Factor

IgG Immunoglobulin G

IL Interleukin

INF Interferon

IS Immunological Synapse

ITAM immunoreceptor tyrosine-based activation motif

KIH Knob-into-Hole

LFA Lymphocyte Function Associated Antigen

mAb Monoclonal Antibody

MACS Magnetic-Activated Cell Sorting

MB Morrison Body

MFI Median Fluorescence Intensity

MHC Major Histocompatibility Complex

MIC MHC Class I Polypeptide–Related Sequence

MR1 Major Histocompatibility Complex Class I-Related

mRNA messenger RNA

MSC Mesenchymal Stem Cell

NCR NK-cell Receptor

NHL Non-Hodgkin's Lymphoma

NKG2 Natural Killer Group 2

NKp Natural Cytotoxicity Triggering Receptor

NKR NK-cell Receptor

NK Natural Killer

NSCLC Non-Small Cell Lung Cancer

PBMC Peripheral Blood Mononuclear Cells

PBS Phosphate Buffered Saline

PCNA Proliferating Cell Nuclear Antigen

PD-1 Programmed Death Receptor 1

PD-L1 Programmed Death Ligand 1

PerCP Peridinin-Chlorophyll-Protein

PE Phycoerythrin

PFN Perforin

PGE-2 Prostaglandin E-2

PHA Phytohaemagglutinin

PID Primary Immunodeficiencies

PVR Poliovirus Receptor

RNA Ribonucleic Acid

RSV Respiratory Syncytial Virus

scFv Single Chain Variable Fragment

SEC Size Exclusion Chromatography

SMAC Supramolecular Activation Cluster

TAA Tumour Associated Antigen

TAM Tumour Associated Macrophage

TCEP Tris(2-carboxyethyl)phosphine

Tcm Central Memory T-cells

TCR T-cell Receptor

TC Tissue Culture

Temra Terminally Differentiated Effector Memory T-cells

Tem Effector Memory T-cells

TGFR Transforming Growth Factor Receptor

TGF Transforming Growth Factor

Th T-Helper

TLR Toll-Like Receptor

TME Tumour Microenvironment

TNFR Tumour Necrosis Factor Receptor

TNF Tumour Necrosis Factor

TRAIL TNF-Related Apoptosis-Inducing Ligand

Treg Regulatory T-cell

TSA Tumour Specific Antigen

ULBP UL16 Binding Protein

VEGF Vascular Endothelial Growth Factor

Chapter 1

Introduction

This thesis aims to investigate the rationale behind targeting Vδ1 T-cells, specifically with an antibody-based engager, to treat cancer. The research focuses on the development of such a Vδ1-targeting engager in the context of CD19$^+$ malignancies and how this treatment can be used to enhance the body's own anti-tumour defences. As an introduction, this first chapter aims to provide an overview of the principle behind onco-immunotherapies, explore the current knowledge-base of $\gamma\delta$ T-cell biology and finally examine why Vδ1 $\gamma\delta$ T-cells warrant further investigation as targets for the next generation of cancer treatments.

1.1 Cancer

Cancer refers to a group of diseases characterized by the abnormal growth of cells. If left untreated, malignant cells can invade the originating organ and spread to other tissues, ultimately leading to fatal disruptions in normal bodily functions. With an ageing population, it is estimated that in the UK 1 in 2 people will develop cancer in their lifetime [1], and globally cancer incidence rates are ever-increasing making cancer a leading cause of death worldwide [2]. Due to the high mortality rates associated with cancer diagnoses, the development of new therapies remains crucial in the ongoing fight against the disease.

1.1.1 Cancer formation

A neoplasm forms from a cell or groups of cells that have sustained genetic mutations that enable them to abnormally divide and grow [3]. The accumulation of mutations facilitates evolution of the cancer which enables its invasive growth due to resultant acquired abilities such as enhanced proliferation, angiogenesis and evasion of growth suppressors, cell-death signals and immune-destruction [3, 4]. Because of these abilities, the resulting tumour is highly heterogenous, not

only between the cancerous cells themselves, but also within the tumour microenvironment (TME) (Figure 1.1).

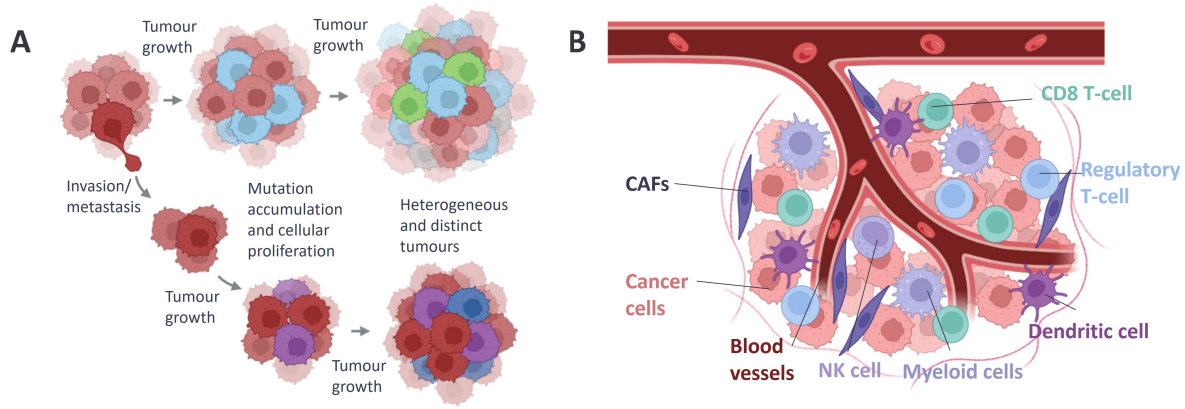


Figure 1.1: ***Tumour Heterogeneity.***

(A) *Heterogeneity of cancer cells. As cancer cells acquire pro-tumoural mutations, the different cell types may present beneficial phenotypes for different reasons, facilitating the growth of different cancer cell populations. This evolution maintains the persistence of varied cancerous cells [5], and will occur separately for the same reasons in any new tumour formations following invasion or metastasis, resulting in distinct and heterogeneous tumours.* ***(B)*** *The tumour microenvironment. A range of non-cancerous cells exist in the tumour microenvironment that may support tumour development, including but not limited to cancer-associated fibroblasts (CAFs), myeloid cells (such as tumour-assocaiated macrophages) and regulatory T-cells. These cells can suppress any anti-tumoural cells such as CD8 T-cells and NK-cells. [6, 7]. [This image was created using BioRender]*

1.1.2 Traditional Cancer Therapies

Surgical removal of a tumour is one of the oldest and most effective treatments for a lot of cancer indications if the tumour is detected early enough, before any invasion or metastases have occured [8]. However, early detection is not always possible and surgery can even expedite tumour growth by increasing cancer cell shedding and inflammation [9]. Other traditional cancer therapies, such as chemotherapy and radiotherapy focus on targeting the uncontrollable growth aspect of a tumour. These therapies use chemicals or radiation to target the rapidly dividing nature of cancer cells to eliminate them; however, the simplicity of this approach fails to address the complexities and heterogenous nature of a malignant tumour that enable the cancer to grow in the first place (Figure 1.1). In failing to recognise the complex hallmarks of cancer[1] [10, 11, 4],

[1]The hallmarks of cancer were first introduced in 2000 by Hanahan and Weinberg to provide clarity on the definition of malignancies but also to understand the defining characteristics of cancers to be able to develop more effective treatments [10]. The hallmarks have been updated over time to include the ever-growing research and

these therapies may not only fail to eradicate a whole tumour but can also aggravate further tumour development [12].

The success of chemotherapy and radiotherapy [13] has thus been variable. These strategies lack tumour-specificity and can affect surrounding healthy tissue leading to severe adverse effects to the patient. Additionally, disease-free survival can remain low due to cancer cells developing resistance mechanisms [14, 15, 16] as well as increased chemotherapy-mediated inflammation [12]. These limitations contribute to disease relapse and thus highlight the continued development these therapies have undergone.

Recent developments in radiotherapy techniques have increased its specificity to reduce its adverse effects and is thus now used in a large proportion of cancer treatments [17]. Despite this, radiotherapy often requires combination with other therapies to improve its efficacy [18] and is not always suitable for all cancer types [19]. Consequently, the development of alternative approaches has gained significant interest.

Over the last decade, immunotherapies have been the focus for many novel cancer therapies, particularly since the development of the CTLA-4 blockade antibody Ipilimumab for advanced melanoma, as well as the PD-1 blockade antibody Nivolumab for NSCLC, which received FDA approval in 2011 and 2015, respectively [20, 21]. Immunotherapies essentially aim to enhance the immune system's inherent capability to recognise and eradicate neoplasms. In comparison to the traditional therapies, immunotherapies can be more cancer-specific reducing potential for detrimental adverse effects. Furthermore, combining traditional therapies with immunotherapy has demonstrated increased efficacy [22], primarily because this approach targets the cancer on multiple fronts, limiting its ability to accumulate mutations quickly enough to evade treatment. Therefore, understanding the immune system's role in cancer could be pivotal in developing more effective treatments.

1.1.3 Cancer and the Immune System

The immune system plays a critical role in keeping us alive by identifying and removing harmful self-derived and foreign entities. This includes safeguarding against cancer formation or tumourigenesis. Under normal conditions, the immune system prevents tumourigenesis through three primary mechanisms [23]:

1. Inhibition of virus-induced tumours by protecting against viral infections.
2. Regulation of persistent inflammation during infections, which might otherwise promote tumourigenesis.

have thus proposed ten hallmarks alongside four enabling characteristics that facilitate neoplasm growth.

3. Elimination of transformed and stressed cells, which have the potential to develop into cancers.

This recognition and elimination of cancerous cells, known as immune surveillance, primarily occurs due to the detection of tumour-associated antigens (TAA), tumour-specific-antigens (TSA) and cell surface proteins indicative of cellular and metabolic stress [24] (Figure 1.2). Tumour antigens can include neoantigens presented via MHC or HLA class I molecules or the abnormal expression of cell surface proteins that facilitate tumour progression. For instance, HER2, a protein normally expressed on breast tissue, is overexpressed in certain cancers to drive cell proliferation [25].

If the neoplasm acquires the right mutations, the tumour can enter a state of equilibrium; where susceptible cancer cells are eliminated by the immune system, while continuous division of further-mutated cancer cells persists [23]. This results in a state of tumour dormancy that is thought to be predominantly maintained by T-cells, IL-12 and IFN-γ [23]. During this state of dormancy, 'editing' of the persisting cancer cell's immunogenicity can occur where occult tumours can acquire mutations that reduce its susceptibility to the immune system which reduces the overall immune response against the cancer. Over time, accumulating advantageous mutations allow persisting cancer cells to escape the equilibrated immune control, shifting the balance to suppress anti-tumourigenic responses and promote tumour growth [23]. This process of immunosurveillance and immunoediting is detailed in figure 1.2. Immune escape, for example, can occur from mutations that reduce expression of tumour antigens, which are essential for immune recognition and elimination [27]. Additionally, mutations that interfere with the HLA presentation of neoantigens can impair activation of CD8 T-cells that are critical for anti-tumour immunity [24]. Immune checkpoint pathways are often dysregulated in cancers, such as overexpressed surface PD-L1, which can effectively silence anti-tumoural T-cell activity [28]. Advantageous mutations can also increase release of cytokines such as IL-6, IL-8, IL-17, and IL-10 which affect the balance of immune signals and drive tumour-promoting inflammation [29]. These signals can recruit immunosuppressive regulatory T cells, specifically $CD4^+CD25^+FoxP3^+$ Tregs, which suppress anti-tumour immune responses by depleting IL-2 supplies essential for T-cell activity and increasing the prevalence of regulatory cytokines in the TME [30, 31].

Understanding the mechanisms by which tumours can affect the immune system has provided critical insights into cancer biology. This knowledge prompted the development of immunotherapies, which aim to restore the immune system's ability to detect and eliminate cancer cells, tipping the balance back in favour of anti-tumour immunity.

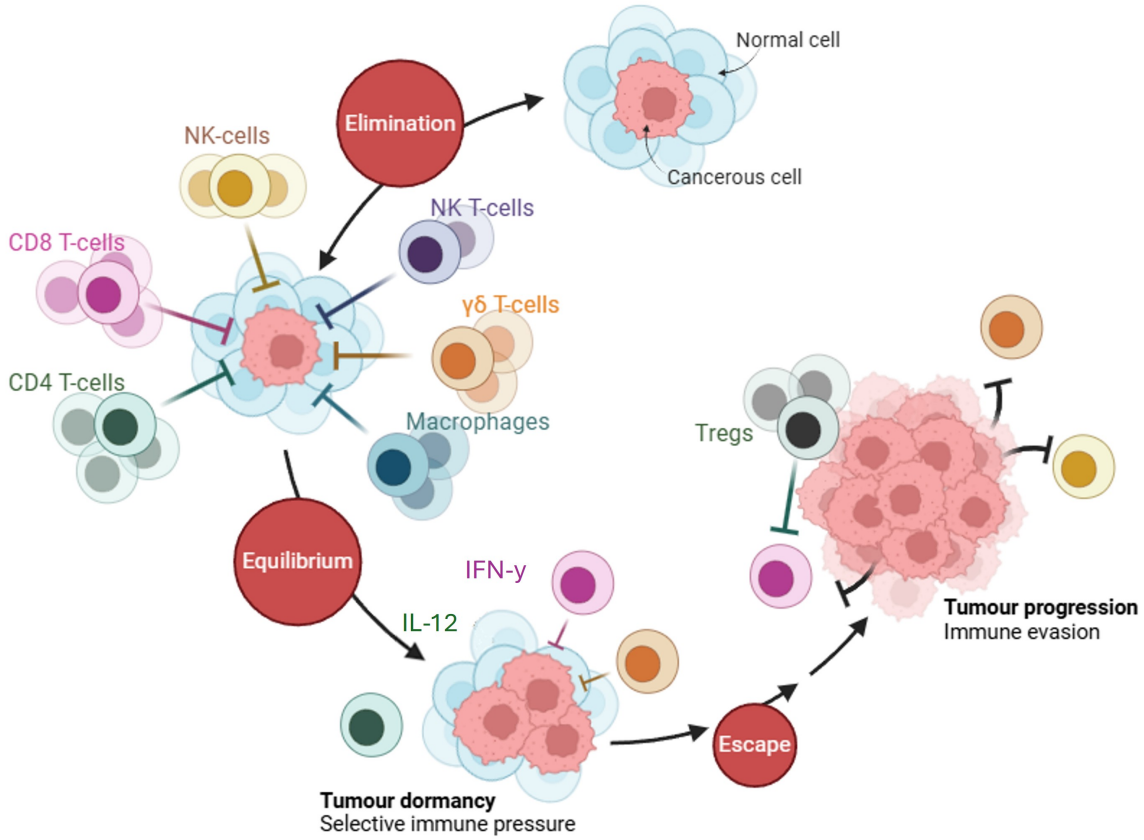


Figure 1.2: ***Cancer Immunoediting.***

Cancer immunoediting is the process in which cancer cells can escape immunosurveillance and elimination through the acquisition of advantageous mutations and interplay with the immune system. Immunoediting is characterised by three stages, elimination, equilibrium and escape.

Elimination*. If intrinsic cellular tumour-suppressor mechanisms fail and a neoplasm forms, such dysregulated cells can be recognised and eliminated by adaptive and innate immune cells. $CD8^+$ T-cells recognise neoantigens expressed via HLA-1 presentation. NK-cells can recognise a lack of HLA-1 molecules on dyregulated cells, and can recognise surface expression of cellular stress ligands. $\gamma\delta$ T-cells may be able to recognise cancerous cells through both of these mechanisms. Dendritic cells and $CD4^+$ helper T-cells can aid macrophage, B-cell and T-cell activation, B-cells can provide an anti-tumour humoural response, and type 1 macrophages can phagocytose tumour cells upon activation.*

Equilibrium*. Equilibrium involves the persistence and dormancy of a tumour, that is maintained by immune cells, particularly T-cells, as well as IL-12 and IFN-γ. The tumour's outgrowth is prevented by these factors which also provides a selection pressure where cancer cells that have acquired the necessary mutations to not be completely eliminated can persist. The persistence of these cells and selection pressure facilitates the capacity of the occult tumour cells to evolve into cells with lower immunogenicity. This state of tumour dormancy can last for years or even a lifetime, though some neoplasms will not even enter this stage and may go straight to elimination.*

Escape *Over time, this equilibrium can progress if the persisted cancerous cells acquire mutations that enable escape or evasion of key anti-tumour immune cells, such as NK-cells and $CD8^+$ T-cells, while promoting the recruitment and activity of pro-tumourigenic immune cells, such as Tregs.*

Adapted from [26] and [23] [This image was created using BioRender]

1.1.4 Onco-Immunotherapy

To restore the immune system's ability to combat cancer, immunotherapies have employed a range of strategies. A description of the current immunotherapy landscape is summarised in figure 1.3.

Despite the advancement and pre-clinical success of these strategies, cancers have still bypassed these efforts through advancing immune evasion and treatment-resistance mechanisms [33]. As many of these strategies aim to enhance the $CD8^+$ T-cell response against the tumour, most of these therapies are susceptible to evasion by increasing immunosuppression within the TME and dampening *any* aspect of the entire antigen presentation mechanism: CD8 T-cells rely on antigen presentation via the MHC-class 1 molecule from both dendritic cells and within the tumour (Figure 1.5). If the tumour accumulates a mutation that disrupts this process in any way, it can result in dysfunctional CD8 cytotoxicity making one line of defence redundant.

CAR T-cell therapies can overcome this problem as they have been genetically engineered to overcome MHC-dependency. CD3-targeting antibodies, or engagers, also bypass the MHC-dependent TCR-mediated activation by stimulation through the common T-cell CD3 molecule [34]. Whilst this bypassing is beneficial to eliminate dependency on MHC-presentation, this also affects the mechanisms for sparing healthy cells from T-cell cytotoxicity. Consequently, these strategies can result in widespread T-cell activation resulting in severe adverse effects such as cytokine release syndrome (CRS) and healthy tissue damage, which has been debilitating if not fatal to patients [35, 36].

Finally, the development of these strategies often overlooks the persistence of cancer stem cells, which play a key role in the formation of neoplasms and the development of treatment resistance. Interestingly, cancer stem cells can contribute to or even drive an immunosuppressive TME [37]. As a result, achieving a cured status is thought to depend on the elimination, or at least attenuation of these cells.

Highlighting the failures of these therapies is not meant to imply that they have been entirely unsuccessful or a wasted effort. On the contrary, these failures highlight areas still in need of improvement, while also expanding our toolkit for designing more effective treatments for individual patients. As has been consistently demonstrated throughout the history of cancer therapy research and development, the most successful strategies often emerge from combining treatments and tailoring approaches to address intra- and inter-tumoural heterogeneity. Therefore, the current landscape of cancer therapies emphasizes the ongoing need to advance these strategies and explore new ones to identify the most effective treatment options for each patient.

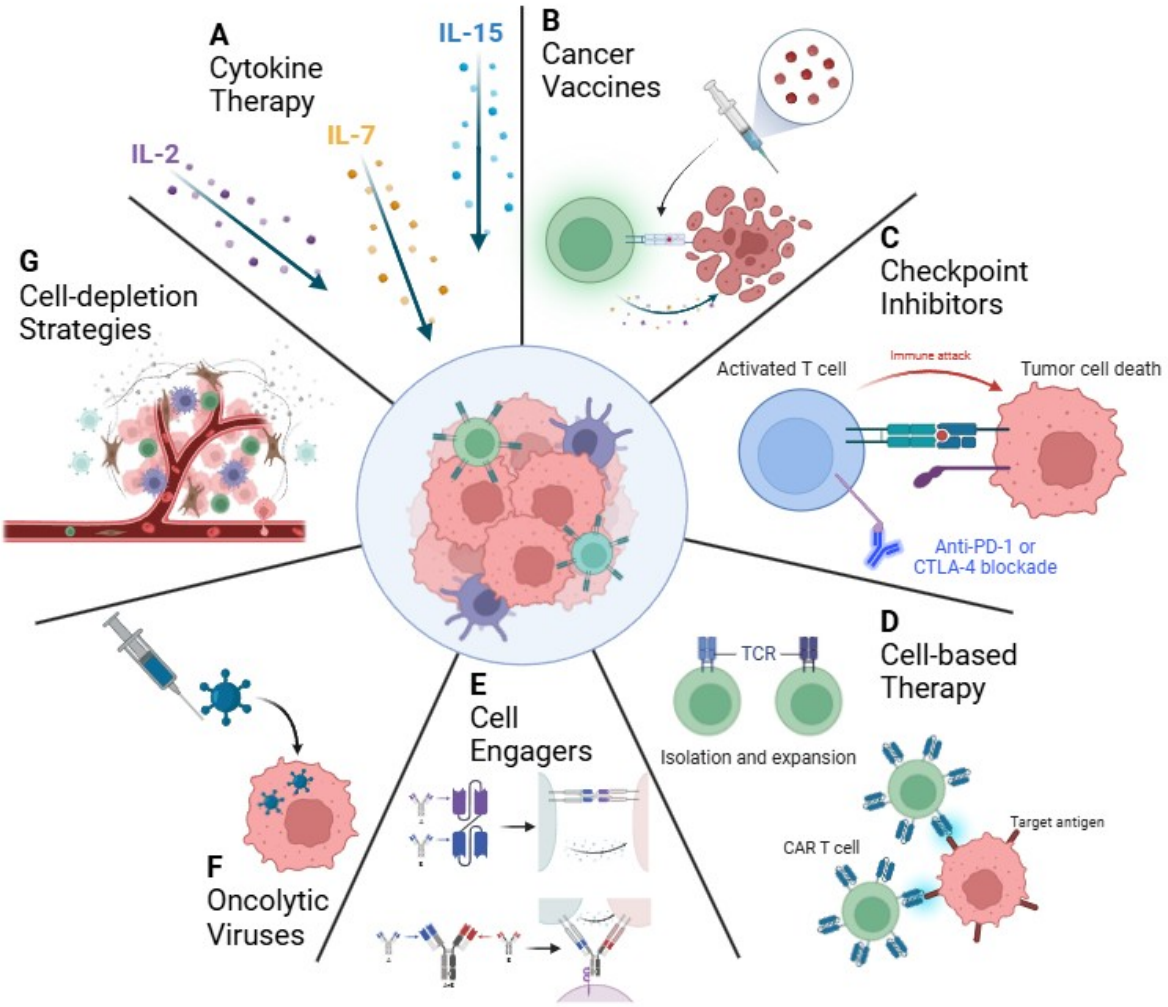


Figure 1.3: ***Immunotherapy Landscape.***

(A) *Cytokine therapy, administration of recombinant cytokines such as IL-2 and IL-15 to boost anti-tumour T-cell activity.* ***(B)*** *Cancer Vaccine, administration of cancer-associated antigens to train dendritic cells to improve the immune system's anti-tumoural response.* ***(C)*** *Checkpoint inhibitors, administration of antagonistic antibodies to inhibit T-cell suppression via receptors such as PD-1 and CTLA-4.* ***(D)*** *Cell-based therapies, administration of activated and/or genetically engineered autologous or allogeneic effector cells to directly enhance the cytotoxic response against maligant cells, such as CAR T-cells* ***(E)*** *Cell engagers, administration of agonistic antibodies to activate effector cells against cancer cells, including CD3 engagement and ADCC and CDC initiating mechanisms.* ***(F)*** *Oncolytic viruses, administration of cancer-specific viral particles that lyse cancer cells to release neoantigens into the TME to train the immune system in a similar mechanism to cancer vaccines.* ***(G)*** *Cell depletion strategies, administration of engagers, chemotherapeutics and/or antagonistic antibodies to deplete immunosuppressive immune cells within the TME such as TAMs. Adapted from [32]. [This image was created using BioRender]*

One addition to the current approaches has been the recent research into the potential of $\gamma\delta$ T-cells. Not only have these cells been associated with increased survival in cancer patients [38, 39, 40, 41, 42, 43, 44, 45, 46, 47], these cells provide a potential solution to some of the pitfalls described above. $\gamma\delta$ T-cells function in an MHC-independent manner [48] and can target a broad range of stress and/transformed related cellular self-antigens. This enables them to act independently of neoantigen generation and not be reliant on the presence of any single molecule [49]. The broad repertoire of activating ligands available to these cells reduces their susceptibility to tumour immune evasion. Moreover, by responding to cellular stress signatures, they can discriminate between healthy and cancerous cells, minimizing the risk of damage to healthy tissue and thus reducing the likelihood of severe adverse effects [50]. Finally, $\gamma\delta$ T-cells have shown promise in recognizing and eliminating cancer stem cells [51, 52].

Given the promise $\gamma\delta$ T-cells hold for cancer therapeutics, the following section will explore the latest research on their mechanisms and assess the potential benefits of targeting Vδ1 $\gamma\delta$ T-cells for immunotherapy.

1.2 Human $\gamma\delta$ T-cells

$\gamma\delta$ T-cells are defined by their TCR, constituting a gamma (γ) chain and delta (δ) chain, as opposed to an alpha (α) and beta (β) chain expressed in the canonical T-cell. Similarly to $\alpha\beta$ T-cells, γ and δ chains undergo V(D)J somatic recombination to express a functional TCR. There are eight types of Vδ gene segments recorded in humans [53] (summarised in figure 1.4), however, the δ chain is often expressed as one of two main types: Vδ1 and Vδ2 [54]. Vδ2 chains often dimerise with γ9 chains [54], and these Vγ9Vδ2 cells typically reside in the blood [55]. Opposingly, Vδ1 chains couple with a wider variety of γ chains [56, 54] and are found both in blood and tissue.

$\gamma\delta$ T-cells, like the more conventional $\alpha\beta$ T-cells, utilise their TCRs to recognise target cells and promote T-cell activation (see section 1.2.1); however there are a few physiological differences between the two cell types. $\alpha\beta$ T-cells are the predominate T-cell type, constituting ˜45-70% of lymphocytes in healthy PBMCs [58], whereas $\gamma\delta$ T-cells represent only ˜0.5-15% [59, 60]. In epithelial cell rich tissues or tumours however, $\gamma\delta$ T-cells can make upto 50% of the lymphocyte population [61]. Furthermore, $\gamma\delta$ T-cells also develop before $\alpha\beta$ T-cells have fully matured [62, 63] allowing $\gamma\delta$ T-cells to act as the 'first line of defence' during development and in adult tissue regulation. This idea that $\gamma\delta$ T-cells surveil and protect the body against infection and tumourigenesis during development was first explored *in vivo* where $\gamma\delta$-depleted mice showed greater tumour susceptibility [64].

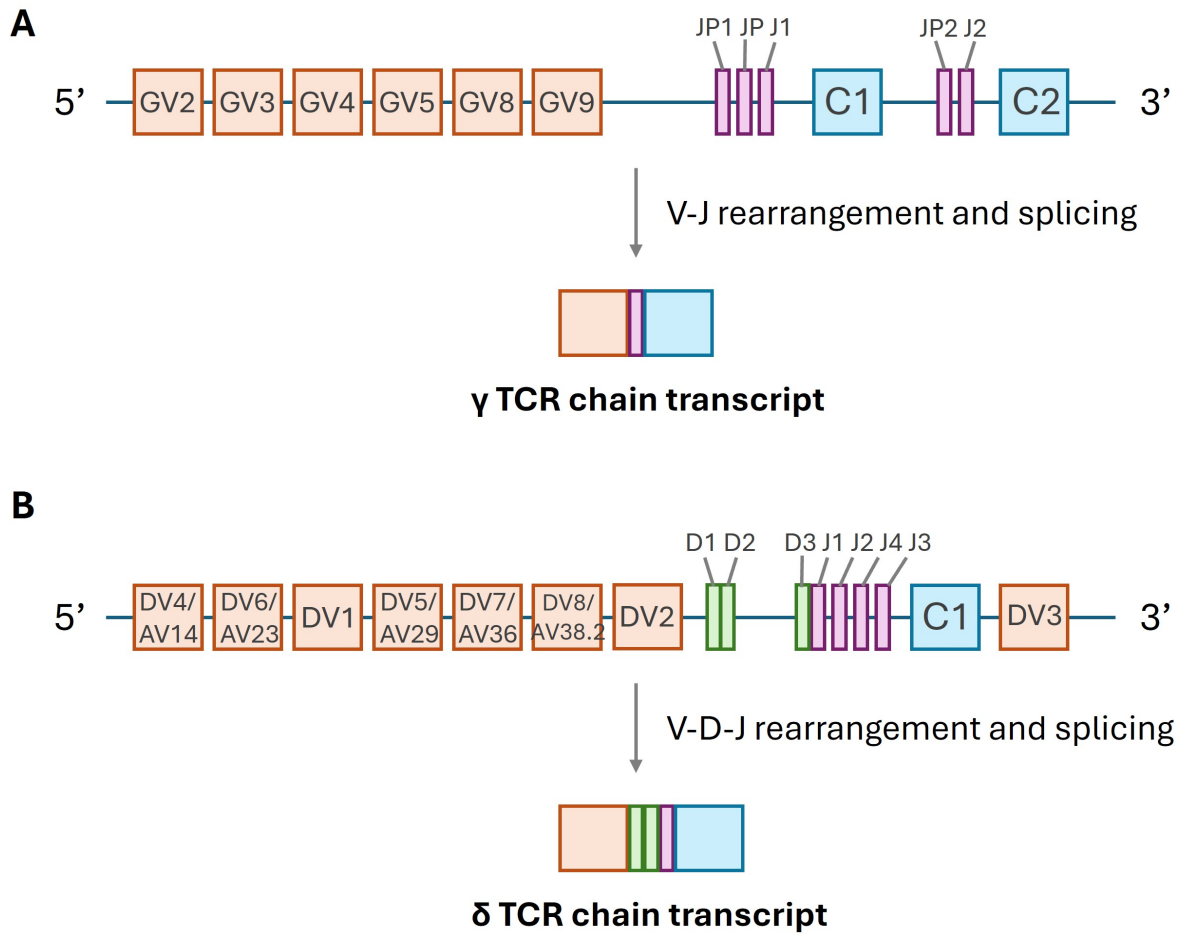


Figure 1.4: ***Somatic Recombination for γ and δ chain expression.***
(A) *Overview of the variable (V), joining (J) and constant (C) gene segments that can make up the γ (G) TCR chain transcript. There are six GV gene segments that determine the Vγ chain type expressed at the protein level following V-J rearrangement.* ***(B)*** *Overview of the variable (V), diversity (D), junctional (J) and constant (C) gene segments that can make up the δ (D) TCR chain transcript. There are eight DV gene segments that determine the Vδ chain type expressed at the protein level following V-D-J rearrangement, where three of these DV segments are only expressed as part of the δ chain, and the remaining five DV gene segments can also be expressed as part of the α chain (AV) of the $\alpha\beta$ TCR. Additional diversity is created in both chain transcripts following the random addition of nucleotides. This diversity increases the variety of TCR binding antigens. Note only functional gene segments have been included in the diagram. Adapted from [57] and [53]*

$\gamma\delta$ T-cells are often described as the link between the adaptive and innate immune systems as they exhibit properties of both [65]. They respond to their TCR ligands and have been suggested to clonally expand in a similar way to $\alpha\beta$ T-cells [54]. Once activated, $\gamma\delta$ T-cells can release proinflammatory cytokines and chemokines to attract and activate antigen presenting

cells [66] as well as other B- and T-cells, and are thus able to orchestrate the immune system [65]. Vδ1 T-cells may be more adaptive than Vδ2 T-cells due to their capacity for differentiation from a wider variety of TCR ligands. Vδ1 T-cells are able to differentiate from naive to effector phenotypes as well as exhibiting a more diverse TCR repertoire to bind to a greater variety of antigens [54].

Alongside their adaptive characteristics, $\gamma\delta$ T-cells can also respond in a more innate-like manner where they do not rely on TCR-mediated signalling to be activated. $\gamma\delta$ T-cells express other receptors such as toll-like receptors (TLR) as well as NK-cell receptors (NKR) that allow them to recognise and activate in response to infection as well as cellular stress-associated ligands in a similar manner to innate NK-cells [67, 49]. This not only enables a faster response than TCR-mediated cytotoxicity but, in the context of anti-tumoural capabilities, because these cells respond to a vast array of ligands, they are less susceptible to immune evasion as their activation and cytotoxicity is not dependent on any single ligand expression mechanism. Therefore, it is useful to understand this activation mechanism and how it differs from the canonical T-cell.

1.2.1 $\gamma\delta$ T-cell Activation

As discussed earlier, conventional T-cells rely on HLA-1 presented antigens to become activated through their TCRs (Figure 1.5). While $\gamma\delta$ T-cells can also become activated via a similar mechanism [68, 69, 70, 71, 72], this is not their sole pathway for TCR-mediated activation and TCR signalling is not the only mechanism that can lead to $\gamma\delta$ T-cell activation (Figure 1.5). While the known repertoire of antigens recognized by $\gamma\delta$ TCRs and other innate receptors remains incomplete, significant progress has been made in identifying and characterizing these targets.

1.2.1.1 $\gamma\delta$ TCR recognition

As Vγ9Vδ2 are the most predominant $\gamma\delta$ T-cell in the periphery, Vγ9Vδ2 TCR ligands have been most extensively studied. Vγ9Vδ2 TCRs recognise butyrophilin (BTN) proteins, such as BTN3A1 and BTN2A1 [74] that are activated by bound intracellular phosphoantigens expressed by infected or metabolically stressed cells [75, 76, 77]. Aminobisphosphonates such as zoledronate can also be used to activate Vδ2 T-cells *in vitro* and *in vivo* as they increase the levels of phosphoantigens in the system [78]. Phosphoantigens activate BTN proteins by binding to the intracellular B30.2 domain of BTN3A1 and BTN2A1 [79]. This BTN 'phosphoantigen sensing' induces a conformational change in the extracellular BTN domains which facilitates BTN-recognition by the Vγ9Vδ2 TCR resulting in Vγ9Vδ2 T-cell activation [79].

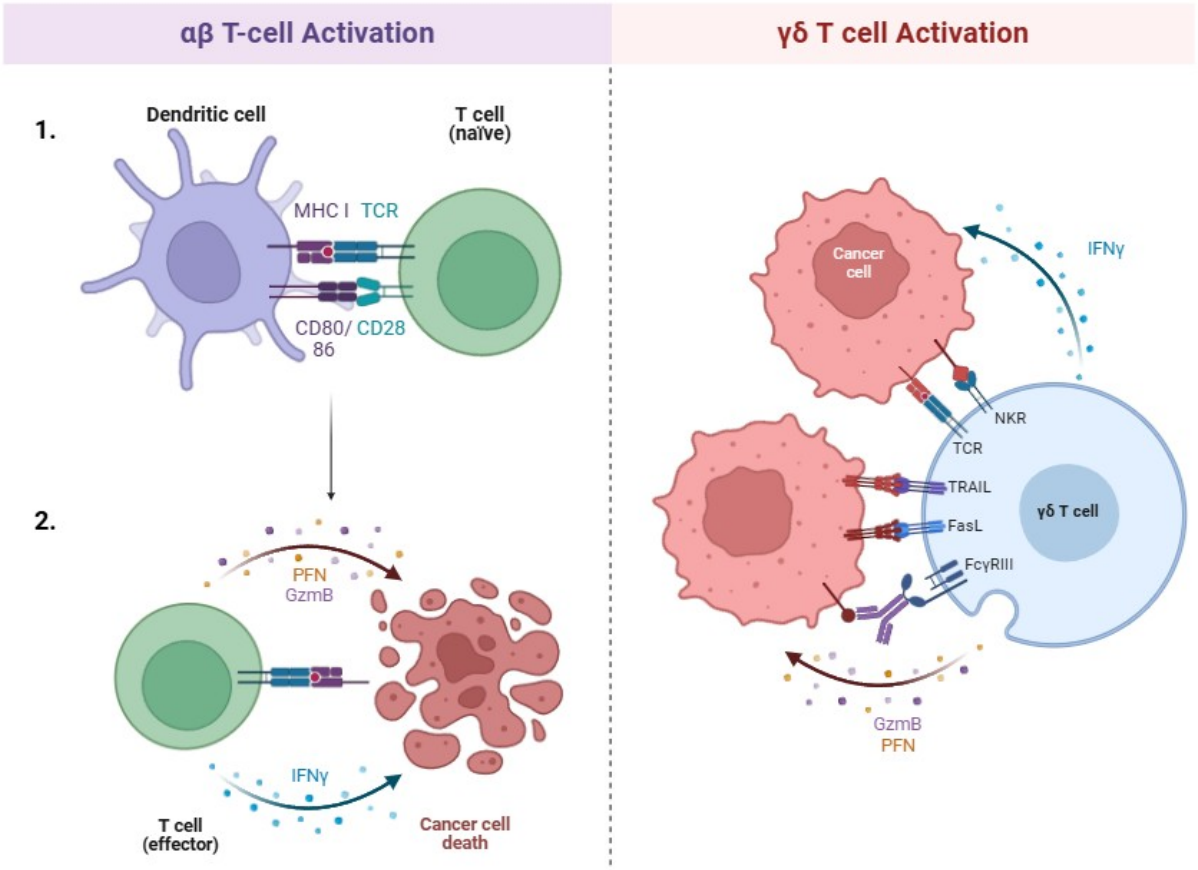


Figure 1.5: $\gamma\delta$ ***vs*** $\alpha\beta$ ***T-cell Activation.***

Left, Simply, CD8$^+$ $\alpha\beta$ T-cells require a 2-step activation process to be able to elicit a cytotoxic response towards their target. Cytotoxic responses include granzyme, perforin and INF-γ release. Peptide-loaded MHC-mediated TCR stimulation is required alongside costimulation through molecules such as CD28 from a professional antigen presenting cell such as dendritic cells. Subsequently, these CD8$^+$ T-cells can recognise peptide-loaded MHC presented on the cancer cell to elicit a cytotoxic response. Without their specific peptide-loaded MHC present on the target cell however, these CD8$^+$ T-cells cannot elicit a cytotoxic response. Right, $\gamma\delta$ T-cells do not require initial co-stimulation to be able to elicit a cytotoxic response and do not rely on any single protein type to be present to become activated as these cells utilise TCR stimulation—that are not MHC-restricted—as well as NKR signalling and death receptor signalling to elicit a cytotoxic response. Adapted from [73]. [This image was created using BioRender]

This mechanism has been leveraged by ImCheck Therapeutics for cancer treatment through a BTN3-targeting antibody, which binds extracellularly to overexpressed BTN3 proteins on the surface of cancer cells, enhancing anti-tumoural Vδ2 T-cell activity [80].

The known repertoire of ligands for the Vδ1 TCR remains incomplete, though evidence suggests a broader range of ligands. Sequencing of the CDR3 regions—the most variable segment of the TCR—from healthy human cord blood and adult blood Vδ1 T-cells revealed a vast clonotype

diversity in cord blood samples, which appears to become more "focused" in adults, likely due to immunological stimuli such as CMV infection [54]. This clonotypic diversity through somatic rearrangement—as well as nucleotide additions during this process—highlights the potential vast array of ligands that could bind the Vδ1 TCR.

Recent research has identified a growing list of ligands that suggest the $\gamma\delta$ TCR binds to MHC and MHC-like complexes that may or may not be presenting an antigen, as well as binding to surface bound cellular-stress related proteins [81]. Among the ligands that have been discovered, CD1c [82] and CD1d [83, 84] antigens have been shown to bind the Vδ1 TCR. CD1d is a lipid-presenting molecule that is usually expressed on antigen-presenting cells to activate NK T-cells. CD1d demonstrated interaction with CDR1 regions of the TCR's δ-chain, whilst the lipid antigen was restricted to binding the CDR3γ loop of the TCR [83]. This dual binding of the Vδ1 TCR was also observed when paired with the Vγ4 chain, where the Vδ1 chain specifically recognized CD1b, while the Vγ4 chain interacted with BTNL3/8 ligands [85]. The Vδ1Vγ8 TCR demonstrated interaction with MR1 presenting vitamin B metabolites [86]. Vitamin B derivatives can originate from bacteria, suggesting MR1 interactions could play a role in Vδ1-mediated pathogen clearance. The Vγ9Vδ1 TCR specifically binds ephrin type-A receptor-2 (EphA2) [87] which facilitates T-cell trafficking and can be upregulated on many cancers. EphA2 could facilitate Vδ1 cancer recognition as EphA2 blocking-techniques reduced Vδ1 cytotoxic responses [88]. This EphA2-dependent response was however not observed with Vδ2 cells, highlighting the distinct responses and roles between the two $\gamma\delta$ T-cell types. Other stress antigens also interact with Vδ1 TCRs including the antigens associated with oxidative stress, annexin A2 and A6 [89], and ligands to the MHC-like natural killer receptor NKG2D [90] (NKG2D interactions are explored further later). Finally, lipid and metabolite recognition from target cells can also occur in a CD1-unrestricted and MR1-unrestricted manner, respectively [91].

The $\gamma\delta$ TCR binds with low affinity to its ligands [81] and therefore likely reaches the threshold of activation through multiple interactions within the immunological synapse (IS) (Figure 1.7) formed between the $\gamma\delta$ T-cell and its target cell. The reliance on multiple signals within the IS to activate $\gamma\delta$ T-cells identifies an important mechanism in which $\gamma\delta$ T-cells can avoid healthy tissue damage and autoimmunity as these cells will only activate if a cell expresses a large number of cellular stress signals, which healthy cells would not be expressing. These signals may be interactions mediated through TCR binding though research has also highlighted the role of $\gamma\delta$-expressed co-receptors within the IS that contribute to $\gamma\delta$ T-cell activation.

1.2.1.2 $\gamma\delta$ Costimulation

In addition to TCR stimulation, $\gamma\delta$ T-cells express other receptors that also result in T-cell activation. Co-stimulation plays a significant role in $\alpha\beta$ T-cell activation, as without this 'signal 2', TCR 'signal 1' stimulation is not sufficient to fully activate the T-cell (reviewed in [92]). This defined role of costimulatory molecules however is not as translatable to $\gamma\delta$ T-cell activation. The $\gamma\delta$ TCR does not ***require*** costimulatory molecules to initiate cell activation, though research has also indicated that specific co-stimulation, or rather stimulation through co-receptors significantly affects the responses observed. A range of co-receptors have been identified on $\gamma\delta$ T-cells to aid their functionality (Figure 1.6).

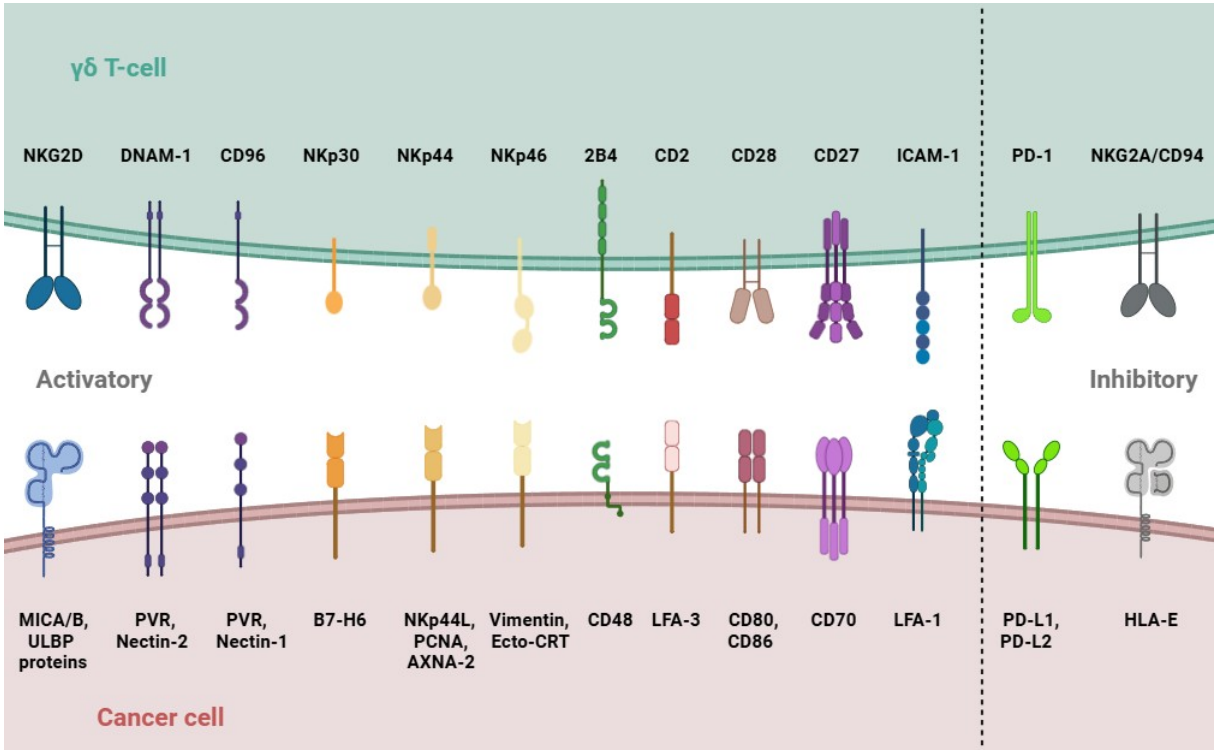


Figure 1.6: $\gamma\delta$ ***T-cell co-receptors and corresponding ligands.***
Adapted from [49]. [This image was created using BioRender]

CD2, canonically expressed on T- and NK-cells, binds CD58 (LFA-3) expressed on APCs and is involved in stabilising cell-to-cell contact in the immunological synapse [49, 93]. CD2 has shown involvement in $\gamma\delta$ T-cell activation when anti-CD2 antibodies improved $\gamma\delta$ T-cell proliferation and IL-2 secretion when in the presence of lymphoma cells [94]. Furthermore, CD2 blockade, in combination with TCR blockade, reduced the cytotoxic capacity of expanded Vδ1 T-cells against CLL B-cells [50], suggesting a role for CD2 in $\gamma\delta$ T-cell cytotoxicity. Another cell adhesion-related receptor, LFA-1 has demonstrated a similar role where Vδ1 cytotoxic ability decreased when LFA-1 binding to ICAM-1—expressed on colorectal cancer cells—was blocked

[95]. This LFA-1 and CD2 reliance highlights the importance of a stable immunological synapse through cell-to-cell contact in facilitating Vδ1 recognition and killing of target cells.

CD28, important for $\alpha\beta$ T-cell proliferation, survival, and cytokine production [92], is minimally expressed on isolated $\gamma\delta$ T-cells from fresh blood [96, 97, 59]. However, TCR-stimulated Vδ1 T-cells have been shown to proliferate following anti-CD28 antibody treatment [97]. This suggests that CD28 may play a role in Vδ1 activation. CD28 may also downregulate upon activation as low-to-negative CD28 expression was observed in mature Vδ1 T-cells from CRC patients, which also correlated with CD27 expression [40]. Vδ1 T-cells lose CD27 as they mature [54]. This differentiation of a naïve T-cell to an effector-like cell—usually with greater cytotoxic responses—can be triggered by immunological stimuli such as CMV and result in a focussing of the TCR repertoire [54], suggestive of clonal expansion and the formation of memory.

In contrast, roughly 80% of human Vγ9Vδ2 cells express CD27 [98]. CD27/CD70 interactions promote proliferation of human Vγ9Vδ2 cells and upregulate anti-apoptotic pathways; human Vδ2 cells proliferated more in response to soluble CD70 whilst blocking CD27 reduced cell expansion *in vitro* [98]. If CD27 expression similarly promotes proliferation in Vδ1 T-cells, its loss in differentiated Vδ1 T-cells with expanded individual TCR clonotypes may indicate a reduced need for further clonal expansion in these effector populations, potentially facilitating the development of a serial-killer-like cytotoxic capability, where each effector cell can kill multiple target cells.

CD27 expression was also observed on a subset of differentiated adult Vδ1 T-cells with low PD-1 expression [99], whereas increased expression of PD-1 correlated to effector-like capabilities [100, 50, 101], opposingly to the canonical $\alpha\beta$ T-cell where increased PD-1 may be a sign of exhaustion as well as activation [101]. This PD-1-effector association was also observed with Vδ2 T-cells [102]. With cell surface expression of CD27 indicating a less differentiated $\gamma\delta$ T-cell, Vδ1 CD27^{+}CD28^{+}PD-1$^{\text{low}}$ cells could indicate a naïve Vδ1 T-cell phenotype.

Another co-receptor, NKG2D, is involved in the recognition of stress-induced ligands, and thus likely plays a key role in cancer cell recognition. On NK cells, NKG2D ligands can result in direct stimulation, whereas NKG2D can have a costimulatory effect on cytotoxic CD8^{+} T-cells indicating TCR stimulation is still required [103]. With $\gamma\delta$ T-cells, NKG2D ligands have been shown to play multiple roles. MICA, an NKG2D ligand, stimulated Vγ9Vδ2 cells [104], and greater expression of the NKG2D ligand ULBP1 on tumour cells resulted in greater susceptibility to Vγ9Vδ2 cytotoxicity [105]. Additionally, blockade of MICA and MICB reduced Vδ1

cytotoxic responses against a leukaemic cell line [106]. MIC proteins were also suggested to bind a specific V$\delta1^+$ TCR clonotype [107, 90] and induce an effector response of Th-1 cytokines [90]. Furthermore, the ligand ULBP4 was suggested to activate Vγ9Vδ2 T-cells through specific binding of the TCR as well as NKG2D [108]. The possibility of NKG2D ligands engaging both the TCR and NKG2D receptor on $\gamma\delta$ T-cells suggests a dual role for NKG2D in $\gamma\delta$ T-cell activation. NKG2D could provide an initial activation signal, analogous to the primary antigen recognition signal ("signal 1"), while also acting as a costimulatory signal ("signal 2") [107, 49]. This mechanism could enable a lower threshold for activation of $\gamma\delta$ T-cells, facilitating their rapid response to stress signals or transformed cells. [2]

Other NK-associated receptors have also been identified on $\gamma\delta$ T-cells. Killer activatory receptors found on $\gamma\delta$ T-cells include natural cytotoxicity receptors (NCRs), CD94/NKG2A, 2B4 (CD244) and DNAX accessory molecule 1 (DNAM-1) [109]. The role of some NCRs is thought to contribute to activation as well as regulation of $\gamma\delta$ T-cells. Following cytokine expansion of blood-derived Vδ1 T-cells, effector capabilities were observed alongside upregulation of NKp30, NKp44, NKG2D, DNAM-1, and 2B4 [50]. Furthermore, cytotoxic capability of these expanded Vδ1 T-cells against AML cells were dependent on DNAM-1 and NKp30 expression [110]. Individual blockade of NKG2D and DNAM-1, as well as the TCR, CD2 and ICAM-1, reduced the specific lysis of a myeloma cell line [111], supporting their role in tumour recognition and cytotoxic responses. The NCRs, NKp30 and NKp44, bind B7-H6—a tumour-associated ligand—and PCNA/ANXA-2, respectively [112]. Blood-derived Vδ1 T-cells were found to express NKp30 following PHA and IL-2 treatment [113]. NKp30 and NKp44 blockade on Vδ1 T-cells decreased killing of lymphocytic leukaemia cells, whereas Vδ1 TCR blockade did not affect this cytotoxic response [113]. Further, blockade of NKp30 reduced the cytotoxic response from PHA and IL-7 expanded Vδ1 T-cells against CRC cancer cell lines [95]. When upregulated by IL-15 and IL-2, NKp46 was observed to facilitate Vδ1 tumour cytotoxicity [39].

Alongside activatory NCRs, $\gamma\delta$ T-cells also express killer inhibitory receptors. NKG2A expression, an NK receptor that inhibits NK-cell mediated killing in the 'missing self hypothesis' via binding to MHC-1 molecule HLA-E [114], was observed on healthy colon and peripheral $\gamma\delta$ T-cells [39]. NKG2A can couple with CD94 to interact with HLA-E and CD94 was minimally expressed on expanded Vδ1 T-cells [50]. This suggests that NKG2A and CD94 may dampen $\gamma\delta$ effector responses and that activated $\gamma\delta$ T-cells may downregulate this receptor to prolong cytotoxic capability. Interestingly, and similar to PD-1 in Vδ1 T-cells, expression of NKG2A

[2] Whilst the role of NKG2D ligands binding the $\gamma\delta$ TCR has been documented by a range of labs, this specific binding has not been reproduced since 2011.

indicated greater effector capabilities in Vδ2 T-cells [115]. This suggests that $\gamma\delta$ T-cells may express both NK- and T-cell regulatory receptors to regulate their effector ability.

Overall, $\gamma\delta$ TCR stimulation is essential for the differentiation and activation of $\gamma\delta$ T cells, while NCRs can further enhance or even initiate this process by recognizing tumour cells and driving a cytotoxic response [109].

1.2.2 $\gamma\delta$ Cytotoxic Responses

$\gamma\delta$ T-cells have been termed as a bridge between the innate and adaptive immune system, and their effector responses further fit this characterisation: $\gamma\delta$ T-cell cytotoxicity exhibit similarities to both NK cells and CD8 T-cells. Both NK-cells and CD8 T-cells utilise degranulation- and TNFR-mediated cytotoxic mechanisms [116, 117] following formation of an immunological synapse (IS) between itself and the target cell (Figure 1.7). In place of the TCR (Figure 1.7), NK-cells exploit NKRs within the IS formed with its target cell, which will elicit a cytotoxic response if the activatory signals outweigh the inhibitory [118].

Degranulation involves reorganisation of the actin cytoskeleton upon effector-cell activation, resulting in the release of granzyme and perforin containing granules directed towards the target cell. Granzymes and perforin will be involved within a lytic IS between cytotoxic T- or NK-cell and its target, contrastingly to a stimulatory IS between a T-cell with an APC (Figure 1.7). Perforin creates pores in the target cell membrane, allowing granzymes to enter the cell and induce apoptosis. Granzyme release correlates to proinflammatory Th1 cytokine release including IL-1β, TNF-α, GM-CSF and INF-γ [120, 117]. INF-γ can play a significant role in promoting an anti-tumour environment as it can trigger upregulation of death receptors expressed on target cells to facilitate TNFR-mediated cell death, as well as promote the presentation of neoantigens in the TME, or even directly inhibit cell proliferation and angiogenesis [121, 122]. Proinflammatory cytokines can also help recruit T-cells and innate immune cells to aid this anti-tumour response [117].

TNFR-mediated cell death involves a variety of molecules and pathways. TNFR family receptors, such as TNFR, Fas, and TRAIL-R, are expressed on the surface of target cells, while their corresponding ligands—TNF, FasL, and TRAIL—are either displayed on the cell surface or secreted by NK cells. Ligand binding to these receptors recruits FADD (Fas-associated death domain), which in turn activates caspase-8, ultimately inducing apoptosis in the target cell [117].

Despite these similarities, key differences exist between NK-cell and T-cell cytotoxicity. As discussed earlier, NK-cells utilize a diverse array of receptors to recognize stressed self-cells

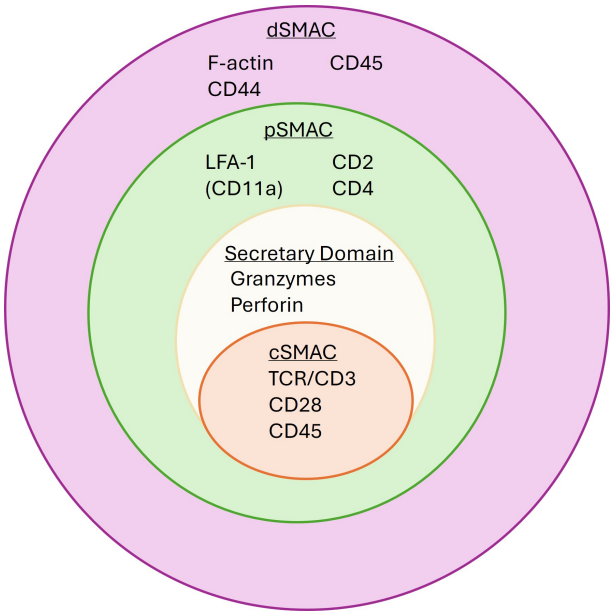


Figure 1.7: ***Structure of a T-cell Immunological Synapse***

The immunological synapse (IS) is a highly organized structure formed at the interface between an immune cell and its interacting cell, characterized by the spatiotemporal arrangement of proteins critical for cell-cell communication and signalling. Many proteins have been identified within the immunological synapse and vary depending on the types of cells involved. Proteins within the IS are categorised into three distinct supramolecular activation clusters (SMAC), distal (dSMAC), peripheral (pSMAC) and central (cSMAC). Typical proteins involved within the IS that T-cells will form with its target cell or APC are portrayed in the image. An IS formed between a cytotoxic CD8$^+$ T-cell and target cell can be termed a lytic IS due to the presence of granzymes and perforin within the secretary domain, whereas a stimulatory IS between T-cell and APC for instance would not contain these cytotoxic proteins. Adapted from [119].

through a broad range of ligands. In contrast, any NK-like receptors expressed on CD8$^+$ T cells primarily serve as co-stimulatory signals to enhance initial TCR activation [103]. NK cells form an immunological synapse with target cells through receptor engagement, initiating ligand-specific responses. Activating receptors on NK cells are linked to adaptor molecules such as DAP10 and DAP12, which associate with immunoreceptor tyrosine-based activation motifs (ITAMs). Ligand binding to these receptors triggers tyrosine kinase-mediated phosphorylation of ITAMs, activating downstream signalling pathways that drive NK cell-mediated target cell death [117].

In addition, NK cells employ antibody-dependent cellular cytotoxicity (ADCC), a mechanism where antibodies bound to target cells or pathogens engage NK cells via the Fc receptor, FcγRIIIA (CD16). This interaction triggers the lysis of the target cell [117].

$\gamma\delta$ T cells exhibit cytotoxicity through both degranulation [113, 39, 100] and TNFR mech-

anisms [51, 123, 124, 95], mediated by both their TCR and NK-cell receptors. These cytotoxic responses can still vary among different $\gamma\delta$ T-cell subsets. For example, blood-derived Vδ1 cells effectively killed neuroblastoma cells and upregulated Th1 cytokines, whereas Vδ2 cells promoted pro-tumourigenic factors such as ANG, VEGF, EGF, and IGF-I [125]. Additionally, while $\gamma\delta$ T cells have demonstrated ADCC via CD16 expression, this activity is predominantly associated with Vδ2 cells rather than Vδ1 cells [126, 99]. The differing responses between $\gamma\delta$ T-cell subsets highlights the importance of selectively stimulating specific subtypes to achieve a controlled and targeted immune response.

1.3 Vδ1 $\gamma\delta$ T-cells

The presence of Vδ1 $\gamma\delta$ T-cells in various cancers is associated with more clinically favourable outcomes [38, 39, 40, 41, 45, 127, 128]. Although Vδ2 cells are the predominant $\gamma\delta$ T-cell subset in circulation, Vδ1 T-cells exhibit greater longevity in the bloodstream and appear less susceptible to activation-induced cell death [129]. Notably, Vδ1 T-cells are thought to exhibit adaptive properties due to their diverse TCR-specific antigen repertoire, expansion of individual clonotypes in response to immunological stimuli, and differentiation into long-lived effectors [54, 130, 131]. Specifically, a memory-like capacity of Vδ1 T-cells has been demonstrated by Vδ1 expansion and resulting accelerated resolution of infection following repeated CMV exposure [131]. These cells are believed to persist in the body for many years, resembling patterns observed in other animals, where distinct developmental waves of $\gamma\delta$ T-cells emerge during pre- and postnatal stages in humans [132]. While the exact duration of their persistence remains uncertain, anti-tumour Vδ1 T-cells have been detected for between months to years post bone marrow-transplantion in leukemia survivors [128, 133] as well as following allogeneic cell therapy infusions enriched for Vδ1 T-cells [134]. Compared to Vδ2 T-cells, Vδ1 T-cells not only exhibit broader TCR ligand recognition (as discussed above) but also reduced susceptibility to the immunosuppressive TME. For example, overexpression of indoleamine-2,3-dioxygenase (IDO) inhibits Vγ9Vδ2 cytotoxic activity against pancreatic adenocarcinoma cells [135], and overexpression of galectins in some tumours suppress Vγ9Vδ2 proliferation [136]. Additionally, cyclooxygenase-2 (COX-2) upregulation in tumour cells and mesenchymal stem cells (MSCs), induced by inflammatory cytokines released by effector cells, indirectly suppresses Vδ2 activity by recruiting Tregs to the TME [137]. Whilst prostaglandins like PGE2 derived from COX-2 activity can inhibit Vδ1 T-cell cytotoxic activity and cytokine release, Vδ2 T-cells are more greatly impacted [138].

Whilst Vδ1 T-cells demonstrate substantial anti-tumoural properties, these cells can also

display regulatory properties. *In vitro* treatment of TGF-β upregulated Fox-P3 expression on peripheral-Vδ1 T-cells which were capable of inhibiting naive CD4$^+$ T-cell [139] and producing further TGF-β [140]. TGF-β is often prominent within the TME [141] as it can facilitate an immunosuppressive environment through encouraging CD4$^+$ Treg selection. High levels of TGF-β within CRC patient TMEs also exhibited greater levels of regulatory Vδ1 T-cells [142]. Despite this, the role of TGF-β is still not fully understood as whilst Vδ2 T-cells have demonstrated similar regulatory roles [143], they have also exhibited enhanced anti-tumoural properties in response to TGF-β treatment, given the right contexts [144]. As the effects of TGF-β on Vδ1 T-cells may vary across different TMEs, coupled with the growing body of research emphasizing the beneficial role of Vδ1 T-cells in various cancers, these cells remain promising targets for onco-immunotherapy and warrant further investigation.

1.3.1 Vδ1 characterisation

Canonical $\alpha\beta$ T-cells are typically classified into four main functional states (Figure 1.8), and these classifications have been extended to Vδ1 T-cells [145, 54, 45]. Vδ1 T-cells can be categorised by their CD27 expression levels. Less cytotoxic, or naive Vδ1 T-cells exhibit higher CD27 expression compared to their more effector-like counterparts [54]. CD27lo/- Vδ1 T-cells are considered more cytotoxic, characterised by elevated levels of granzymes and perforin [54], higher expression of CD69 [40] and reportedly greater IFN-γ production [45]. This CD27-based classification contrasts murine $\gamma\delta$ T-cells, where CD27high cells are more cytotoxic, and CD27lo/- are associated with tumour-promoting IL-17A production [146]. These distinctions, alongside the little to no phylogenetic homology between murine and human γ chains, highlight the fundamental differences between human and murine Vδ1 T-cells suggesting that murine $\gamma\delta$1 T-cells may not a suitable model for studying human Vδ1 T-cell biology.

With $\alpha\beta$ T-cells, downregulation of CD45RA is indicative of a memory phenotype (Figure 1.8), however, within the Vδ1 T-cell compartment, CD45RA expression may only hold significance primarily in inflammatory contexts such as cancer as opposed to in healthy contexts. In healthy individuals, TCR focussing is associated with the downregulation of CD27 while retaining CD45RA expression [54], suggesting that CD45RA may not play a role in healthy Vδ1 memory cells. However, in NSCLC patients, an increased prevalence of CD27-CD45RA- Vδ1 T-cells was associated with better prognoses [45], indicating that CD27-CD45RA- Vδ1 phenotype may represent Vδ1 ***effector*** memory in the context of cancer.

While the majority of studies highlight the anti-tumoural capabilities of Vδ1 T-cells, a subset

of human Vδ1 T-cells has demonstrated immunosuppressive roles in cancer, however this was only observed in human breast cancer [48, 147, 148, 149]. Furthermore, IL-17A production and negative correlations associated with human Vδ1 T-cell presence have been reported during HIV infection [150, 151]. Despite this, the addition of TLR ligands has been shown to reverse the immunosuppressive effect observed in breast cancer [48, 149]. Overall, these findings demonstrate the potential of Vδ1 T-cell targeted therapies to benefit a wide range of cancers, though certain tumours may require additional stimulation to fully harness their anti-tumour capabilities [67].

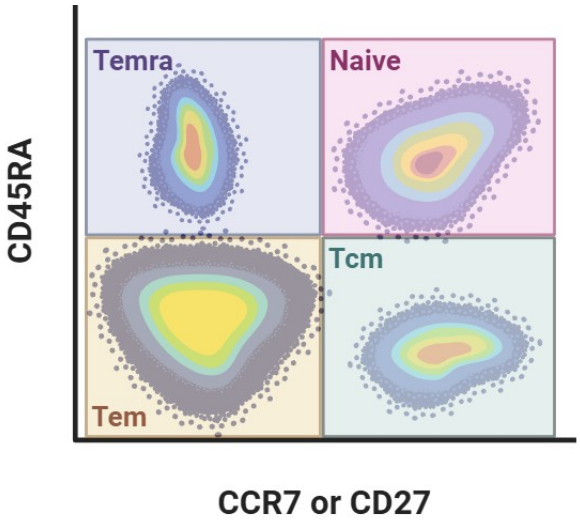


Figure 1.8: ***T-cell characterisation.***
T-cell characterisation by CD27 or CCR7 and CD45RA expression, represented by a flow cytometric plot. $CD45RA^{+}CD27^{+}$ represent naive T-cells, $CD45RA^{-}CD27^{+}$ represent central memory T-cells (Tcm), $CD45RA^{-}CD27^{-}$ represent effector memory T-cells (Tem), $CD45RA^{+}CD27^{-}$ represent terminally differentiated effector memory T-cells (Temra). Adapted from [145]. [This image was created using BioRender]

1.3.2 Blood vs tissue Vδ1 T-cells

Despite the majority of Vδ1 T-cells residing in tissue, the small Vδ1 T-cell subset in circulation—where Vδ2 T-cells are the predominant $\gamma\delta$ T-cell type within the periphery—has demonstrated potential in controlling cancer progression. Interestingly, research indicates key differences in their phenotypes and mechanisms of recognition. Tissue-resident Vδ1 T-cells typically express the tissue-resident memory marker CD103, which may also correlate with greater anti-tumour properties in lung cancer [45]. Circulating-Vδ1 T-cells upregulate NCRs, in particular NKp30 and NKp44, in response to IL-2 and TCR-stimulation [109]; whereas intraepithelial Vδ1 T-cells, isolated from healthy tissue of CRC patients, displayed greater NKp46 expression with little to no NKp30 and NK44 expression [39]. Furthermore, tissue infiltrating Vδ1 T-cells released more INF-γ than peripheral-blood Vδ1 T-cells when cultured with ovarian tumour cells

[56]. This may suggest that solid cancer cells are more susceptible to cytotoxic responses from tissue-resident Vδ1 T-cells over peripheral blood Vδ1 T-cells. Despite these findings, circulating Vδ1 T-cells express high levels of chemokine receptors, in particular CCR4 and CXCR5 [95], indicating that circulating-Vδ1 may have chemokine-mediated infiltration capabilities where these Vδ1 T-cells may undergo infiltration-dependent phenotypic changes resulting in the cytotoxic response observed from tissue-infiltrated Vδ1 T-cells. This infiltration capability is supported by the higher levels of cytotoxic Vδ1 T-cells in circulation observed in CRC patients with better prognoses than patients with lower Vδ1 numbers [40]. Finally, ADCC, the cytotoxic mechanism used by NK-cells mediated by the Fc receptor CD16, has been demonstrated by some $\gamma\delta$ T-cells. CD16 expression has however only been reported on blood-derived Vδ1 T-cells, suggesting ADCC-mediated killing may not be a tissue-resident Vδ1 cytotoxicity mechanism [126, 152].

The site of Vδ1 tissue residency can also implicate its function. Vδ1 T-cells within the gut display unique capabilites where their TCRs—mainly consisting of Vδ1 pairing with Vγ4 chains—can recognise organ-specific BTNL proteins [153]. Furthermore, as mentioned above, only breast-resident Vδ1 T-cells have demonstrated IL-17A production in a cancer context and thus can display a distinct phenotype and role within the TME.

1.4 Vδ1 T-cells as an onco-therapeutic target

Vδ1 T-cells were first identified in the late 1980s [154], and their therapeutic potential has only recently gained attention. The Silva-Santos lab has developed DOT (Delta One T-cell) cells, a cytokine-expanded allogeneic Vδ1-based therapy, for use as treatment for AML [155] as well as a CD123 CAR T-cell approach [156]. Additionally, these DOT cells have demonstrated cytotoxicity against CLL [50]. Other gene-engineered CAR-T therapies derived from expanded Vδ1 T-cells have entered clinical trials, such as a therapy targeting relapsed/refractory B-cell Non-Hodgkin Lymphoma (Clinical trial ID: NCT04735471). While both treatments have shown promise in leukaemic indications, they rely on cell-based strategies which pose logistical challenges including high costs, labour-intensive production and difficulties in the transport and storing of efficacious products [157]. Biologics, such as Vδ1-directed engagers, offer a potential alternative. These could not only provide deeper insights into the therapeutic benefits of Vδ1-targeted approaches, but also serve as a more cost-effective and accessible strategy, addressing the manufacturability challenges associated with cell-based therapies.

The success of therapeutic engagers has already been demonstrated in Vδ2-targeted approaches. Companies such as ImCheck Therapeutics and Lava Therapeutics have developed

strategies that effectively activate Vδ2 T-cells *in situ* for the treatment of both solid and haematological cancers [158]. Imcheck's approach focuses on enhancing the availability of activated Vδ2 ligands in the system, whereas Lava's strategy directly stimulates Vδ2 T-cells through their TCR.

Lava's LAVA-1207 bispecific antibody not only activates Vδ2 T-cells directly, but also directs them to PSMA expressing prostate cancer cells [159]. This bispecific approach provides a dual advantage: it enhances the specificity of Vδ2 T-cell responses and artificially increases $\gamma\delta$ T-cell infiltration within the TME. Building on this success, similar bispecific strategies could be explored for targeting Vδ1 T-cells, offering new avenues for therapeutic development.

1.4.1 Bispecific Antibodies for Vδ1-directed therapy

Therapeutic antibodies were initially developed on the immunoglobulin G (IgG) antibodies produced *in situ* by human plasma B-cells (Figure 1.9), with engineered variable regions designed to bind a specific antigen, such as PD-1 and CTLA-4. This monospecific format of therapeutic antibody is advantageous when the desired response involves the interaction with a single protein. For example, rituximab targets the B-cell-restricted protein CD20, facilitating antibody dependent cellular cytotoxicity (ADCC) specifically against CD20-expressing cells, ensuring that ADCC and other cytotoxic mechanisms would be directed toward cancerous B-cells [160].

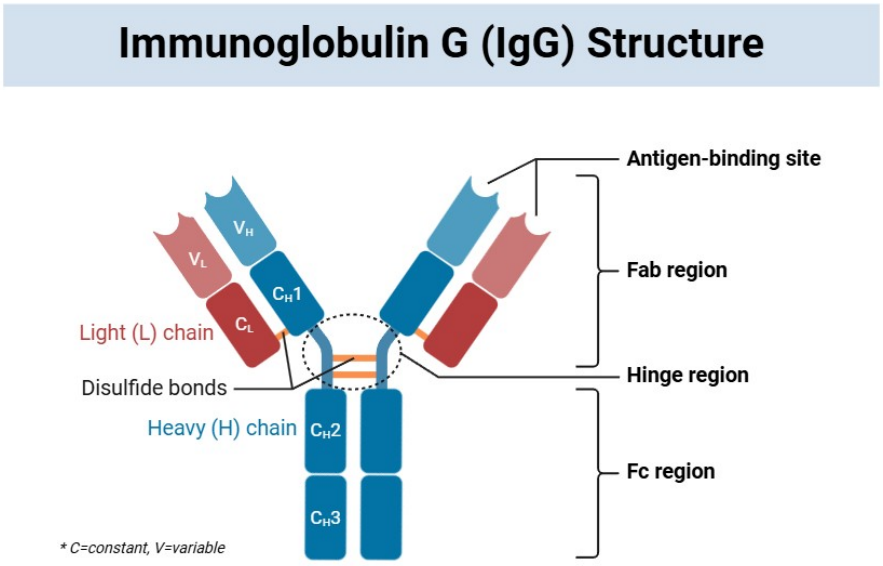


Figure 1.9: ***IgG Antibody Structure.***
Structure of an IgG antibody. V, variable region; C, constant region; H, heavy chain; L, light chain. [This image was created using BioRender]

Bispecific antibodies, or engagers, are engineered to interact with the immune system while utilising the cancer-specific approach of therapeutic antibodies. These bispecific molecules are

engineered to bind two distinct proteins through their two variable regions, which differ in specificity. The format of bispecific antibodies significantly influences their function, which led to the development of various designs tailored to specific therapeutic effects (Figure 1.10). Some formats have even modified the Fc receptor-binding region to either enhance or inhibit ADCC, depending on the intended outcome.

Blinatumomab, the first bispecific T-cell engager (BiTE), exemplifies this approach by linking two single-chain variable fragments (scFv). Each scFv targets a distinct antigen—CD3 on T-cells and CD19 on cancer cells. A flexible linker between the scFv regions acts like a hinge, similar to the design of monoclonal antibodies, enabling simultaneous binding. As discussed earlier, CD3-engaging antibodies activate T-cells; in this case, the additional CD19-binding moiety directs activated T-cells toward CD19-expressing cancer cells, facilitating a targeted immune response [161].

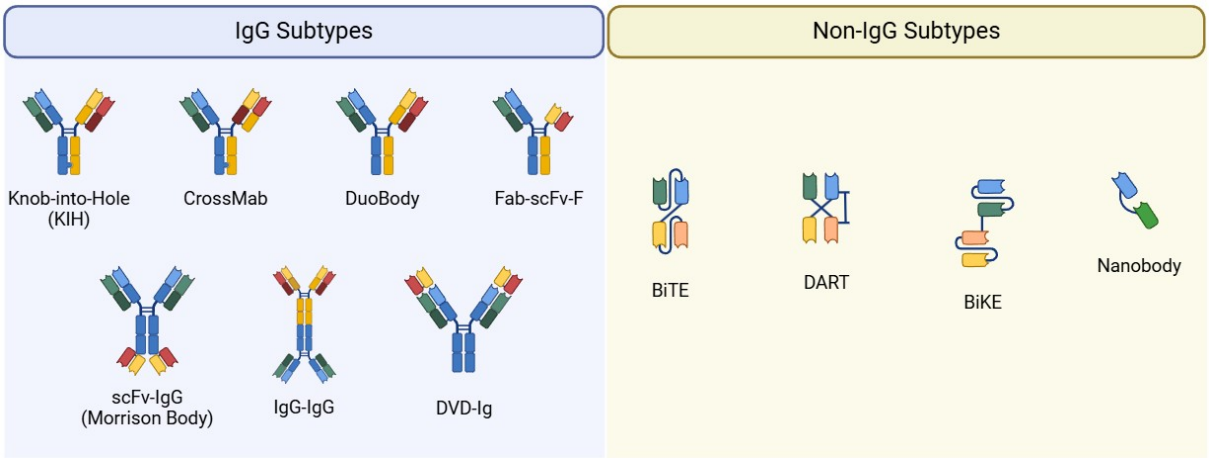


Figure 1.10: ***Bispecific Format Examples.***
A range of bispecific formats have been developed which can affect their resulting biological function. Many bispecific antibodies are based on the classical IgG antibody format, and alter the position, size or orientation of the different binding moieties. Non-IgG subtypes remove the constant regions of the typical IgG, and link the two variable regions together, often with a flexible glycine-serine amino acid linker sequence. Adapted from [162]. [This image was created using BioRender]

In 2022, Takeda Pharmaceutical Company acquired Adaptate Biotherapeutics and Gamma Delta Biotherapeutics to advance the development of the first therapeutic Vδ1 engagers (Patent ID PCT/GB2020/051959). Following the success of CD3 engagers, there was growing interest in engineering these molecules as bispecific antibodies (Patent ID PCT/IB2021/057509). However, the novel nature of Vδ1-directed engagers highlighted a significant gap in the literature regarding their effects on Vδ1 T-cells and a comprehensive understanding of Vδ1 T-cell activation. To address this, this thesis investigates CD19—an established cancer-associated antigen—as a proof-

of-concept target to evaluate the potential advantages that Vδ1-directed bispecific antibodies could bring to the cancer immunotherapy landscape.

1.4.2 CD19$^+$ cancers as a target for a Vδ1-directed engager

CD19 is a B-cell-restricted transmembrane glycoprotein involved in the normal development of B-cells, B-cell receptor (BCR)-mediated activation, and amplification of BCR signals during B-cell selection in the bone marrow [163].

CD19 expression is restricted to B-cells and B-cell malignancies, making it an attractive biomarker and therapeutic target. CD19 is expressed in 80% of ALL, 88% of B-cell lymphomas and 100% of B-cell leukaemias [164]. In the case of Non-Hodgkin's lymphoma (NHL) patients, low doses of blinatumomab increased lysis of CD19$^+$ B cells in the periphery as well as the bone marrow and liver [161]. Furthermore, blinatumomab achieved high complete remission rates in refractory B-precursor acute lymphoblastic leukaemia patients, however, 83% of patients experienced grade 3 or higher adverse effects, including cyokine-release syndrome (CRS) [165].

In parallel, Vδ1 T-cells have gained attention for their potential against B-cell malignancies, especially with CLL where the Vδ1 population is significantly elevated [166]. In addition to the DOT cells [50] described above, polyclonal $\gamma\delta$ cells engineered as CAR19 cells—$\gamma\delta$ T-cells that have been genetically engineered to express a chimeric antigenic receptor that binds external CD19 (Figure 1.3D)—have also been investigated. These CAR19 cells increased specific lysis of CD19$^+$ cell lines and increased tumour shrinkage against NALM-6 tumours in mice [167]. Furthermore, Vδ1 cells from B-cell Chronic lymphocytic leukaemia (B-CLL) patients showed selective recognition and activation against autologous B-CLL PBMCs but not healthy PBMCs, with increased proliferation and cytokine production, including IFN-γ and TNF-α [127]. This cytotoxicity correlated with ULBP3 expression on leukaemic B cells, and blocking of this NKG2D ligand reduced the cytotoxic response. Interestingly, upregulation of ULBP3 with trans-retinoic acid treatment maintained Vδ1 activity, suggesting potential therapeutic strategies for sustaining responses [127].

The feasibility of bridging Vδ1 T-cells to CD19$^+$ targets was demonstrated using an engager-like biologic where NKG2D ligands were fused to an anti-CD20 scFv [168]. These ligands enabled Vδ1-mediated killing of Raji cells, a CD19$^+$ leukaemia cell line, whereas NKG2D ligands alone were insufficient, indicating the necessity of bridging for stable immunological synapse formation. This highlights the promise of Vδ1-directed engagers for CD19$^+$ malignancies.

Building on this, the established CD19-binding moiety from Blinatumomab could be adapted to a Vδ1 antibody to form a bispecific engager. This would allow for the exploration of Vδ1

T-cell responses against $CD19^+$ malignancies, opening new avenues for cancer immunotherapy.

Add how CD19 binding with blinatumomab and other CD19 antibodies affects B-cells - at least CD19 ligands/CD19 signalling.

1.5 Summary

Cancer is a multifaceted disease that requires the development of many treatment options that can accommodate a cancer's inherent heterogeneity. Current cancer therapies are still not able to maintain consistent disease-free survival rates as tumour evasion and immunosuppression remain causes for relapse. Even in therapies that demonstrate success, treatment adverse effects can severely affect the patient's quality of life. Recent research of Vδ1 $\gamma\delta$ T-cells highlight a promising new approach to the current pitfalls in cancer immunotherapies. Their advantages stem from their ability to function in an MHC-independent manner and their ability to recognise a broad range of stress-related self-antigens which reduces their susceptibility to tumour immune evasion. Furthermore, Vδ1 $\gamma\delta$ T-cells have shown promise in recognizing and eliminating cancer stem cells as well as being able to discriminate between healthy and cancerous cells which facilitates the total eradication of the cancer whilst minimizing the risk of adverse damage to healthy tissue. The research presented in this thesis aims to support the development of Takeda's Vδ1 engagers by generating a CD19 targeting Vδ1 engager as proof-of-concept for the treatment of CD19 haematological malignancies with a Vδ1-modulating biologic.

Chapter 2

Hypothesis and Aims

2.1 Hypothesis

Vδ1 T-cells play a crucial role in the eradication of stressed and cancerous cells within the body and have already demonstrated anti-tumour efficacy in onco-immunotherapeutic cell-based therapies. Despite this, the need for cheaper, less labour-intensive drug generation and administration remains, making antibody-based treatments a desirable alternative to expedite the development of Vδ1-targeted therapies. Accordingly, this study will explore the hypothesis that Vδ1 engagers can target Vδ1 $\gamma\delta$ T-cells to improve the overall immune response against haematological cancers by enhancing the cancer-directed Vδ1 $\gamma\delta$ T-cell cytotoxic responses through the involvement of co-receptors.

2.2 Aims

I will investigate my hypothesis in the following aims:

1. To design and validate a Vδ1 engager that can enhance the effector response against haematological cancer cells using CD19 as a target.

2. To identify co-receptors that enable the Vδ1 cytotoxic response to be directed at malignant over healthy cells.

3. To investigate the mechanisms of how these co-receptors affect the Vδ1 response and how Vδ1 engagers affect Vδ1 co-receptor function.

Chapter 3

Methods

3.1 Antibody Design

Variable light (V_L) and heavy chain (V_H) sequences (table 3.1) from a proprietary anti-Vδ1 sequence (with a binding epitope of the variable delta 1 (Vδ1) chain as described in patents PCT/GB2020/051959 and PCT/IB2021/057509) and a commercial CD3/CD19 engager (BPS Bioscience) were implemented to form Vδ1/CD19 engagers in various formats: Bispecific T-cell engager (BiTE), Knob-into-Hole (KIH) and Morisson Body (MB) (Fig 3.1 and tables 3.2 - 3.4). Each V_L and V_H was also substituted for V_L and V_H sequences from an anti-RSV sequence to create a control IgG arm. For ensuing assays using a CD3/CD19 engager, the scFv-scFv bispecific antibody against human CD19 and human CD3 from Invivogen was used.

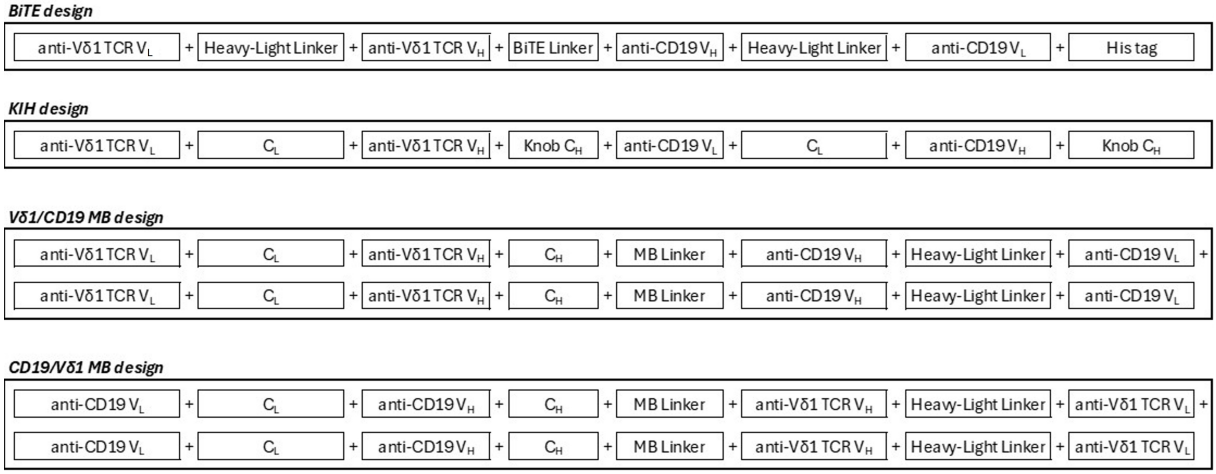


Figure 3.1: ***Design of each bispecific antibody format.***

V_L refers to variable light chain; V_H refers to variable heavy chain;C_L refers to constant light chain;C_H refers to constant heavy chain.

Table 3.1: Variable chain sequences used in Figure 3.1

Variable sequences	**V_H sequence**	**V_L sequence**
anti-Vδ1 TCR	*Proprietary to Takeda*	*Proprietary to Takeda*
anti-CD19	Q V Q L Q Q S G A E L V R P G S S V K I S C K A S G Y A F S S Y W M N W V K Q R P G Q G L E W I G Q I W P G D G D T N Y N G K F K G K A T L T A D E S S S T A Y M Q L S S L A S E D S A V Y F C A R R E T T T V G R Y Y Y A M D Y W G Q G T T V T V S S	D I Q L T Q S P A S L A V S L G Q R A T I S C K A S Q S V D Y D G D S Y L N W Y Q Q I P G Q P P K L L I Y D A S N L V S G I P P R F S G S G S G T D F T L N I H P V E K V D A A T Y H C Q Q S T E D P W T F G G G T K L E I K
IgG control (anti-RSV)	Q V T L R E S G P A L V K P T Q T L T L T C T F S G F S L S T A G M S V G W I R Q P P G K A L E W L A D I W W D D K K H Y N P S L K D R L T I S K D T S K N Q V V L K V T N M D P A D T A T Y Y C A R D M I F N F Y F D V W G Q G T T V T V S S	D I Q M T Q S P S T L S A S V G D R V T I T C S A S S R V G Y M H W Y Q Q K P G K A P K L L I Y D T S K L A S G V P S R F S G S G S G T E F T L T I S S L Q P D D F A T Y Y C F Q G S G Y P F T F G G G T K V E I K
anti-CD3	Q V Q L Q Q S G A E L A R P G A S V K M S C K T S G Y T F T R Y T M H W V K Q R P G Q G L E W I G Y I N P S R G Y T N Y N Q K F K D K A T L T T D K S S S T A Y M Q L S S L T S E D S A V Y Y C A R Y Y D D H Y C L D Y W G Q G T T L T V S S	D I Q L T Q S P A I M S A S P G E K V T M T C R A S S S V S Y M N W Y Q Q K S G T S P K R W I Y D T S K V A S G V P Y R F S G S G S G T S Y S L T I S S M E A E D A A T Y Y C Q Q W S S N P L T F G A G T K L E I K

Table 3.2: BiTE-specific sequences used in Figure 3.1

BiTE-specific sequences	Sequence
Heavy-Light Linker	G G G G S G G G G S G G G G S
BiTE Linker	G G G G S
His tag	H H H H H H

Table 3.3: KIH-specific sequences used in Figure 3.1

KIH-specific sequences	Sequence
C_L	R T V A A P S V F I F P P S D E Q L K S G T A S V V C L L N N F Y P R E A K V Q W K V D N A L Q S G N S Q E S V T E Q D S K D S T Y S L S S T L T L S K A D Y E K H K V Y A C E V T H Q G L S S P V T K S F N R G E C
Knob C_H	A S T K G P S V F P L A P S S K S T S G G T A A L G C L V K D Y F P E P V T V S W N S G A L T S G V H T F P A V L Q S S G L Y S L S S V V T V P S S S L G T Q T Y I C N V N H K P S N T K V D K K V E P K S C D K T H T C P P C P A P E L A G A P S V F L F P P K P K D T L M I S R T P E V T C V V V D V S H E D P E V K F N W Y V D G V E V H N A K T K P R E E Q Y N S T Y R V V S V L T V L H Q D W L N G K E Y K C K V S N K A L P A P I E K T I S K A K G Q P R E P Q V Y T L P P C R D E L T K N Q V S L W C L V K G F Y P S D I A V E W E S N G Q P E N N Y K T T P P V L D S D G S F F L Y S K L T V D K S R W Q Q G N V F S C S V M H E A L H N H Y T Q K S L S L S P G K
Hole C_H	A S T K G P S V F P L A P S S K S T S G G T A A L G C L V K D Y F P E P V T V S W N S G A L T S G V H T F P A V L Q S S G L Y S L S S V V T V P S S S L G T Q T Y I C N V N H K P S N T K V D K K V E P K S C D K T H T C P P C P A P E L A G A P S V F L F P P K P K D T L M I S R T P E V T C V V V D V S H E D P E V K F N W Y V D G V E V H N A K T K P R E E Q Y N S T Y R V V S V L T V L H Q D W L N G K E Y K C K V S N K A L P A P I E K T I S K A K G Q P R E P Q V C T L P P S R D E L T K N Q V S L S C A V K G F Y P S D I A V E W E S N G Q P E N N Y K T T P P V L D S D G S F F L V S K L T V D K S R W Q Q G N V F S C S V M H E A L H N H Y T Q K S L S L S P G K

Table 3.4: MB-specific sequences used in Figure 3.1

MB-specific sequences	Sequence
C_L	R T V A A P S V F I F P P S D E Q L K S G T A S V V C L L N N F Y P R E A K V Q W K V D N A L Q S G N S Q E S V T E Q D S K D S T Y S L S S T L T L S K A D Y E K H K V Y A C E V T H Q G L S S P V T K S F N R G E C
C_H	A S T K G P S V F P L A P S S K S T S G G T A A L G C L V K D Y F P E P V T V S W N S G A L T S G V H T F P A V L Q S S G L Y S L S S V V T V P S S S L G T Q T Y I C N V N H K P S N T K V D K K V E P K S C D K T H T C P P C P A P E L A G A P S V F L F P P K P K D T L M I S R T P E V T C V V V D V S H E D P E V K F N W Y V D G V E V H N A K T K P R E E Q Y N S T Y R V V S V L T V L H Q D W L N G K E Y K C K V S N K A L P A P I E K T I S K A K G Q P R E P Q V Y T L P P S R D E L T K N Q V S L T C L V K G F Y P S D I A V E W E S N G Q P E N N Y K T T P P V L D S D G S F F L Y S K L T V D K S R W Q Q G N V F S C S V M H E A L H N H Y T Q K S L S L S P
MB Linker	G G G G G S G G G G S G G G G G S
Heavy-Light Linker	G G G G S G G G G S G G G G S

3.2 Antibody Production

Antibody production was outsourced to FairJourney Biologics, where antibodies were produced in an ExpiCHO-STM culture system for 14 days. Antibody titres were assessed with POROS A (20μm). KIHs and MBs were initially purified with HiTrap MabSelect Sure Protein A and BiTEs with HisTrap High performance column. A polishing step was conducted using size exclusion chromatography (pSEC) where antibodies were loaded onto HiLoad 26/600 Superdex 200pg column. TCEP reduction was performed for KIHs before further purification of KIHs and BiTEs by immobilized metal ion affinity chromatography (IMAC). All antibodies were desalted into the formulation buffer 1x PBS + 100mM L-arginine pH6.5 – 6.7 and stored at -80°C.

3.3 High Performance Liquid Chromatography (HPLC)

Antibody stability was validated using HPLC following incubation at 4°C and 37°C for 31 days. At Day 0, 1, 6, 14, 20 and 31 antibodies were prepared in HPLC buffer (50 mM sodium phosphate pH 7.0, 200 mM potassium chloride) at 0.5mg/ml (or undiluted stock if antibody concentration was less than 0.5mg/ml). 10ul of sample was injected into a BioResolve SEC mAb 200Å, 2.5µm, 4.6x300mm column at 0.2ml/min using the Waters Alliance HPLC system. The sample was measured at A280 for 30 minutes. Monomeric content was calculated using Empower's ApexTrack Integration method where all peaks up to 19 minutes were assessed and the percentage of the monomeric peak was taken.

3.4 Cell Lines

Reh (CRL-8286, ATCC), Daudi cells (CCL-213, ATCC) and THP-1 cells (TIB-202, ATCC) were cultured in RPMI-1640 (ATCC), modified to contain 2 mM L-glutamine, 10 mM HEPES, 1 mM sodium pyruvate, 4500 mg/L glucose, and 1500 mg/L sodium bicarbonate, with 10% foetal calf serum (FCS). MEC-1 cells (ACC 497, DSMZ) were culture in McCoy's 5A (Modified) medium (Gibco) containing 20% FCS. Cells were maintained in culture for upto 6 weeks following methods from ATCC and DSMZ, respectively.

3.5 Primary tissue collection

Human skin tissue samples, were commercially obtained from Tissue Solutions Ltd, whole blood and fresh leukopaks from healthy donors, and PBMCs from healthy and CLL patients were commercially obtained from Cambridge Bioscience, ensuring all samples were collected with

informed donor consent and in compliance with ethical regulations for use in accordance with consent given.

3.6 Whole Blood processing

Blood from whole blood collection was removed from its packaging and diluted 1:1 in PBS with 10% FBS. Samples were centrifuged in Ficoll-Paque (Ficoll® Paque Plus, Merck) in a volume ratio of 1:1 for 20 minutes at 300g, without brake. The interphase buffy coat containing PBMCs was collected in PBS with 10% FBS. Excess red blood cells were lysed from samples using RBC lysis buffer (ThermoFisher), following manufacturer's instructions.

3.7 Vδ1 expansion from skin

Isolation and Expansion. Skin tissue-resident Vδ1 T-cells were isolated and expanded following a protocol described previously: WO2020095058A1. In brief, skin samples that were negative for HIV I/II, HBV and HCV were biopsied and placed onto Tantalum coated reticulated vitreous carbon scaffolds (also called grids) (Ultramet, California, USA) which were cultured in G-Rex plates (Wilson Wolf) with isolation medium (AIM-V with phenol red, L-glutamine, streptomycin and gentamycin (Gibco, 0870112DK), 1% Amphotericin B (Gibco, 15290-018), 5% CTS immune serum replacement (Gibco, A25961-02) and a cytokine supplementation of IL-15, IL-2, IL-4 and IL-21) for 3 weeks with a media feed after 7 and 14 days. Cells to be expanded after the 3-week isolation procedure were removed from the cell suspension in the G-rex plates and were frozen at -80°C before the expansion protocol. Cells were then cultured in CellStack plates (Corning, 431123) with expansion medium (TexMACS Medium (Miltenyi, 130-097-196) with 5% CTS Immune Serum replacement, 1% Penicillin/Streptomycin and cytokine supplementation), for 3 weeks with a media feed after 7 and 14 days. Before freezing cells for long-term storage in liquid nitrogen, $\alpha\beta$ T-cells were depleted from the cell suspension using the CliniMACS TCR$\alpha\beta$ Kit (Miltenyi) with the MultiMACS Cell24 Separator Plus (Miltenyi). $\alpha\beta$ and Vδ1 T-cell contents were assessed using flow cytometry (Method 3.23) to validate the percentage of isolated Vδ1 cells.

Culturing. $\alpha\beta$-depleted Vδ1 cells are thawed into SKIN-R medium and cultured for 5-7 days with cytokine supplementation (described in WO2020095058A1) at Day 0 and Day 3. The cells are removed from culture after 5-7 days using Accutase® solution for *in vitro* based assays.

3.8 Vδ1 expansion from blood

Isolation and Expansion. Blood cells obtained by leukapheresis from healthy volunteers were centrifuged to collect lymphocytes then red blood cells lysed (10X RBC Lysis Buffer, Gibco). $\alpha\beta$ T-cells were depleted (CliniMACS® TCR$\alpha\beta$ Kit, Miltenyi) following manufacturer's instructions. Remaining cells were cultured in complete OpTmizer in GREX 100M (WilsonWolf) for 17 days with confidential cytokine and an anti-CD3 mAb supplementation before harvesting.

Culturing. $\alpha\beta$-depleted Vδ1 cells are thawed into complete OpTmizer (A1048501) supplemented and cultured for 1-3 days with IL-15 supplementation (concentration confidential) before using *in vitro* based assays.

3.9 Binding Assay

Freshly thawed PBMCs, expanded Vδ1 T-cells and cell lines from culture were resuspended in efluor780 solution and plated in a 96-well round bottomed plate (400,000 PBMCs/well and 35,000 cultured cells/well). Titrated engagers were added to the plated cells and incubated for 30 minutes at 4°C. Surface-bound BiTE was detected using an anti-His-PE tag secondary antibody and surface-bound KIH and MB was detected using anti-hIgG-AF647 followed by flow cytometry (Method 3.23 and table 3.8).

3.10 Cell Trace Violet (CTV) Staining

Primary cell suspensions were centrifuged at 300g for 10 minutes, and cell lines cell suspensions 400g for 5 minutes before resuspending in CTV solution (diluted 1 in 10 000 in PBS). Cells were incubated for 20 minutes at 37°C before adding double the volume cell culture media and incubating for a further 5 minutes at 37°C. Cells were centrifuged and resuspended in cell culture media in preparation for use in subsequent assays.

3.11 Primary B-cell isolation

Primary B-cells from healthy and CLL PBMCs were isolated using the Pan B cell isolation kit (130-101-638, Miltenyi) following manufacturer's instructions.

3.12 Activation and Cytotoxicity assays with expanded Vδ1 T-cells

CTV-stained cell lines, or primary B-cells were plated in a TC-treated 96-well round bottomed plate (35,000 cells/well). Expanded Vδ1 T-cells were removed from culture and washed in culture media (absent of cytokine supplementation), then added at a 1:1 ratio to the plated target cells, followed by engager treatment titrated in Vδ1 culture media (absent of cytokine supplementation). For 4-hour activation assays, anti-CD107a-PE was also added to wells at 1 in 100 at T0. Cells were cultured for 4 hours at 37°C, to detect surface Vδ1 TCR, CD107a and 41BB, and cultured for 24 hours for 37°C to detect CD25 and live target cells, using flow cytometry (Method 3.23 and table 3.9 and 3.10).

3.13 Vδ1 proliferation from PBMCs

PBMCs were thawed, stained with CTV and plated in ATCC modified RPMI with 10% FCS at 350,000 cells/well in a TC-treated 96-well round bottomed plate. Plated PBMCs were cultured with engagers titrated in media for 7 days at 37°C. At day 6, anti- Vδ1-PE was added to each well at 1 in 150 to improve the detection of Vδ1 cells following TCR stimulation. Vδ1, Vδ2, $\alpha\beta$ and NK ($CD3^{-}CD56^{+}$) cells were detected using flow cytometry (Method 3.23 and table 3.11). This assay was also conducted with the addition of a CD44 blockade antibody (MA4400, Invitrogen) added at T0.

3.14 Vδ1 cytotoxicity from PBMCs

Following the Vδ1 proliferation setup, without CTV staining PBMCs, CTV-stained isolated primary CLL B-cells (primary and MEC-1) were added at day 6 of culture and cultured for another 24 hours before detecting live target cells using flow cytometry (Method 3.23 and table 3.12).

3.15 RNA expression analysis

RNA was sequenced from cell lysates using nCounter PanCancer IO360 Panel from Nanostring following manufacturer's instructions and differential RNA expression analysis was conducted using Rosalind software. Cell lysates were collected following protocol from Nanostring (MAN-10151-07) using Buffer RLT (Qiagen®, 79216) for primary isolated B-cells and iScript (BioRad, 170-8898) for cell lines from culture.

3.16 B-cell Phenotyping

$CD19^+$ cell lines from culture and isolated primary B-cells from PBMCs were phenotyped for stress ligand expression using flow cytometry (Method 3.23 and table 3.13 - 3.18).

3.17 Vδ1 phenotyping assay

Freshly thawed PBMCs were plated in ATCC modified RPMI with 10% FCS at 350,000 cells/well in a TC-treated 96-well round bottomed plate. Plated PBMCs were cultured with 100pM engager and with or without MEC-1 cells in media for 14 days at 37°C. 100pM engager and MEC-1 cells were added at day 0 and added again after day 7. Cells were removed from culture at day 0, 1, 3, 7, 10 and 14 to stain for CD3, Vδ1, CD27, CD45RA, NKG2D, DNAM-1, CD44, LY-9, CD96, 2B4, NKp30, NKp44, NKp46, Fas-L, CD11a, CD2, ICAM-3, NKG2A, CD94, CD5, PD-1, CTLA-4, CD28, ICOS, CD69, 41BB, CD25 and GZMB using flow cytometry (Method 3.23). 24 hours prior to removal from culture, anti-Vδ1-PE was added to each well at 1 in 150 to improve the detection of Vδ1 cells following TCR stimulation. Intracellular staining of granzyme B was conducted using the FoxP3 staining kit (00-5523-00, Invitrogen) following manufacturer's instructions. (see tables 3.19 - 3.24).

3.18 Cytokine Analysis

Supernatants from cytotoxicity assays were collected and assessed for cytokine presence using the MSD U-plex assay (K151AEM-1, MesoScaleDiscovery) following manufacturer's instructions.

3.19 Cytotoxicity Blockade

MEC-1 cells were stained with CTV, incubated with 10μg/ml blocking antibodies for MICA/B (MAB13001, Biotechne), ULBP1 (AF1380, Biotechne), ULBP3 (AF1517, Biotechne), ULBP2/5/6 (MAB1298, Biotechne), LFA-3 (AF1689, Biotechne), PVR (MAB 25301, Biotechne), Nectin-1 (AF2880, Biotechne), Nectin-2 (337424, Biotechne), CD48 (947104, Biotechne), B7-H6 (605953, Biotechne) for 45 minutes at 37°C and then washed with MEC-1 culture media. Following the Vδ1 proliferation setup, pre-incubated MEC-1 cells, alongside anti-CD107a-PEVio770, were added at day 7 of culture and cultured for 5 hours before detecting live target cells using flow cytometry (Method 3.23 and table 3.25). At day 6, anti-Vδ1-PE was added to each well at 1 in 150 to improve the detection of Vδ1 cells following TCR stimulation.

3.20 Magnetic-Activated Cell Sorting (MACS)

PBMCs were removed from culture and any adhered cells were removed from the cell culture flasks using accutase (A1110501, Thermofisher). Cells were centrifuged for 10 minutes at 300g and resuspended in MACS buffer (PBS pH 7.2, 0.5% bovine serum albumin (BSA), and 2 mM EDTA) with biotin-conjugated antibodies specific to $\alpha\beta$ TCR (130-113-537, Miltenyi), Vδ2 TCR (130-111-008, Miltenyi), CD19 (130-113-644, Miltenyi) and CD14 (130-110-517, Miltenyi) (table 3.5).

Table 3.5: MACS depletion antibody conditions

Solution	**μl per 1e^8 cells**
MACS buffer	80
anti-$\alpha\beta$ TCR-biotin	10
anti-Vδ2 TCR-biotin	2
anti-CD19-biotin	2
anti-CD14-biotin	5

Cells were incubated for 10 minutes at 4°C then washed with MACS buffer before resuspending in MACS buffer and anti-biotin microbeads (130-105-637, Miltenyi) (table 3.6).

Table 3.6: MACS depletion microbead conditions

Solution	**μl per 1e^8 cells**
MACS buffer	80
anti-biotin microbeads	20

Cells were incubated for 15 minutes at 4°C before washing in MACS buffer. Cells were resuspended in 500μl/1e8 cells MACS buffer and added to LS columns (130-042-401, Miltenyi) inserted into QuadroMACS™ Separator (Miltenyi) to deplete the microbead-labelled cells. Negative fraction was collected for Vδ1 T-cell isolation by fluorescence-activated cell sorting (FACS).

3.21 Vδ1 T-cell isolation

MACS-sorted cells were stained with anti-Vδ1 TCR-PE (1 in 100) using flow cytometry methods (Method 3.23) and resuspended in 500μl/2.5e7 cells MACS buffer. Propidium iodide (PI) (130-093-233, Miltenyi) was added just prior to sorting. Live Vδ1 T-cells (PI^- $V\delta1^+$) were selected for using BD FACSymphony™ S6 Cell Sorter and resuspended in 10% FBS ATCC RPMI to use in subsequent assays.

3.22 Plate-bound recombinant ligand activation assay

MICA (1300-MA-050, Biotechne), MICB (1599-MB-050, Biotechne), ULBP1 (1380-ul-050, Biotechne), ULBP2 (1298-ul-050, Biotechne), ULBP3 (1517-ul-050, Biotechne), LFA-3 (10068-CD-050, Biotechne), Nectin-1 (10697-N1-050, Biotechne), PVR (9174-CD-050, Biotechne), Nectin-2 (9317-N2-050, Biotechne), and B7-H6 (AVI7144-050, Biotechne) recombinant ligands were plated in PBS at 1μg/ml in TC-treated 96-well round bottomed plates at incubated at 4°C overnight. Vδ1 T-cells were proliferated from PBMCs with 0pM and 100pM Vδ1/CD19 engager for 7 days in 10% FCS ATCC modified RPMI and anti-Vδ1-PE was added at day 6 (1 in 200) to label Vδ1 T-cells for FACS. Vδ1 T-cells were then isolated (Method 3.21). Recombinant ligand solution was flicked out of the plates, and isolated Vδ1 T-cells were added to the plates (20,000 cells/well) in 10% FCS ATCC modified RPMI. Cells were cultured for 24 hours at 37°C and stained for activation markers with flow cytometry (Method 3.23 and table 3.26).

3.23 Flow Cytometry

Cells were washed using PBS and stained with efluor780 viability marker (Invitrogen, 65-0865-18) and blocked with FcR block (Miltenyi, 130-059-901) for 10 minutes at 4oC. This was followed by cell surface marker staining for 15 minutes at 4oC before washing out and resuspending in PBS. Stained cells were acquired using Miltenyi MACSQuant Analyzer 10/16 Flow Cytometer or BD LSR Fortessa™ Cell Analyzer and data was analysed using FlowLogic v8.5 or FlowJo v10. MFI was calculated as the median fluorescent intensity. Dead cells and doublets were excluded from analyses. For PBMC experiments, Vδ1 T-cells were identified as $CD3^+$ $V\delta1^+$.

3.24 Statistical Analysis

Graphical representation of data and any statistical analysis was conducted using Graphpad Prism 9. Specific statistical tests are detailed in appropriate figure legends. Statistical analysis

was conducted in assays where all conditions within the assay utilised more than three biological replicates.

3.24.1 Flow Panels

3.24.1.1 Binding assay

Table 3.7: PBMC Binding flow panel

Target	Fluorophore	Dilution	Catalogue number	Supplier
Dead cell stain	efluor780	1 in 1000	65-0865-18	Invitrogen
Vδ1 TCR	PE	1 in 100	130-120-440	Miltenyi
CD3	BV650	1 in 25	317324	Biolegend
$\alpha\beta$ TCR	APC	1 in 50	130-113-535	Miltenyi
Vδ2 TCR	Viogreen	1 in 50	130-111-016	Miltenyi
CD19	PEVio615	1 in 50	130-114-522	Miltenyi
CD20	PEVio615	1 in 50	130-111-347	Miltenyi
CD56	FITC	1 in 50	318304	Biolegend
His tag	PE	1 in 50	130-120-718	Miltenyi
IgG	AF647	1 in 200	109-607-008	JIR Labs

Table 3.8: Cell line and Isolated Vδ1 T-cell Binding flow panel

Target	Fluorophore	Dilution	Catalogue number	Supplier
Dead cell stain	efluor780	1 in 1000	65-0865-18	Invitrogen
His tag	PE	1 in 50	130-120-718	Miltenyi
IgG	AF647	1 in 200	109-607-008	JIR Labs

3.24.1.2 Activation with expanded Vδ1 T-cells assay

Table 3.9: 4hr Activation with expanded Vδ1 T-cells flow panel

Target	**Fluorophore**	**Dilution**	**Catalogue number**	**Supplier**
Dead cell stain	efluor780	1 in 1000	65-0865-18	Invitrogen
Vδ1 TCR	PEVio770	1 in 100	130-117-697	Miltenyi
Target cells	CTV	1 in 10 000	C34571	Invitrogen
CD107a	PE	1 in 100	130-111-629	Miltenyi
41BB	BV650	1 in 25	309828	Biolegend

3.24.1.3 Activation and cytotoxicity with expanded Vδ1 T-cells assay

Table 3.10: 24hr activation and cytotoxicity with expanded Vδ1 T-cells flow panel

Target	Fluorophore	Dilution	Catalogue number	Supplier
Dead cell stain	efluor780	1 in 1000	65-0865-18	Invitrogen
Vδ1 TCR	PEVio770	1 in 100	130-117-697	Miltenyi
Target cells	CTV	1 in 10 000	C34571	Invitrogen
CD25	APC	1 in 50	130-113-284	Miltenyi

3.24.1.4 Vδ1 proliferation assay

Table 3.11: Vδ1 Proliferation flow panel

Target	Fluorophore	Dilution	Catalogue number	Supplier
Dead cell stain	efluor780	1 in 1000	65-0865-18	Invitrogen
Vδ1 TCR	PE	1 in 100	130-120-440	Miltenyi
PBMCs	CTV	1 in 10 000	C34571	Invitrogen
CD3	BV650	1 in 25	317324	Biolegend
CD27	PerCPVio700	1 in 50	130-120-037	Miltenyi
$\alpha\beta$ TCR	APC	1 in 50	130-113-535	Miltenyi
Vδ2 TCR	Viogreen	1 in 50	130-111-016	Miltenyi
CD19	PEVio615	1 in 50	130-114-522	Miltenyi
CD20	PEVio615	1 in 50	130-111-347	Miltenyi
CD56	FITC	1 in 50	318304	Biolegend

3.24.1.5 PBMC Cytotoxicity assay

Table 3.12: PBMC cytotoxicity flow panel

Target	Fluorophore	Dilution	Catalogue number	Supplier
Dead cell stain	efluor780	1 in 1000	65-0865-18	Invitrogen
Vδ1 TCR	PE	1 in 100	130-120-440	Miltenyi
Target cells	CTV	1 in 10 000	C34571	Invitrogen
CD3	BV650	1 in 25	317324	Biolegend

3.24.1.6 B-cell Phenotyping

Table 3.13: B-cell phenotyping flow panel 1

Target	Fluorophore	Dilution	Catalogue number	Supplier
Dead cell stain	efluor780	1 in 1000	65-0865-18	Invitrogen
Nectin-2	APC	1 in 50	130-122-771	Miltenyi
MICA/B	PerCPVio700	1 in 50	130-118-834	Miltenyi
TNFR1	PEVio770	1 in 50	130-127-484	Miltenyi
TRAILR2	PE	1 in 25	307406	Biolegend
TNFR2	FITC	1 in 50	130-119-777	Miltenyi
LFA-3	V423	1 in 50	130-128-544	Miltenyi

Table 3.14: B-cell phenotyping flow panel 2

Target	**Fluorophore**	**Dilution**	**Catalogue number**	**Supplier**
Dead cell stain	efluor780	1 in 1000	65-0865-18	Invitrogen
Nectin-1	APC	1 in 50	130-123-217	Miltenyi
CD86	VB515	1 in 50	130-116-165	Miltenyi
ICOSLG	PEVio770	1 in 50	130-116-805	Miltenyi
CD44	PE	1 in 50	130-113-342	Miltenyi
ULBP2/5/6	AF405	1 in 25	FAB1298V	Biotechne

Table 3.15: B-cell phenotyping flow panel 3

Target	**Fluorophore**	**Dilution**	**Catalogue number**	**Supplier**
Dead cell stain	efluor780	1 in 1000	65-0865-18	Invitrogen
PD-L1	V423	1 in 50	130-127-200	Miltenyi
LY-9	APC	1 in 50	130-116-004	Miltenyi
CD48	PEVio770	1 in 50	130-106-469	Miltenyi
ULBP1	PerCP	1 in 25	FAB1380C	Biotechne

Table 3.16: B-cell phenotyping flow panel 4

Target	Fluorophore	Dilution	Catalogue number	Supplier
Dead cell stain	efluor780	1 in 1000	65-0865-18	Invitrogen
PVR	VB515	1 in 50	130-119-003	Miltenyi
CD19	PerCPVio700	1 in 50	130-113-648	Miltenyi
ULBP3	PE	1 in 25	FAB1517P	Biotechne
CD5	PEVio615	1 in 25	130-110-996	Miltenyi

Table 3.17: B-cell phenotyping flow panel 5

Target	Fluorophore	Dilution	Catalogue number	Supplier
Dead cell stain	efluor780	1 in 1000	65-0865-18	Invitrogen
Fas	PE	1 in 50	130-113-004	Miltenyi
CD11a	PerCPVio700	1 in 50	130-121-048	Miltenyi

Table 3.18: B-cell phenotyping flow panel 6

Target	Fluorophore	Dilution	Catalogue number	Supplier
Dead cell stain	efluor780	1 in 1000	65-0865-18	Invitrogen
CD80	VBR720	1 in 50	130-128-249	Miltenyi
HLA-E	PEVio615	1 in 50	130-117-551	Miltenyi
ICAM-3	Viogreen	1 in 50	130-115-210	Miltenyi

3.24.1.7 Vδ1 Phenotyping

Table 3.19: Vδ1 phenotyping flow panel 1

Target	Fluorophore	Dilution	Catalogue number	Supplier
Dead cell stain	efluor780	1 in 1000	65-0865-18	Invitrogen
Vδ1 TCR	PE	1 in 100	130-120-440	Miltenyi
CD3	BV650	1 in 25	317324	Biolegend
CD27	PerCPVio700	1 in 50	130-120-037	Miltenyi
CD45RA	BV570	1 in 25	304132	Biolegend
DNAM-1	Vioblue	1 in 50	130-123-522	Miltenyi
ICOS	Viogreen	1 in 20	130-100-739	Miltenyi
2B4	FITC	1 in 50	130-099-039	Miltenyi
NKG2D	PEVio770	1 in 50	130-111-646	Miltenyi
CD96	APC	1 in 50	130-118-337	Miltenyi

Table 3.20: Vδ1 phenotyping flow panel 2

Target	**Fluorophore**	**Dilution**	**Catalogue number**	**Supplier**
Dead cell stain	efluor780	1 in 1000	65-0865-18	Invitrogen
Vδ1 TCR	PE	1 in 100	130-120-440	Miltenyi
CD3	BV421	1 in 25	317344	Biolegend
CD27	BV605	1 in 25	302830	Biolegend
CD45RA	BV510	1 in 25	304142	Biolegend
PD-1	VB515	1 in 50	130-120-386	Miltenyi
CD2	PE-Cy5	1 in 25	300210	Biolegend
CD69	PEVio770	1 in 50	130-112-612	Miltenyi
Ly-9	APC	1 in 50	130-116-004	Miltenyi

Table 3.21: Vδ1 phenotyping flow panel 3

Target	**Fluorophore**	**Dilution**	**Catalogue number**	**Supplier**
Dead cell stain	efluor780	1 in 1000	65-0865-18	Invitrogen
Vδ1 TCR	PE	1 in 100	130-120-440	Miltenyi
CD3	BV421	1 in 25	317344	Biolegend
CD27	BV605	1 in 25	302830	Biolegend
CD45RA	BV510	1 in 25	304142	Biolegend
Fas-L	VB515	1 in 100	130-118-092	Miltenyi
CD11a	PerCPVio700	1 in 50	130-121-048	Miltenyi
CTLA-4	PEVio770	1 in 50	130-130-455	Miltenyi
CD94	APC	1 in 50	130-098-976	Miltenyi

Table 3.22: Vδ1 phenotyping flow panel 4

Target	**Fluorophore**	**Dilution**	**Catalogue number**	**Supplier**
Dead cell stain	efluor780	1 in 1000	65-0865-18	Invitrogen
Vδ1 TCR	PE	1 in 100	130-120-440	Miltenyi
CD3	BV650	1 in 25	317324	Biolegend
CD27	PEVio770	1 in 50	130-113-641	Miltenyi
CD45RA	BV570	1 in 25	304132	Biolegend
CD28	V423	1 in 50	130-127-175	Miltenyi
ICAM-3	Viogreen	1 in 75	130-115-210	Miltenyi
CD44	FITC	1 in 25	338804	Biolegend
CD5	PEVio615	1 in 25	130-110-996	Miltenyi
NKG2A	AF700	1 in 25	130-128-577	Miltenyi

Table 3.23: Vδ1 phenotyping flow panel 5

Target	**Fluorophore**	**Dilution**	**Catalogue number**	**Supplier**
Dead cell stain	efluor780	1 in 1000	65-0865-18	Invitrogen
Vδ1 TCR	PE	1 in 100	130-120-440	Miltenyi
CD3	BV421	1 in 25	317344	Biolegend
CD27	PerCPVio700	1 in 50	130-120-037	Miltenyi
CD45RA	BV570	1 in 25	304132	Biolegend
41BB	BV650	1 in 25	309828	Miltenyi
CD25	PEVio770	1 in 50	130-114-541	Miltenyi
Granzyme B	AF647	1 in 25	515406	Biolegend

Table 3.24: Vδ1 phenotyping flow panel 6

Target	Fluorophore	Dilution	Catalogue number	Supplier
Dead cell stain	efluor780	1 in 1000	65-0865-18	Invitrogen
Vδ1 TCR	PE	1 in 100	130-120-440	Miltenyi
CD3	BV421	1 in 25	317344	Biolegend
CD27	PEVio770	1 in 50	130-113-641	Miltenyi
CD45RA	BV570	1 in 25	304132	Biolegend
NKp44	VB515	1 in 50	130-120-361	Miltenyi
NKp30	PEVio615	1 in 25	130-112-434	Miltenyi
NKp46	APC	1 in 50	130-112-122	Miltenyi

3.24.1.8 Cytotoxicity Blockade assay

Table 3.25: Cytotoxicity blockade flow panel

Target	Fluorophore	Dilution	Catalogue number	Supplier
Dead cell stain	efluor780	1 in 1000	65-0865-18	Invitrogen
Vδ1 TCR	PE	1 in 100	130-120-440	Miltenyi
Target cells	CTV	1 in 10 000	C34571	Invitrogen
CD3	BV650	1 in 50	317324	Biolegend
CD27	PerCPVio700	1 in 100	130-120-037	Miltenyi
Fas-L	VB515	1 in 100	130-118-092	Miltenyi
CD25	APC	1 in 100	130-113-284	Miltenyi
CD107a	PEVio770	1 in 100	130-111-622	Miltenyi

3.24.1.9 Plate-bound recombinant ligand activation assay

Table 3.26: Plate-bound recombinant activation flow panel

Target	**Fluorophore**	**Dilution**	**Catalogue number**	**Supplier**
Dead cell stain	efluor780	1 in 1000	65-0865-18	Invitrogen
Vδ1 TCR	PE	1 in 100	130-120-440	Miltenyi
CD3	BV650	1 in 50	317324	Biolegend
CD27	PerCPVio700	1 in 100	130-120-037	Miltenyi
Fas-L	VB515	1 in 100	130-118-092	Miltenyi
CD25	APC	1 in 100	130-113-284	Miltenyi
CD107a	PEVio770	1 in 100	130-111-622	Miltenyi
41BB	PEVio615	1 in 50	130-110-766	Miltenyi

Chapter 4

Results

4.1 Vδ1/CD19 Antibody Design and Selection

4.1.1 Antibody Design

As explored in the introduction, the format of a bispecific antibody can affect an antibody's function. To generate a bispecific antibody that can not only specifically bind to Vδ1 TCR and CD19 but also enhance the Vδ1 effector cell capability, three different bispecific formats were implemented in the pursuit of at least one format functioning in the desired way. The chosen antibody designs were based on the bispecific T-cell engager (BiTE), Knob-into-Hole (KIH) and Morrison Body (MB) formats. Resultingly, four Vδ1/CD19 antibodies, one BiTE, one KIH and two MBs were generated (Figure 4.1).

Each bispecific antibody design utilised variable light, V_L, and heavy, V_H, amino acid sequences from a Takeda proprietary anti-Vδ1 TCR monoclonal antibody and the CD19 moiety from a commercially available anti-CD3/anti-CD19 BiTE (Figure 4.1). These V_L and V_H sequences were appended to each bispecific antibody template sequence (see Chapter 3.1). A monoclonal antibody (mAb) specific only to Vδ1 TCR was also generated to use as a control engager in appropriate subsequent assays.

4.1.2 Antibody Validation

Once generated (see Chapter 3.2), the antibodies were validated for their stability in solution, as well as their specific binding capacity to their intended targets. To ensure the antibodies were stable enough to use in cell-based assays, monomer content was assessed over time using high-performance liquid chromatography (HPLC) (Figure 4.2). Monomer content defines the amount of antibody that is not fragmented (peaks post the monomer peak in a HPLC plot) nor aggregated (peaks preceding the monomer peak in a HPLC plot), thus a high monomer

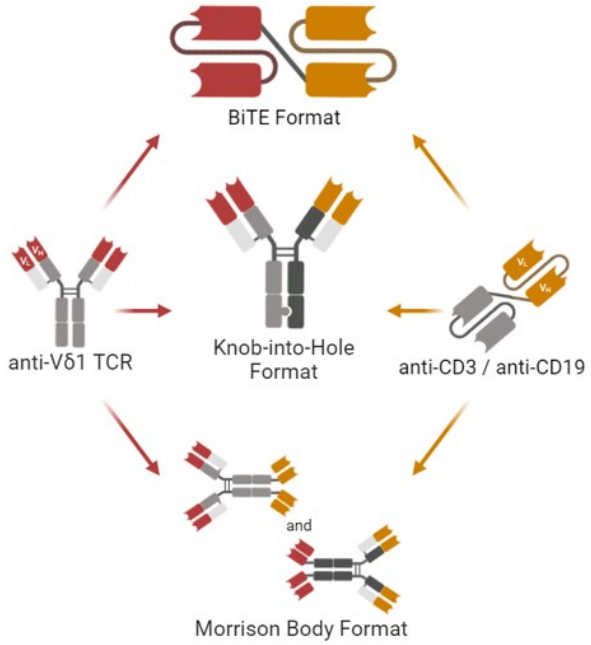


Figure 4.1: ***Design of Vδ1/CD19 bispecific engagers.***
Graphical representation of the three bispecific formats designed and generated to bind both Vδ1 TCR and CD19. [This image was created using BioRender]

content that remains high over time indicates a stable antibody structure. The HPLC plots in Figure 4.2 portray the antibody content in each sample. A ˜19-minute buffer peak was observed in all samples. The height of this peak varied between samples as dilution was required in some samples due to higher stock concentrations. The KIH monomer peak was detected at ˜12 minutes, the BiTE monomer peak at ˜15 minutes, and the MB monomer peaks at ˜13 minutes. KIH samples did not aggregate and showed little to no fragmentation. Despite BiTE samples displaying some degree of aggregation, the monomer content remained above 90% for up to 2 weeks at both 4°C and 37°C. The MBs, specifically Vδ1/CD19 MB (as opposed to the CD19/Vδ1 orientated MB (Figure 3.1)), had a very low percentage of pure monomer due to both aggregation and fragmentation. Excess aggregate can facilitate exaggerated antibody function [169] and therefore could increase the antibody's toxicity potential, indicating that the Vδ1/CD19 MB may not be suitable for understanding Vδ1 effector responses to Vδ1 engagers. Nevertheless, this antibody format, alongside the others, were still investigated in subsequent assays.

For antibody validation, Vδ1 T-cells isolated and expanded from blood and skin were used in subsequent *in vitro* assays (see method sections 3.7 and 3.8 for isolation protocols). The resulting populations from these protocols were between 50 and 60% pure Vδ1 T-cells (Figure

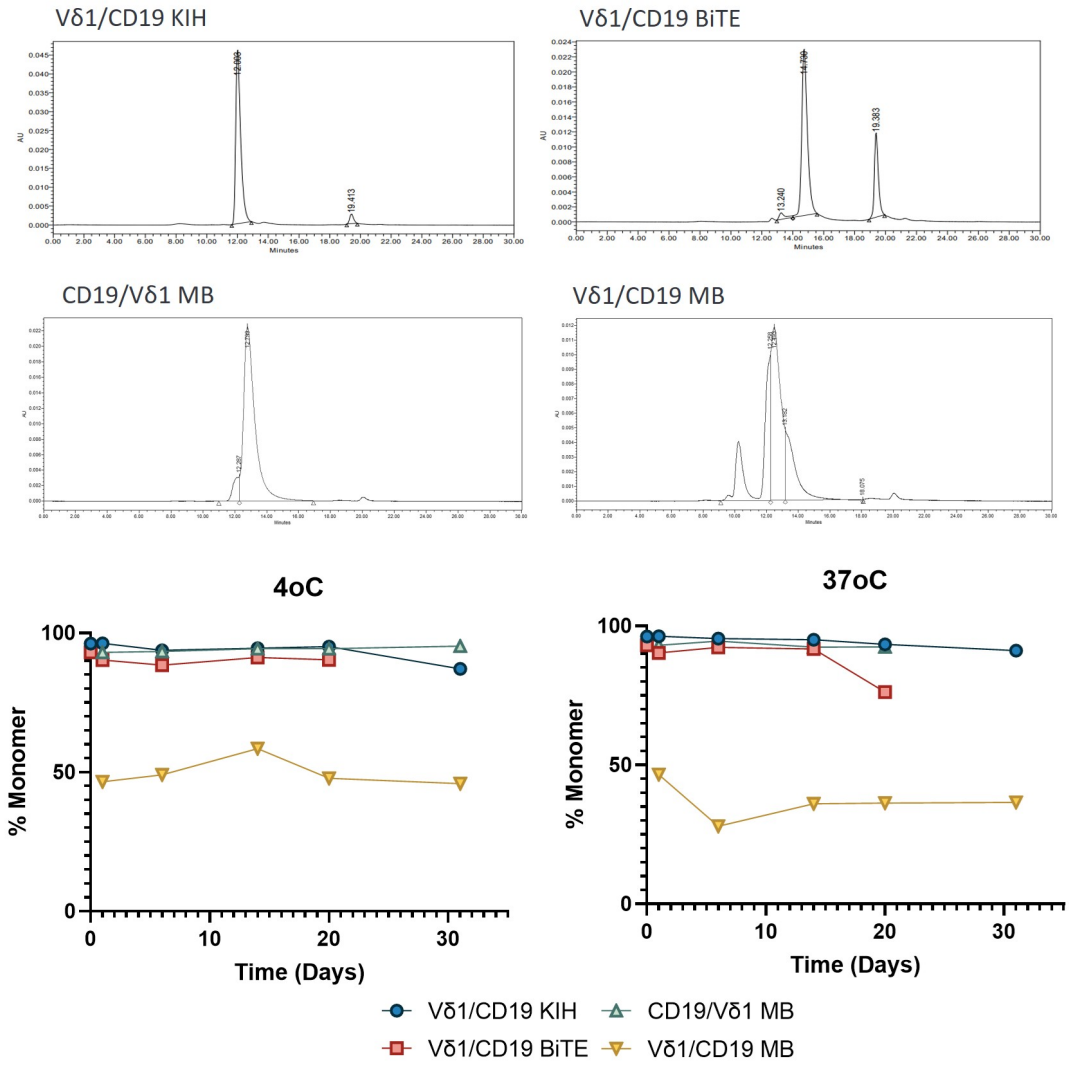


Figure 4.2: ***Vδ1/CD19 engager stability.***

Top, Vδ1/CD19 engager composition from HPLC analysis prior to storage at -80° C. Bottom, percentage monomer of the Vδ1/CD19 bispecific antibodies, calculated following the integration of each peak, excluding the buffer peak at ~19 minutes, over time post thaw from -80° C, incubated at 4° C and 37° C.

4.3). These populations were isolated using a negative-selection isolation technique. A positive selection technique would have resulted in purer Vδ1 T-cell populations, however, this method was avoided as a positive-selection protocol would utilise an anti-Vδ1 TCR antibody that could stay bound to the TCR on the final Vδ1 T-cell population. Binding from this selection antibody did not affect activation of Vδ1 T-cells for upto 48-hours (data not shown), however, this selection antibody, whilst not interfering with activation could interfere with TCR and Vδ1 detection as the selection antibody and the detection antibody are the same (Vδ1 TCR, Miltenyi, REA format). Other anti-Vδ1 TCRs do exist, however, such antibodies historically interfere with activation or may compete with the established Vδ1/CD19 engagers. Therefore, to ensure no

residual isolation antibodies remained attached to the Vδ1 T-cells, the negative selection method was adopted.

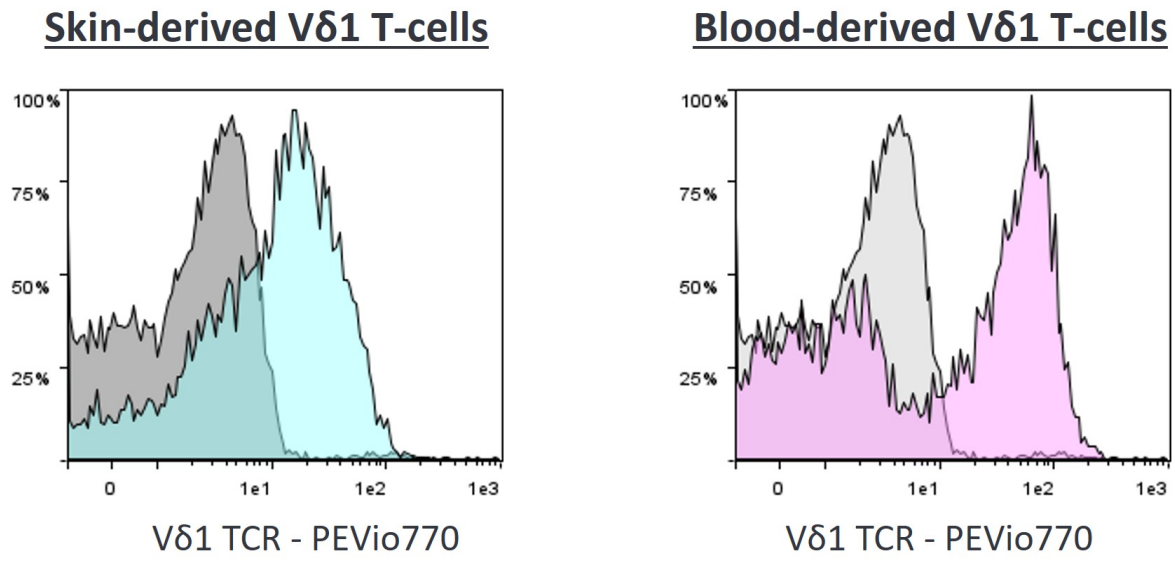


Figure 4.3: ***Vδ1 T-cell purity following isolation protocols.***
Left, Histogram from flow cytometric analysis of Vδ1 TCR$^+$ cells following Vδ1 T-cell-specific isolation and expansion protocol from a representative human skin donor. Right, Histogram from flow cytometric analysis of Vδ1 TCR$^+$ cells following Vδ1 T-cell-specific isolation and expansion protocol from a representative human blood donor. Unstained control samples are coloured in grey.

To validate their specificity, the antibodies were assessed for binding against expanded Vδ1 T-cells, CD19$^+$ B-cell cancer lines and the Vδ1$^-$CD19$^-$ cell line THP-1 (Figure 4.4 and 4.5). Mono-cultured cells were incubated with the bispecific antibodies for 30 minutes at 4°C before assessing surface-bound bispecific antibody using a secondary antibody and flow cytometry. All Vδ1/CD19 bispecific antibodies, as well as the Vδ1 monoclonal antibody, were detected on the surface of both skin-expanded and blood-expanded Vδ1 T-cells. All bispecific antibodies also bound to the CD19$^+$ cell lines Reh, MEC-1 and Daudi. This binding to CD19$^+$ cells was not observed from Vδ1 mAb which highlights the specificity of the Vδ1 binding moieties to only the Vδ1 TCR. Additionally, none of the antibodies bound to the CD19$^-$ control cell line THP-1 cells, suggesting no non-specific binding. Non-specific binding is crucial to identify so that subsequent mixed cell-based assays can be interpreted assuming that the antibodies are interacting only with their intended targets. Whilst not binding to Vδ1$^-$ and CD19$^-$ THP-1 T-cells, it would have been beneficial to assess such binding with Vδ1 T-cells with its TCR knocked-out, as well as CD19 KO MEC-1, Daudi and Reh cells for more conclusive results of non-specific binding.

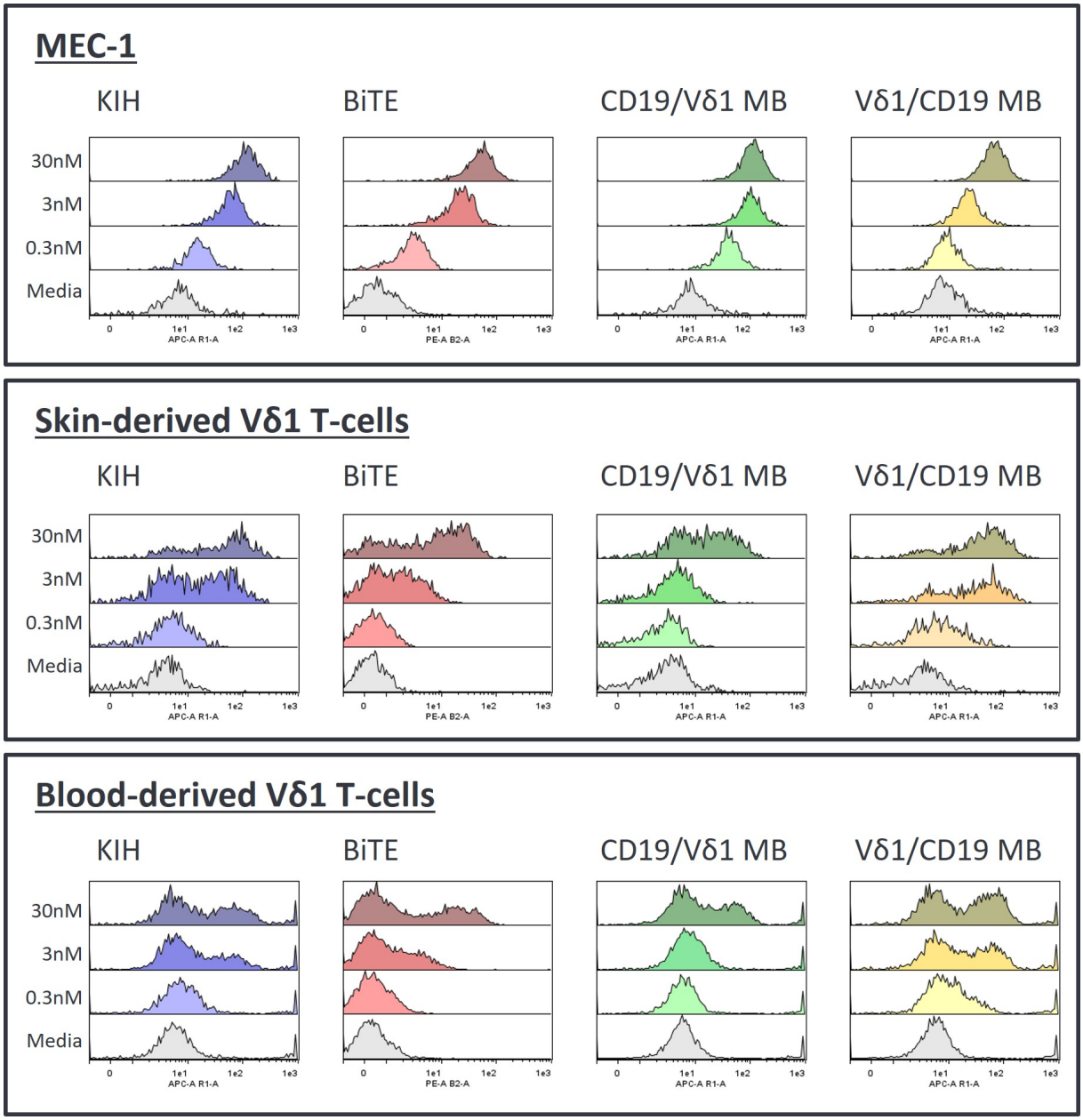


Figure 4.4: ***Representative histograms of Vδ1/CD19 engager binding.***

Binding of Vδ1/CD19 engagers to skin expanded Vδ1 T-cells (representative donor from n=3), blood expanded Vδ1 T-cells (representative donor from n=2) and CD19$^+$ MEC-1 cells. Cells were cultured alone with engagers for 30 minutes at 4oC before assessing for surface bound engager. KIH and MBs binding was assessed with an anti-IgG secondary antibody, and BiTE binding was assessed with an anti-His tag secondary antibody, all using flow cytometry. Concentration of engager in shown sample is indicated in nM.

The maximal binding observed to these cells interestingly varied (Figure 4.5). The reduced binding observed to Reh cells over MEC-1 and Daudi cells is likely due to lower levels of CD19 expressed by Reh cells. This effect is explored later. The low maximal binding to the Vδ1 T-cells (40 - 60 % cells detected bound to engager) may be due to a similar reason where the number of TCRs available on the surface of these cells may not be in great enough numbers to detect 100% of cells binding. Furthermore, as the isolation and expansion process did not have yield 100% pure Vδ1 T-cell populations (Figure 4.3), the maximum possible Vδ1 T-cell binding could only be upto 60%. This is highlighted by the bimodal peaks observed at the highest antibody concentrations when binding to the Vδ1 cells and not by the cell lines (Figure 4.4). Due to these unpure populations, an anti-Vδ1 TCR detection antibody should have been used to gate on these populations first before assessing Vδ1 TCR binding of the bispecific engagers. Nevertheless, as specific binding was consistently observed, these engagers were assessed in further functional assays.

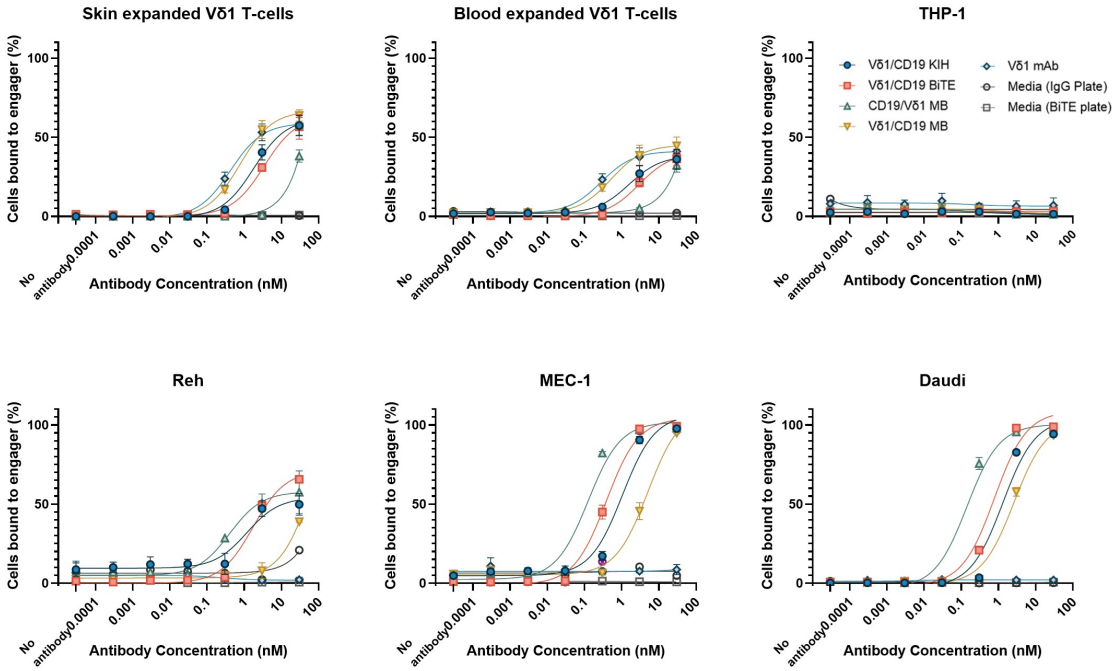


Figure 4.5: ***Vδ1/CD19 engager binding.***

Binding of Vδ1/CD19 engagers to skin expanded Vδ1 T-cells (n=3), blood expanded Vδ1 T-cells (n=2) and $CD19^+$ (Reh, MEC-1 and Daudi) and $CD19^-$ (THP-1) cell lines. Cells were cultured alone with engagers for 30 minutes at 4oC before assessing for surface bound engager. KIH and MBs binding was assessed with an anti-IgG secondary antibody, and BiTE binding was assessed with an anti-His tag secondary antibody, all using flow cytometry. Error bars of Vδ1 graphs represent SEM, where for each donor, values from two technical replicates were first averaged, and these per-donor averages were used to calculate the fold change and plot the overall mean and SEM across all donors. Error bars of the cell line graphs represent SD of two technical replicates.

4.1.3 Vδ1 engager function

As all bispecific antibodies exhibited specific binding to Vδ1 T-cells and CD19$^+$ cell lines, these engagers were subsequently assessed in functional assays to identify the most effective biologically functional engager.

4.1.3.1 TCR Downregulation

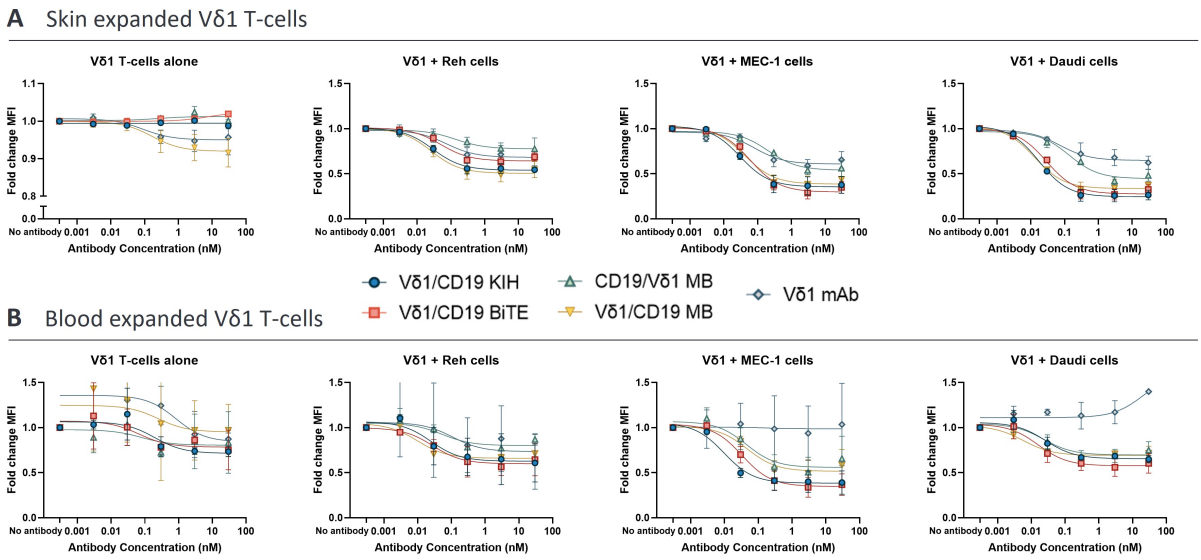


Figure 4.6: ***Vδ1/CD19 antibody-mediated TCR Downregulation.***
Vδ1 TCR expression on skin expanded (n=3) and blood expanded (n=2) Vδ1 T-cells was assessed using flow cytometry following treatment with Vδ1/CD19 antibodies and with or without the presence of CD19$^+$ cell lines. Vδ1 T-cells were co-cultured with the indicated cell lines and incubated with the bispecific antibodies for 4 hours before assessing residual surface-expressed Vδ1 TCR. Data is showing the fold change MFI of surface Vδ1 TCR expression where raw MFI values from each treatment were normalised to the MFI values from the media-treatment controls. Error bars represent the SEM. For each donor, MFI values from two technical replicates were first averaged, and these per-donor averages were used to plot the overall mean and SEM across all donors.

As with canonical $\alpha\beta$ T-cells, the $\gamma\delta$ TCR is downregulated and internalised from the cell surface when it is engaged [170]. Accordingly, to validate that the Vδ1/CD19 engager is capable of activating Vδ1 T-cells, antibody-mediated TCR downregulation was assessed from expanded skin-derived (Figure 4.6A and 4.7) and blood-derived Vδ1 T-cells (Figure 4.6B and 4.7) co-cultured with and without CD19$^+$ tumour targets. These expanded and isolated Vδ1 T-cells were incubated with the bispecific antibodies and cell lines for 4 hours before assessing residual surface-expressed Vδ1 TCR by flow cytometry. TCR downregulation is indicated by the reduction of surface Vδ1 TCR and thus reduction of surface staining with higher concentrations of Vδ1/CD19

antibody treatments (Figure 4.7). Minimal to no TCR downregulation was observed when Vδ1 T-cells were treated alone; however, once in co-culture with $CD19^+$ cells, the Vδ1 TCR was downregulated following Vδ1/CD19 antibody treatment in a dose-dependent manner. The Vδ1 mAb also displayed little to no effect across all co-culture conditions. These minimal responses could be due to the Vδ1 binding moiety only being able to sufficiently engage the TCR when binding is stabilised through co-engagement with target cell-expressed CD19. This effect was observed to similar degrees with both the skin-derived and blood-derived Vδ1 T-cells.

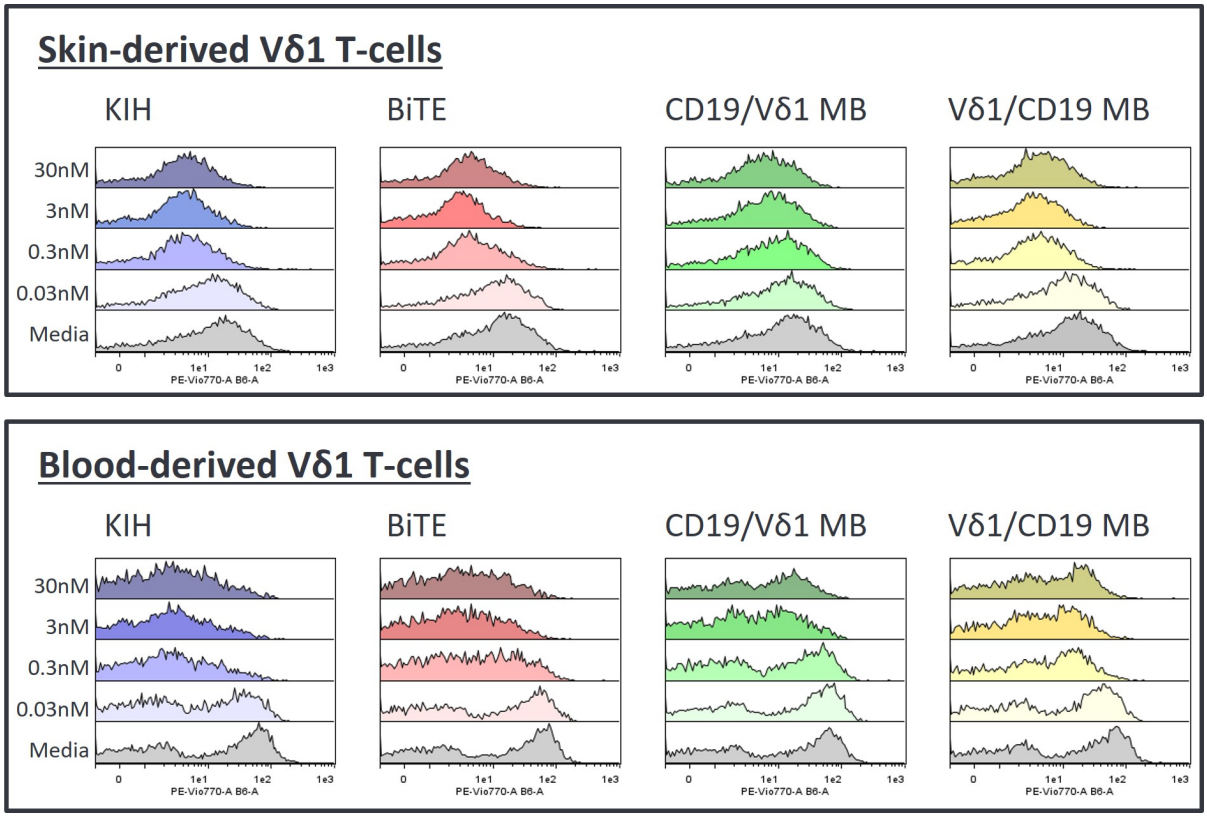


Figure 4.7: ***Representative histograms of Vδ1/CD19 antibody-mediated TCR Downregulation.***

Vδ1 TCR expression on skin expanded (representative donor from n=3) and blood expanded (representative donor from n=2) Vδ1 T-cells was assessed using flow cytometry following treatment with Vδ1/CD19 antibodies and with or without the presence of $CD19^+$ MEC-1 cells. Vδ1 T-cells were co-cultured with MEC-1 cells and incubated with the bispecific antibodies for 4 hours before assessing residual surface-expressed Vδ1 TCR. Concentration of engager in shown sample is indicated in nM.

Notably, all bispecific antibody formats engaged and downregulated the TCR to a similar extent, perhaps with the exception of the CD19/Vδ1 MB where less TCR downregulation was observed. This particular MB form positions the Vδ1 binding moieties at the base of the Fc region, as opposed to the normal mAb configuration (Figure 4.1). This positioning may impair the Vδ1 binding as the Vδ1-binding variable regions may not be able to interact with the TCR epi-

tope in the most efficient manner. However, as all Vδ1/CD19 bispecific antibodies demonstrated *some* level of TCR engagement, their functional capabilities were further investigated.

4.1.3.2 T-cell activation

To assess the ability of Vδ1/CD19 bispecific antibodies to activate Vδ1 T-cells, expression of the canonical T-cell activation markers 41BB (Figure 4.8 and 4.9) and CD25 (Figure 4.10 and 4.11) were assessed on skin-derived and blood-derived Vδ1 T-cells. These activation markers were assessed following Vδ1/CD19 antibody treatment in Vδ1 T-cell co-cultures with and without CD19$^+$ tumour cell lines. Antibody-treated co-cultures were assessed after 4-hours to detect surface 41BB expression on the Vδ1 T-cells, and after 24-hours to detect surface CD25 expression on the Vδ1 T-cells using flow cytometry.

In response to Vδ1/CD19 antibody stimulation, both Vδ1 T-cell types upregulated 41BB and CD25 in some but not all of the conditions. First, a response was only observed when co-cultured with CD19$^+$ malignant cells. This dependency on Vδ1 *and* CD19 presence reflects the same dependency observed from the antibody-mediated TCR downregulation response. This dependency highlights the importance of sufficient TCR stimulation for Vδ1 T-cell activation.

Furthermore, despite consistent binding and TCR engagement from all Vδ1/CD19 bispecific antibodies, 41BB and CD25 were noticeably only consistently upregulated in response to the BiTE antibody form. This emphasises the need for specialised antibody design to achieve the desired response.

Additionally, CD25 was not upregulated on skin-derived Vδ1 T-cells in any condition where upregulation *was* observed from blood-derived Vδ1 T-cells. Interestingly, at 6 hours post-BiTE treatment—as opposed to 24 hours—CD25 upregulation could be observed from skin-derived Vδ1 T-cells, and appeared to decline thereafter (Appendix 8.1). This early upregulation might explain why CD25 levels appeared unchanged at 24 hours (Figure 4.10) as the cells may have already downregulated CD25 by that time. These time-dependent differences in CD25 expression suggest that skin-derived and blood-derived Vδ1 T-cells may respond differently to BiTE treatment, highlighting the importance of using relevant Vδ1 T-cell models for analysis. Other Vδ1 T-cell models will be explored in subsequent sections.

To note, 41BB was assessed after 4 hours of antibody treatment whereas CD25 expression was assessed after 24 hours. Therefore, it was decided to stain for CD25 within the 24-hour *cytotoxicity* assay instead of the 4-hour 41BB and TCR downregulation assay. At the time of running the cytotoxicity assay, it was also decided that the *Vδ1 alone* condition was unnecessary

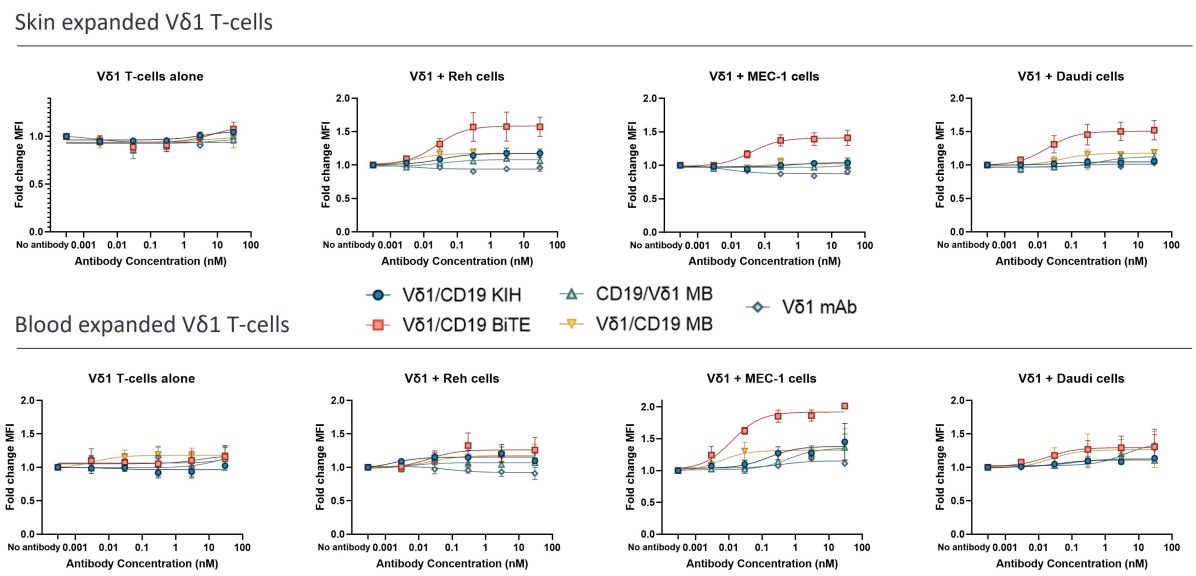


Figure 4.8: ***Vδ1/CD19 antibody-mediated 41BB upregulation.***

41BB expression on skin expanded (n=3) and blood expanded (n=2) Vδ1 T-cells was assessed using flow cytometry 4-hours following treatment with Vδ1/CD19 antibodies, co-cultured with and without CD19$^+$ cell lines. Data is showing the fold change MFI of surface 41BB expression where raw MFI values from each treatment were normalised to the raw MFI values from the media-treatment controls. Error bars represent SEM. For each donor, MFI values from two technical replicates were first averaged, and these per-donor averages were used to calculate the fold change and plot the overall mean and SEM across all donors.

to conduct. Therefore, CD25 expression data on Vδ1 T-cells cultured alone was not collected. This data absence was only realised during the consolidation of this thesis at which point materials were no longer available to repeat this experiment. Therefore, future work should validate this CD25 response from Vδ1 T-cells alone.

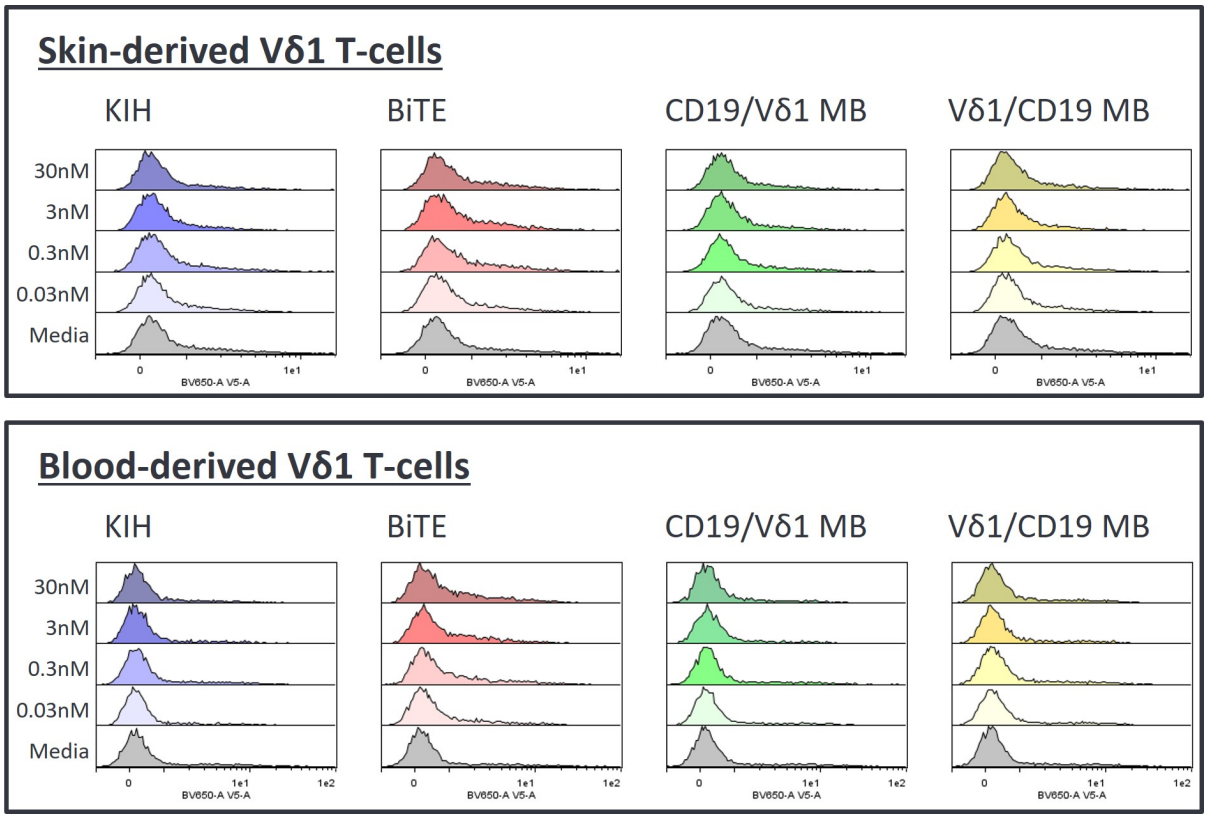


Figure 4.9: ***Representative histograms Vδ1/CD19 antibody-mediated 41BB upregulation.*** *Representative histograms of 41BB expression from skin-expanded (representative donor from n=3) and blood-expanded (representative donor from n=2) Vδ1 T-cells assessed using flow cytometry 4-hours following treatment with Vδ1/CD19 antibodies, co-cultured with and without MEC-1 cells. Concentration of engager in shown sample is indicated in nM.*

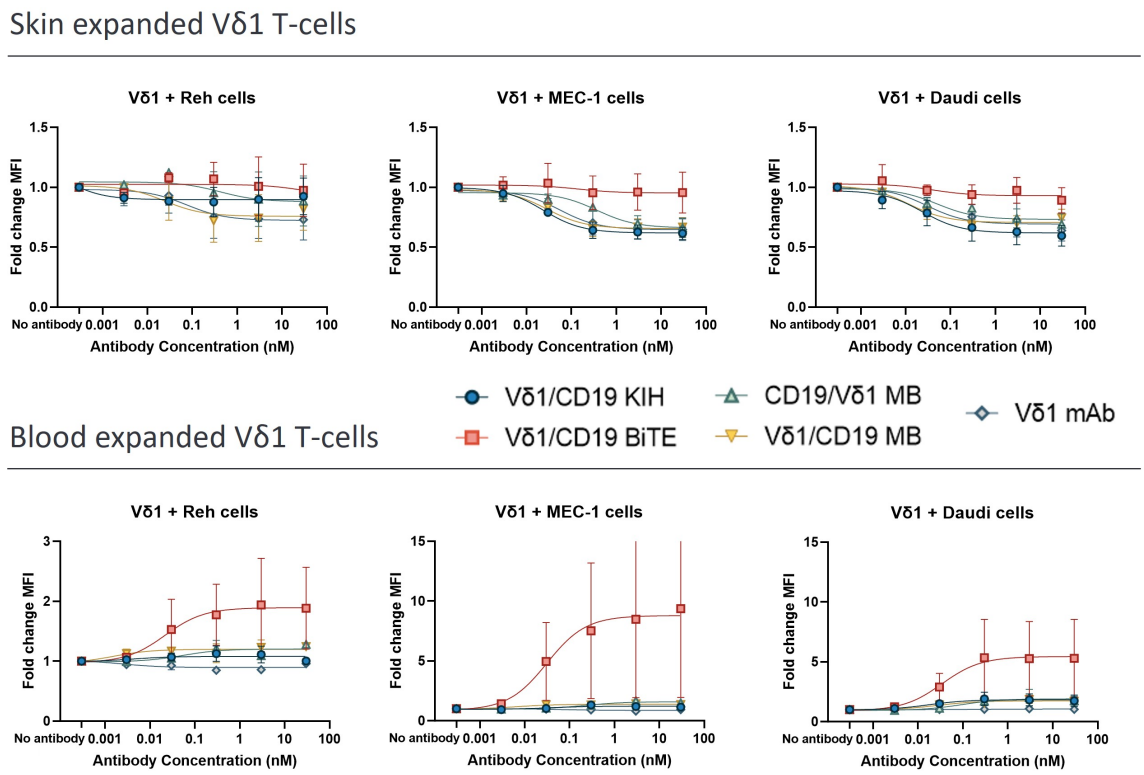


Figure 4.10: ***Vδ1/CD19 antibody-mediated CD25 upregulation.***

CD25 expression on skin expanded (n=3) and blood expanded (n=2) Vδ1 T-cells was assessed using flow cytometry 24-hours following treatment with Vδ1/CD19 antibodies, co-cultured with and without $CD19^+$ cell lines. Data is showing the fold change MFI of surface CD25 expression where raw MFI values from each treatment were normalised to the raw MFI values from the media-treatment controls. Error bars represent SEM. For each donor, MFI values from two technical replicates were first averaged, and these per-donor averages were used to calculate the fold change and plot the overall mean and SEM across all donors.

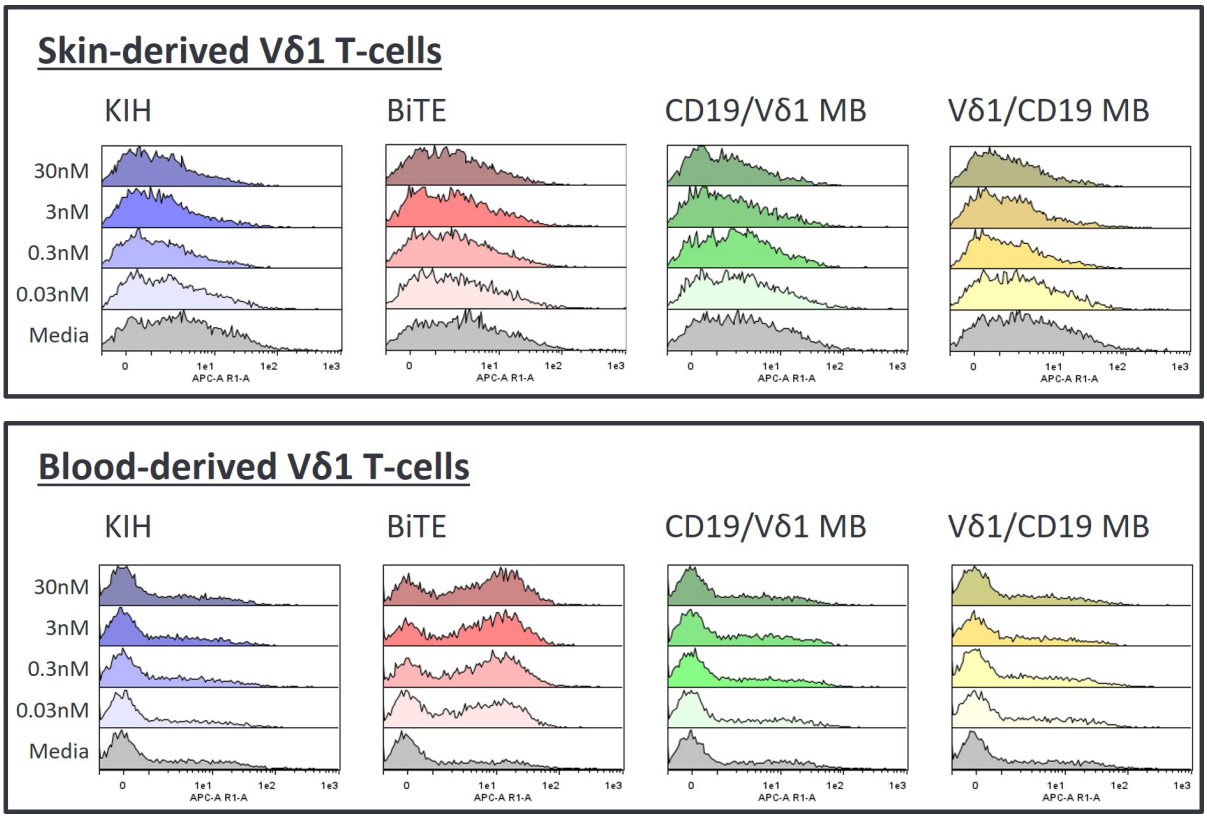


Figure 4.11: ***Representative histograms of Vδ1/CD19 antibody-mediated CD25 upregulation.*** *Representative histograms of CD25 expression from skin-expanded (representative donor from n=3) and blood-expanded (representative donor from n=2) Vδ1 T-cells assessed using flow cytometry 24-hours following treatment with Vδ1/CD19 antibodies, co-cultured with and without MEC-1 cells. Concentration of engager in shown sample is indicated in nM.*

4.1.3.3 Cytotoxicity

To assess whether Vδ1/CD19 antibody-mediated activation may result in greater cytotoxic capability, degranulation was measured as expression of CD107a on skin-derived and blood-derived Vδ1 T-cells following Vδ1/CD19 antibody treatment in co-culture with and without CD19$^+$ tumour cell lines (Figure 4.12 and 4.13). CD107a, also known as LAMP-1 (Lysosomal-Associated Membrane Protein-1), is a marker commonly used to assess degranulation resulting in granzyme and perforin release from cytotoxic cells. Upon degranulation, vesicles containing these cytotoxic molecules merge with the cell membrane, exposing CD107a on the cell surface. Therefore, the upregulation or increased surface expression of CD107a serves as an indicator of enhanced degranulation and a proxy for cytotoxic activity. This 'surface-exposed' CD107a was detected using flow cytometry, 4-hours following treatment of the co-cultures (see method section 3.12 for protocol details).

Similar to the TCR downregulation and activation responses, stimulated Vδ1 T-cells alone were unable to upregulate CD107a; a co-culture with CD19$^+$ cancer cells was necessary to induce a degranulation response, highlighting the importance of sufficient TCR engagement for Vδ1 T-cell activation and cytotoxicity. CD107a upregulation was observed following Vδ1/CD19 engager treatment, however, only BiTE treatment, similarly to 41BB and CD25 measurements, reliably induced a response compared to the other Vδ1/CD19 bispecific antibodies. This BiTE-specific response suggests that the BiTE may be the most functional engager to enhance Vδ1 capabilities. It should be noted that the increased CD107a response from skin-derived Vδ1 T-cells was less prominent than from blood-derived Vδ1 T-cells. Alongside the differential CD25 response, these activation results could suggest that blood- and skin-derived Vδ1 T-cells may rely on different co-receptors and cytotoxicity mechanisms. These differences are explored later.

The engager-mediated degranulation response also corresponded to the remaining live target cell population after 24 hours (Figure 4.14 and 4.15), where BiTE-treatment mediated a consistent decrease in live CD19$^+$ cancer cell numbers. The increased target cell death, alongside increased Vδ1-specific CD107a expression suggests that BiTE treatment enhances the Vδ1 T-cell cytotoxic capabilities.

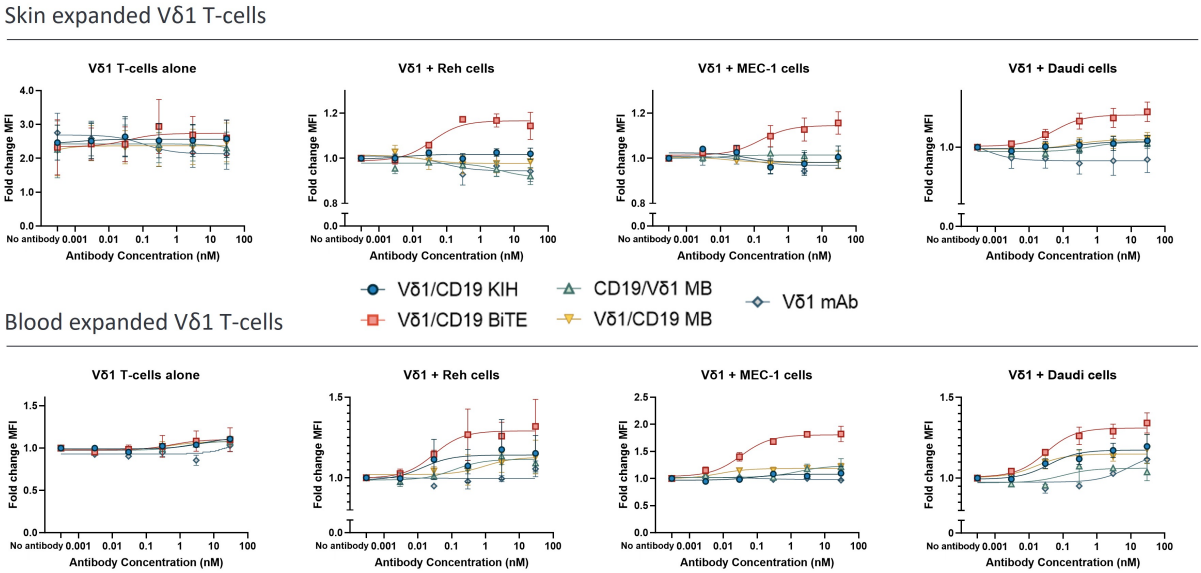


Figure 4.12: ***Vδ1/CD19 antibody-mediated CD107a upregulation.***

CD107a expression on skin expanded (n=3) and blood expanded (n=2) Vδ1 T-cells was assessed using flow cytometry 4-hours following treatment with Vδ1/CD19 antibodies, co-cultured with and without CD19$^+$ cell lines. Data is showing the fold change MFI of surface-exposed CD107a where raw MFI values from each treatment were normalised to the raw MFI values from the media-treatment controls. Error bars represent SEM. For each donor, MFI values from two technical replicates were first averaged, and these per-donor averages were used to calculate the fold change and plot the overall mean and SEM across all donors.

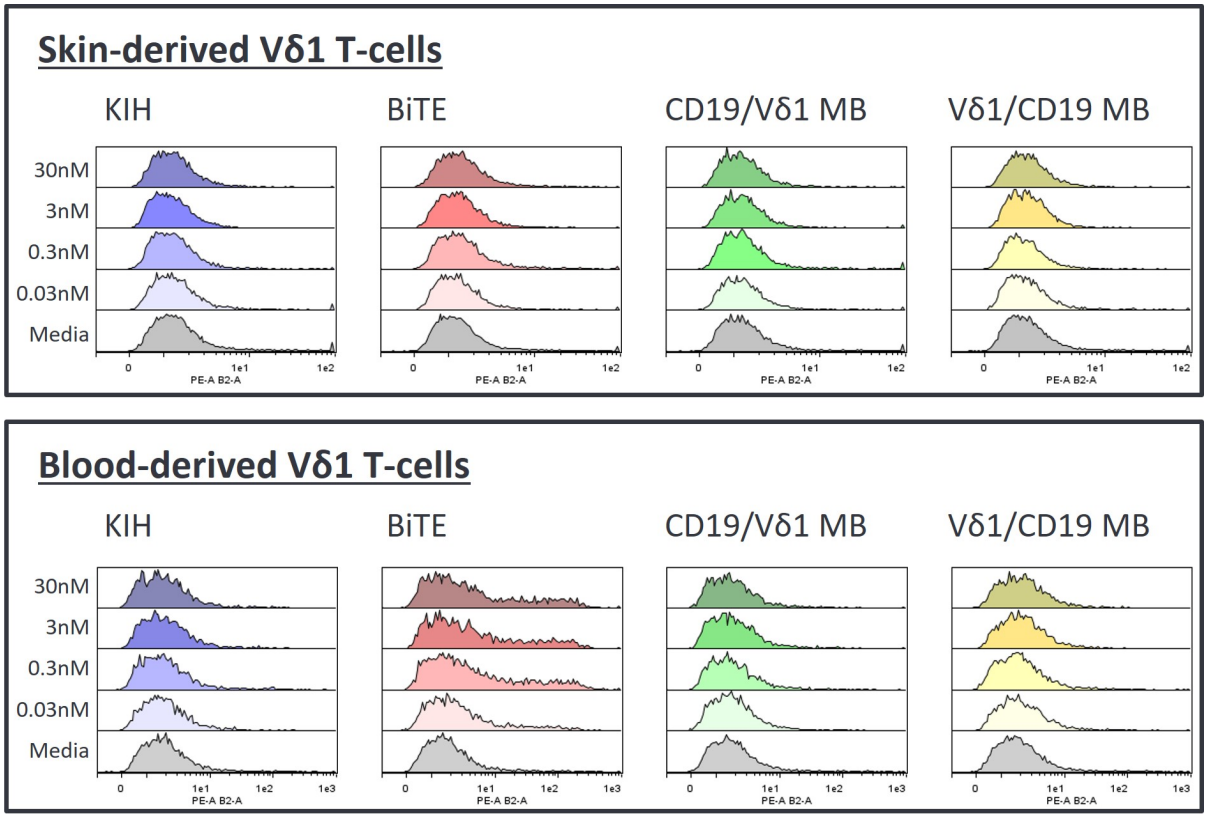


Figure 4.13: ***Representative histograms of Vδ1/CD19 antibody-mediated CD107a upregulation.***

Representative histograms of CD107a expression from skin-expanded (representative donor from n=3) and blood-expanded (representative donor from n=2) Vδ1 T-cells assessed using flow cytometry 4-hours following treatment with Vδ1/CD19 antibodies, co-cultured with and without MEC-1 cells. Concentration of engager in shown sample is indicated in nM.

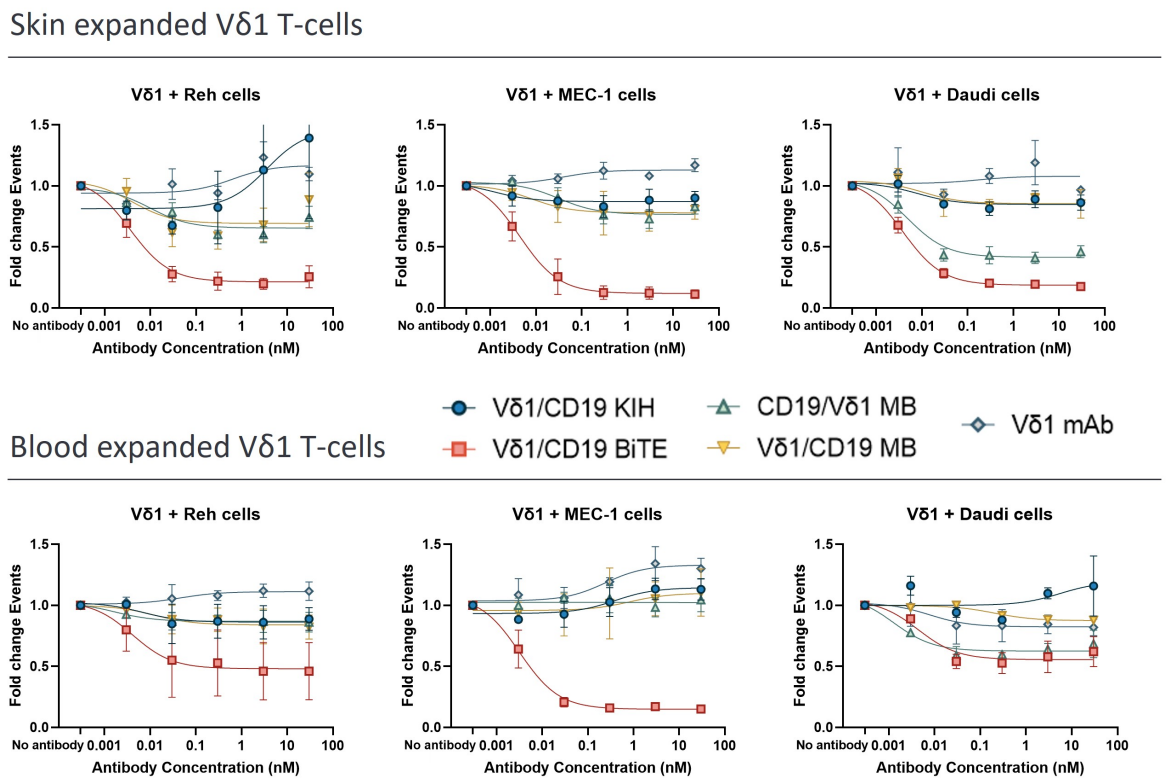


Figure 4.14: ***Vδ1/CD19 engager-mediated enhanced Vδ1 cytotoxicity.***

Remaining live cancer target cell events was assessed using flow cytometry following 24-hour culture with skin expanded (n=3) and blood expanded (n=2) Vδ1 T-cells and Vδ1/CD19 engager treatment. Data is showing fold change events of the remaining live indicated target cells in the co-culture. Each event represents a single live target cell recorded on the flow cytometer. Fold change events represents the raw live event numbers from each treatment normalised to the raw live event numbers from the media-treatment controls. Error bars represent SEM. For each donor, values from two technical replicates were first averaged, and these per-donor averages were used to calculate the fold change and plot the overall mean and SEM across all donors.

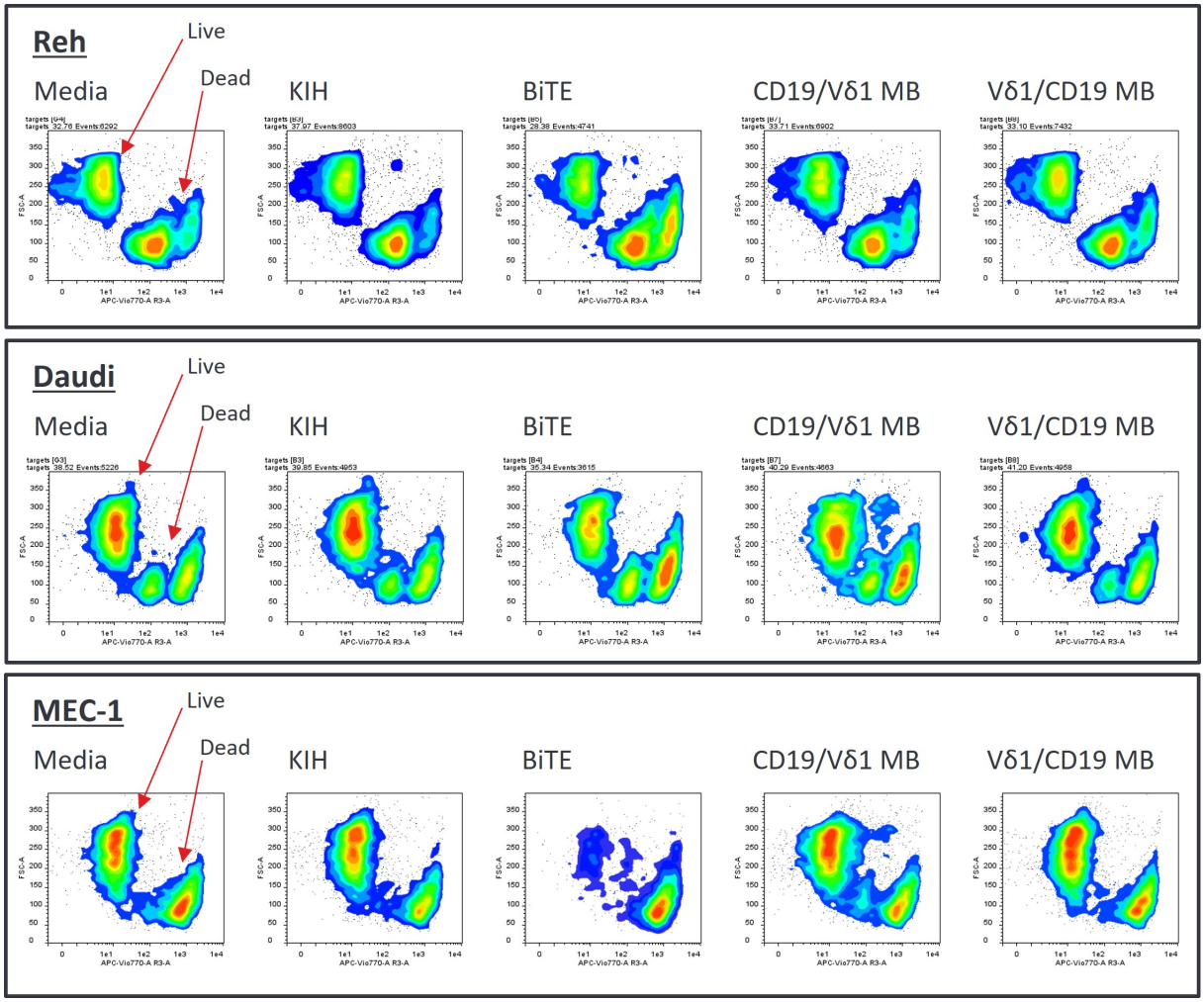


Figure 4.15: ***Representative flow plots of Vδ1/CD19 engager-mediated enhanced Vδ1 cytotoxicity.***

Representative flow plots of live and dead populations of the indicated target cells after 24 hours of culture with blood-derived Vδ1 T-cells (representative donor from n=2) treated with 30nM of the indicated Vδ1/CD19 bispecific antibody. Flow plots are displaying the live dead marker (x-axis, efluor780-A) against forward scatter (y-axis, FSC-A). Live and dead populations are indicated with arrows.

4.1.3.4 Proliferation

In response to CD3-engager treatment, peripheral T-cells undergo several activation processes, one of which includes proliferation [171, 172, 173]. As the Vδ1 T-cell peripheral population is small, increasing this population would be a beneficial response from Vδ1/CD19 engager-treatment. Therefore, Vδ1 T-cell numbers were assessed from primary PBMC samples after culture with Vδ1/CD19 antibody treatment over 7 days (Figure 4.16). Interestingly, despite only the BiTE displaying functional activity thus far, *all* the bispecific formats induced Vδ1 proliferation; however, notably the BiTE-format remained the most efficacious treatment. This effect is observed in the flow plots of these samples (Figure 4.17). Interestingly, both CD27 populations proliferated in all treatment conditions. Furthermore, the CD27$^+$ populations from all samples expressed higher levels of TCR compared to their CD27$^-$ counterparts, except for the BiTE-treated where two populations of CD27$^-$ cells, based on TCR expression emerged. Both BiTE-stimulated CD27$^-$ and CD27$^+$ Vδ1 T-cell populations demonstrated a vast increase in forward and side scatter, which can be indicators of increased T-cell activation and proliferation [174]. BiTE-stimulated cells may therefore be undergoing increased activation as well as proliferation compared to the other formats. This response will be explored further later.

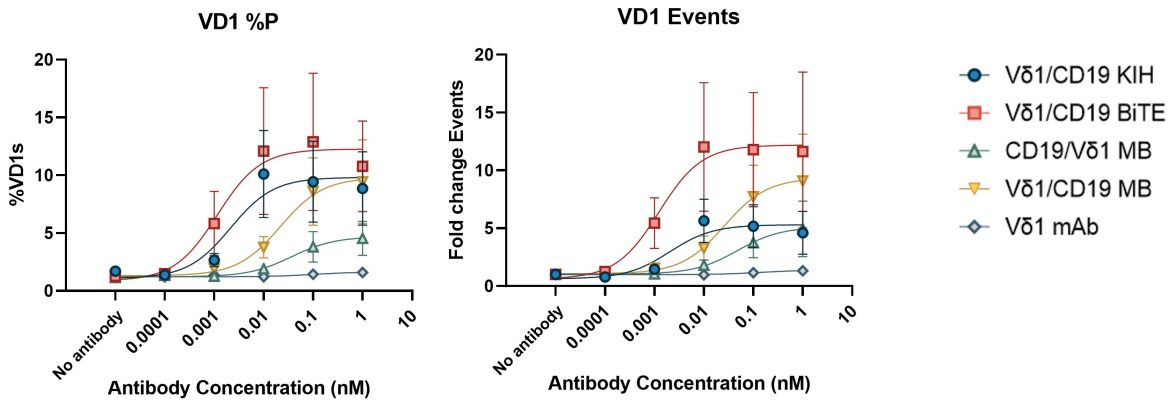


Figure 4.16: ***Vδ1/CD19 engager-mediated Vδ1 proliferation.***
Vδ1 populations from PBMC cultures (n=3) were assessed using flow cytometry after treatment with Vδ1/CD19 engagers for 7 days. Left, data is showing the percentage of live cells from whole PBMC culture that are Vδ1 positive. Right, data is showing fold change events of Vδ1 T-cells. Each event represents a single live Vδ1 T-cell recorded on the flow cytometer. Fold change events represents the raw live event numbers from each treatment normalised to the raw live event numbers from the media-treatment controls. Error bars represent SEM. For each donor, values from two technical replicates were first averaged, and these per-donor averages were used to calculate the fold change and plot the overall mean and SEM across all donors.

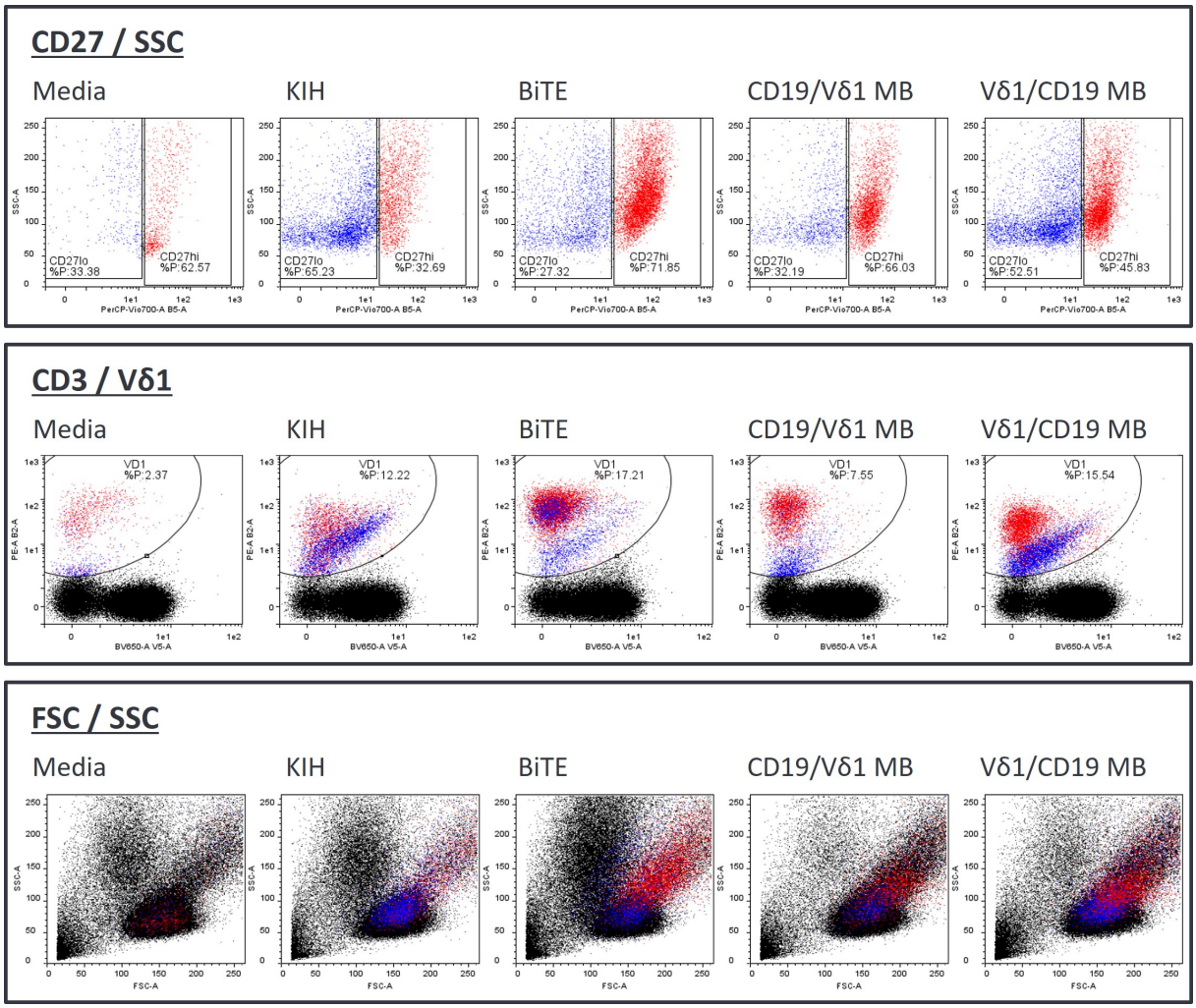


Figure 4.17: ***Representative flow plots of Vδ1/CD19 engager-mediated Vδ1 proliferation.*** *Vδ1 populations from PBMC cultures (representative donor from n=3) were assessed using flow cytometry after treatment with 30nM Vδ1/CD19 engagers for 7 days. Top panel is showing the $CD27^{high}$ (right, red) and $CD27^{low/-}$ (left, blue) Vδ1 population gating following treatment of indicated antibodies, with the events displayed as CD27 staining (x-axis) vs side scatter (SSC, y-axis). The middle panel is showing the Vδ1 population gating of the same samples in the above panel, with the events displayed as CD3 staining (x-axis) vs Vδ1 TCR staining (y-axis). The according CD27 populations have been coloured in these plots. The bottom panel is showing the forward (x-axis) and side scatter (y-axis) of all the cells in the same samples as the above panels with the CD27 high and low populations of Vδ1 T-cells coloured accordingly.*

4.1.4 Summary

Overall, these assays were used to validate the capacity of Vδ1/CD19 bispecific antibodies to enhance Vδ1 T-cell function. All Vδ1/CD19 antibodies demonstrated binding to their specific targets, which resulted in stable TCR engagement in expanded Vδ1 T-cells, as well as proliferation of primary PBMC-based Vδ1 T-cells. Despite *all* these engagers displaying functionality in these assays, only the BiTE format mediated subsequent Vδ1 T-cell activation which led to enhanced cytotoxicity against CD19$^+$ malignant tumour cell lines. Therefore, the BiTE format was chosen to be used in subsequent assays to investigate the remaining aims of this study. The Vδ1/CD19 BiTE will henceforth be referred to as *Vδ1/CD19* and/or the *engager*.

4.2 Selected Vδ1/CD19 Engager Evaluation

To evaluate the selected Vδ1/CD19 engager, and to instill confidence in the decision, data from the section above was consolidated and repeated with additional control conditions. This was to provide a foundation for further understanding the function of this engager for investigating the further aims of this study. An assessment of this chosen engager is summarised in a journal article currently in review.

Thus far, both skin-derived and blood-derived Vδ1 T-cells have been utilised to validate basic engager function; however, as the Vδ1/CD19 targets the haematological marker CD19, further involvement of skin-derived Vδ1 T-cells was deemed unnecessary as blood-derived Vδ1 T-cells are more physiologically relevant. Therefore, results hereafter focus on blood-derived Vδ1 T-cells, either cytokine-expanded or PBMC-based.

4.2.1 Binding

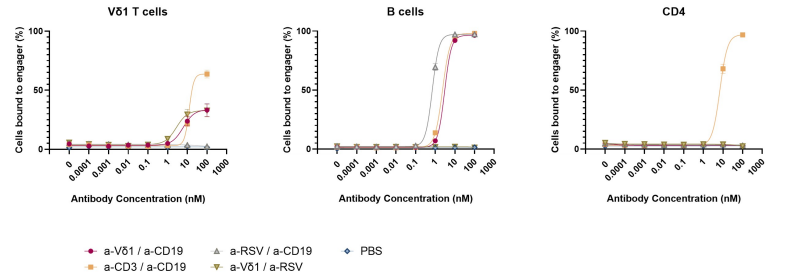
In addition to the binding observed in figure 4.5, binding of Vδ1/CD19 to PBMCs was assessed (Figure 4.18A). The engager bound to PBMC-based Vδ1 T-cells as well as $CD19^+CD20^+$ B-cells[1]. The engager did not bind to $CD4^+$ cells which were used as a control cell type to assess non-specific binding of Vδ1/CD19. The positive control CD3/CD19 engager, as expected, bound to all three cell types as both Vδ1 and CD4 T-cells express CD3.

Binding EC50s of Vδ1/CD19 were lower than the CD3/CD19 engager which would suggest that Vδ1/CD19 binds more efficiently to Vδ1 T-cells than the CD3 engager. Despite this Vδ1-binding difference, the binding EC50s of Vδ1/CD19 and CD3/CD19 binding to $CD19^+$ cells were comparable. As the CD19-binding amino acid sequence used to generate Vδ1/CD19 was taken from the CD3/CD19 engager, it is ideal that the efficiency of binding to CD19 remains intact as it suggests that the Vδ1-binding sequence, did not interfere with the CD19 moiety binding capacity. This comparability ensures confidence that the Vδ1 engager is interacting with $CD19^+$ target cells in an appropriate manner.

Control BiTEs were also used in this binding assay to further ensure that each binding moiety of the Vδ1/CD19 engager was not affecting the overall binding capacity of the engager to its intended targets. The control BiTEs generated substituted an anti-RSV sequence for each binding moiety separately (see section 3.1 for more details). Both the Vδ1 and CD19 binding moieties of the Vδ1/CD19 engager were slightly less efficient, if not similarly efficient, compared to the control BiTEs; however, the maximum binding capacity remained comparable.

[1]Engager binding to CD19 interfered with the flow cytometry detection of B-cells via the CD19 marker so an anti-CD20 flow antibody was used in addition to an anti-CD19 antibody as a method to gate on B-cells.

A



B

Cell type	Binding EC50	
	a-Vδ1/a-CD19	a-CD3/a-CD19
THP-1	-	-
Reh	1.72	3.33
Daudi	0.50	0.99
MEC-1	0.33	0.67
B cells	3.00	2.33
CD4	-	6.98
Vδ1 T-cells	6.20	12.44
Skin-derived Vδ1 T-cells	3.43	*Too low binding to calculate*
Blood-derived Vδ1 T-cells	2.54	166.40

Figure 4.18: ***Selected Vδ1/CD19 engager specifically binds to Vδ1 and B-cells in PBMCs.*** *Binding of engagers to cells in vitro using flow cytometry after 30 minutes incubation at 4oC.* ***(A)*** *Binding of Vδ1, CD19 and CD3 bispecific engagers in BiTE format to $Vδ1^+$, $CD19^+CD20^+$ and $CD4^+$ cells in whole PBMC cultures (n=3). Error bars represent SEM. For each donor, values from two technical replicates were first averaged, and these per-donor averages were used to plot the overall mean and SEM across all donors.* ***(B)*** *Binding EC50s (nM) of Vδ1/CD19 and CD3/CD19 engagers to all cell types assessed in* ***(A)*** *and in figure 4.5.*

Therefore, this similar binding suggested that the Vδ1/CD19 engager was binding specifically, and to a suitable degree to PBMC-based cells.

To note, the maximal binding of CD3/CD19 engager to $CD4^+$ T-cells is likely to be greater than the maximal binding observed to Vδ1 T-cells (Figure 4.18A), as this binding assay was conducted in whole PBMCs, meaning that more of the CD3/CD19 engager would bind to the more prevalent $CD4^+$ T-cells. Furthermore, as mentioned above, the lower maximal binding could be due to available epitope numbers on the cell surface. The nearly double difference in maximal binding between the CD3 and Vδ1 engagers could highlight the greater numbers of CD3 present on the surface of T-cells, where two CD3 subunits are expressed per TCR [175].

4.2.2 Engager-mediated Vδ1 activation and cytotoxicity

As explored in the previous section, the Vδ1 T-cell alone condition—without target cell co-culture—was not efficient in downregulating the TCR and subsequently activating Vδ1 T-cells. This observation was likely due to the lack of CD19 in the system that would enable stable binding of Vδ1/CD19 to the TCR. Therefore, if a lack of CD19 affects engager capabilities, perhaps increased levels of CD19 in the system could further enhance Vδ1/CD19-mediated responses. The Vδ1 activation and enhanced cytotoxicity results in figures 4.6 - 4.14 utilised Vδ1 T-cell co-cultures with different $CD19^+$ cell lines. These cell lines expressed varying levels of CD19 (Figure 4.19). Therefore to understand the effect of CD19 expression on engager function, the results from figures 4.6 - 4.14 were consolidated to compare Vδ1 activation and cytotoxicity

across the different co-culture conditions (Figure 4.20).

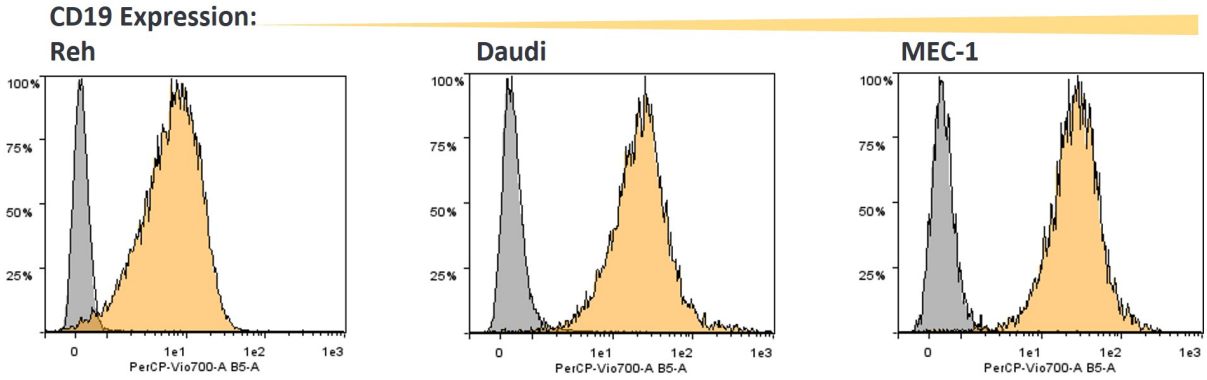


Figure 4.19: ***Cell line CD19 expression.***
Reh, Daudi and MEC-1 cells were assessed for their levels of CD19 expression using flow cytometry. Grey histograms represent the FMO control sample, and yellow histograms represent the samples stained with an anti-CD19-PerCPVio700 flow antibody.

With an increase in target cell CD19 expression, TCR downregulation, activation marker upregulation, and cytotoxicity were all improved. This supports the notion that Vδ1/CD19 is dependent on epitope availability to sufficiently engage the TCR. Of course this differential response may not solely be due to CD19 expression as these target cells also express varied cancer-associated stress ligand signatures (see next chapter for phenotyping). For example, when cultured without the engager, Vδ1 T-cells differentially downregulated their TCRs in response to the different target cell phenotypes (Appendix 8.2). Despite this response, the level of engager-mediated activation—assessed by 41BB, CD107a and CD25—was not affected by the baseline TCR downregulation observed (Appendix 8.2). This suggests that the CD19-mediated engager binding is more likely to instigate these differential responses.

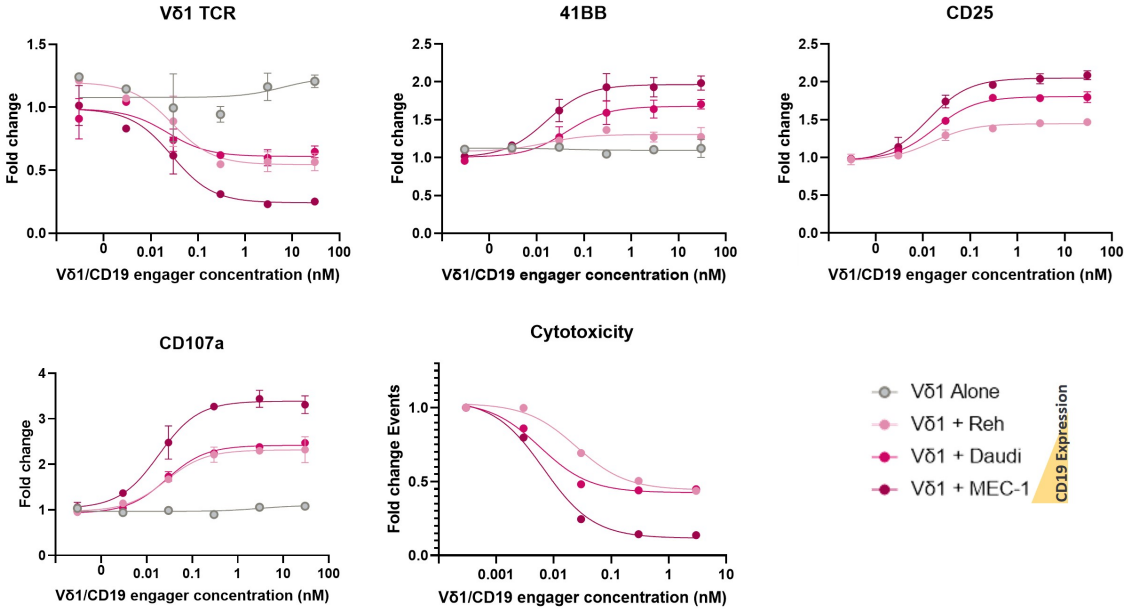


Figure 4.20: ***Selected Vδ1/CD19 engager activates and enhances cytotoxicity of Vδ1 T-cells.*** *Vδ1 activation and cytotoxicity from blood expanded Vδ1 T-cells (representative donor from n=2) cultured alone and with Reh, Daudi or MEC-1 cells with Vδ1/CD19 BiTE treatment where Vδ1 TCR, CD107a and 41BB expression was assessed using flow cytometry after 4 hours of culture and CD25 expression and remaining live target cells were assessed after 24 hours of culture. Expression data of each indicated marker is presented as fold change MFI where raw MFI values from each treatment were normalised to the raw MFI values from the media-treatment co-culture controls. Fold change events is presented fold change events of the remaining live target cells in the co-culture. Each event represents a single live target cell recorded on the flow cytometer. Fold change events represents the raw live event numbers from each treatment normalised to the raw live event numbers from the media-treatment co-culture controls. Error bars represent SD where two technical replicates were conducted.*

4.2.3 Engager-mediated Vδ1 proliferation

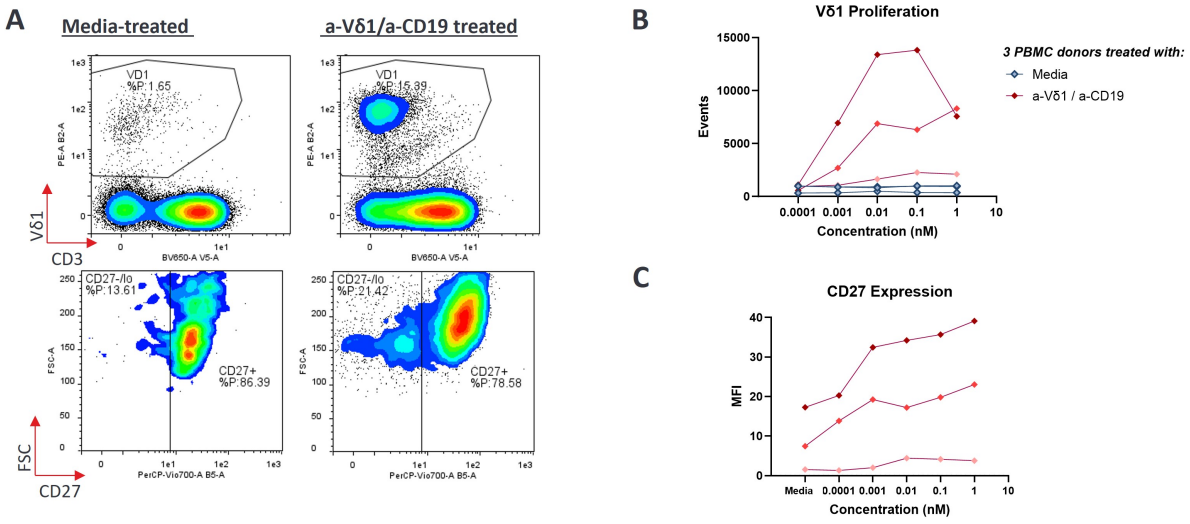


Figure 4.21: ***Selected Vδ1/CD19 engager induces proliferation of Vδ1 T-cells.*** *Proliferation of Vδ1 T-cells in whole PBMC cultures assessed by flow cytometry.* ***(A)*** *Top, Representative histogram of Vδ1 T-cells proliferation from whole PBMC culture after 7 days with and without 1nM Vδ1/CD19 BiTE treatment, bottom, Representative histogram of CD27 expression from corresponding Vδ1 populations.* ***(B)*** *Proliferation of Vδ1 T-cells from whole PBMC cultures (n=3) after 7 days treatment with and without Vδ1/CD19 stimulation. Data is showing events where each event represents a single live Vδ1 T-cell recorded on the flow cytometer.* ***(C)*** *Raw MFI of CD27 expression of corresponding Vδ1 T-cells (corresponding donors are coloured accordingly) treated with Vδ1/CD19 engager (n=3).*

To assess how the selected Vδ1/CD19 engager can induce Vδ1 T-cell proliferation, PBMCs were cultured with Vδ1/CD19 for 7 days, similarly to figure 4.16. The engager consistently induced proliferation of PBMC-based Vδ1 T-cells (Figure 4.21). Interestingly, Vδ1 proliferation corresponded to an increase in CD27 expression (Figure 4.21). As high CD27 expression is a marker of naive Vδ1 T-cells [54], in these healthy PBMC cultures, Vδ1/CD19-mediated TCR stimulation may maintain a naive Vδ1 phenotype.

Additionally, the extent of Vδ1 proliferation correlated to the basal Vδ1 CD27 expression profile (Figure 4.22) where greater basal CD27 expression suggested greater engager-mediated Vδ1 proliferative capacity. These results support previous findings that demonstrate higher proliferative capacity of CD27+ than CD27- Vδ2 T-cells [98]. Consequently, Vδ1/CD19-mediated proliferation may be dependent on homeostatic Vδ1 CD27 status and individuals with higher CD27 levels may have greater reactivity to Vδ1-engager stimulation. The relevance of CD27 and Vδ1 engager-stimulated Vδ1 T-cells will be examined in more detail in subsequent sections.

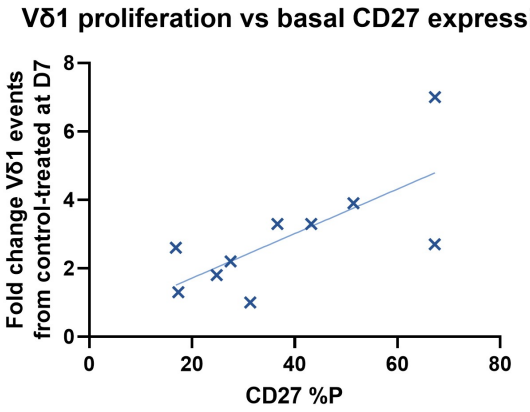


Figure 4.22: ***Vδ1/CD19-mediated Vδ1 proliferation correlates to basal CD27 expression.*** *Engager-mediated proliferation (y-axis) correlates to the percentage of CD27+ PBMC-based Vδ1 T-cells (CD27%P) at day 0 (n=11, where 1 donor was excluded from the linear regression model following ROUT outlier identification) assessed by flow cytometry. Engager-mediated proliferation (y-axis) is presented as the fold change of Vδ1 events, from the same PBMC donors, where fold change is calculated as Vδ1 events from Vδ1/CD19-treated PBMCs normalised to Vδ1 events from control engager-treated PBMCs after 7 days in culture. Each event represents a single live Vδ1 T-cell recorded on the flow cytometer. A linear regression model was used to calculate the correlation between basal CD27 expression and engager-mediated Vδ1 proliferation where R=0.5 and p=0.02.*

4.2.4 Engager-mediated PBMC-based Vδ1 cytotoxicity

In addition to the cytotoxicity observed from cytokine-expanded Vδ1 T-cells (Figure 4.20), PBMC-based engager-stimulated Vδ1 T-cells were also assessed for cytotoxic capability (Figure 4.23). As the Vδ1 T-cell population makes up a small percentage of the PBMC composition, a broader targeting CD3/CD19 engager was used here as a positive control where all $CD3^+$ T-cells would be stimulated. In this assay, whole PBMCs were cultured for 6 days with engager-stimulation prior to the addition of the CLL cell line MEC-1 (Figure 4.23A) or primary CLL B-cells (Figure 4.23B). Co-cultures were then incubated for 24 hours before measuring the remaining live target cells. Thus far, a range of $CD19^+$ cancers have been assessed as a target for Vδ1/CD19 stimulated Vδ1 T-cells. $CD19^+$ cell lines were used to do this as cell lines are often used as cancer models for oncotherapeutic research. They provide an accessible and repeatable system to assess drug mechanisms; however, due to the immortilisation process and large passage numbers, cell lines can tend to differ from the primary indication that they were designed to model. This study utilises $CD19^+$ cell lines for the same advantages, but also incorporated primary cells where possible in response to the potential disadvantages.

This study aimed to investigate a range of $CD19^+$ cancers whenever possible; however, where

cell availability or time constraints were an issue, it was decided to focus on the one CD19$^+$ indication, Chronic Lymphocytic Leukaemia (CLL). Thus in this particular experiment, only CLL was investigated using primary CLL B-cells and the CLL cell line, MEC-1.

The Vδ1 T-cell engager enhanced the cytotoxicity of PBMC cultures against both the MEC-1

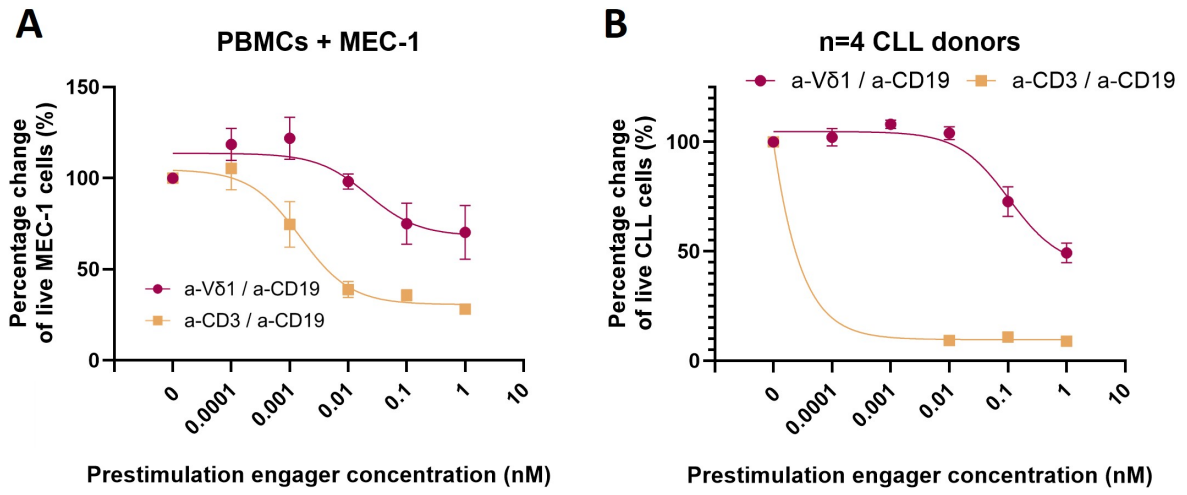


Figure 4.23: ***Vδ1/CD19 engager treatment enhances PBMC cytotoxicity against CLL cancer cells.***

Susceptibility of CLL B-cells to engager-treated PBMCs assessed by flow cytometry. ***(A)*** *Healthy PBMCs cultures (n=3) prestimulated for 6 days with Vδ1/CD19 and CD3/CD19 engagers were then assessed for cytotoxic capability where MEC-1 cells were added to the PBMC cultures for 24 hours. Remaining live target cells were assessed after the 24 hours of co-culture. Live target cells presented as percentage fold change from live MEC-1 cells in non-prestimulated culture. Error bars represent SEM. For each donor, cell numbers from two technical replicates were first averaged, and these per-donor averages were used to calculate the percentage change to plot the overall mean and SEM across all donors.* ***(B)*** *Healthy PBMCs cultures (n=1) prestimulated for 6 days with Vδ1/CD19 and CD3/CD19 engagers were then assessed for cytotoxic capability where isolated primary CLL B-cells (n=4) were added to the PBMC cultures for 24 hours.Remaining live target cells were assessed after the 24 hours of culture. Live target cells presented as percentage fold change from live CLL cells in non-prestimulated culture. Error bars represent SEM. For each donor, cell numbers from two technical replicates were first averaged, and these per-donor averages were used to calculate the percentage change to plot the overall mean and SEM across all donors.*

cell line and primary CLL B-cells. As these are whole PBMC cultures, these data cannot *prove* that the Vδ1/CD19-dose dependent enhanced cytotoxicity is solely due to engager-mediated *Vδ1* activation; however, it is unlikely that this increased cell death is due to toxicity from the engager as direct treatment to MEC-1 cells alone did not result in increased cell death (Figure 4.24). However, it should be noted that binding to CD19 may instigate killing of target cells with low cell viability (Appendix 8.3). Direct killing from CD19 binding has been documented

from the therapeutic mAb Tafasitamab [176] though the mechanism is not fully understood and therefore CD19 binding-associated cell death would require further investigation.

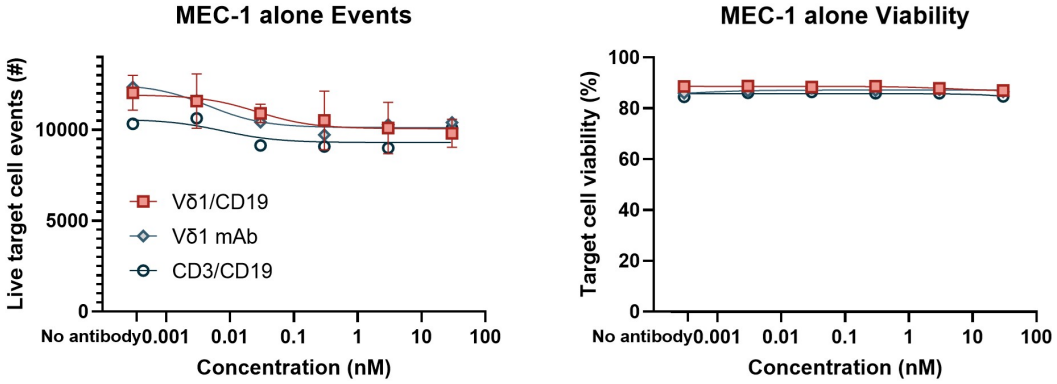


Figure 4.24: ***Vδ1/CD19 treatment does not induce MEC-1 cell death without Vδ1 T-cell presence.***

Remaining live MEC-1 cells following culture alone with specified engager treatment for 24 hours assessed using flow cytometry. Bars indicate SD where two technical replicates were conducted. Each event represents a single live MEC-1 cell recorded on the flow cytometer. Left, Live MEC-1 events. Right, percentage of live MEC-1 cells identified using the dead cell dye efluor780.

As non-specific binding was previously assessed, it is likely that the enhanced PBMC cytotoxic response is Vδ1 specific. Using Vδ1 T-cells isolated from PBMCs to assess Vδ1/CD19-mediated cytotoxicity would have been a more accurate assay to assess specific Vδ1 responses; however, this was attempted unsuccessfully. The absolute numbers obtained from Vδ1 isolation were very low due to the small fraction of the peripheral Vδ1 population alongside cellular loss during FACS isolation. FACS isolation *was* successful during later studies (see Section 4.4.2.3), however, fewer cell numbers were acceptable in such an assay whereas greater cell numbers were required here for a suitable E:T and a full engager titration. As this assay method was unreliable, it was decided to conduct the cytotoxicity assay with whole PBMCs as to not potentially waste the primary CLL PBMC samples. If more time was available, generating a more reliable protocol to assess isolated Vδ1 cytotoxicity would have been preferred.

Although CD3/CD19 prestimulation resulted in a stronger cytotoxic response (Figure 4.23), the enhanced cytotoxicity was comparable when normalised to the number of effector cells present (Figure 4.25). Furthermore, Vδ1/CD19 treatment demonstrated a safer toxicity profile (Figure 4.26). As discussed in the introduction, CD3 engagers are widely being investigated to treat a range of malignant indications, following suit from the FDA-approved CD3/CD19

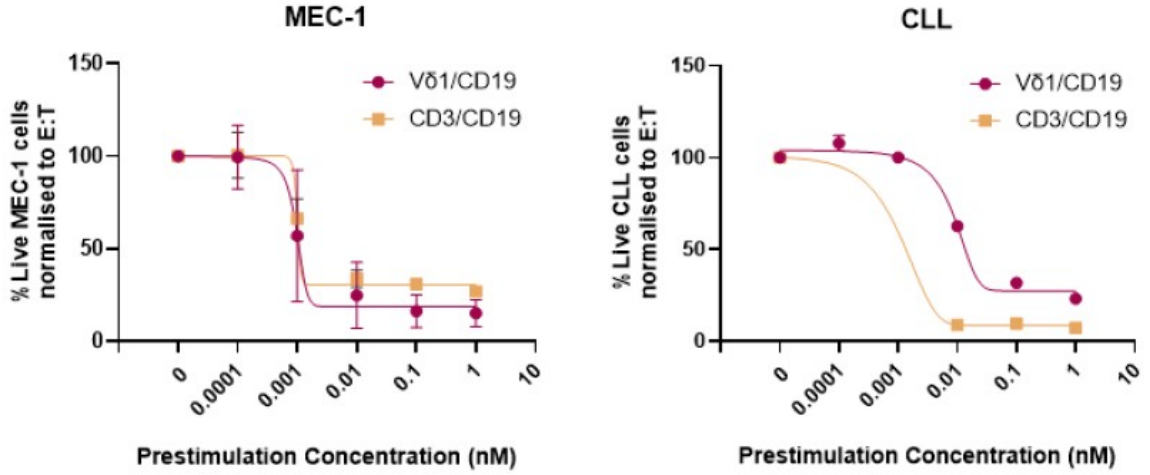


Figure 4.25: ***Vδ1/CD19 treatment enhances cytotoxicity comparably to CD3/CD19 when normalised to effector cell numbers***

Data from figure 4.23, susceptibility of CLL B-cells to engager-treated PBMCs assessed by flow cytometry, normalised to the number of engager-targeted effector cells. Left, PBMCs cultures (n=3) prestimulated for 6 days with Vδ1/CD19 and CD3/CD19 engagers were then assessed for cytotoxic capability where MEC-1 cells were added for 24 hours. Remaining live target cells were assessed after the 24 hours of culture. Live target cells presented as percentage fold change from live MEC-1 cells in non-prestimulated culture normalised to the E:T. Right, PBMCs cultures (n=1) prestimulated for 6 days with Vδ1/CD19 and CD3/CD19 engagers were then assessed for cytotoxic capability where isolated primary CLL B-cells (n=4) were added for 24 hours. Remaining live target cells were assessed after the 24 hours of culture. Live target cells presented as percentage fold change from live CLL cells in non-prestimulated culture normalised to the E:T.

Error bars represent SEM. For each donor, cell numbers from two technical replicates were first averaged, and these per-donor averages were used to calculate the normalised percentage change to plot the overall mean and SEM across all donors.

BiTE, Blinatumomab. Despite this widespread interest, CD3 engagers struggle to find a balance between efficacy and toxicity to the patient, often due to CRS. Therefore, to observe such differences, healthy PBMCs were treated with a CD3/CD19 engager and the Vδ1/CD19 engager over 7 days to compare resulting cell numbers and treatment-mediated cytokine release (Figure 4.26). As the Vδ1 population in PBMCs is smaller than the $CD3^+$ (Figure 4.26A), the Vδ1/CD19 engager treatment specifically only targeted the small Vδ1 population, whereas the CD3/CD19 engager targeted and induced proliferation of a greater T-cell population (Figure 4.26A). Whilst this broad T-cell targeting facilitated greater cytotoxic efficacy, it also resulted in an adverse cytokine release profile where CD3/CD19 stimulation greatly increased GZMB, IFNγ, IL-10, IL-17, Perforin and TRAIL, and decreased IL-2 in the absence of cancerous cells (Figure 4.26B).

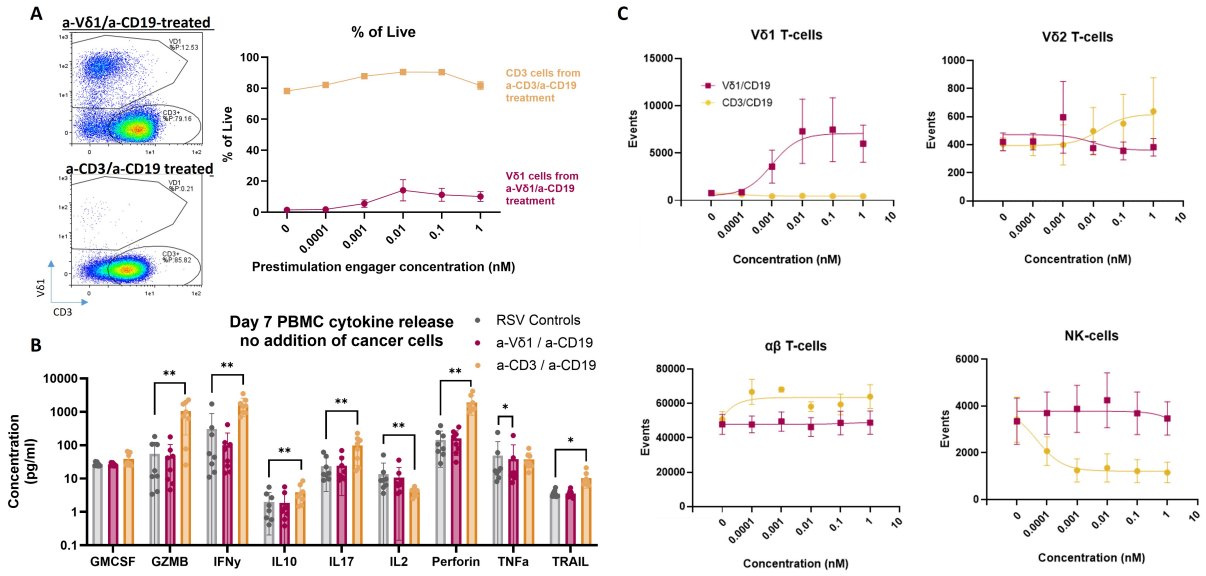


Figure 4.26: ***Vδ1/CD19 engager treatment targets Vδ1 T-cells allowing for controlled cytotoxic and proliferative response.***

(A) *Left, Representative flow plot of Vδ1 T-cell populations assessed by flow cytometry after 7 days prestimulation with 1nM Vδ1/CD19 engager (top) and CD3/CD19 engager (bottom) treatment. Right, Vδ1+ and CD3+ populations from the same PBMC cultures in 4.23A (n=3) following 7 days prestimulation with Vδ1/CD19 and CD3/CD19 engager treatments, respectively. Error bars represent SEM. For each donor, percentages from two technical replicates were first averaged, and these per-donor averages were used to plot the overall mean and SEM across all donors.* ***(B)*** *Cytokine release profile from whole PBMC cultures (n=8) following 7 days prestimulation with Vδ1/CD19 and CD3/CD19 engager treatments. Concentrations calculated from MSD standards (Method 3.18). Paired wilcoxon non-parametric statistical test performed against the RSV control-treated samples. Each asterisk (*) denotes a level of significance: $p < 0.05$, $p < 0.01$, $p < 0.001$, and $p < 0.0001$. Error bars denote SD.* ***(C)*** *Events of different cell populations in Vδ1/CD19-treated and CD3/CD19-treated PBMCs after 7 days in culture assessed by flow cytometry. Each event represents a single live cell recorded on the flow cytometer. Error bars represent SEM. For each donor, cell numbers from two technical replicates were first averaged, and these per-donor averages were used to plot the overall mean and SEM across all donors.*

Vδ1/CD19 stimulation importantly did not mediate overall IL-17 production (4.26B). IL-17 release is characteristic of pro-tumoural $\gamma\delta$ T-cells [177] so the absence of IL-17 suggests that Vδ1/CD19 engager-stimulated Vδ1 T-cells are not immunosuppressive and thus more likely to facilitate an anti-tumour response, however, Vδ1-specific release of IL-17 and TGF-β should be further investigated. CD3/CD19 prestimulation also affected the PBMC cell populations where NK cells were greatly reduced (Figure 4.26C). Despite increased Vδ2 and $\alpha\beta$ T-cells—that express CD3—a decrease in NK cells could be detrimental to overall anti-tumour responses

and general immune activity. Opposingly, a high fold increase in Vδ1 T-cell numbers (Figure 4.26A) did not facilitate an adverse cytokine release profile (Figure 4.26B) nor an adverse PBMC composition (Figure 4.26C) but was still able to increase the cytotoxic potential of PBMCs against MEC-1 and primary CLL cells (Figure 4.23). It should be noted that a statistically significant decrease in TNFα was recorded following Vδ1/CD19 treatment, however, the absolute decrease in TNFα was minimal and may not be as biologically relevant as the other differences observed.

4.2.5 Summary

This study thus far aimed to develop a Vδ1 engager that specifically binds the Vδ1 TCR and the haematological leukaemic marker CD19, which would subsequently enhance Vδ1 cytotoxicity towards malignant CD19$^+$ cells. The BiTE format of the Vδ1/CD19 engager demonstrated ability to specifically bind both epitopes in individual cell cultures, as well as mixed co-cultures. The engager sufficiently engaged the TCR when CD19 was present which resulted in Vδ1 T-cell activation and subsequent cytotoxicity towards CD19$^+$ target cells. Furthermore, the engager was able to induce proliferation of PBMC-based Vδ1 T-cells, with available CD19 expressed by healthy CD19$^+$ B-cells. Overall, these results have satisfied the first aim of this study—outlined in Chapter 2—to establish a Vδ1/CD19 engager that can be used to further investigate the potential for Vδ1 engagers to treat haematological malignancies.

4.3 Identification of Vδ1 receptors involved in cancer cell recognition

This study aims to investigate how Vδ1 engagers can enhance the effector and anti-tumor functions of Vδ1 T-cells through co-receptors. At this stage, a functional Vδ1 engager has been successfully generated. The final objective of this study aims to explore the mechanisms by which the engager enhances Vδ1 cytotoxicity, but before this can be done, how Vδ1 T-cells recognize cancer cells must first be explored. As discussed in the introduction, the mechanisms by which Vδ1 T-cells recognize stressed or malignant cells are not yet fully understood; therefore, *this* results section aims to deepen the understanding of how Vδ1 T-cells recognise their targets through co-receptors before further examining the effects of the engager.

4.3.1 Target cell phenotyping

The literature suggests that Vδ1 T-cells can distinguish between healthy and stressed or malignant cells. To evaluate their recognition of CD19$^+$ B-cells, cytokine-expanded blood-derived Vδ1 T-cells were cultured with both healthy and CLL B-cells, and the number of surviving target cells was measured. However, the resulting target cell counts from co-cultures with healthy and CLL B-cells did not differ (Figure 4.27A), indicating that this Vδ1 T-cell model might not effectively differentiate between healthy and cancerous B-cells. This inability may be due to the cytokine stimulation during the Vδ1 T-cell expansion process, leading to high baseline cytotoxicity that masks discrimination between cell types.

Interestingly, when treated with the engager, CLL B-cells showed greater susceptibility to Vδ1 cytotoxicity over healthy B-cells (Figure 4.27B). In this setup, primary CLL B-cells, as well as Nalm-6 and Reh cells, were killed more than healthy B-cells. The engager might enhance Vδ1 T-cell cytotoxicity by promoting stress ligand recognition rather than relying on baseline activity. This suggests that Vδ1 T-cells can differentiate between healthy and cancerous cells, though further optimization using PBMC-based Vδ1 T-cells would have better explore this capability.

To investigate the different phenotypes and stress ligands that healthy and CLL B-cells may be expressing to facilitate Vδ1 recognition, mRNA transcripts from healthy and CLL B-cells were assessed using the nCounter technology from Nanostring (Figure 4.28). mRNA transcripts of housekeeping genes and additional engineered transcripts were assessed as controls to ensure the quality and reliability between samples (Appendix 8.4).

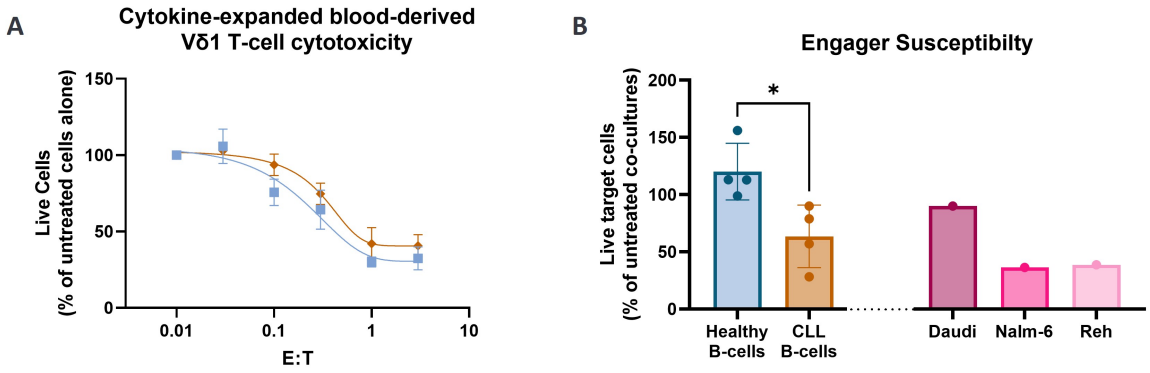


Figure 4.27: ***CLL B-cells are more susceptible than healthy B-cells to Vδ1 cytotoxicity when treated with Vδ1/CD19.***

Susceptibility of B-cells to blood-derived cytokine-expanded Vδ1 T-cells assessed by flow cytometry. ***(A)*** *Remaining live primary B-cells after 24 hours culture with cytokine-expanded blood-derived Vδ1 T-cells. B-cells were negatively isolated from healthy (n=4) and CLL (n=4) PBMCs. E:T (effector : target) represents the ratio of Vδ1 T-cells to target B cells in each culture. Data is normalised to the number of untreated B-cells from each individual donor. Error bars represent SEM. For each donor, cell numbers from two technical replicates were first averaged, and these per-donor averages were used to calculate the percentage live cells and plot the overall mean and SEM across all donors.* ***(B)*** *Remaining live primary B-cells (left) and CD19$^+$ cell lines (right) after 24 hours culture with cytokine-expanded blood derived Vδ1 T-cells and 100pM Vδ1/CD19 engager treatment. Primary B-cells were negatively isolated from healthy (n=4) and CLL (n=4) PBMCs. Vδ1 T-cells were added to target B cells at a 1:1 E:T. B-cell susceptibility to Vδ1/CD19 engager treatment is represented by the number of remaining live target cells from co-cultures treated with engager normalised to the number of remaining live target cells from untreated co-culture from each individual donor. Error bars represent SD. Statistics by unpaired student's t-test, * indicates $p < 0.05$.*

Differential expression analysis comparing healthy and CLL B-cell transcriptomes revealed that CLL B-cells express higher levels of apoptotic genes, such as caspase 3 and caspase 8 (Figure 4.28A). This observation suggested that cancerous B-cells may be more susceptible to effector cell-mediated apoptosis. Caspase 8, for instance, is activated in response to death receptor-mediated cytotoxicity. Effector cells, such as Vδ1 cells, can express death ligands like Fas-L, which can thus activate caspase 8 and subsequently activate caspase 3. This finding aligns with the higher expression levels of TNFRSF1A and TNFRSF10B genes observed in CLL cells (Figure 4.28B); these genes encode death receptors TNFR and TRAILR, which bind to effector cell-produced TNF-α and TRAIL, respectively, to induce apoptosis. This greater expression of apoptotic receptors further suggests that CLL B-cells may be more susceptible to effector Vδ1-directed responses.

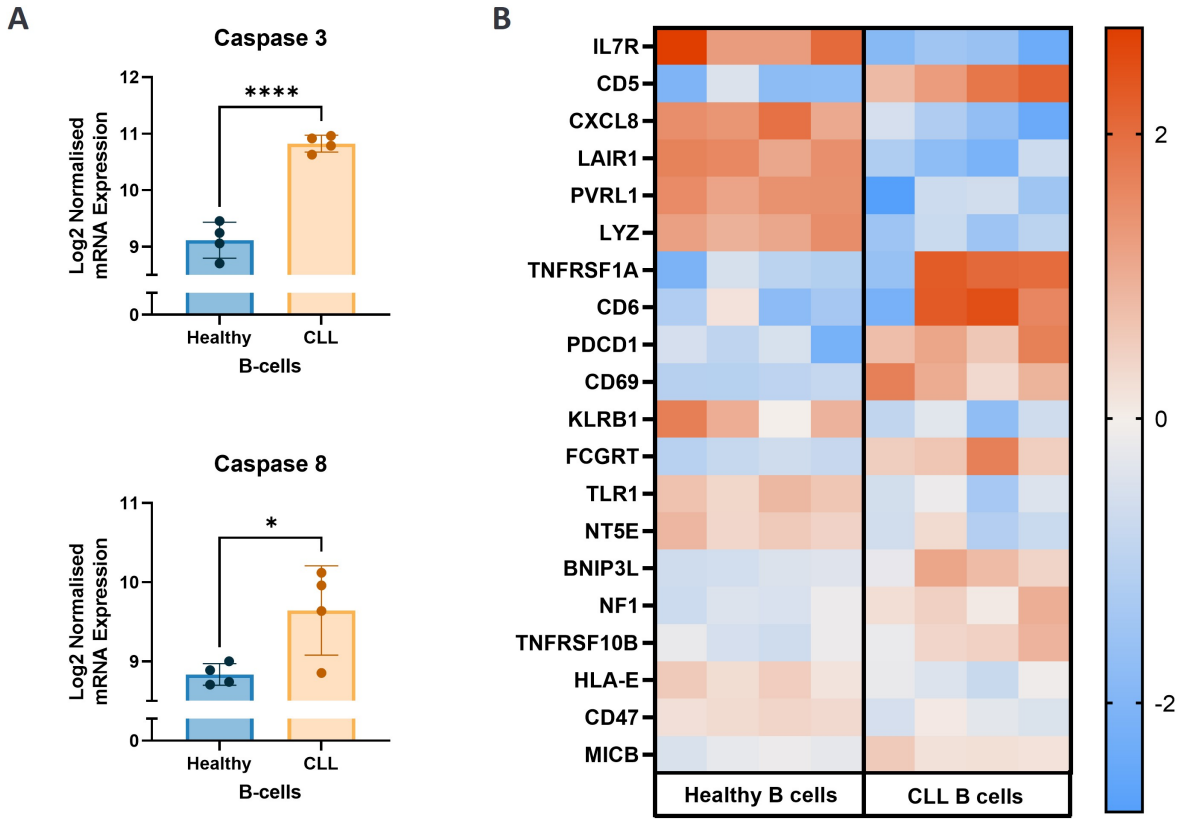


Figure 4.28: ***Healthy and CLL B cells differentially express membrane-expressed and apoptotic-associated genes.***

Healthy versus CLL primary B-cell RNA expression differences assessed using Nanostring technologies. ***(A)*** *RNA expression levels of IDO, caspase 3 and caspase 8 genes from primary healthy (n=4, blue) and primary CLL B cells (n=4, orange). An unpaired student's t test was performed to calculate significance p-values when comparing expression levels to those of healthy B cells. Each asterisk (*) denotes a level of significance:* $p < 0.05$, $p < 0.01$, $p < 0.001$, *and* $p < 0.0001$. *Error bars represent SD.* ***(B)*** *Differentially expressed genes of membrane-bound proteins from primary healthy (n=4) and primary CLL (n=4) B cells represented as [log2(sample RNA counts) – average(log2(total RNA counts))] per gene, with greatest differentially expressed genes ordered from top to bottom.*

Other genes encoding cell surface-bound proteins were also more highly expressed in CLL cells compared to healthy cells (Figure 4.28B). CD5, a marker frequently used to characterize CLL B-cells [178], was expressed more in primary CLL B-cells. Furthermore, MICB expression was elevated in CLL cells, suggesting a potential mechanism for activating Vδ1 cell cytotoxicity via the activating receptor NKG2D. Despite expressing lower levels of the T-cell inhibitory gene PD-L1, healthy B cells exhibited higher expression of another inhibitory ligand HLA-E, which could regulate Vδ1 cytotoxicity. While other gene expression differences may also influence the

differential Vδ1 T-cell response, this analysis primarily focused on proteins implicated in T-cell or NK-cell effector cytotoxicity based on current literature.

The cell lines assessed above displayed differential responses to engager-stimulated cytokine-expanded blood-derived Vδ1 T-cells (Figure 4.27B), where Nalm-6 and Reh cells were more susceptible to treatment over primary cells as well as, interestingly, Daudi cells. To understand and uncover proteins that may facilitate this differential response, these cancer cell lines were also assessed for RNA expression (Figure 4.29). To note, the Daudi cells used in this experiment had a low viability (Appendix 8.5). In hindsight, this experiment should have been repeated, thus serious conclusions were not taken from this cytotoxicity experiment. Despite these suboptimal conditions, the phenotypic differences observed when comparing these cells were confirmed later with suitably viable cells (Figure 4.31). Whilst the setup for this cytotoxicity experiment was essentially flawed, the proteins identified from these comparisons were later found to be of interest. Therefore, it was deemed necessary to highlight these experiments to indicate the thought-process.

Unfortunately, at the time of transcriptome analysis, the CLL cell line MEC-1 was not available; however, four different CD19$^+$ cell lines were assessed for RNA expression, and flow cytometry analysis of all cell lines, MEC-1 inclusive, was later conducted to maintain continuity.

When comparing the overall RNA content of all cell types assessed, the primary cells, both healthy and CLL B-cells, clustered separately from the cell lines assessed (Figure 4.29A). Furthermore, Nalm-6 and Reh cells are both CD19$^+$ models of acute lymphoblastic leukemia (ALL) whereas Daudi cells are from Burkitt's Lymphoma which was evident by separate clustering of these two disease types (Figure 4.29A). The previously identified MICB and HLA-E were also differentially expressed in the cell lines when compared to primary CLL and healthy B-cells (Figure 4.29B). The cell lines showed higher MICB and lower HLA-E expression, exaggerating the CLL expression profile. This further highlights the potential roles of these ligands in Vδ1 T-cell function. Differential expression was also observed of the indoleamine 2,3-dioxygenase gene IDO (Figure 4.29B). IDO protein is a secreted ligand that has previously demonstrated regulatory activity towards effector $\gamma\delta$ T-cells [135], which could, in addition to HLA-E, represent potential mechanisms for reduced Vδ1 cytotoxicity towards healthy B-cells over cancerous B-cells.

When comparing the differences between the ALL cell lines and primary B-cells, Reh and Nalm-6 cells most notably expressed fewer genes for T-cell costimulatory proteins than healthy B-cells (Figure 4.29C). This was interesting as it could suggest that T-cell-associated costimulatory proteins could also be involved in the Vδ1 T-cell response. Of note, CD80 and CD86 (which

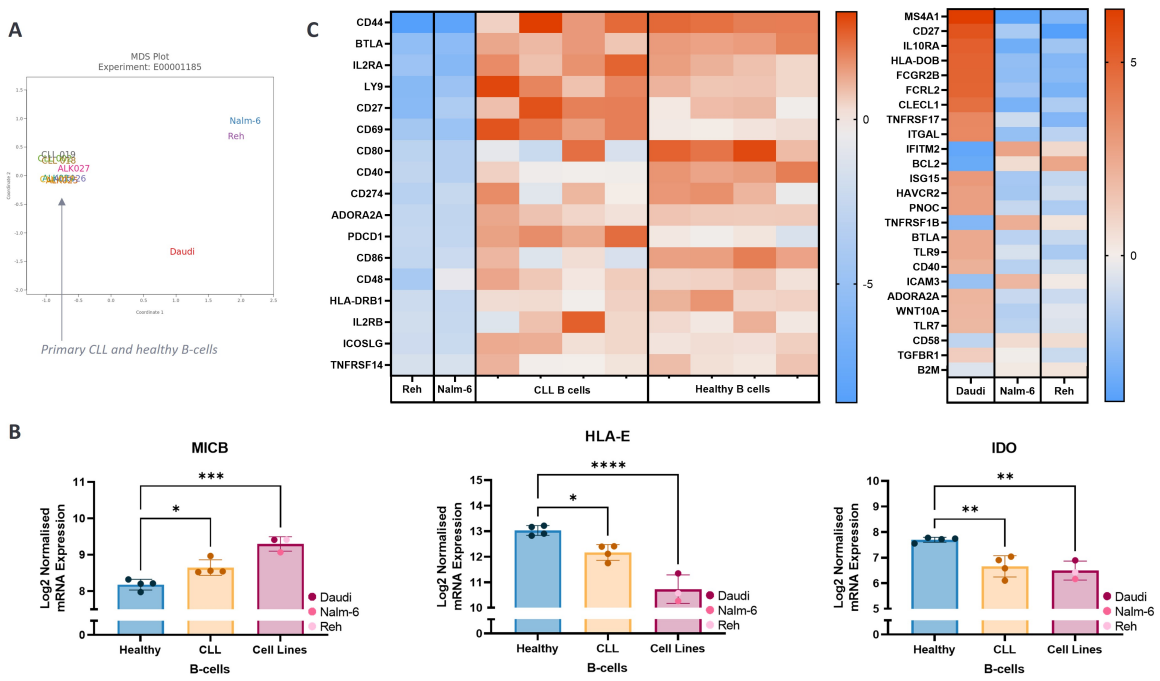


Figure 4.29: ***Cancer B-cell lines and primary B cells differentially express genes encoding for membrane-bound and costimulatory-associated proteins.***

B-cell RNA expression differences assessed using Nanostring technologies. ***(A)*** *MDS plot to represent similarities between total RNA signatures from all healthy (n=4), primary CLL B cells (n=4) and CD19+ cell lines.* ***(B)*** *RNA expression levels of Vδ1 and NK receptor-related genes were assessed in primary healthy B cells (n=4, blue), primary CLL B cells (n=4, orange), and three CD19+ cell lines: Daudi, Nalm-6, and Reh (pink). RNA counts were normalized to housekeeping gene counts and subsequently transformed using a log2 scale (log2[sample RNA counts]). A one-way ANOVA was performed to calculate significance p-values when comparing expression levels to those of healthy B cells. Each asterisk (*) denotes a level of significance: $p < 0.05$, $p < 0.01$, $p < 0.001$, and $p < 0.0001$.* ***(C)*** *Differentially expressed genes of membrane-bound proteins (left) and costimulatory proteins (right) from primary healthy (n=4), primary CLL (n=4) B cells and CD19+ cell lines represented as [log2(sample RNA counts) – average(log2(total RNA counts))] per gene, with greatest differentially expressed genes ordered from top to bottom. Error bars represent SD.*

can bind to the regulatory CTLA-4 receptor as well as CD28), PD-L1 (CD274) and TNFRSF14 (which binds to the inhibitory receptors BTLA and CD160) could highlight potential mechanisms for reduced Vδ1 cytotoxicity. Interestingly, the ligands, CD48, ICOSLG, and CD44, associated with activatory receptors, were also expressed less in the cell lines suggesting that these cell lines express other ligands that are sufficient to activate Vδ1 T-cells. The role of these proteins will be explored in more detail later.

As Daudi cells did not appear to be affected by Vδ1/CD19 stimulated Vδ1 T-cells (Figure

4.27B), differential transcriptomes between Daudi and the ALL cell lines may highlight essential Vδ1 T-cell pathways (Figure 4.29C) [2]. While there were few differences, it was notable that ICAM3 and CD58 (LFA-3) were significantly less expressed in Daudi cells compared to Nalm-6 and Reh, suggesting an activatory role for ICAM-3 and LFA-3 on Vδ1 T-cell function.

All gene-expressions identified above were consolidated to provide a resource for the remainder of this study (Figure 4.30A). Corresponding binding ligand/receptors were identified from the literature and detailed alongside the consolidated gene-expression list. Additionally, to incorporate existing knowledge from the literature, other Vδ1 T-cell associated co-receptors were also detailed (Figure 4.30B).

RNA sequencing can be useful to identify differential gene expression, however, the number of RNA transcripts does not always correlate to expression of functional proteins. Therefore, expression of the identified proteins was assessed on the primary B-cells and cell lines using flow cytometry (Figure 4.31). Despite significant transcriptome distinctions, the phenotypic differences between primary healthy and primary CLL B-cells were few on the protein level. LFA-3 expression and CD5 expression (Figure 4.31A) were the two most notable differences. LFA-3 is the ligand for CD2 which plays a role in T-cell activation by stabilising the immunological synapse between the T-cell and target cell [179]. It is interesting that CLL B-cells may express more LFA-3 than healthy B-cells as it suggests that CLL B-cells may facilitate Vδ1 T-cell activation through the LFA-3/CD2 pathway. Despite this, healthy B-cells still largely express LFA-3 so reactivity to varying levels of LFA-3 would need to be assessed further.

CD5 was only detected on the surface of CLL B-cells, and not healthy B-cells. Despite being a CLL marker, CD5 could also indicate another mechanism for the increased cytotoxicity of Vδ1 T-cells. For example, target cell CD5 can bind CD5 on canonical T-cells, and if CD5 is not bound by its ligands, T-cell CD5 will translocate to the immunological synapse with the TCR to modulate TCR signalling [180]. Therefore, with greater CD5 expression on CLL cells, less CD5 may be available to dampen TCR signalling, thus improving Vδ1 T-cell activation.

As the primary CLL differences were subtle, CD19$^+$ cell lines may provide a more useful model to highlight the role of other stress-ligands (Figure 4.31B). MEC-1 cells expressed nearly all of the chosen ligands with the exception of the NKG2D ligands ULBP1 and ULBP3, the DNAM-1 and CD96 ligands PVR and CD5, and TRAILR2. This greater stress ligand expression corresponded to increased susceptibility of MEC-1 cells to Vδ1 cytotoxicity, in the absence

[2] Whilst the viability of the Daudi cells was not acceptable in the cytotoxicity assay, the involvement of such differentially expressed proteins are explored later in more suitable conditions.

A

Differentially expressed genes between:

Primary healthy vs primary CLL B cells

Ligand/receptor identified on CD19+ cells	Corresponding receptor/ligand on Vδ1 T-cells
HLA-E	NKG2A KLRD1 (CD94)
MICB	NKG2D
TNFRsf10b	TRAIL
TNFRsf1a	TNFa
CD5	CD5
PD-L1	PD-1
PVRL1 (Nectin1)	CD96 (acts similarly to DNAM-1)

Primary vs Nalm-6 and Reh

Ligand/receptor identified on CD19+ cells	Corresponding receptor/ligand on Vδ1 T-cells
CD44	CD44
LY9	LY9
CD80	CD28/CTLA-4
CD86	CD28/CTLA-4
ICOSLG	ICOS

Daudi vs Nalm-6 and Reh

Ligand/receptor identified on CD19+ cells	Corresponding receptor/ligand on Vδ1 T-cells
CD58 (LFA-3)	CD2
ICAM-3	CD11a (part of LFA-1)

B

Other Vδ1- and γδ-associated receptors from the literature:

Vδ1 receptors	Corresponding Ligand(s)
NKG2D	MICA/B ULBP1/2/5/6
CD96	Nectin-1 PVR
DNAM-1	Nectin-2 PVR
2B4	CD48
NKp30	B7-H6
NKp44	NKp44L
NKp46	Unknown tumour-associated ligands

Figure 4.30: ***Identified co-receptors and corresponding ligands potentially capable of regulating the Vδ1 cytotoxic response.***

(A) *Selected key ligand/receptors from differential expression analysis, triaged using suggested roles from literature.* ***(B)*** *Other Vδ1 co-receptors and corresponding ligands that have been suggested to regulate Vδ1 effector cytotoxicity in published literature.*

of Vδ1/CD19 (Figure 4.32). To note, MEC-1 cells may therefore express a more exaggerated phenotype of primary CLL B-cells, thus their use in subsequent assays, whilst informative, would need to be followed up with primary cells to provide more accurate conclusions.

The minimal variations observed between healthy and CLL B-cells may indicate a potential

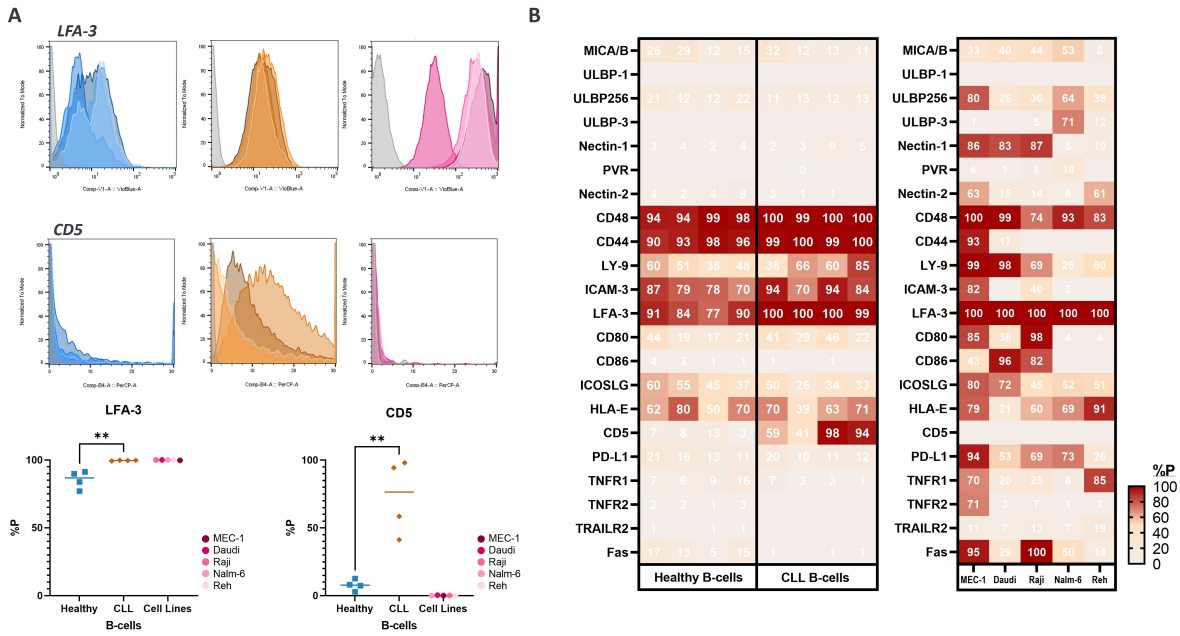


Figure 4.31: ***CD19$^+$ cell line protein expression validation of ligands potentially capable of initiating Vδ1 cytotoxic response.***

B-cell protein expression differences assessed using flow cytometry. ***(A)*** *Expression of LFA-3 and CD5 on isolated primary healthy (blue, n=4) and CLL (orange, n=4) B-cells and CD19$^+$ cell lines (pink) presented as flow cytometry histograms (top) and percentage of cells expressing marker (bottom). An unpaired student's t test was performed to calculate significance p-values when comparing expression levels to those of healthy B cells. Each asterisk (*) denotes a level of significance: $p < 0.05$, $p < 0.01$, $p < 0.001$, and $p < 0.0001$.* ***(B)*** *Percentage of cells expressing the proteins from the list 4.30 presented in a heat map of primary cells (left) and cell lines (right).*

limitation in the method used to identify differential phenotypes. The underlying hypothesis for this method was that CLL B-cells would express stress-related ligands that healthy B-cells would not. Thus, a sample size of *n=4* should have been sufficient to detect ligands that are either completely expressed or absent. However, it appears that healthy B-cells also express these ligands. Cancerous B-cells may alter their phenotypes in more subtle ways, but these changes might only be apparent when compared to healthy B-cells from the same individual. Therefore, any differences between healthy and cancerous B-cells may only be detectable through within-patient comparisons. This individual shift in stress-related phenotypes could be what the patient's Vδ1 T-cells are responding to. Since cancerous B-cells can dominate the peripheral B-cell population, it becomes challenging to distinguish in the lab between healthy and cancerous cells from a patient's blood sample. To distinguish these two B-cell types more accurately and reliably, a larger sample size would have been necessary. A greater *n* number could have highlighted dysregulated signatures in cancerous cells, with more significant variation in altered

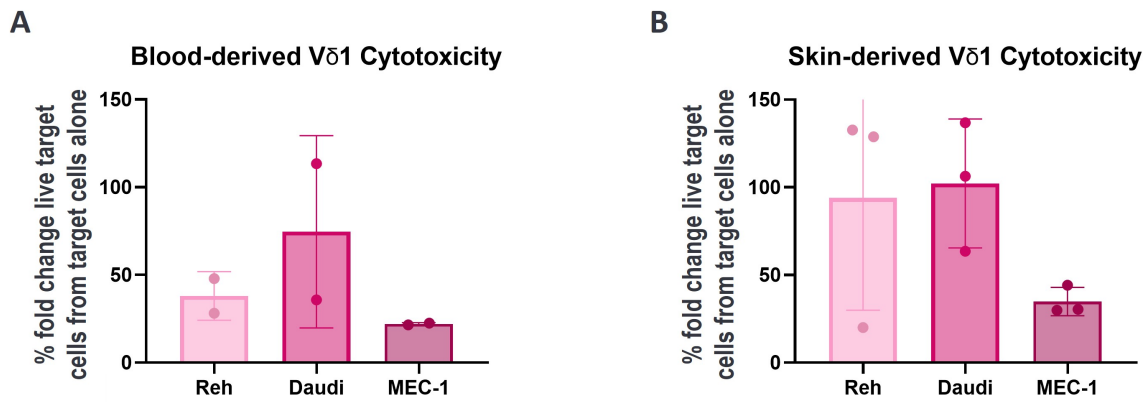


Figure 4.32: ***CD19$^+$ cell line susceptibility Vδ1 cytotoxic response.***
CD19+ Cell line susceptibility to Vδ1 T-cells assessed by flow cytometry. ***(A)*** *Remaining live target cells after 24 hours of culture with cytokine-expanded blood-derived Vδ1 T-cells presented as a percentage of target cells cultured alone.* ***(B)*** *Remaining live target cells after 24 hours of culture with cytokine-expanded skin-derived Vδ1 T-cells presented as a percentage of target cells cultured alone.*
Bars represent SD with two technical replicates.

stress ligand expression as opposed to simply *'yes-or-no'* expression. Therefore, retrospectively more donors should have been assessed but with the data available, both RNA and protein expression patterns will be investigated further.

Overall, this list of potential ligands provided a useful resource to reference throughout the project and will be referred back to in subsequent sections.

4.3.2 Vδ1 T-cell models

To identify Vδ1 T-cell co-receptors involved in the cytotoxic response, expression of the proteins from figure 4.30 were assessed on all Vδ1 T-cell models used using flow cytometry (Figure 4.33). See Appendix 8.6 for representative flow plots of these expression profiles. As explored in the introduction, Vδ1 T-cells can be categorised into naive and effector phenotypes based on CD27 expression, where high CD27 expression indicates a more naive and less cytotoxic Vδ1 T-cell. The CD27$^-$ and CD27$^+$ [3] Vδ1 phenotypes were assessed from PBMC-based Vδ1 T-cells to investigate which receptors corresponded to the effector and naive Vδ1 classifications (Figure 4.33A). This analysis highlighted greater granzyme B expression from the CD27$^-$ Vδ1 populations, as previously observed [54]. Additionally, greater expression of the typically activatory co-receptors DNAM-1 and 2B4 was detected on the effector CD27$^-$ cells, alongside greater expression of the typically regulatory co-receptors CD94 and CD5. It should be noted that CD5 and DNAM-1

[3]The Vδ1 T-cell subpopulations were gated on as CD27$^{-/low}$ and CD27^{high}, as shown in figure 4.21, but for ease in text, these subpopulations are also referred to as CD27$^-$ and CD27$^+$, respectively.

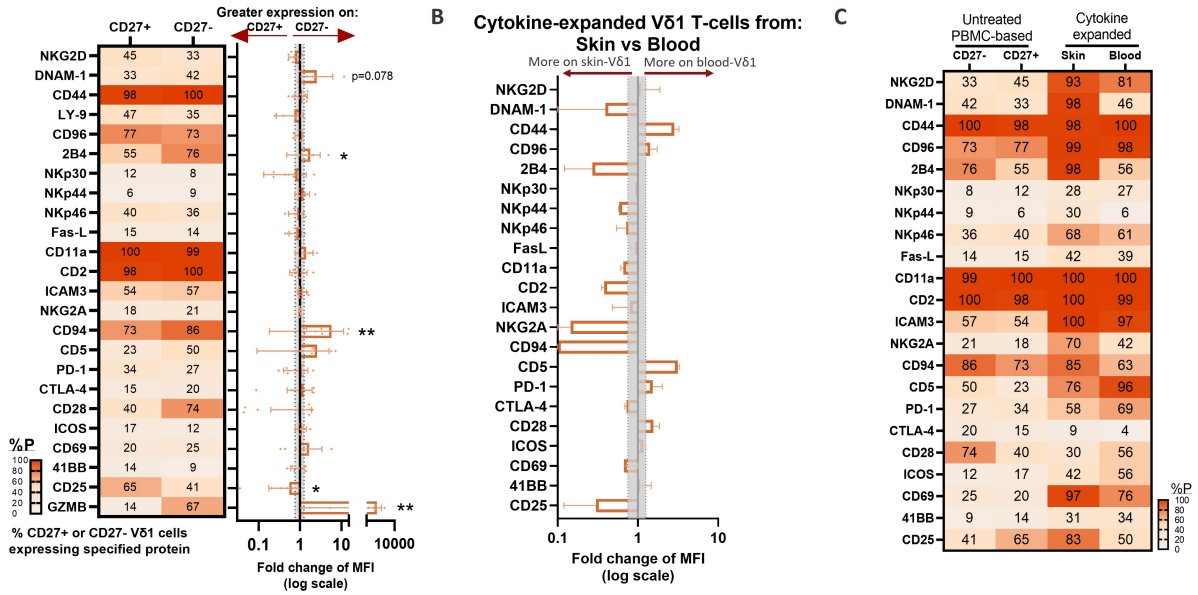


Figure 4.33: ***Protein expression by PBMC-based, blood or skin-derived Vδ1 T-cell populations.***

Selected protein expression by the PBMC-based, blood and skin-derived Vδ1 T-cell populations used throughout this study was assessed by flow cytometry. Error bars indicate SD. ***(A)*** *Vδ1 T-cell phenotype from PBMCs (n=8) analysed as CD27$^+$ and CD27$^-$ subpopulations. Left, comparing percentage of CD27$^+$ and CD27$^-$ Vδ1 T-cells expressing the specified proteins. Right, comparing MFIs of the specified proteins as fold change of CD27$^+$ to CD27$^-$ Vδ1 T-cells. Statistically significant MFI differences were calculated using paired wilcoxon test where each asterisk (*) denotes a level of significance: $p < 0.05$, $p < 0.01$, $p < 0.001$, and $p < 0.0001$.* ***(B)*** *Phenotype of cytokine-expanded skin-derived and blood-derived Vδ1 T-cells, presented as fold change MFI of specified protein expressed on blood-derived to skin-derived Vδ1 T-cells.* ***(C)*** *Vδ1 phenotype of each Vδ1 T-cell model used, comparing the percentage of the specified Vδ1 T-cells expressing the specified protein.*

were not significantly differentially expressed, they trended towards greater expression on the CD27$^-$ Vδ1 T-cells. More donors should be assessed to validate these differences. Overall, the Vδ1 T-cell phenotype highlights how the effector Vδ1 T-cells may respond to stress ligands with 2B4 whilst still maintaining self-regulatory capabilities with CD94 as to not contribute to immune-driven pathology.

In addition to PBMC-based Vδ1 T-cells, phenotypes of the cytokine-expanded Vδ1 T-cells were also assessed (Figure 4.33B and C). To understand the differences between the skin-derived and blood-derived cytokine-expanded Vδ1 T-cells, the percentage of marker expression was presented as fold change between the two Vδ1 T-cell models (Figure 4.33B). This analysis highlighted that the skin-derived Vδ1 T-cells expressed greater levels of DNAM-1, 2B4 and CD94 (similarly to the PBMC-based CD27$^-$ Vδ1 T-cells), as well as CD2, NKG2A and CD25.

Despite the skin-derived Vδ1 T-cells displaying a more cytotoxic phenotype, the blood-derived Vδ1 T-cells displayed greater basal cytotoxic capabilities than the skin-derived towards the CD19$^+$ cell lines (Figure 4.32). As explored in the introduction, tissue-resident Vδ1 T-cells display greater cytotoxicity to solid tumour targets over blood-resident Vδ1 T-cells, which could then imply that blood-derived Vδ1 T-cells are more equipped to respond to blood-based target cells. This specialised capability may then be facilitated by the receptors CD44, CD96, CD5 and CD28 which are expressed more on the blood-derived Vδ1 T-cells (Figure 4.33B).

Whilst CD27$^-$ PBMC-based Vδ1 T-cells expressed greater DNAM-1, 2B4, CD94, CD5 and granzyme B, and the expansion with cytokines and CD3 stimulation increased NKG2D, CD96, NKp30, NKp46, Fas-L, ICAM-3, NKG2A, CD5, PD-1, ICOS, CD69 and 41BB levels (Figure 4.33C), the increased co-receptor expression of the cytokine-expanded Vδ1 T-cells suggests that these co-receptors facilitate their greater cytotoxic potential and thus should be further explored.

4.3.3 Summary

B-cell transcriptomes and phenotypes were assessed to identify differentially expressed proteins that corresponded to differing Vδ1 cytotoxic susceptibilities. Primary B-cells from healthy and CLL-patients were included in this analysis, alongside CD19$^+$ cell lines. The complementary proteins that bind to the proteins identified from this analysis, as well as known $\gamma\delta$ T-cell co-receptors, were identified using literature search. Expression of these proteins was measured on the primary PBMC-based and cytokine-expanded Vδ1 T-cells used previously in this study. Phenotypic analysis revealed that Vδ1 T-cells express many of these co-receptors (Table 4.1) which could facilitate the activation of Vδ1 cytotoxicity and enable differential responses towards healthy and cancerous B-cells. The next sections will explore the role of these identified co-receptors in the context of Vδ1/CD19 engager treatment.

4.4 Engager-mediated Vδ1 Cytotoxicity

4.4.1 Engager-mediated Vδ1 phenotype

This study has demonstrated increased cytotoxicity from PBMCs that were treated with the BiTE Vδ1/CD19 engager (Figure 4.23). In this particular experimental design, the increased cytotoxicity could be attributed to the increase in Vδ1 T-cell numbers that this model facilitates (Figure 4.21). However, a greater Vδ1-to-target cell ratio does not necessarily mean increased cytotoxicity as Vδ1 T-cell proliferation mediated by the other bispecific antibody formats (Figure 4.16) ***did not*** correspond to increased target cell death (Figure 4.34).

Table 4.1: Identified co-receptors that may affect Vδ1 cytotoxicity

Vδ1 co-receptor	**Associated ligands**
NKG2D	ULBP1/2/3/5/6, MICA/B
DNAM-1	Nectin-2, PVR
CD44	Extracellular matrix components
CD96	Nectin-1, PVR
2B4	CD48
Fas-L	Fas
CD11a (part of LFA-1)	ICAM-3
CD2	LFA-3
NKG2A	HLA-E
CD94	HLA-E
CD5	CD5
PD-1	PD-L1
CTLA-4	CD80, CD86
CD28	CD80, CD86

The increased Vδ1/CD19 engager-mediated cytotoxicity may therefore not only be attributed to Vδ1 proliferation but also engager-mediated phenotypic changes of the Vδ1 T-cell. Accordingly, changes in cell-surface expression of Vδ1 T-cells in whole PBMC cultures were assessed, using flow cytometry, after 7 days with engager treatment (Figure 4.35 and 4.36). Results showed that CD27$^+$ Vδ1 T-cells significantly increased their expression of the typically activatory receptors NKG2D, DNAM-1, CD96, CD2 and ICOS, and reduced expression of the inhibitory T-cell receptor CTLA-4. This increased expression of activatory receptors and decreased expression of CTLA-4 could improve sensitivity of the activatory receptors to their respective ligands which in turn would facilitate Vδ1 activation. Interestingly, the inhibitory receptor PD-1 was *upregulated*,

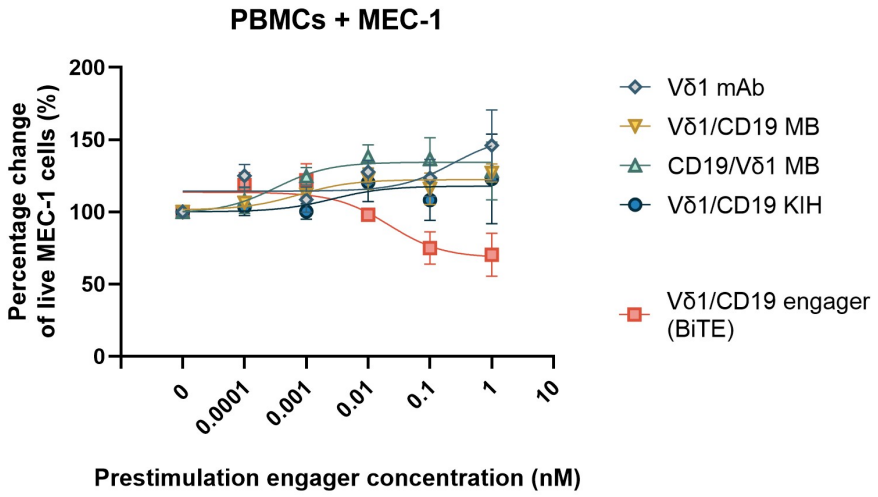


Figure 4.34: ***Engager-mediated PBMC cytotoxicity using different bispecific formats.*** *Cytotoxicity of PBMCs cultures (n=3) prestimulated for 7 days with different formats of Vδ1/CD19 engagers against MEC-1 cells where remaining live target cells was assessed after 24 hours of culture using flow cytometry. Live target cells presented as percentage fold change from live MEC-1 cells in non-prestimulated culture. Error bars represent SEM. For each donor, cell numbers from two technical replicates were first averaged, and these per-donor averages were used to calculate the percentage change and plot the overall mean and SEM across all donors.*

though PD-1 has previously been associated with a more effector-like Vδ1 phenotype [100]. This could suggest that PD-1 upregulation occurs to regulate a more activated Vδ1 T-cell in a similar vain to the CD94 and CD5 expressed on homestatic CD27$^-$ Vδ1 T-cells (Figure 4.33A). The increased cytotoxic capability and greater activatory receptor expression and PD-1 upregulation on the naive CD27$^+$ Vδ1 T-cells following Vδ1/CD19 engager treatment suggests that the engager may encourage Vδ1 maturation from a naive to effector state.

On the other hand, CD27$^-$ Vδ1 T-cells did not upregulate any receptors in response to Vδ1/CD19 treatment in a normal setting. These cells instead downregulated the typically activatory receptors 2B4, CD11a and CD2 (Figure 4.35). However, when activated with cancerous cells in the culture, they increased expression of granzyme B (Figure 4.37).

It should be noted that after the 7-day priming of these PBMCs, some non-cancerous B-cell death was observed in these cultures (data not shown). The observed cell death could be attributed to a percentage of these B-cells expressing stress ligands due to the *in vitro* culture conditions. However, to confirm whether these B-cells were healthy or stressed, additional experiments should have been conducted, such as incorporating Annexin V and PI into the flow panel to identify apoptotic cells.

The CD27$^-$ response differed from the CD27$^+$ Vδ1 T-cells where engager stimulation perhaps

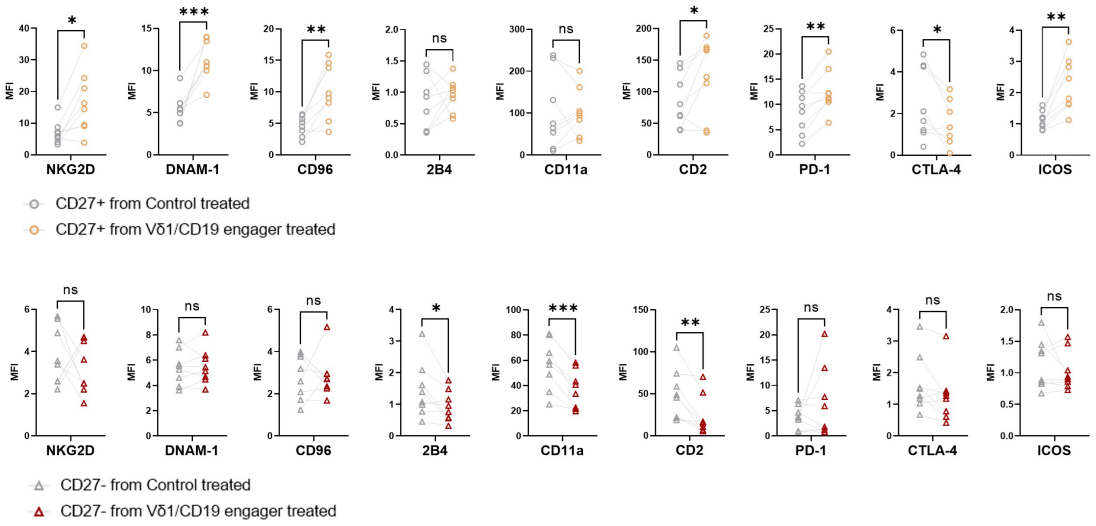


Figure 4.35: ***Vδ1/CD19 engager treatment affects Vδ1 T-cell phenotype***

$CD27^+$ and $CD27^-$ Vδ1 T-cell phenotype after 7 days in whole-PBMC culture (n=8) treated with control (RSV BiTEs) and 100pM Vδ1/CD19 engager assessed by flow cytometry. Expression of each surface marker presented as averaged MFI values per donor. A paired student's t test was performed to calculate significance p-values when comparing expression levels to those of control treated PBMCs. Each asterisk (*) denotes a level of significance: $p < 0.05$, $p < 0.01$, $p < 0.001$, and $p < 0.0001$.

primes or initiates maturation of $CD27^+$ Vδ1 T-cells but have not induced a full effector phenotype, indicated by the increased levels of CD27 expression (Figure 4.38) alongside no marked increase in granzyme B expression (Figure 4.37). Interestingly, Vδ1/CD19-treated $CD27^+$ Vδ1 T-cells downregulated CD45RA (Figure 4.39) which could further support the idea that engager treatment is priming the naive Vδ1 T-cells as decreased CD45RA suggests a memory-like T-cell phenotype [54]. Vδ1 T-cells may therefore only fully mature into memory effector-like cells in the presence of stressed or cancerous cells. This idea is supported by the phenotypic changes observed from both $CD27^+$ and $CD27^-$ Vδ1 T-cells when cultured with MEC-1 cells. These Vδ1 T-cells display fewer engager-mediated changes than without MEC-1 cells (Appendix 8.7) indicating that as these cells may be more effector-like—due to the cancerous cell presence—Vδ1 T-cells may need to maintain their co-receptor expressions whilst the target cells persist. It is interesting that the intrinsic Vδ1 reactivity to cancerous over healthy cells is maintained with engager-mediated Vδ1 TCR stimulation because like with canonical $\alpha\beta$ T-cells, the naive Vδ1 T-cells may still require some level of co-stimulation. This co-stimulation may be provided by the target cells for full activation where TCR stimulation alone may not be sufficient. The observation that Vδ1 granzyme B release and CD27 downregulation is not occurring in a non-cancerous setting is important, as the ability to maintain discrimination between healthy and

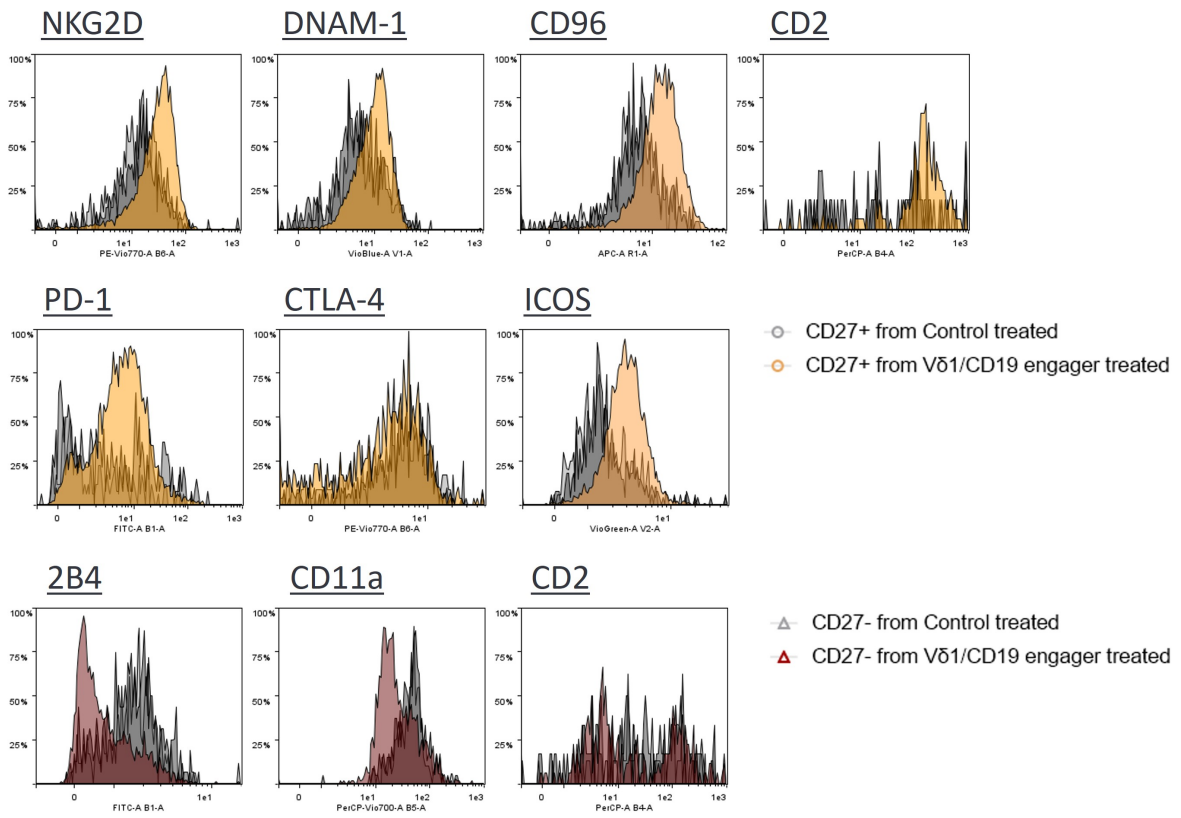


Figure 4.36: ***Representative histograms of affected Vδ1 T-cell phenotype following Vδ1/CD19 engager treatment.***

Co-receptor expression of $CD27^{high}$ (yellow) and $CD27^{low/-}$ (red) Vδ1 T-cell populations after 7 days in whole-PBMC culture (representative donor from n=8) treated with 100pM Vδ1/CD19 engager assessed by flow cytometry. Expression of indicated marker from control-treated (RSV BiTEs) samples is highlighted in grey.

cancerous cells following engager treatment could help to minimise adverse responses.

These engager-mediated phenotypic differences may highlight receptors that are involved in Vδ1 activation to allow the increase in cytotoxic function that was observed. The $CD27^{+}$ Vδ1 changes suggested a primed Vδ1 T-cell phenotype in a healthy context, characterised by CD45RA, NKG2D, DNAM-1, CD96, CD2, PD-1 and ICOS upregulation and CTLA-4 downregulation. The $CD27^{-}$ Vδ1 changes suggested a limiting of effector function in a healthy context through the downregulation of 2B4, CD11a and CD2. The role of these receptors, potentially as co-receptors to engager-mediated TCR stimulation, will be further investigated in the next section to explore how engager-mediated TCR stimulation can enhance the Vδ1 effector capabilities.

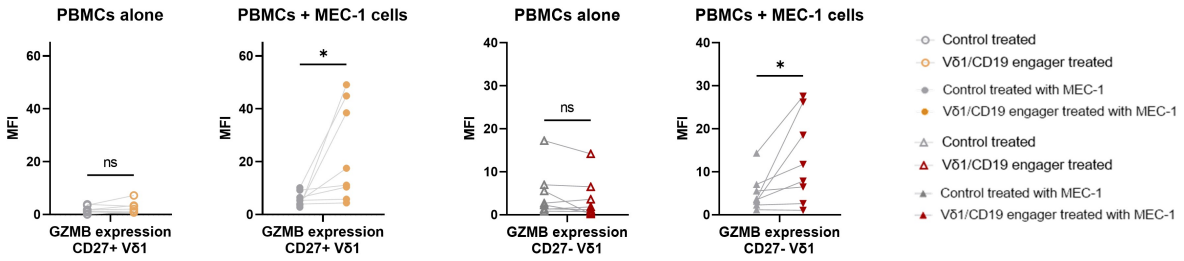


Figure 4.37: ***Vδ1/CD19 engager treatment promotes granzyme B upregulation only in a cancerous context.***

$CD27^+$ (yellow circles) and $CD27^-$ (red triangles) Vδ1 T-cell intracellular expression of granzyme B, assessed by flow cytometry, after 7 days in whole-PBMC cultures (n=8) with and without MEC-1 cells, treated with control (RSV BiTEs) and 100pM Vδ1/CD19 engager. Expression is presented as averaged MFI values per donor. A paired student's t test was performed to calculate significance p-values when comparing expression levels to those of control treated PBMCs. Each asterisk (*) denotes a level of significance: $p < 0.05$, $p < 0.01$, $p < 0.001$, and $p < 0.0001$.

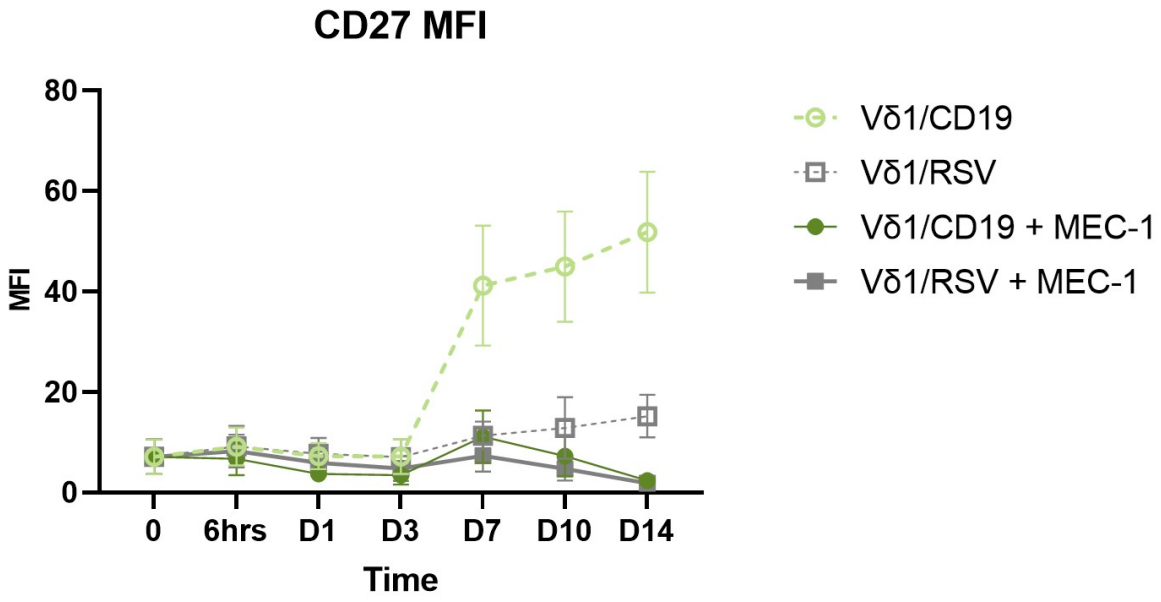


Figure 4.38: ***CD27 expression on Vδ1 T-cells with Vδ1/CD19 engager treatment.***

Vδ1 T-cell expression of CD27 over 14 days in whole-PBMC cultures (n=8) treated with control and 100pM Vδ1/CD19 engager and with and without MEC-1 cells, assessed by flow cytometry. 100pM of engager and MEC-1 cells were added at day 0 and again after day 7. Expression is presented as averaged MFI values of each donor. Error bars represent SEM, with one technical replicate.

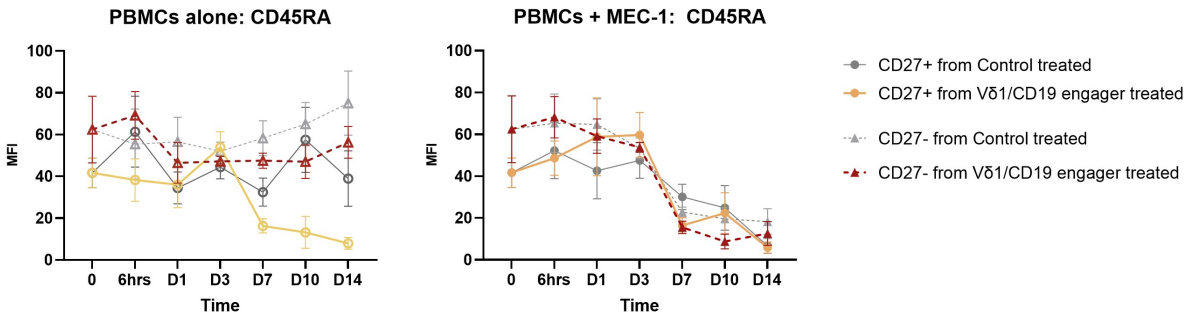


Figure 4.39: ***CD45RA expression on Vδ1 T-cells with Vδ1/CD19 engager treatment.*** *$CD27^+$ and $CD27^-$ Vδ1 T-cell expression of CD45RA over 14 days in whole-PBMC cultures (n=8) treated with control and 100pM Vδ1/CD19 engager and with and without MEC-1 cells, assessed by flow cytometry. 100pM of engager and MEC-1 cells were added at day 0 and again after day 7. Expression is presented as averaged MFI values per donor. Error bars denote SEM, with one technical replicate.*

4.4.2 Co-receptor role in engager-mediated Vδ1 function

4.4.2.1 Proliferation

During proliferation assay development, different culture conditions were assessed where differing levels of proliferation were observed. Notably, Vδ1 T-cells seemed to proliferate well in PBMC alone cultures treated with engager, where Vδ1 T-cells are presumably cross-linking with healthy B-cells via CD19; but in co-cultures where Vδ1 T-cells would also be cross-linked to Nalm-6 cells, proliferation was reduced, and in co-cultures with MEC-1 cells, proliferation was greatly increased (Figure 4.40). This differing proliferative response suggested that different target cell phenotypes may facilitate or hinder Vδ1 engager-mediated proliferation of Vδ1 T-cells. When exploring the phenotypic differences between healthy B-cells, Nalm-6 and MEC-1 cells, the expression of CD44 and ICAM-3 varied, with Nalm-6 cells expressing considerably less CD44 and ICAM-3 (Figure 4.41). CD44 can bind to extracellular matrix components that in turn bind to CD44 expressed on other immune cells; and ICAM-3 binds LFA-1. Interestingly, CD44 and LFA-1 have previously been implicated in canonical T-cell immunological synapse stabilisation, which can facilitate TCR-mediated activation [119]. This correlation of CD44 expression on the target cell and the degree of engager-mediated proliferation does not indicate direct cause and effect as these cells could be expressing other proteins that are also affecting this proliferative response. Therefore, to investigate the potential role of CD44 within engager-mediated Vδ1 T-cell proliferation, PBMC cultures were cultured with Vδ1/CD19 and a CD44 neutralising antibody for 7 days before measuring Vδ1 events (Figure 4.42).

The addition of the CD44 neutralising antibody considerably reduced the level of engager-mediated Vδ1 T-cell proliferation. Increased proliferation was demonstrated by increased Vδ1

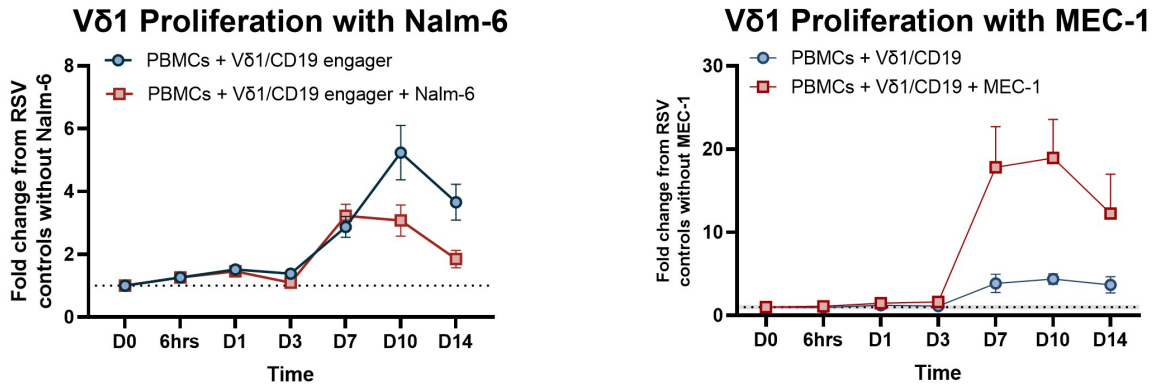


Figure 4.40: ***Vδ1 T-cells proliferate to different extents depending on the co-culture.***
Proliferation of PBMC-based Vδ1 T-cells cultured with Nalm-6 and MEC-1 cells, assessed by flow cytometry. Left, Vδ1 T-cell events assessed from PBMC cultures (n=3) with and without Nalm-6 cells following 100pM Vδ1/CD19 engager treatment over 14 days. Events were normalised to control-treated cultures. Right, Vδ1 T-cell events assessed from PBMC cultures (n=8) with and without MEC-1 cells following 100pM Vδ1/CD19 engager treatment over 14 days. Events were normalised to control-treated cultures. 100pM of engager and MEC-1 cells were added at day 0 and again after day 7.
Error bars represent SEM, with one technical replicate.

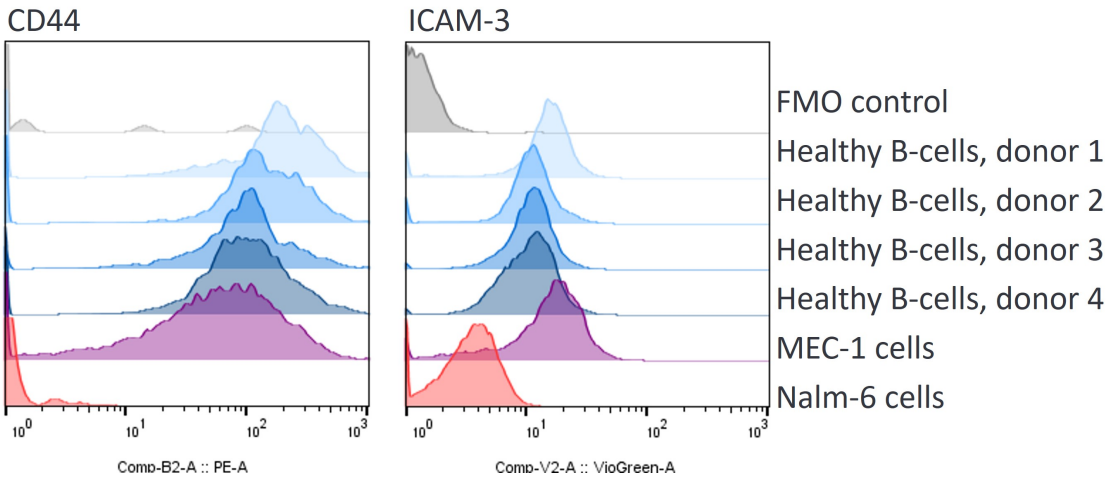


Figure 4.41: ***CD44 and ICAM-3 expression on MEC-1, Nalm-6 and healthy B-cells.***
Flow cytometry histograms displaying CD44 and ICAM-3 expression on MEC-1, Nalm-6 and isolated healthy B-cells.

events and reduced fluorescence from the proliferation dye CTV. In this assay design, the response observed suggests that Vδ1 T-cell proliferation may at least in part be dependent on the levels of functional CD44 within the immunological synapse. Further work would be required to investigate this hypothesis as well as the potentially linked role of ICAM-3 and LFA-1 in the immunological synapse. To note, an isotype control antibody should have also been utilised as

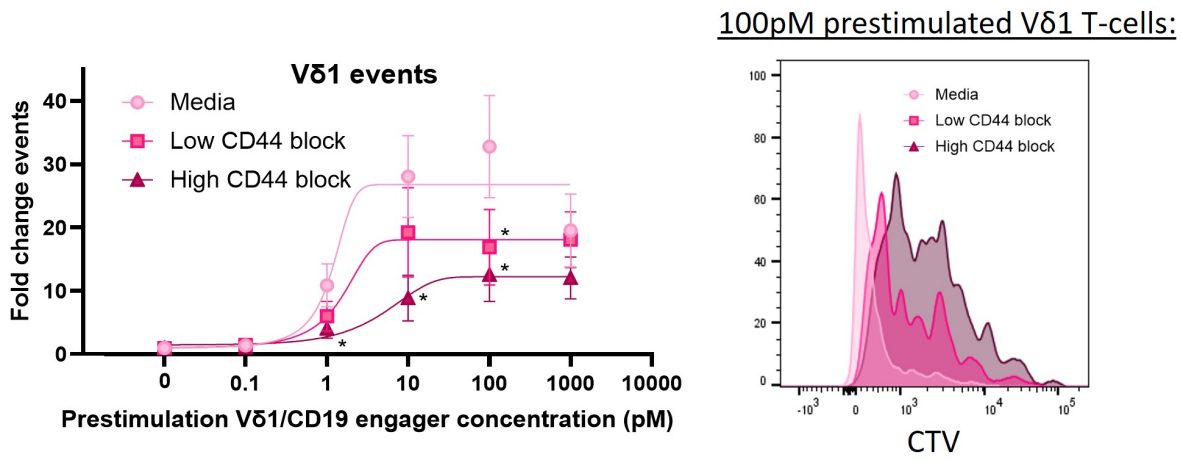


Figure 4.42: ***Neutralising CD44 reduces engager-mediated Vδ1 proliferation.***
Proliferation of Vδ1 T-cells after CD44 neutralisation assessed by flow cytometry. Left, Vδ1 T-cell proliferation from whole PBMC cultures (n=6) after 7 days treatment with Vδ1/CD19 engager and none (Media), low (0.3ug/ml) or high (30ug/ml) CD44 blockade. Paired wilcoxon non-parametric statistical test performed against the media treated samples. Each asterisk (*) denotes a level of significance: $p < 0.05$, $p < 0.01$, $p < 0.001$, and $p < 0.0001$. Error bars represent SEM. For each donor, cell numbers from two technical replicates were first averaged, and these per-donor averages were used to calculate the fold change events and plot the overall mean and SEM across all donors. Right, Histogram depicts CellTrace Violet (CTV) proliferation staining on 100pM Vδ1/CD19 engager treated Vδ1 T-cells from one representative donor.

a negative control to improve the reliability of the observed response.

4.4.2.2 Cytotoxicity

The role of co-receptors in engager-mediated Vδ1 cytotoxicity was investigated by blocking the cancer-associated proteins on MEC-1 cells prior to their addition to Vδ1/CD19 engager-prestimulated PBMC cultures. After 7 days of prestimulation, PBMC cytotoxic capability

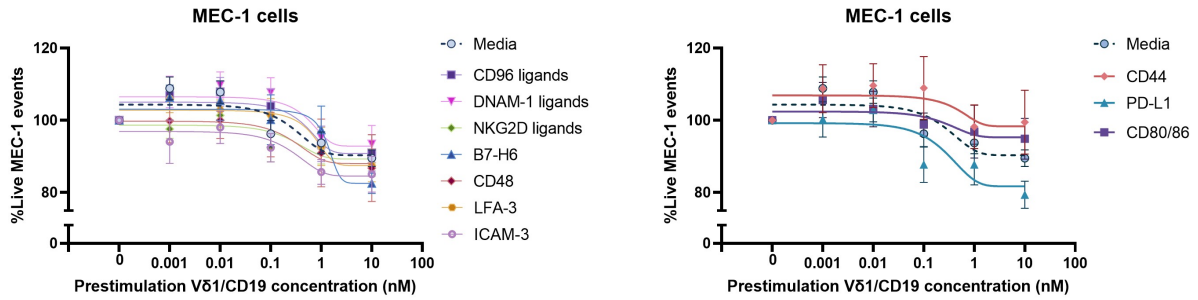


Figure 4.43: ***MEC-1 cell cytotoxicity following blockade of cancer-associated ligands.*** *PBMCs cultures (n=6) prestimulated for 7 days with Vδ1/CD19 engager were assessed for cytotoxicity where MEC-1 cells, blocked for specified stress ligands, were added and remaining live MEC-1 target cells were assessed after 5 hours of co-culture using flow cytometry. Live target cells are presented as percentage fold change from live MEC-1 cells in co-culture with PBMCs that were not prestimulated (but still cultured for 7 days prior to the addition of MEC-1 cells). MEC-1 cells were blocked with 10μg/ml blocking antibodies for NKG2D (MICA/B, ULBP1, ULBP3, ULBP2/5/6), DNAM-1 ligands (PVR and Nectin-2), CD96 ligands (PVR and Nectin-1), LFA-3, CD48, B7-H6, ICAM-3, CD80, CD86, PD-L1 and CD44. Left and Right graphs with specified blocking antibodies are separated for clarity of observing the data. Error bars represent SEM with one technical replicate.*

against blocked MEC-1 cells was assessed over a short 5-hour incubation (Figure 4.43). This timeframe was chosen to minimize potential unknown effects from the neutralizing antibodies and is consistent with previous studies [50, 127]. However, the short incubation likely limited the assay window, making small changes in response to blocked ligands harder to detect. Additionally, since whole PBMC cultures were used, responses from other cell types contributed to the overall effect. This confounding factor is evident in the PD-L1 blockade, where MEC-1 cell death increased across all conditions compared to no blockade (Figure 4.43), likely due to enhanced canonical effector T-cell activity. Thus, this assay was not optimal for exploring the roles of individual ligands. Future work should focus on using isolated Vδ1 T-cells and knocking out ligands in target cells to improve sensitivity.

Nevertheless, to investigate the Vδ1-specific response within this assay design, Vδ1 Fas-L and CD107a were also measured from these cultures. Blockade of the ligands individually did not reliably impact Vδ1 Fas-L and CD107a expression (Appendix 8.8 and 8.9), mimicking the minimal cell death from individual blockade (Figure 4.43). However, when a ***combination*** of

the ligands were blocked instead of individual blockade, MEC-1 cell death was reduced (Figure 4.44) and there was correspondingly reduced Vδ1 T-cell expression of Fas-L and CD107a (Figure 4.45). The CD27$^+$ Vδ1 T-cells demonstrated a greater reduction in Fas-L expression than their CD27$^-$ counterparts in response to ligand blockade, though not in response to Vδ1/CD19 treatment (Figure 4.45A). This data suggests that CD27$^+$ Vδ1 T-cells may be able to perform some cytotoxic functions via a Fas-mediated pathway in response to co-receptor stimulation and irrespective of Vδ1 engager treatment. Constrastingly, CD107a expression did not change from the CD27$^+$ population (Figure 4.45B). Furthermore, a reduced CD107a expression was observed from the CD27$^-$ Vδ1 T-cells in response to ligand blockade but only from the 1nM Vδ1/CD19 prestimulation condition (Figure 4.45B). This data suggests that Vδ1/CD19 treatment may encourage CD27$^-$ Vδ1 T-cell cytotoxicity through degranulation.

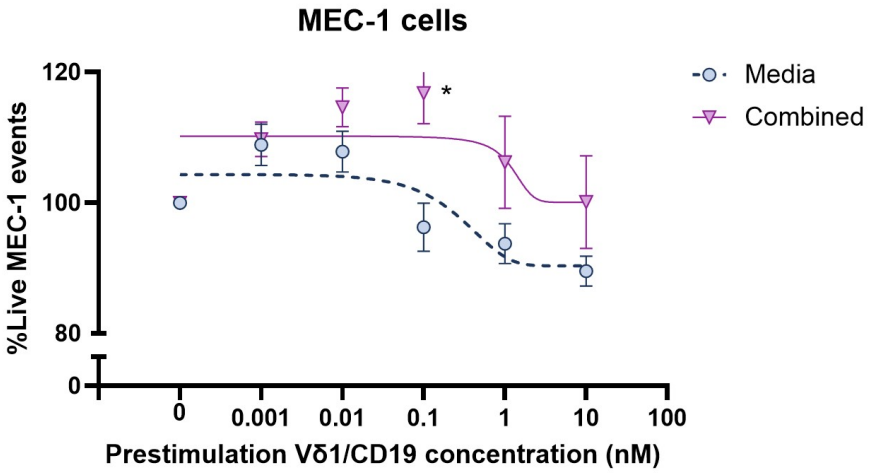


Figure 4.44: ***MEC-1 cell death reduced by blockade of a combination of cancer-associated ligands.***

PBMCs cultures (n=6) prestimulated for 7 days with Vδ1/CD19 engager were then assessed for cytotoxicity using flow cytometry where MEC-1 cells blocked for specified stress ligands were added and remaining live target cells were assessed after 5 hours of co-culture. Live target cells are presented as percentage fold change from live MEC-1 cells in co-culture with PBMCs that were not prestimulated (but still cultured for 7 days prior to the addition of MEC-1 cells). MEC-1 cells were blocked with a combination of 10µg/ml blocking antibodies for NKG2D (MICA/B, ULBP1, ULBP3, ULBP2/5/6), DNAM-1 ligands (PVR and Nectin-2), CD96 ligands (PVR and Nectin-1), LFA-3, CD48 and B7-H6. Paired wilcoxon non-parametric statistical test performed against the media treated samples. Each asterisk (*) denotes a level of significance: $p < 0.05$, $p < 0.01$, $p < 0.001$, and $p < 0.0001$. Error bars represent SEM with one technical replicate.

The reduced cytotoxicity observed when testing combined ligand blockade compared to individual blockade suggests that Vδ1 T-cells do not rely on a single stress ligand to function,

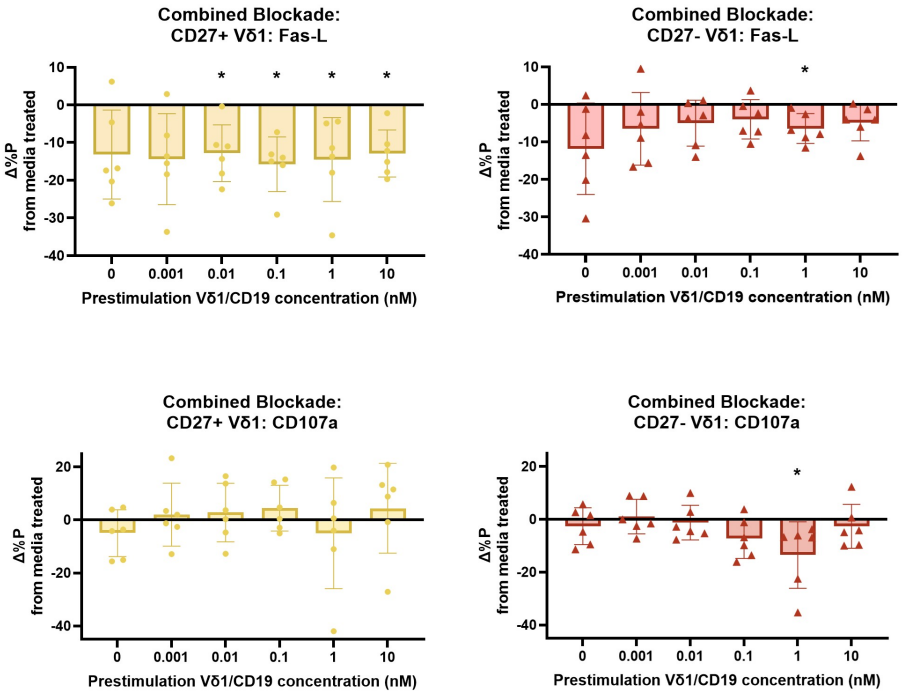


Figure 4.45: ***Engager-treated Vδ1 T-cell cytotoxicity reduces with combined blockade of MEC-1 ligands.***

Cytotoxicity marker expression, ***(A)*** *Fas-L and* ***(B)*** *CD107a, assessed by flow cytometry, on CD27$^-$ (red triangles) and CD27$^+$ (yellow circles) Vδ1 T-cells from combined ligand block in figure 4.44 compared to non-blocked (media-treated) conditions, calculated as the difference in percentage (△%P) of Vδ1 T-cells expressing Fas-L or CD107a. Paired wilcoxon non-parametric statistical test performed against the media treated samples. Each asterisk (*) denotes a level of significance: $p < 0.05$, $p < 0.01$, $p < 0.001$, and $p < 0.0001$. Bars represent SD with one technical replicate.*

but instead respond to a range of stress ligands to appropriately target stressed or malignant cells over healthy ones. Notably, this broad stress ligand dependency remained intact after Vδ1/CD19 engager treatment. This maintained dependency lowers the risk of adverse effects from Vδ1 engager therapy, as treated Vδ1 T-cells would still primarily target stressed and malignant cells.

4.4.2.3 Activation

Activation of PBMC-based Vδ1 T-cells in response to the co-receptor ligands was also assessed (Figure 4.46). In this assay, Vδ1 T-cells were isolated from both non-prestimulated and engager-prestimulated PBMCs to be cultured with plate-bound ligands for 24 hours. Since only three donors were assessed, statistical analysis was not performed; instead, the data was used to observe numerical trends without drawing definitive conclusions.

When cultured with recombinant ligands for the activatory receptors NKG2D, DNAM-1, CD96, CD2, and NKp30, isolated Vδ1 T-cells showed increased expression of 41BB, CD25, Fas-L, and CD107a (Figure 4.46). Vδ1/CD19-prestimulated Vδ1 T-cells exhibited a reasonably greater activation response compared to non-prestimulated cells, suggesting that Vδ1/CD19 treatment may enhance Vδ1 reactivity to these stress ligands. Notably, in $CD27^+$ Vδ1/CD19-prestimulated T-cells, only 41BB and CD25 were upregulated, while CD25, Fas-L, and CD107a were more highly expressed in $CD27^-$ cells. Despite the proposed maturation of engager-treated $CD27^+$ Vδ1 T-cells, the activation profile suggests that $CD27^-$ Vδ1 T-cells may retain stronger cytotoxic potential. Furthermore, as $CD27^+$ Vδ1 T-cells did not upregulate the cytotoxicity proxy markers of Fas-L and CD107a, but the $CD27^-$ population did, the primed $CD27^+$ Vδ1 T-cells may still require further stimulation for enhanced cytotoxicity, for example, via TCR stimulation. This could suggest that $CD27^-$ Vδ1 T-cells are less dependent on TCR stimulation and perhaps more reliant on co-receptor engagement, though further work would be required.

Overall, the data indicates that Vδ1/CD19 treatment maintains stress ligand-dependent activation, enabling Vδ1 T-cells to discriminate between healthy and stressed cells.

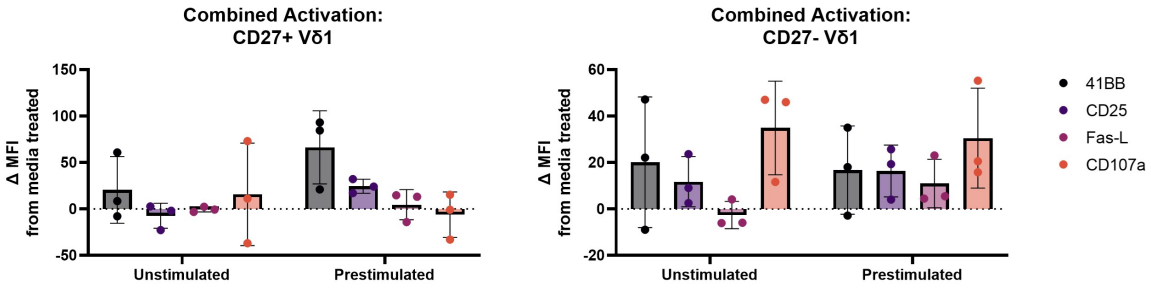


Figure 4.46: ***Engager-treated Vδ1 T-cells upregulate activation receptors in response to a combination of plate-bound ligands.***

Activation of FACS-sorted Vδ1 T-cells were assessed by flow cytometry staining for 41BB, CD25, Fas-L and CD107a. PBMCs (n=3) were prestimulated for 7 days with 0pM or 100pM Vδ1/CD19 engager, Vδ1 T-cells isolated and then cultured with recombinant plate-bound stress ligands (NKG2D ligands, DNAM-1 ligands, CD96 ligands, LFA-3, B7-H6) for 24 hours. Bars represent SD, with one technical replicate.

Vδ1 T-cell reactivity to the individual ligands was also assessed (Appendix 8.10). Interestingly, CD44, ICAM-3, and LFA-3, which are known to stabilize the immunological synapse in canonical T-cells, showed similar responses. However, since only three donors were evaluated, these observations are speculative, and further investigation is needed to draw definitive conclusions. Further experiments to explore the role of LFA-3 were also initiated (Appendix 8.11), however, time constraints limited the capacity to fully understand the involvement of these proteins.

4.4.3 Summary

This study demonstrates that Vδ1/CD19 engager stimulation enhances the cytotoxicity of Vδ1 T-cells against CD19$^+$ malignant cells The conclusions are summarised and illustrated in figure 4.47. In PBMC cultures without cytokine supplementation, increased cytotoxicity is attributed to both the proliferation of Vδ1 T-cells and the phenotypic maturation of naive CD27$^+$ Vδ1 T-cells (Figure 4.47B). Vδ1/CD19 treatment encouraged CD45RA, NKG2D, DNAM-1, CD96, CD2, PD-1, and ICOS upregulation as well as CTLA-4 downregulation, indicating a priming of naive Vδ1 T-cells. However, the persistence of CD27 suggests they were not fully effector-ready in healthy contexts.

In contrast, in cancerous conditions, the downregulation of CD27 and upregulation of granzyme B indicate a shift toward an effector Vδ1 phenotype with enhanced cytotoxic capacity (Figure 4.47B). Importantly, even with engager stimulation, Vδ1 T-cells were able to regulate their activation, reducing the risk of immune dysregulation. Moreover, engager-stimulated Vδ1 T-cells maintained stress ligand-dependent activation, which would allow for healthy cell discrimination while potentially improving reactivity to stress ligands. These findings suggest a controlled yet effective cytotoxic response from engager-stimulated Vδ1 T-cells, particularly in malignant environments.

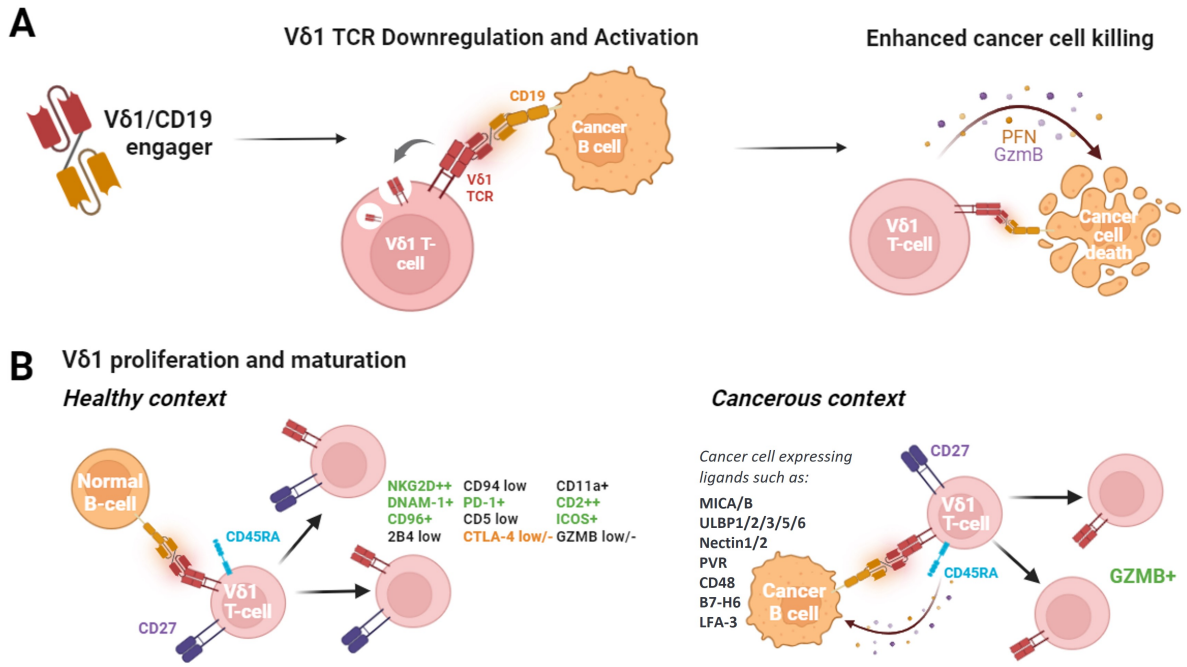


Figure 4.47: ***Diagram to illustrate the current model of enhanced Vδ1 activation following Vδ1/CD19 engager treatment.***

(A) Short-term effects of Vδ1/CD19 engager treatment, resulting in TCR downregulation and activation of Vδ1 T-cells, leading to enhanced cancer cell killing. **(B)** Longer term effects of Vδ1/CD19 treatment in healthy (left) and cancerous (right) contexts. In the healthy setting, CD27 expression is maintained or upregulated whilst CD45RA is downregulated. Activatory receptors are upregulated whilst granzyme B expression remains low. Collectively this indicates an engager-mediated memory Vδ1 phenotype that is primed for further activation. Proteins in green denote upregulation and orange indicate downregulation in response to Vδ1/CD19 engager stimulation. In a cancerous context, CD27 and CD45RA are downregulated suggesting an effector memory Vδ1 phenotype which is supported by the increase in granzyme B expression. $CD27^-$ effector Vδ1 T-cells may depend on the balance of signals fom co-receptor engagement as well as TCR signalling to elicit a cytotoxic response. [This image was created using BioRender]

Chapter 5

Discussion

Vδ1 $\gamma\delta$ T-cells have historically demonstrated oncostatic properties that highlight potential for the next generation of cancer therapeutics. This thesis has explored the use of a novel Vδ1-targeting engager to enhance the anti-tumoural immune response against CD19$^+$ malignancies. This Vδ1/CD19 engager activated, proliferated and enhanced the cytotoxic potential of Vδ1 T-cells (Figure 4.47A). Engager-stimulation also matured naive Vδ1 T-cells into effector memory cells that exhibited enhanced stress ligand reactivity with, importantly, maintained preferential Vδ1 reactivity to cancerous over healthy cells (Figure 4.47B). The results here support the use of Vδ1 engagers for the treatment of CD19$^+$ malignancies, as well as highlighting their potential for the treatment of other cancers. As the engager developed here was generated for research purposes and as a tool for demonstrating proof-of-concept, there are several considerations required to be explored prior to implementation into a functioning therapy. The following discussion will first identify limitations in the study before exploring the relevance of this thesis's findings within key themes introduced in Chapter 1, alongside any areas that would need further exploration to be able to utilise Vδ1-targeting engagers as a therapy.

5.1 Study Design Limitations

Despite yielding meaningful findings, certain experiments were constrained by limitations in design or material availability. While some of these limitations were addressed within the Results section in the context of the specific experiments, this section will provide a broader discussion of the study's limitations, particularly focusing on aspects that would require further attention in order to support the development of Vδ1-based therapies.

As explored in the introduction, Vδ1 T-cells may become immunosuppressive in response to TGF-β treatment. As TGF-β is a common cytokine within the TME, it is crucial to investigate

its effects on Vδ1-based engagers. Understanding whether these cells are at risk of developing immunosuppressive properties is essential for determining appropriate combination treatments and identifying patient populations that may benefit from these therapies. It has been suggested that $\gamma\delta$ T-cell-based engagers alone might not suffice to overcome the immunosuppressive TME [181], whereas there may be more flexibility regarding a cell-based approach. For example, Adicet Bio have developed an allogeneic CD27 CAR $\gamma\delta$ cell-based therapy engineered to resist TGF-β signals [182]. Accordingly, this study would have benefited from evaluating whether Vδ1/CD19 engager therapy can protect Vδ1 T-cells from potential TGF-β–induced immunosuppression, for instance, by assessing the Vδ1 T-cell expression levels of TGF-β receptors and immunosuppressive proteins such as PD-L1, IL-17A and IL-10 expression following Vδ1/CD19 treatment.

Additionally, it may have been valuable to investigate the signalling pathways within engager-treated Vδ1 T-cells in greater detail. While some preliminary analysis was performed (Appendix 8.11), this study would have benefited from examining engager-treated Vδ1 T-cells from both healthy and cancerous *ex vivo* models. For instance, although PBMCs from CLL patients were used to study target cell phenotypes, investigating Vδ1 T-cells derived from CLL patient PBMCs could have provided insights into how these cells, already exposed to the TME, would respond to treatment. Comparing the Vδ1 T-cell responses from healthy and TME-exposed contexts might have clarified their signalling dependencies and functional responses. Furthermore, this approach could have identified potential immunosuppressive or immunosuppressed phenotypes in Vδ1 T-cells before and after treatment, offering a more comprehensive understanding of their behaviour under different conditions.

Further investigation of these signalling dependencies could help identify suitable patients for treatment and potential combination therapies that might provide mutual benefits. The observed increase in expression of activatory receptors following Vδ1/CD19 engager treatment (Figure 4.35) suggests that these Vδ1 T-cells may require less stimulation to activate, potentially due to a lowered activation threshold. This hypothesis was preliminarily explored using plate-bound recombinant ligands to assess activation responses of treated Vδ1 T-cells (Figure 4.46). While the experiment demonstrated cell activation, additional studies would be necessary to determine how engager-treated Vδ1 T-cells respond to a mix of activatory and inhibitory signals. Such research could clarify whether engager treatment enhances sensitivity to activatory signals or offers protection against immunosuppressive signals, such as those mediated by PD-L1 and HLA-E.

Furthermore, although this study investigated the role of co-receptors on engager-treated Vδ1

T-cells, the contribution of additional TCR stimulation—via ligands beyond the engager—remains an important area for future exploration. These additional signals could significantly influence the overall activation of these cells. Understanding the specific target cell phenotypes required for optimal activation of engager-treated Vδ1 T-cells would ensure more effective treatment strategies and better patient outcomes.

The healthy cell-sparing assessment in this study demonstrated increased granzyme B expression in engager-treated Vδ1 T-cells following co-culture with MEC-1 cells, whereas no such increase was observed in the absence of cancer cells (Figure 4.37). While this is a meaningful finding, it would require further validation through direct measurements of healthy versus cancerous B-cell killing. A straightforward approach would have been to use the already established 7-day PBMC killing assay to compare the killing of CLL-isolated B cells with that of healthy-isolated B cells. Although this experiment was not conducted due to time constraints, it represents the minimum necessary step to substantiate the claim that Vδ1/CD19 engager treatment does not induce healthy B-cell killing.

Finally, as this study is based entirely on *in vitro* and *ex vivo* models, future work should focus on testing engager-based assays in more complex systems. Although murine Vδ1 T-cells are not directly comparable to their human counterparts, recent advancements in humanized mouse models have demonstrated more similar Vδ1 phenotypes [183]. These models provide a promising starting point for investigating the findings of this study in an *in vivo* context.

5.2 Considerations for Vδ1 engagers as a therapy

5.2.1 Engager Format

Initial studies assessed the abilities of four different Vδ1/CD19 bispecific antibody formats to bind, activate, proliferate and enhance cytotoxicity of isolated and PBMC-based Vδ1 T-cells against CD19$^+$ cell lines. Whilst all formats were able to bind and proliferate Vδ1 T-cells, only the BiTE format was capable of enhancing Vδ1 T-cell activation and cytotoxicity.

Immunotherapeutic engagers have demonstrated efficacy in cancer-treating strategies, not only in their ability to activate T-cells through CD3 engagement, but also due to increased formation of immunological synapses (IS) between T-cell and target [184]. When canonical T-cells form an IS, TCRs will accumulate or cluster at the centre of the interface of interaction [185] (Figure 1.7). The strength of peptide-loaded MHC binding can affect TCR clustering which is

suggested to initiate differing signals where more TCR clusters indicate a more mature IS capable of T-cell activation [186]. The data presented here demonstrates that only the BiTE format is capable of Vδ1 T-cell activation. Therefore, this BiTE-specific response could suggest that the other formats, whilst able to engage the TCR, are not able to induce sufficient TCR clustering to reach the threshold of activation. Bispecific antibodies have previously demonstrated improved IS formation [187] and BiTEs have specifically been implicated in lytic IS formation due to the increase in perforin and granzyme presence within the IS [184]. As only the Vδ1/CD19 BiTE enhanced degranulation (Figure 4.12), perhaps only the BiTE format was capable of increasing this lytic IS formation. Interestingly, the other formats were able to enhance Vδ1 proliferation, however, this could suggest that initiation of the Vδ1 proliferation mechanism may rely on limited TCR clustering and can thus also occur in the naive CD27$^+$ Vδ1 T-cell population.

The structure of each bispecific format is hypothesised to affect the degree of TCR-clustering within the IS. There are a number of differences that could affect the overall avidity of the antibody to facilitate efficient binding. The most obvious difference between these engager formats is their size, with the BiTE being a third of the size of the KIH, and a quarter of the size of the MB (Tables 3.2-3.4). A smaller engager may simply 'fit' into the IS more efficiently to facilitate and perhaps stabilise the interactions of other proteins in the synapse. Additionally, the BiTE utilises a flexible glycine-serine (GS) linker between each scFv (Table 3.2) which could facilitate improved orientation of binding to both the TCR and CD19 within the IS [188].

The flexibility and geometry of the BiTE may provide an advantage over both the KIH and MB formats. The lack of a GS linker, as well as the positioning of the KIH binding moieties may be more restricted than the BiTE and therefore not conducive towards sufficient TCR clustering. The MB employs an IgG structure (Figure 4.1), binding either Vδ1 TCR or CD19, connected with a GS linker to two scFv regions binding either CD19 or Vδ1 TCR, respectively. Despite the use of the flexible GS linker, the MB's scFv binding moieties did not bind as effectively as the MB's IgG binding moieties (Figure 4.5). This was unexpected as it was hypothesised that by increasing the valency—utilising two binding moieties per target instead of one—the MB's avidity to each binding target would improve. Instead, the scFv binding capabilities were reduced, suggesting that when in a MB format, scFv avidity is reduced. Increasing the affinity or avidity of either binding moiety in a bispecific antibody is thought to improve an engager's potency [188]. The MB orientation is also suggested to significantly limit CD3 engager potency [189]. Therefore, the reduced MB avidity could reduce its capability to effectively engage and cluster TCRs within the IS.

A GS linker of less than 12 amino acids in length have been proposed to form multimers [190,

191] due to a lack of separation between the fusion proteins [192]. This would suggest the BiTE used here could form multimers which would increase its avidity and thus improve its efficacy in TCR clustering. However, multimerisation has not been documented with Blinatumomab and the Vδ1/CD19 BiTE bound to cells in a similar capacity to the CD3/CD19 engager, suggesting that this BiTE is functioning as a monomer.

The finding that only the BiTE was biologically functional was surprising as other formats have previously demonstrated efficacy with CD3 [193, 189]. This finding may highlight the difference between canonical and Vδ1 T-cells, however, it may also indicate that the mechanism of action that results in Vδ1 activation when binding the Vδ1 TCR may be more dependent on the TCR clustering effect, over the downstream signalling that CD3-engagement initiates.

Overall, the differences between engager formats can significantly affect not only their manufacturability but also their biological effects including both the initial binding downstream biological activity which all determine the feasibility of the engager being developed into a therapy. When comparing KIH and MB formats to the Vδ1/CD19 BiTE, only the BiTE could elicit Vδ1 T-cell activation, however, this is not to say that other formats may not be suitable. For example, the DART format (Figure 1.10) may be more stable than a BiTE format and provide advantages during the manufacturing process due to additional linkers [194]. Furthermore, alternative IgG formats, despite being larger than a BiTE have demonstrated ability to improve IS formation [195] and could provide additional benefits such as improving drug half-life. Therefore, further work would be required to determine which format would be most beneficial in regards to pharmacokinetics and dynamics, which determines how long the engager may be required in the system per dose to elicit the desired response. Further work in validating whether the BiTE, in a Vδ1 context, functions through an IS-specific mechanism is also necessary to determine a suitable size and geometry of the engager.

5.2.2 Implications of co-receptors for Vδ1-based therapies

This thesis has explored the involvement of co-receptors (Table 4.1) within the Vδ1 cytotoxic response. Co-receptor expression was demonstrated on three different Vδ1 T-cell models in both *ex vivo* and cytokine-expanded populations (Figure 4.33), where *ex vivo* CD27$^-$ Vδ1 T-cells expressed greater DNAM-1, 2B4, CD94, CD5 and granzyme B than their CD27$^+$ naive counterparts; and cytokine-expansion increased NKG2D, CD96, NKp30, NKp46, Fas-L, ICAM-3, NKG2A, CD5, PD-1, ICOS, CD69 and 41BB levels. Vδ1/CD19 engager treatment upregulated the co-receptors NKG2D, DNAM-1, CD96, CD2, ICOS and PD-1 (Figure 4.35), placing

this engager-stimulated phenotype in-between the basal CD27$^-$ cytotoxic Vδ1 T-cell and the cytokine-expanded Vδ1 T-cell. Upregulation of such co-receptors corresponded to increased cytotoxic capability (Figure 4.32, 4.23 and Figure 4.37), and combined blockade of such receptors reduced Vδ1 cytotoxicity (Figure 4.44 and 4.45), highlighting the importance of co-receptors in Vδ1 cytotoxicity. Similarly, the Vδ1 cell-therapy 'DOT cells' demonstrate co-receptor involvement as they upregulate NKG2D, exhibit DNAM-1 dependency, and express *de novo* NKp30 and NKp44 alongside increased cytotoxic capacity [50, 155, 110]. Despite differing methods of stimulation, these similarities between both DOT cells and Vδ1 engager-stimulated PBMC-based Vδ1 T-cells suggest a common blood-resident Vδ1 mechanism, where co-receptor stimulation may be essential for the maturation and/or capability of cytotoxic effector Vδ1 T-cells.

The importance of co-receptor engagement for Vδ1 cytotoxicity may also explain their inherent healthy cell sparing capabilities. The downregulation of co-receptors on CD27$^-$ Vδ1 T-cells following engager treatment (Figure 4.35) suggest that these co-receptors are used as a mechanism for sensing target cells, and as no cytotoxicity was observed in this healthy context (Figure 4.37), it would suggest that such signals were not sufficient to initiate a killing response. Furthermore, the upregulation of co-receptors on CD27$^+$ Vδ1 T-cells in the same context (Figure 4.35) alongside their **primed** cytotoxic capability (Figure 4.23) suggest that these upregulated co-receptors *facilitate* the priming of these cells to initiate a cytotoxic response when sufficient signals (i.e. the addition of cancer cells) are present. Overall, these results highlight a co-receptor-dependency for Vδ1 cytotoxicity and healthy cell sparing that is sustained with Vδ1-specific engager treatment.

The differing responses of engager-treated CD27$^+$ and CD27$^-$ Vδ1 T-cells suggest a varying dependency of these subpopulations on TCR and co-receptor stimulation to elicit specific responses. First of all, the importance of co-receptors is observed in homeostatic Vδ1 T-cells where there was increased basal expression of co-receptors on CD27$^-$ compared to CD27$^+$ Vδ1 T-cells (Figure 4.33). Secondly, in a healthy context, TCR stimulation, via the engager, resulted in upregulation of CD27$^+$ co-receptors, where as the same TCR stimulation resulted in a downregulation of 2B4, CD2 and CD11a[1] on the CD27$^-$ Vδ1 T-cell population (Figure 4.35). This engager-treated CD27$^-$ Vδ1 phenotype could suggest a post-IS formation state where decreased LFA-1 expression decreases after stimulation in canonical T-cells [196]. As the CD27$^+$ Vδ1 T-cells demonstrated a *primed* phenotype following engager treatment, it could suggest that these cells rely on TCR stimulation to *initiate* differentiation and maturation, whereas the CD27$^-$

[1]CD11a heterodimerises with CD18 to form LFA-1

Vδ1 T-cells may instead utilise TCR signalling more in combination with the other co-receptor signals within the lytic IS to elicit a cytotoxic response, provided signals are sufficient to surpass the threshold of cytotoxic activation. These primed CD27$^+$ Vδ1 T-cells can then perhaps utilise their new co-receptor expression to induce cytotoxicity in the presence of respective stress ligands (Figure 4.23), however, such primed cells were not as easy to activate to a cytotoxic state as the pre-stimulated CD27$^-$ Vδ1 T-cells with plate bound stress ligands (Figure 4.46) suggesting that these primed CD27$^+$ Vδ1 T-cells may require higher levels of stimulation facilitated through further TCR stimulation and/or more co-receptor signalling over time. This differential mechanism of TCR involvement is supported by cytokine-expanded blood-derived Vδ1 T-cell cytotoxicity not being affected by TCR blockade [113], highlighting that the effector Vδ1 T-cells may rely on the balance of signals within the IS more than definitively requiring TCR signalling.

This TCR and co-receptor dependency, specifically cell-adhesion related co-receptors, is also observed in canonical T-cell cytotoxicity, where CD2 and LFA-1 form part of the canonical T-cell lytic IS with APCs as well as in lytic synapses formed with bispecific engagers that indirectly signal through the TCR via CD3-engagement [119, 197]. Furthermore, cytokine-expanded Vδ1 cytotoxicity against myeloma cells was also seen to be dependent on TCR, CD2, ICAM-1, NKG2D and DNAM-1 signalling [111]. Interestingly, cytokine-expanded Vδ1 cytotoxicity against CLL cells was dependent on CD2 but only when TCR stimulation was also impaired [50], highlighting that TCR stimulation can add to the combination of signals within the IS for effector Vδ1 cytotoxicity.

The data presented here also supports a similar theory previously proposed [109] where the development of cytotoxic DOT cells requires TCR stimulation (via CD3 engagement) alongside further differentiation into a cytotoxic product using cytokines [50]. Further investigation is needed to fully understand the nuances between TCR and co-receptor signalling that drive these differential responses, as well as how these mechanisms translate between naive versus effector and blood-resident versus tissue-resident Vδ1 T-cells.

CD2 and LFA-1 have demonstrated a role in stabilising IS formation, and NK-cell associated co-receptors may contribute to healthy cell discrimination by balancing the signals to reach the threshold of activation. In addition to these co-receptors, Vδ1/CD19 engager-mediated proliferation of Vδ1 T-cells was dependent on CD44 (Figure 4.42), however, as CD44 can bind CD44 on other cells via extracellular matrix components, it is unclear whether the engager-mediated proliferative response was affected by Vδ1-expressed CD44 or CD44 expressed on other cells. Canonical T-cells utilise CD44 in IS formation ([198, 199]) suggesting that neutralising CD44 on the surface of Vδ1 T-cells may have negatively impacted the IS necessary for proliferation.

CD44 may be more useful in Vδ1 stimulatory ISs over lytic ISs as CD44 dependency affected the Vδ1 proliferative response which is more prominent in the CD27$^+$ Vδ1 population that does not form lytic ISs so readily as discussed above. If TCR stimulation is essential for Vδ1 maturation and proliferation within CD27$^+$CD44$^+$ T-cells, it suggests potential interplay between the Vδ1 TCR, CD27, and CD44, possibly within the immunological synapse, that warrants further exploration.

Target cell-expressed CD44 may also impact Vδ1-expressed CD44 function within the IS (Figure 4.40 and 4.41). This mechanism may occur if, through binding extracellular matrix components, target cell expressed CD44 facilitates stable Vδ1-expressed CD44 presence within the IS. This feedback mechanism could be disturbed in the presence of the CD44 neutralising antibody and thus affect engager-mediated Vδ1 T-cell proliferation as the stimulatory IS may not function appropriately. This suggested co-receptor involvement in the Vδ1 IS would need to be explored further in the field to understand the necessity for CD2, LFA-1 and CD44 for Vδ1 T-cell activation for other Vδ1 T-cell based therapies. Further investigation would be required to understand the specific role that CD44 has to play and whether CD44 is more important for Vδ1 proliferation when expressed on the Vδ1 T-cell or external available CD44, particularly if Vδ1-based therapies' efficacy are relying on proliferative mechanisms.

Overall, Vδ1 based therapies must consider that co-receptor expression should be maintained or encouraged to not only facilitate activation, but also to maintain healthy cell discrimination and thus increasing efficacy whilst reducing the likelihood of adverse effects. This may impact Vδ1-based therapy strategies as TCR stimulation as well as co-receptor engagement would need to be ensured to choose patients that are likely to respond.

5.2.3 Therapy for cancer

This study highlights the use of a Vδ1 engager targeting CD19 as a proof of concept. While CD19 was the primary target in this work, this work supports targeting Vδ1 T-cells with antibody engagers for cancer treatment and suggests exploring other TAAs for future development.

As discussed above, the overall avidity of an antibody binding to its target influences its functionality. In addition to enhancing the affinity of each binding moiety, increasing the accessibility of one or both epitopes of a bispecific antibody can further boost its overall avidity [188, 200]. Vδ1/CD19 engager function corresponded to CD19 expression and whilst it could bind to isolated Vδ1 T-cells, the engager could not engage the TCR without a CD19 target cell present (Section 4.2), suggesting that the Vδ1/CD19 engager's avidity was facilitated and

improved by increasing the CD19 levels in the system. This TAA-dose dependency has also been observed with CD3 bispecific antibodies [201, 202, 203]. Whilst not necessarily surprising, this TAA dependency may pose a potential issue for the function of Vδ1 T-cell engagers because if the cancer manipulates the expression of the TAA then the therapy may become redundant. For example, leukaemic B-cells have historically demonstrated CD19 downregulating resistance mechanisms in response to CD19-specific treatments [204, 205]. There are strategies however to overcome such an issue. As explored in the introduction, the best current strategy we have for the successful treatment of cancer is to combine treatment strategies to fight the cancer on multiple fronts, targeting the tumour's heterogeneity as well as reducing the likelihood of the cancer to develop any resistance mechanisms. Therefore, if Vδ1 T-cell engagers are utilised in combination with other strategies targeting a different aspect of the tumour, the likelihood of the cancer developing a TAA-related resistance mechanism would reduce. Furthermore, as the Vδ1 engager demonstrated both proliferative capacity and the maturation of naive Vδ1 T-cells, it is possible that treated Vδ1 T-cells could sustain an enhanced anti-tumour response if healthy cells continue to express the TAA, such as CD19. As discussed in the introduction, co-receptor-dependent cytotoxicity is less vulnerable to tumour resistance mechanisms compared to MHC-dependent cytotoxicity, as it does not rely on the expression of a specific ligand within the TME. Although the data suggest the maturation of effector memory Vδ1 T-cells following engager treatment (Figure 4.39), further investigation is needed to assess the persistence and effector function of Vδ1 T-cells *in situ* over time.

As the work here has provided support for the use of Vδ1 engagers in non-CD19 contexts, other TAA binding moieties could be explored that are less susceptible to modification. The development of tri-specific antibodies has identified an alternative mechanism by which one would be able to target multiple TAAs in one engager [187], which could reduce the likelihood of succumbing to tumour resistance mechanisms. For example, resistance to HER protein family-directed therapies can occur following the upregulation of HER-3, therefore, targeting both of these proteins may make it more difficult for the cancer to overcome the therapy [206].

Nonetheless, as long as these Vδ1 T-cell engagers are dependent on TAA expression, the range of cancers that these engagers can be used to treat remains limited to tumours with definable markers. Therefore, future development of such engagers may benefit from exploring alternative bispecific moieties to direct Vδ1-specific engagers.

Accordingly, if Vδ1 engagers function similarly to the Vδ1/CD19 engager described here, selecting patients for Vδ1 engager treatment would require sufficient expression of both the TAA and CD27, as discussed above. Since new cancer therapies are often tested on patients

who have relapsed or failed to respond to gold standard treatments like surgery, chemotherapy, or checkpoint inhibition, further studies are necessary to understand how post-treatment cancers may respond to Vδ1 T-cell engagers. For example, surgery and chemotherapy are known to increase inflammation within the TME [9, 12], which can amplify immunosuppressive signals from the tumour. Understanding the extent of the anti-tumour properties of stimulated Vδ1 T-cells in these contexts will help determine whether these therapies are suitable for such patients or if alternative strategies might be more effective.

Furthermore, while Vδ1/CD19 engager-treated Vδ1 T-cells rely on stress ligand expression and exhibit PD-1 upregulation, the overall tumour signals must maintain a balance favouring activation over inhibition. Although potentially less susceptible to immunosuppression than CD8$^+$ T-cells as discussed in Chapter 1, Vδ1 T-cells are not invulnerable. Therefore, exploring the potential for combining Vδ1-based therapies with strategies that enhance tumour immunogenicity could prove beneficial.

The state of the tumour also influences the suitability of Vδ1-engager-based therapies, including factors such as whether the tumour is classified as "hot" or "cold" and its mutational burden. Cold tumours, which exhibit limited immune cell infiltration, are often resistant to checkpoint inhibition [207]. In contrast, hot tumours are characterized by greater immune-cell infiltration, including higher CD8$^+$ T-cell presence, and generally respond more effectively to checkpoint inhibitors [208]. If Vδ1-directed therapies can enhance tissue infiltration, the distinction between hot and cold tumours might become less critical. However, combining Vδ1 T-cell therapies with approaches designed to improve tumour-immune infiltration warrants further investigation.

Similarly, CD8-directed therapies are more effective in tumours with a high mutational burden, as these tumours tend to express higher levels of neoantigens that stimulate T-cell activity [208]. Since Vδ1 T-cells can respond to—though not dependent on—peptide-loaded MHC, future studies should explore whether the effectiveness of Vδ1-directed therapies depends on these same conditions. This research could clarify the circumstances under which Vδ1-engager therapies are most likely to benefit patients.

Finally, as Vδ1 T-cells exhibit different properties depending on their residency within the body (see Section 1.3.2), the development of Vδ1-based engagers would need to separately assess the response on each Vδ1 T-cell subpopulation. For example, as breast cancer-associated Vδ1 T-cells have demonstrated IL-17 producing capabilities (see Section 1.3.1), combined treatment with TLR ligands could be essential in restoring anti-tumoural capabilities to these Vδ1 T-cell populations [48, 149]. Overall, as Vδ1-based therapies are only beginning to emerge in the

cancer treatment landscape, significant exploration is still required to discern which patients could benefit most from these therapies.

5.2.4 Therapy for other indications

Whilst this thesis has focused on targeting cancer, the potential benefits of Vδ1 directed therapies are not limited to oncology as these cells are involved in a variety of immune responses.

Vδ1 T-cells have demonstrated expansion in response to a range of infections [130]. For example, individuals infected with CMV exhibit more differentiated CD27$^-$ T-cells [54], suggesting that cytotoxic Vδ1 T-cells may play a role in the management of this infection. Therefore, improved expansion and effector-like maturation using a Vδ1 T-cell engager could aid patients that may be struggling to clear such viral infections.

Interestingly, CMV infection has recently also been associated with Vδ1 T-cell expansion in patients with common variable immunodeficiency (CVID) [209]. CVID is a primary immunodeficiency disorder (PID) that presents with very low antibody levels within the body and reduced and abnormal T-cells, resulting in greater susceptibility to infections [209]. Despite this, CVID patients infected with CMV demonstrated functional $\gamma\delta$ T-cell effector capabilities [209]. Therefore, in combination with other therapies to aid the treatment of this complex disease, perhaps a Vδ1-targeting engager may provide some additional protection against infectious agents to CVID patients providing the expansion of these cells. Furthermore, PIDs can be a result of actin cytoskeleton defects which can affect the capacity for IS formation [210]. As the Vδ1/CD19 engager may facilitate IS formation, this capability could be exploited in PIDs and other diseases where Vδ1 T-cell IS formation is affected.

Despite the expansion of Vδ1 T-cells in HIV patients [211], their impact on HIV remains unclear due to their ability to produce IL-17A. While IL-17A plays a crucial role in immune responses against pathogens—and Vδ1 T-cells may help fulfil this role when IL-17-producing CD4$^+$ T-cells are suppressed [212]—Vδ1-derived IL-17A has also been shown to facilitate HIV function [213]. Therefore, the application of a Vδ1-directed engager in this context requires further investigation and careful justification, as it may not be suitable.

As discussed in Chapter 1, Vδ1 T-cells are abundant in the gut, and their populations are often disrupted in individuals with irritable bowel disease (IBD). Notably, these gut-resident Vδ1 T-cells have shown a protective role in preventing damage to the gut epithelium, suggesting that restoring the gut-resident $\gamma\delta$ T-cell population could support IBD treatment [153]. This raises the possibility that a Vδ1-based therapeutic engager, enhancing the proliferation and activation of these cells, could provide an alternative approach to IBD therapy.

5.3 Summary

This study has explored the therapeutic potential of Vδ1-targeting engagers by developing and evaluating a Vδ1/CD19 engager. While the engager demonstrated activity *in vitro*, further studies are essential to assess its healthy cell-sparing capabilities and to validate its functionality in more physiologically relevant *in vivo* models. Additionally, potential immunosuppressive and immunosuppressed phenotypes of Vδ1 T-cells following engager treatment should be investigated to confirm the suitability of such therapies.

The format of the engager plays a critical role in its functionality. While the BiTE format used in this study may facilitate immunological synapse formation between Vδ1 T-cells and target cells, further exploration of alternative formats is warranted. This work also highlights the importance of TCR signalling in the maturation of peripheral naive Vδ1 T-cells. The balance of co-receptor signalling appears to differ between naive and effector Vδ1 T-cells, where there may be a lower threshold for activation with effector Vδ1 T-cells though additional study is required to optimize cytotoxicity.

For the development into cancer therapies, TAA availability is crucial for engager function. Limited TAA expression could lead to tumour resistance, emphasizing the need for careful patient selection and a combination of therapeutic approaches. Additional criteria, such as tumour type and TME must also be investigated, as certain TMEs may not support Vδ1 T-cell activation, infiltration, or cytotoxicity.

Beyond oncology, Vδ1-specific engagers could potentially be applied to treat infectious diseases and downstream sequalae of immunodeficiencies. However, the role of Vδ1 T-cells varies significantly across cancer types and other indications, necessitating substantial investigation to define their broader applicability.

Overall, while this study supports the development of Vδ1-based engagers as promising therapeutic agents, further research is essential before they can be integrated into the oncologist's toolkit.

Chapter 6

Concluding Remarks

This thesis has explored the hypothesis that Vδ1-targeting engagers improve the overall immune response against CD19$^+$ malignancies, in order to support their general use in the treatment of cancer. Whilst the work conducted is not extensive, the overall findings demonstrate that the Vδ1/CD19 engager enhances Vδ1 anti-tumoural responses through the involvement of co-receptors.

Various engager formats were explored where binding and TCR engagement were observed; however, only the BiTE format successfully performed in initial biological functional assays. The BiTE format may be more capable in enhancing Vδ1 anti-tumoural function due to its suggested ability in facilitating IS formation. As Vδ1/CD19 BiTE function was dependent on sufficient TAA expression, other bispecific formats also capable of improved IS formations are worth investigating.

The BiTE Vδ1/CD19 engager was capable of specific stable binding to both the Vδ1 TCR and CD19 which led to downregulation of the TCR, enhanced Vδ1 T-cell activation, proliferation and cytotoxicity against CD19$^+$ cancer cells. Various co-receptors and ligands were identified to explain Vδ1 T-cell healthy cell sparing capabilities, though methods should be improved to explore the nuances between healthy and cancerous discrimination more effectively.

Naive Vδ1 T-cells may rely on TCR stimulation to facilitate maturation into effector Vδ1 T-cells. Whereas, effector Vδ1 T-cells may depend more on co-receptor stimulation to elicit a cytotoxic response, and importantly rely on the balance of signals within the IS to discriminate between healthy and cancerous cells. Naive and effector Vδ1 T-cells may also rely on co-receptors such as CD44 within the IS to facilitate proliferation. These responses were suggested to be maintained in Vδ1/CD19-stimulated Vδ1 T-cells.

Overall, this work supports the continued investigation of Vδ1 T-cell engagers as a promising approach for cancer treatment. Further research is crucial to determine whether engager-mediated Vδ1 responses are consistent with primary healthy and cancerous cells, validated within *in vivo* models, and applicable across a broader range of cancer types.

Chapter 7

References

Bibliography

[1] A. S. Ahmad, N. Ormiston-Smith, and P. D. Sasieni, "Trends in the lifetime risk of developing cancer in great britain: comparison of risk for those born from 1930 to 1960," *British journal of cancer*, vol. 112, no. 5, pp. 943–947, 2015.

[2] . World Health Organisation, "Cancer," 2022.

[3] B. Vogelstein, N. Papadopoulos, V. E. Velculescu, S. Zhou, L. A. Diaz Jr, and K. W. Kinzler, "Cancer genome landscapes," *science*, vol. 339, no. 6127, pp. 1546–1558, 2013.

[4] D. Hanahan, "Hallmarks of cancer: new dimensions," *Cancer discovery*, vol. 12, no. 1, pp. 31–46, 2022.

[5] I. Dagogo-Jack and A. T. Shaw, "Tumour heterogeneity and resistance to cancer therapies," *Nature reviews Clinical oncology*, vol. 15, no. 2, pp. 81–94, 2018.

[6] E. Hanna, J. Quick, and S. Libutti, "The tumour microenvironment: a novel target for cancer therapy," *Oral diseases*, vol. 15, no. 1, pp. 8–17, 2009.

[7] M. R. Junttila and F. J. De Sauvage, "Influence of tumour micro-environment heterogeneity on therapeutic response," *Nature*, vol. 501, no. 7467, pp. 346–354, 2013.

[8] L. Wyld, R. A. Audisio, and G. J. Poston, "The evolution of cancer surgery and future perspectives," *Nature reviews Clinical oncology*, vol. 12, no. 2, pp. 115–124, 2015.

[9] S. Tohme, R. L. Simmons, and A. Tsung, "Surgery for cancer: a trigger for metastases," *Cancer research*, vol. 77, no. 7, pp. 1548–1552, 2017.

[10] R. Weinberg and D. Hanahan, "The hallmarks of cancer," *Cell*, vol. 100, no. 1, pp. 57–70, 2000.

[11] D. Hanahan and R. A. Weinberg, "Hallmarks of cancer: the next generation," *cell*, vol. 144, no. 5, pp. 646–674, 2011.

[12] N. Behranvand, F. Nasri, R. Zolfaghari Emameh, P. Khani, A. Hosseini, J. Garssen, and R. Falak, "Chemotherapy: a double-edged sword in cancer treatment," *Cancer immunology, immunotherapy*, vol. 71, no. 3, pp. 507–526, 2022.

[13] C. Hennequin, S. Guillerm, and L. Quero, "Combination of chemotherapy and radiotherapy: A thirty years evolution," *Cancer/Radiothérapie*, vol. 23, no. 6-7, pp. 662–665, 2019.

[14] R. S. Kalra and S. A. Bapat, "Enhanced levels of double-strand dna break repair proteins protect ovarian cancer cells against genotoxic stress-induced apoptosis," *Journal of ovarian research*, vol. 6, pp. 1–10, 2013.

[15] H.-Y. Min and H.-Y. Lee, "Mechanisms of resistance to chemotherapy in non-small cell lung cancer," *Archives of pharmacal research*, vol. 44, no. 2, pp. 146–164, 2021.

[16] V. Lohiya, J. B. Aragon-Ching, and G. Sonpavde, "Role of chemotherapy and mechanisms of resistance to chemotherapy in metastatic castration-resistant prostate cancer," *Clinical Medicine Insights: Oncology*, vol. 10, pp. CMO–S34535, 2016.

[17] R. Atun, D. A. Jaffray, M. B. Barton, F. Bray, M. Baumann, B. Vikram, T. P. Hanna, F. M. Knaul, Y. Lievens, T. Y. Lui, *et al.*, "Expanding global access to radiotherapy," *The lancet oncology*, vol. 16, no. 10, pp. 1153–1186, 2015.

[18] L. Barazzuol, R. P. Coppes, and P. van Luijk, "Prevention and treatment of radiotherapy-induced side effects," *Molecular oncology*, vol. 14, no. 7, pp. 1538–1554, 2020.

[19] X. Liu, Z. Li, and Y. Yin, "Clinical application of mr-linac in tumor radiotherapy: a systematic review," *Radiation Oncology*, vol. 18, no. 1, p. 52, 2023.

[20] C. Robert, "A decade of immune-checkpoint inhibitors in cancer therapy," *Nature communications*, vol. 11, no. 1, p. 3801, 2020.

[21] S. Gettinger, N. A. Rizvi, L. Q. Chow, H. Borghaei, J. Brahmer, N. Ready, D. E. Gerber, F. A. Shepherd, S. Antonia, J. W. Goldman, *et al.*, "Nivolumab monotherapy for first-line treatment of advanced non–small-cell lung cancer," *Journal of Clinical Oncology*, vol. 34, no. 25, pp. 2980–2987, 2016.

[22] C. Sordo-Bahamonde, S. Lorenzo-Herrero, A. P. Gonzalez-Rodriguez, A. Martínez-Pérez, J. P. Rodrigo, J. M. García-Pedrero, and S. Gonzalez, "Chemo-immunotherapy: a new trend in cancer treatment," *Cancers*, vol. 15, no. 11, p. 2912, 2023.

[23] R. D. Schreiber, L. J. Old, and M. J. Smyth, "Cancer immunoediting: Integrating immunity's roles in cancer suppression and promotion," *Science*, vol. 331, no. 6024, pp. 1565–1570, 2011.

[24] S. Jhunjhunwala, C. Hammer, and L. Delamarre, "Antigen presentation in cancer: insights into tumour immunogenicity and immune evasion," *Nature Reviews Cancer*, vol. 21, no. 5, pp. 298–312, 2021.

[25] M. Yan, M. Schwaederle, D. Arguello, S. Z. Millis, Z. Gatalica, and R. Kurzrock, "Her2 expression status in diverse cancers: review of results from 37,992 patients," *Cancer and Metastasis Reviews*, vol. 34, pp. 157–164, 2015.

[26] M. Sadeghalvad, H.-R. Mohammadi-Motlagh, and N. Rezaei, *Introduction to Cancer Immunology*, pp. 1–29. Cham: Springer International Publishing, 2022.

[27] D. S. Vinay, E. P. Ryan, G. Pawelec, W. H. Talib, J. Stagg, E. Elkord, T. Lichtor, W. K. Decker, R. L. Whelan, H. Shantha Kumara, E. Signori, K. Honoki, A. G. Georgakilas, A. Amin, W. G. Helferich, C. Boosani, G. Guha, M. R. Ciriolo, S. Chen, S. I. Mohammed, and B. S. Kwon, "Immune evasion in cancer: Mechanistic basis and therapeutic strategies," vol. 35, pp. S185–S198, 2015.

[28] Y. Han, D. Liu, and L. Li, "Pd-1/pd-l1 pathway: current researches in cancer," *American journal of cancer research*, vol. 10, no. 3, p. 727, 2020.

[29] A. E. Kartikasari, C. S. Huertas, A. Mitchell, and M. Plebanski, "Tumor-induced inflammatory cytokines and the emerging diagnostic devices for cancer detection and prognosis," *Frontiers in oncology*, vol. 11, p. 692142, 2021.

[30] T. Curiel, G. Coukos, L. Zou, X. Alvarez, P. Cheng, P. Mottram, M. Evdemon-Hogan, J. Conejo-Garcia, L. Zhang, M. Burow, Y. Zhu, S. Wei, I. Kryczek, B. Daniel, A. Gordon, L. Myers, A. Lackner, M. Disis, K. Knutson, L. Chen, and W. Zou, "Specific recruitment of regulatory t cells in ovarian carcinoma fosters immune privilege and predicts reduced survival," *Nat Med*, vol. 10, pp. 900–901, 2004.

[31] I. Lee, L. Wang, A. D. Wells, M. E. Dorf, E. Ozkaynak, and W. W. Hancock, "Recruitment of foxp3+ t regulatory cells mediating allograft tolerance depends on the ccr4 chemokine receptor," *The Journal of experimental medicine*, vol. 201, no. 7, pp. 1037–1044, 2005.

[32] N. E. Welty and S. I. Gill, "Cancer immunotherapy beyond checkpoint blockade: Jacc: Cardiooncology state-of-the-art review," *Cardio Oncology*, vol. 4, no. 5, pp. 563–578, 2022.

[33] C. B. Johnson and S. Y. Win, "Combination therapy with pd-1/pd-l1 blockade: an overview of ongoing clinical trials," *Oncoimmunology*, vol. 7, no. 4, p. e1408744, 2018.

[34] P. Cech, K. Skórka, L. Dziki, and K. Giannopoulos, "T-cell engagers—the structure and functional principle and application in hematological malignancies," *Cancers*, vol. 16, no. 8, p. 1580, 2024.

[35] G. Martinelli, N. Boissel, P. Chevallier, O. Ottmann, N. Gökbuget, A. Rambaldi, E. K. Ritchie, C. Papayannidis, C. A. Tuglus, J. D. Morris, *et al.*, "Long-term follow-up of blinatumomab in patients with relapsed/refractory philadelphia chromosome–positive b-cell precursor acute lymphoblastic leukaemia: Final analysis of alcantara study," *European Journal of Cancer*, vol. 146, pp. 107–114, 2021.

[36] R. Houot, E. Bachy, G. Cartron, F.-X. Gros, F. Morschhauser, L. Oberic, T. Gastinne, P. Feugier, R. Duléry, C. Thieblemont, *et al.*, "Axicabtagene ciloleucel as second-line therapy in large b cell lymphoma ineligible for autologous stem cell transplantation: a phase 2 trial," *Nature Medicine*, vol. 29, no. 10, pp. 2593–2601, 2023.

[37] D. Bayik and J. D. Lathia, "Cancer stem cell–immune cell crosstalk in tumour progression," *Nature Reviews Cancer*, vol. 21, no. 8, pp. 526–536, 2021.

[38] S. Meraviglia, E. Lo Presti, M. Tosolini, C. La Mendola, V. Orlando, M. Todaro, V. Catalano, G. Stassi, G. Cicero, S. Vieni, *et al.*, "Distinctive features of tumor-infiltrating $\gamma\delta$ t lymphocytes in human colorectal cancer," *Oncoimmunology*, vol. 6, no. 10, p. e1347742, 2017.

[39] J. Mikulak, F. Oriolo, E. Bruni, A. Roberto, F. S. Colombo, A. Villa, M. Bosticardo, I. Bortolomai, E. L. Presti, S. Meraviglia, *et al.*, "Nkp46-expressing human gut-resident intraepithelial vδ1 t cell subpopulation exhibits high antitumor activity against colorectal cancer," *JCI insight*, vol. 4, no. 24, 2019.

[40] E. Bruni, M. M. Cimino, M. Donadon, R. Carriero, S. Terzoli, R. Piazza, S. Ravens, I. Prinz, V. Cazzetta, P. Marzano, *et al.*, "Intrahepatic cd69+ vδ1 t cells re-circulate in the blood of patients with metastatic colorectal cancer and limit tumor progression," *Journal for Immunotherapy of Cancer*, vol. 10, no. 7, 2022.

[41] Y. Wu, F. Kyle-Cezar, R. T. Woolf, C. Naceur-Lombardelli, J. Owen, D. Biswas, A. Lorenc, P. Vantourout, P. Gazinska, A. Grigoriadis, *et al.*, "An innate-like vδ1+ $\gamma\delta$ t cell compartment in the human breast is associated with remission in triple-negative breast cancer," *Science translational medicine*, vol. 11, no. 513, p. eaax9364, 2019.

[42] N. Zakeri, A. Hall, L. Swadling, L. J. Pallett, N. M. Schmidt, M. O. Diniz, S. Kucykowicz, O. E. Amin, A. Gander, M. Pinzani, *et al.*, "Characterisation and induction of tissue-resident gamma delta t-cells to target hepatocellular carcinoma," *Nature Communications*, vol. 13, no. 1, p. 1372, 2022.

[43] J. Wang, C. Lin, H. Li, R. Li, Y. Wu, H. Liu, H. Zhang, H. He, W. Zhang, and J. Xu, "Tumor-infiltrating $\gamma\delta$t cells predict prognosis and adjuvant chemotherapeutic benefit in patients with gastric cancer," *Oncoimmunology*, vol. 6, no. 11, p. e1353858, 2017.

[44] H. Lu, W. Dai, J. Guo, D. Wang, S. Wen, L. Yang, D. Lin, W. Xie, L. Wen, J. Fang, *et al.*, "High abundance of intratumoral $\gamma\delta$ t cells favors a better prognosis in head and neck squamous cell carcinoma: a bioinformatic analysis," *Frontiers in Immunology*, vol. 11, p. 573920, 2020.

[45] Y. Wu, D. Biswas, I. Usaite, M. Angelova, S. Boeing, T. Karasaki, S. Veeriah, J. Czyzewska-Khan, C. Morton, M. Joseph, *et al.*, "A local human vδ1 t cell population is associated with survival in nonsmall-cell lung cancer," *Nature cancer*, vol. 3, no. 6, pp. 696–709, 2022.

[46] N. A. Gherardin, K. Waldeck, A. Caneborg, L. G. Martelotto, S. Balachander, M. Zethoven, P. M. Petrone, A. Pattison, J. S. Wilmott, S. M. Quiñones-Parra, *et al.*, "$\gamma\delta$ t cells in merkel cell carcinomas have a proinflammatory profile prognostic of patient survival," *Cancer immunology research*, vol. 9, no. 6, pp. 612–623, 2021.

[47] S. Nguyen, M. F. Chevalier, S. Benmerzoug, V. Cesson, A. K. Schneider, S.-C. Rodrigues-Dias, F. Dartiguenave, I. Lucca, P. Jichlinski, B. Roth, *et al.*, "Vδ2 t cells are associated with favorable clinical outcomes in patients with bladder cancer and their tumor reactivity can be boosted by bcg and zoledronate treatments," *Journal for Immunotherapy of Cancer*, vol. 10, no. 8, 2022.

[48] G. Peng, H. Y. Wang, W. Peng, Y. Kiniwa, K. H. Seo, and R.-F. Wang, "Tumor-infiltrating $\gamma\delta$ t cells suppress t and dendritic cell function via mechanisms controlled by a unique toll-like receptor signaling pathway," *Immunity*, vol. 27, no. 2, pp. 334–348, 2007.

[49] J. C. Ribot, A. Debarros, and B. Silva-Santos, "Searching for "signal 2": costimulation requirements of $\gamma\delta$ t cells," *Cellular and Molecular Life Sciences*, vol. 68, pp. 2345–2355, 2011.

[50] A. R. Almeida, D. V. Correia, A. Fernandes-Platzgummer, C. L. da Silva, M. G. da Silva, D. R. Anjos, and B. Silva-Santos, "Delta one t cells for immunotherapy of chronic lymph-

ocytic leukemia: clinical-grade expansion/differentiation and preclinical proof of concept," *Clinical Cancer Research*, vol. 22, no. 23, pp. 5795–5804, 2016.

[51] M. Todaro, M. D'Asaro, N. Caccamo, F. Iovino, M. G. Francipane, S. Meraviglia, V. Orlando, C. La Mendola, G. Gulotta, A. Salerno, *et al.*, "Efficient killing of human colon cancer stem cells by $\gamma\delta$ t lymphocytes," *The Journal of Immunology*, vol. 182, no. 11, pp. 7287–7296, 2009.

[52] D. Lai, F. Wang, Y. Chen, C. Wang, S. Liu, B. Lu, X. Ge, and L. Guo, "Human ovarian cancer stem-like cells can be efficiently killed by $\gamma\delta$ t lymphocytes," *Cancer Immunology, Immunotherapy*, vol. 61, pp. 979–989, 2012.

[53] M.-P. Lefranc, "Nomenclature of the human t cell receptor genes," *Current protocols in immunology*, vol. 40, no. 1, pp. A–1O, 2000.

[54] M. S. Davey, C. R. Willcox, S. P. Joyce, K. Ladell, S. A. Kasatskaya, J. E. McLaren, S. Hunter, M. Salim, F. Mohammed, D. A. Price, D. M. Chudakov, and B. E. Willcox, "Clonal selection in the human vδ1 t cell repertoire indicates $\gamma\delta$ tcr-dependent adaptive immune surveillance," *Nature communications*, vol. 8, no. 1, p. 14760, 2017.

[55] S. C. De Rosa, J. P. Andrus, S. P. Perfetto, J. J. Mantovani, L. A. Herzenberg, L. A. Herzenberg, and M. Roederer, "Ontogeny of $\gamma\delta$ t cells in humans," *The Journal of Immunology*, vol. 172, no. 3, pp. 1637–1645, 2004.

[56] H.-H. Oberg, L. Janitschke, V. Sulaj, J. Weimer, D. Gonnermann, N. Hedemann, N. Arnold, D. Kabelitz, M. Peipp, D. Bauerschlag, *et al.*, "Bispecific antibodies enhance tumor-infiltrating t cell cytotoxicity against autologous her-2-expressing high-grade ovarian tumors," *Journal of leukocyte biology*, vol. 107, no. 6, pp. 1081–1095, 2020.

[57] M. Legut, D. K. Cole, and A. K. Sewell, "The promise of $\gamma\delta$ t cells and the $\gamma\delta$ t cell receptor for cancer immunotherapy," *Cellular & molecular immunology*, vol. 12, no. 6, pp. 656–668, 2015.

[58] D. Lozano-Ojalvo, R. López-Fandiño, and I. López-Expósito, "Pbmc-derived t cells," *The Impact of Food Bioactives on Health: in vitro and ex vivo models*, pp. 169–180, 2015.

[59] S. Fonseca, V. Pereira, C. Lau, M. d. A. Teixeira, M. Bini-Antunes, and M. Lima, "Human peripheral blood gamma delta t cells: report on a series of healthy caucasian portuguese adults and comprehensive review of the literature," *Cells*, vol. 9, no. 3, p. 729, 2020.

[60] M. Sanz, B. T. Mann, P. L. Ryan, A. Bosque, D. J. Pennington, H. Hackstein, and N. Soriano-Sarabia, "Deep characterization of human $\gamma\delta$ t cell subsets defines shared and lineage-specific traits," *Frontiers in Immunology*, vol. 14, p. 1148988, 2023.

[61] T. Verkerk, A. T. Pappot, T. Jorritsma, L. A. King, M. C. Duurland, R. M. Spaapen, and S. M. van Ham, "Isolation and expansion of pure and functional $\gamma\delta$ t cells," *Frontiers in immunology*, vol. 15, p. 1336870, 2024.

[62] M. E. Parker and M. Ciofani, "Regulation of $\gamma\delta$ t cell effector diversification in the thymus," *Frontiers in immunology*, vol. 11, p. 42, 2020.

[63] J. C. Ribot, N. Lopes, and B. Silva-Santos, "$\gamma\delta$ t cells in tissue physiology and surveillance," *Nature Reviews Immunology*, vol. 21, no. 4, pp. 221–232, 2021.

[64] M. Girardi, D. E. Oppenheim, C. R. Steele, J. M. Lewis, E. Glusac, R. Filler, P. Hobby, B. Sutton, R. E. Tigelaar, and A. C. Hayday, "Regulation of cutaneous malignancy by $\gamma\delta$ t cells," *Science*, vol. 294, no. 5542, pp. 605–609, 2001.

[65] O. Nussbaumer and M. Koslowski, "The emerging role of $\gamma\delta$ t cells in cancer immunotherapy," *Immuno-Oncology Technology*, vol. 1, pp. 3–10, 2019.

[66] J. Ismaili, V. Olislagers, R. Poupot, J.-J. Fournié, and M. Goldman, "Human $\gamma\delta$ t cells induce dendritic cell maturation," *Clinical immunology*, vol. 103, no. 3, pp. 296–302, 2002.

[67] D. Wesch, C. Peters, H.-H. Oberg, K. Pietschmann, and D. Kabelitz, "Modulation of $\gamma\delta$ t cell responses by tlr ligands," *Cellular and Molecular Life Sciences*, vol. 68, pp. 2357–2370, 2011.

[68] G. J. Kierkels, W. Scheper, A. Meringa, I. Johanna, D. Beringer, A. Janssen, M. Schiffler, T. Aarts-Riemens, L. Kramer, T. Straetemans, *et al.*, "Identification of a tumor-specific allo-hla–restricted $\gamma\delta$tcr," *Blood advances*, vol. 3, no. 19, pp. 2870–2882, 2019.

[69] P. M. Benveniste, S. Roy, M. Nakatsugawa, E. L. Chen, L. Nguyen, D. G. Millar, P. S. Ohashi, N. Hirano, E. J. Adams, and J. C. Zúñiga-Pflücker, "Generation and molecular recognition of melanoma-associated antigen-specific human $\gamma\delta$ t cells," *Science immunology*, vol. 3, no. 30, p. eaav4036, 2018.

[70] H. Spits, X. Paliard, V. Engelhard, and J. De Vries, "Cytotoxic activity and lymphokine production of t cell receptor (tcr)-alpha beta+ and tcr-gamma delta+ cytotoxic t lymphocyte (ctl) clones recognizing hla-a2 and hla-a2 mutants. recognition of tcr-gamma delta+

ctl clones is affected by mutations at positions 152 and 156.," *Journal of immunology (Baltimore, Md.: 1950)*, vol. 144, no. 11, pp. 4156–4162, 1990.

[71] E. Ciccone, O. Viale, D. Pende, M. Malnati, G. B. Ferrara, S. Barocci, A. Moretta, and L. Moretta, "Specificity of human t lymphocytes expressing a γ/δ t cell antigen receptor. recognition of a polymorphic determinant of hla class i molecules by a γ/δ clone," *European journal of immunology*, vol. 19, no. 7, pp. 1267–1271, 1989.

[72] P. Del Porto, M. D'Amato, M. T. Fiorillo, L. Tuosto, E. Piccolella, and R. Sorrentino, "Identification of a novel hla-b27 subtype by restriction analysis of a cytotoxic gamma delta t cell clone.," *Journal of immunology (Baltimore, Md.: 1950)*, vol. 153, no. 7, pp. 3093–3100, 1994.

[73] C. Q. Wang, P. Y. Lim, and A. H.-M. Tan, "Gamma/delta t cells as cellular vehicles for anti-tumor immunity," *Frontiers in Immunology*, vol. 14, p. 1282758, 2024.

[74] L. Yuan, X. Ma, Y. Yang, Y. Qu, X. Li, X. Zhu, W. Ma, J. Duan, J. Xue, H. Yang, *et al.*, "Phosphoantigens glue butyrophilin 3a1 and 2a1 to activate vγ9vδ2 t cells," *Nature*, vol. 621, no. 7980, pp. 840–848, 2023.

[75] C. Harly, Y. Guillaume, S. Nedellec, C.-M. Peigné, H. Mönkkönen, J. Mönkkönen, J. Li, J. Kuball, E. J. Adams, S. Netzer, *et al.*, "Key implication of cd277/butyrophilin-3 (btn3a) in cellular stress sensing by a major human $\gamma\delta$ t-cell subset," *Blood, The Journal of the American Society of Hematology*, vol. 120, no. 11, pp. 2269–2279, 2012.

[76] M. Rigau, S. Ostrouska, T. S. Fulford, D. N. Johnson, K. Woods, Z. Ruan, H. E. McWilliam, C. Hudson, C. Tutuka, A. K. Wheatley, *et al.*, "Butyrophilin 2a1 is essential for phosphoantigen reactivity by $\gamma\delta$ t cells," *Science*, vol. 367, no. 6478, p. eaay5516, 2020.

[77] Y. Yang, L. Li, L. Yuan, X. Zhou, J. Duan, H. Xiao, N. Cai, S. Han, X. Ma, W. Liu, *et al.*, "A structural change in butyrophilin upon phosphoantigen binding underlies phosphoantigen-mediated vγ9vδ2 t cell activation," *Immunity*, vol. 50, no. 4, pp. 1043–1053, 2019.

[78] M. Kondo, T. Izumi, N. Fujieda, A. Kondo, T. Morishita, H. Matsushita, and K. Kakimi, "Expansion of human peripheral blood $\gamma\delta$ t cells using zoledronate," *Journal of visualized experiments: JoVE*, no. 55, 2011.

[79] T. Herrmann and M. M. Karunakaran, "Phosphoantigen recognition by vγ9vδ2 t cells," *European Journal of Immunology*, vol. 54, no. 11, p. 2451068, 2024.

[80] A. De Gassart, K.-S. Le, P. Brune, S. Agaugué, J. Sims, A. Goubard, R. Castellano, N. Joalland, E. Scotet, Y. Collette, *et al.*, "Development of ict01, a first-in-class, anti-btn3a antibody for activating vγ9vδ2 t cell–mediated antitumor immune response," *Science Translational Medicine*, vol. 13, no. 616, p. eabj0835, 2021.

[81] M. Deseke and I. Prinz, "Ligand recognition by the $\gamma\delta$ tcr and discrimination between homeostasis and stress conditions," *Cellular & molecular immunology*, vol. 17, no. 9, pp. 914–924, 2020.

[82] S. Roy, D. Ly, C. D. Castro, N.-S. Li, A. J. Hawk, J. D. Altman, S. C. Meredith, J. A. Piccirilli, D. Moody, and E. J. Adams, "Molecular analysis of lipid-reactive vδ1 $\gamma\delta$ t cells identified by cd1c tetramers," *The Journal of Immunology*, vol. 196, no. 4, pp. 1933–1942, 2016.

[83] A. P. Uldrich, J. Le Nours, D. G. Pellicci, N. A. Gherardin, K. G. McPherson, R. T. Lim, O. Patel, T. Beddoe, S. Gras, J. Rossjohn, *et al.*, "Cd1d-lipid antigen recognition by the $\gamma\delta$ tcr," *Nature immunology*, vol. 14, no. 11, pp. 1137–1145, 2013.

[84] L. Bai, D. Picard, B. Anderson, V. Chaudhary, A. Luoma, B. Jabri, E. J. Adams, P. B. Savage, and A. Bendelac, "The majority of cd1d-sulfatide-specific t cells in human blood use a semiinvariant vδ1 tcr," *European journal of immunology*, vol. 42, no. 9, pp. 2505–2510, 2012.

[85] J. F. Reijneveld, T. A. Ocampo, A. Shahine, B. S. Gully, P. Vantourout, A. C. Hayday, J. Rossjohn, D. B. Moody, and I. Van Rhijn, "Human $\gamma\delta$ t cells recognize cd1b by two distinct mechanisms," *Proceedings of the National Academy of Sciences*, vol. 117, no. 37, pp. 22944–22952, 2020.

[86] J. Le Nours, N. A. Gherardin, S. H. Ramarathinam, W. Awad, F. Wiede, B. S. Gully, Y. Khandokar, T. Praveena, J. M. Wubben, J. J. Sandow, *et al.*, "A class of $\gamma\delta$ t cell receptors recognize the underside of the antigen-presenting molecule mr1," *Science*, vol. 366, no. 6472, pp. 1522–1527, 2019.

[87] C. Harly, S. P. Joyce, C. Domblides, T. Bachelet, V. Pitard, C. Mannat, A. Pappalardo, L. Couzi, S. Netzer, L. Massara, *et al.*, "Human $\gamma\delta$ t cell sensing of ampk-dependent metabolic tumor reprogramming through tcr recognition of epha2," *Science Immunology*, vol. 6, no. 61, p. eaba9010, 2021.

[88] R. Hudecek, B. Kohlova, I. Siskova, M. Piskacek, and A. Knight, "Blocking of epha2 on endometrial tumor cells reduces susceptibility to vδ1 gamma-delta t-cell-mediated killing," *Frontiers in Immunology*, vol. 12, p. 752646, 2021.

[89] R. Marlin, A. Pappalardo, H. Kaminski, C. R. Willcox, V. Pitard, S. Netzer, C. Khairallah, A.-M. Lomenech, C. Harly, M. Bonneville, *et al.*, "Sensing of cell stress by human $\gamma\delta$ tcr-dependent recognition of annexin a2," *Proceedings of the National Academy of Sciences*, vol. 114, no. 12, pp. 3163–3168, 2017.

[90] B. Xu, J. C. Pizarro, M. A. Holmes, C. McBeth, V. Groh, T. Spies, and R. K. Strong, "Crystal structure of a $\gamma\delta$ t-cell receptor specific for the human mhc class i homolog mica," *Proceedings of the National Academy of Sciences*, vol. 108, no. 6, pp. 2414–2419, 2011.

[91] A. C. Hayday, "$\gamma\delta$ t cell update: adaptate orchestrators of immune surveillance," *The Journal of Immunology*, vol. 203, no. 2, pp. 311–320, 2019.

[92] L. Chen and D. B. Flies, "Molecular mechanisms of t cell co-stimulation and co-inhibition," *Nature reviews immunology*, vol. 13, no. 4, pp. 227–242, 2013.

[93] N. Espagnolle, D. Depoil, R. Zaru, C. Demeur, E. Champagne, M. Guiraud, and S. Valitutti, "Cd2 and tcr synergize for the activation of phospholipase cγ1/calcium pathway at the immunological synapse," *International immunology*, vol. 19, no. 3, pp. 239–248, 2007.

[94] G. Pawelec, K. Schaudt, A. Rehbein, D. Olive, and H.-J. Bühring, "Human t cell clones with $\gamma\delta$ and $\alpha\beta$ receptors are differently stimulated by monoclonal antibodies to cd2," *Cellular immunology*, vol. 129, no. 2, pp. 385–393, 1990.

[95] D. Wu, P. Wu, X. Wu, J. Ye, Z. Wang, S. Zhao, C. Ni, G. Hu, J. Xu, Y. Han, *et al.*, "Ex vivo expanded human circulating vδ1 $\gamma\delta$t cells exhibit favorable therapeutic potential for colon cancer," *Oncoimmunology*, vol. 4, no. 3, p. e992749, 2015.

[96] V. Lafont, J. Liautard, A. Gross, J. P. Liautard, and J. Favero, "Tumor necrosis factor-α production is differently regulated in $\gamma\delta$ and $\alpha\beta$ human t lymphocytes," *Journal of Biological Chemistry*, vol. 275, no. 25, pp. 19282–19287, 2000.

[97] R. Testi and L. L. Lanier, "Functional expression of cd28 on t cell antigen receptor γ/δ-bearing t lymphocytes," *European journal of immunology*, vol. 19, no. 1, pp. 185–188, 1989.

[98] A. DeBarros, M. Chaves-Ferreira, F. d'Orey, J. C. Ribot, and B. Silva-Santos, "Cd70–cd27 interactions provide survival and proliferative signals that regulate t cell receptor-driven

activation of human $\gamma\delta$ peripheral blood lymphocytes," *European journal of immunology*, vol. 41, no. 1, pp. 195–201, 2011.

[99] L. Tan, A. S. Fichtner, E. Bruni, I. Odak, I. Sandrock, A. Bubke, A. Borchers, C. Schultze-Florey, C. Koenecke, R. Förster, *et al.*, "A fetal wave of human type 3 effector $\gamma\delta$ cells with restricted tcr diversity persists into adulthood," *Science immunology*, vol. 6, no. 58, p. eabf0125, 2021.

[100] D. Davies, S. Kamdar, R. Woolf, I. Zlatareva, M. L. Iannitto, C. Morton, Y. Haque, H. Martin, D. Biswas, S. Ndagire, M. Munonyara, C. Gillett, O. O'Neill, O. Nussbaumer, A. Hayday, and Y. Wu, "Pd-1 defines a distinct, functional, tissue-adapted state in vδ1+ t cells with implications for cancer immunotherapy," *Nature Cancer*, vol. 5, no. 3, pp. 420–432, 2024.

[101] C. Rancan, M. Arias-Badia, P. Dogra, B. Chen, D. Aran, H. Yang, D. Luong, A. Ilano, J. Li, H. Chang, *et al.*, "Exhausted intratumoral vδ2- $\gamma\delta$ t cells in human kidney cancer retain effector function," *Nature Immunology*, vol. 24, no. 4, pp. 612–624, 2023.

[102] M. Iwasaki, Y. Tanaka, H. Kobayashi, K. Murata-Hirai, H. Miyabe, T. Sugie, M. Toi, and N. Minato, "Expression and function of pd-1 in human $\gamma\delta$ t cells that recognize phosphoantigens," *European journal of immunology*, vol. 41, no. 2, pp. 345–355, 2011.

[103] F. M. Wensveen, V. Jelenčić, and B. Polić, "Nkg2d: a master regulator of immune cell responsiveness," *Frontiers in immunology*, vol. 9, p. 441, 2018.

[104] B. Rincon-Orozco, V. Kunzmann, P. Wrobel, D. Kabelitz, A. Steinle, and T. Herrmann, "Activation of vγ9vδ2 t cells by nkg2d," *The Journal of Immunology*, vol. 175, no. 4, pp. 2144–2151, 2005.

[105] A. Q. Gomes, D. V. Correia, A. R. Grosso, T. Lança, C. Ferreira, J. F. Lacerda, J. T. Barata, M. G. da Silva, and B. Silva-Santos, "Identification of a panel of ten cell surface protein antigens associated with immunotargeting of leukemias and lymphomas by peripheral blood $\gamma\delta$ t cells," *Haematologica*, vol. 95, no. 8, p. 1397, 2010.

[106] V. Groh, R. Rhinehart, H. Secrist, S. Bauer, K. H. Grabstein, and T. Spies, "Broad tumor-associated expression and recognition by tumor-derived $\gamma\delta$ t cells of mica and micb," *Proceedings of the National Academy of Sciences*, vol. 96, no. 12, pp. 6879–6884, 1999.

[107] J. Wu, V. Groh, and T. Spies, "T cell antigen receptor engagement and specificity in the recognition of stress-inducible mhc class i-related chains by human epithelial $\gamma\delta$ t cells," *The Journal of Immunology*, vol. 169, no. 3, pp. 1236–1240, 2002.

[108] Y. Kong, W. Cao, X. Xi, C. Ma, L. Cui, and W. He, "The nkg2d ligand ulbp4 binds to tcrγ9/δ2 and induces cytotoxicity to tumor cells through both tcr$\gamma\delta$ and nkg2d," *Blood, The Journal of the American Society of Hematology*, vol. 114, no. 2, pp. 310–317, 2009.

[109] D. V. Correia, A. C. Lopes, and B. Silva-Santos, "Tumor cell recognition by $\gamma\delta$ t lymphocytes: T-cell receptor vs. nk-cell receptors," *Oncoimmunology*, vol. 2, no. 1, p. e22892, 2013.

[110] S. Mensurado, C. Condeço, D. Sánchez-Martínez, S. Shirley, R. M. Coelho, N. Tirado, M. Vinyoles, R. Blanco-Domínguez, L. Barros, B. Galvão, *et al.*, "Cd155/pvr determines acute myeloid leukemia targeting by delta one t cells," *Blood*, vol. 143, no. 15, pp. 1488–1495, 2024.

[111] A. Knight, S. Mackinnon, and M. W. Lowdell, "Human vdelta1 gamma-delta t cells exert potent specific cytotoxicity against primary multiple myeloma cells," *Cytotherapy*, vol. 14, no. 9, pp. 1110–1118, 2012.

[112] A. D. Barrow, C. J. Martin, and M. Colonna, "The natural cytotoxicity receptors in health and disease," *Frontiers in immunology*, vol. 10, p. 909, 2019.

[113] D. V. Correia, M. Fogli, K. Hudspeth, M. G. da Silva, D. Mavilio, and B. Silva-Santos, "Differentiation of human peripheral blood vδ1+ t cells expressing the natural cytotoxicity receptor nkp30 for recognition of lymphoid leukemia cells," *Blood, The Journal of the American Society of Hematology*, vol. 118, no. 4, pp. 992–1001, 2011.

[114] D. H. Raulet, "Missing self recognition and self tolerance of natural killer (nk) cells," in *Seminars in immunology*, vol. 18, pp. 145–150, Elsevier, 2006.

[115] V. Cazzetta, E. Bruni, S. Terzoli, C. Carenza, S. Franzese, R. Piazza, P. Marzano, M. Donadon, G. Torzilli, M. Cimino, *et al.*, "Nkg2a expression identifies a subset of human vδ2 t cells exerting the highest antitumor effector functions," *Cell Reports*, vol. 37, no. 3, 2021.

[116] J. H. Russell and T. J. Ley, "Lymphocyte-mediated cytotoxicity," *Annual review of immunology*, vol. 20, no. 1, pp. 323–370, 2002.

[117] R. Zambello, G. Barilà, S. Manni, F. Piazza, and G. Semenzato, "Nk cells and cd38: implication for (immuno) therapy in plasma cell dyscrasias," *Cells*, vol. 9, no. 3, p. 768, 2020.

[118] S.-C. Oh, S.-E. Kim, I.-H. Jang, S.-M. Kim, S. Y. Lee, S. Lee, I.-S. Chu, S. R. Yoon, H. Jung, I. Choi, *et al.*, "Ngr1 is an nk cell inhibitory receptor that destabilizes the immunological synapse," *Nature Immunology*, vol. 24, no. 3, pp. 463–473, 2023.

[119] W. R. Strohl and M. Naso, "Bispecific t-cell redirection versus chimeric antigen receptor (car)-t cells as approaches to kill cancer cells," *Antibodies*, vol. 8, no. 3, p. 41, 2019.

[120] S. Paul and G. Lal, "The molecular mechanism of natural killer cells function and its importance in cancer immunotherapy," *Frontiers in immunology*, vol. 8, p. 1124, 2017.

[121] N. Vigneron, "Human tumor antigens and cancer immunotherapy," *BioMed research international*, vol. 2015, no. 1, p. 948501, 2015.

[122] M. Mojic, K. Takeda, and Y. Hayakawa, "The dark side of ifn-γ: its role in promoting cancer immunoevasion," *International journal of molecular sciences*, vol. 19, no. 1, p. 89, 2017.

[123] G. M. Siegers, H. Dhamko, X.-H. Wang, A. M. Mathieson, Y. Kosaka, T. C. Felizardo, J. A. Medin, S. Tohda, J. Schueler, P. Fisch, and A. Keating, "Human vδ1 $\gamma\delta$ t cells expanded from peripheral blood exhibit specific cytotoxicity against b-cell chronic lymphocytic leukemia-derived cells," *Cytotherapy*, vol. 13, no. 6, pp. 753–764, 2011.

[124] F. Dieli, D. Vermijlen, F. Fulfaro, N. Caccamo, S. Meraviglia, G. Cicero, A. Roberts, S. Buccheri, M. D'Asaro, N. Gebbia, *et al.*, "Targeting human $\gamma\delta$ t cells with zoledronate and interleukin-2 for immunotherapy of hormone-refractory prostate cancer," *Cancer research*, vol. 67, no. 15, pp. 7450–7457, 2007.

[125] K. Schilbach, K. Frommer, S. Meier, R. Handgretinger, and M. Eyrich, "Immune response of human propagated $\gamma\delta$-t-cells to neuroblastoma recommend the vδ1+ subset for $\gamma\delta$-t-cell–based immunotherapy," *Journal of Immunotherapy*, vol. 31, no. 9, pp. 896–905, 2008.

[126] J. P. Fisher, M. Yan, J. Heuijerjans, L. Carter, A. Abolhassani, J. Frosch, R. Wallace, B. Flutter, A. Capsomidis, M. Hubank, *et al.*, "Neuroblastoma killing properties of vδ2 and vδ2-negative $\gamma\delta$t cells following expansion by artificial antigen-presenting cells," *Clinical Cancer Research*, vol. 20, no. 22, pp. 5720–5732, 2014.

[127] A. Poggi, C. Venturino, S. Catellani, M. Clavio, M. Miglino, M. Gobbi, A. Steinle, P. Ghia, S. Stella, F. Caligaris-Cappio, and M. R. Zocchi, "Vδ1 t lymphocytes from b-cll patients recognize ulbp3 expressed on leukemic b cells and up-regulated by trans-retinoic acid," *Cancer research*, vol. 64, no. 24, pp. 9172–9179, 2004.

[128] K. Godder, P. Henslee-Downey, J. Mehta, B. Park, K. Chiang, S. Abhyankar, and L. Lamb, "Long term disease-free survival in acute leukemia patients recovering with increased $\gamma\delta$ t cells after partially mismatched related donor bone marrow transplantation," *Bone marrow transplantation*, vol. 39, no. 12, pp. 751–757, 2007.

[129] G. M. Siegers and L. S. Lamb, "Cytotoxic and regulatory properties of circulating vδ1+ $\gamma\delta$ t cells: a new player on the cell therapy field?," *Molecular Therapy*, vol. 22, no. 8, pp. 1416–1422, 2014.

[130] M. S. Davey, C. R. Willcox, A. T. Baker, S. Hunter, and B. E. Willcox, "Recasting human vδ1 lymphocytes in an adaptive role," *Trends in immunology*, vol. 39, no. 6, pp. 446–459, 2018.

[131] V. Pitard, D. Roumanes, X. Lafarge, L. Couzi, I. Garrigue, M.-E. Lafon, P. Merville, J.-F. Moreau, and J. Déchanet-Merville, "Long-term expansion of effector/memory vδ2- $\gamma\delta$ t cells is a specific blood signature of cmv infection," *Blood, The Journal of the American Society of Hematology*, vol. 112, no. 4, pp. 1317–1324, 2008.

[132] G. Sanchez Sanchez, Y. Tafesse, M. Papadopoulou, and D. Vermijlen, "Surfing on the waves of the human $\gamma\delta$ t cell ontogenic sea," *Immunological reviews*, vol. 315, no. 1, pp. 89–107, 2023.

[133] L. Lamb Jr, P. Henslee-Downey, R. Parrish, K. Godder, J. Thompson, C. Lee, and A. Gee, "Increased frequency of tcr gamma delta+ t cells in disease-free survivors following t cell-depleted, partially mismatched, related donor bone marrow transplantation for leukemia.," *Journal of hematotherapy*, vol. 5, no. 5, pp. 503–509, 1996.

[134] L. J. Knowles, M. Malik, O. Nussebaumer, A. Brown, S. van Wetering, and M. Koslowski, "Abstract ct525: Gdx012u-001 a phase 1, open-label, dose escalation, and dose expansion study to assess the safety, tolerability, and preliminary antileukemic activity of gdx012 in patients with mrd positive aml," *Cancer Research*, vol. 82, no. 12_Supplement, pp. CT525–CT525, 2022.

[135] H. Jonescheit, H.-H. Oberg, D. Gonnermann, M. Hermes, V. Sulaj, C. Peters, D. Kabelitz, and D. Wesch, "Influence of indoleamine-2, 3-dioxygenase and its metabolite kynurenine

on $\gamma\delta$ t cell cytotoxicity against ductal pancreatic adenocarcinoma cells," *Cells*, vol. 9, no. 5, p. 1140, 2020.

[136] D. Gonnermann, H.-H. Oberg, M. Lettau, M. Peipp, D. Bauerschlag, S. Sebens, D. Kabelitz, and D. Wesch, "Galectin-3 released by pancreatic ductal adenocarcinoma suppresses $\gamma\delta$ t cell proliferation but not their cytotoxicity," *Frontiers in immunology*, vol. 11, p. 1328, 2020.

[137] L. Martinet, S. Fleury-Cappellesso, M. Gadelorge, G. Dietrich, P. Bourin, J.-J. Fournié, and R. Poupot, "A regulatory cross-talk between vγ9vδ2 t lymphocytes and mesenchymal stem cells," *European journal of immunology*, vol. 39, no. 3, pp. 752–762, 2009.

[138] D. Tawfik, C. Groth, J.-P. Gundlach, M. Peipp, D. Kabelitz, T. Becker, H.-H. Oberg, A. Trauzold, and D. Wesch, "Trail-receptor 4 modulates $\gamma\delta$ t cell-cytotoxicity toward cancer cells," *Frontiers in Immunology*, vol. 10, p. 2044, 2019.

[139] X. Li, N. Kang, X. Zhang, X. Dong, W. Wei, L. Cui, D. Ba, and W. He, "Generation of human regulatory $\gamma\delta$ t cells by tcr$\gamma\delta$ stimulation in the presence of tgf-β and their involvement in the pathogenesis of systemic lupus erythematosus," *The Journal of Immunology*, vol. 186, no. 12, pp. 6693–6700, 2011.

[140] A. A. Kühl, N. N. Pawlowski, K. Grollich, M. Blessenohl, J. Westermann, M. Zeitz, C. Loddenkemper, and J. C. Hoffmann, "Human peripheral $\gamma\delta$ t cells possess regulatory potential," *Immunology*, vol. 128, no. 4, pp. 580–588, 2009.

[141] E. Batlle and J. Massagué, "Transforming growth factor-β signaling in immunity and cancer," *Immunity*, vol. 50, no. 4, pp. 924–940, 2019.

[142] G. Hu, P. Wu, P. Cheng, Z. Zhang, Z. Wang, X. Yu, X. Shao, D. Wu, J. Ye, T. Zhang, *et al.*, "Tumor-infiltrating cd39+ γ δ tregs are novel immunosuppressive t cells in human colorectal cancer," *Oncoimmunology*, vol. 6, no. 2, p. e1277305, 2017.

[143] R. Casetti, C. Agrati, M. Wallace, A. Sacchi, F. Martini, A. Martino, A. Rinaldi, and M. Malkovsky, "Cutting edge: Tgf-β1 and il-15 induce foxp3+ $\gamma\delta$ regulatory t cells in the presence of antigen stimulation," *The Journal of Immunology*, vol. 183, no. 6, pp. 3574–3577, 2009.

[144] R. E. Beatson, A. C. Parente-Pereira, L. Halim, D. Cozzetto, C. Hull, L. M. Whilding, O. Martinez, C. A. Taylor, J. Obajdin, K. N. L. Hoang, *et al.*, "Tgf-β1 potentiates vγ9vδ2 t cell adoptive immunotherapy of cancer," *Cell Reports Medicine*, vol. 2, no. 12, 2021.

[145] K. Odaira, S.-n. Kimura, N. Fujieda, Y. Kobayashi, K. Kambara, T. Takahashi, T. Izumi, H. Matsushita, and K. Kakimi, "Cd27-cd45+ $\gamma\delta$ t cells can be divided into two populations, cd27-cd45int and cd27-cd45hi with little proliferation potential," *Biochemical and biophysical research communications*, vol. 478, no. 3, pp. 1298–1303, 2016.

[146] G. Qu, S. Wang, Z. Zhou, D. Jiang, A. Liao, and J. Luo, "Comparing mouse and human tissue-resident $\gamma\delta$ t cells," *Frontiers in immunology*, vol. 13, p. 891687, 2022.

[147] C. Ma, Q. Zhang, J. Ye, F. Wang, Y. Zhang, E. Wevers, T. Schwartz, P. Hunborg, M. A. Varvares, D. F. Hoft, *et al.*, "Tumor-infiltrating $\gamma\delta$ t lymphocytes predict clinical outcome in human breast cancer," *The Journal of Immunology*, vol. 189, no. 10, pp. 5029–5036, 2012.

[148] G. Chabab, C. Barjon, N. Abdellaoui, L. Salvador-Prince, C. Dejou, H.-A. Michaud, F. Boissière-Michot, E. Lopez-Crapez, W. Jacot, D. Pourquier, *et al.*, "Identification of a regulatory vδ1 gamma delta t cell subpopulation expressing cd73 in human breast cancer," *Journal of leukocyte biology*, vol. 107, no. 6, pp. 1057–1067, 2020.

[149] J. Ye, C. Ma, E. C. Hsueh, C. S. Eickhoff, Y. Zhang, M. A. Varvares, D. F. Hoft, and G. Peng, "Tumor-derived $\gamma\delta$ regulatory t cells suppress innate and adaptive immunity through the induction of immunosenescence," *The Journal of Immunology*, vol. 190, no. 5, pp. 2403–2414, 2013.

[150] M. F. Chevalier, N. Bhatnagar, C. Didier, M. Lopez-Gonzalez, J. Pavie, D. Bollens, C. Duvivier, L. Collias, C. Jung, D. Scott-Algara, *et al.*, "$\gamma\delta$ t-cell subsets in hiv controllers: potential role of t$\gamma\delta$17 cells in the regulation of chronic immune activation," *Aids*, vol. 33, no. 8, pp. 1283–1292, 2019.

[151] G. S. Olson, S. W. Moore, J. M. Richter, J. J. Garber, B. A. Bowman, C. A. Rawlings, M. Flagg, B. Corleis, and D. S. Kwon, "Increased frequency of systemic pro-inflammatory vδ1+ $\gamma\delta$ t cells in hiv elite controllers correlates with gut viral load," *Scientific Reports*, vol. 8, no. 1, p. 16471, 2018.

[152] C. K. Muller, J. Spagnuolo, A. Audigé, A. Chancellor, D. Russenberger, A. U. Scherrer, M. Hoffmann, R. Kouyos, M. Battegay, G. De Libero, *et al.*, "Immunophenotypic characterization of tcr $\gamma\delta$ t cells and mait cells in hiv-infected individuals developing hodgkin's lymphoma," *Infectious Agents and Cancer*, vol. 16, pp. 1–15, 2021.

[153] R. J. Dart, I. Zlatareva, P. Vantourout, E. Theodoridis, A. Amar, S. Kannambath, P. East, T. Recaldin, J. C. Mansfield, C. A. Lamb, *et al.*, "Conserved $\gamma\delta$ t cell selection by btnl pro-

teins limits progression of human inflammatory bowel disease," *Science*, vol. 381, no. 6663, p. eadh0301, 2023.

[154] Y. Hu, Q. Hu, Y. Li, L. Lu, Z. Xiang, Z. Yin, D. Kabelitz, and Y. Wu, "$\gamma\delta$ t cells: origin and fate, subsets, diseases and immunotherapy," *Signal Transduction and Targeted Therapy*, vol. 8, no. 1, p. 434, 2023.

[155] B. Di Lorenzo, A. E. Simoes, F. Caiado, P. Tieppo, D. V. Correia, T. Carvalho, M. G. Da Silva, J. Déchanet-Merville, T. N. Schumacher, I. Prinz, *et al.*, "Broad cytotoxic targeting of acute myeloid leukemia by polyclonal delta one t cells," *Cancer immunology research*, vol. 7, no. 4, pp. 552–558, 2019.

[156] D. S. Martínez, N. Tirado, S. Mensurado, A. Martínez-Moreno, P. Romecín, F. G. Agüera, D. V. Correia, B. Silva-Santos, and P. Menéndez, "Generation and proof-of-concept for allogeneic cd123 car-delta one t (dot) cells in acute myeloid leukemia," *Journal for immunotherapy of cancer*, vol. 10, no. 9, 2022.

[157] A. Rotolo, C. Chabannon, and R. Gramignoli, "Identification of hurdles in the development of cell-based therapies," 2020.

[158] L. Paniagua-Herranz, C. Díaz-Tejeiro, A. Sanvicente, J. Bartolomé, C. Nieto-Jiménez, and A. Ocana, "Overcoming limitations for antibody-based therapies targeting $\gamma\delta$ t (vg9vd2) cells," *Frontiers in Immunology*, vol. 15, p. 1432015, 2024.

[159] N. Mehra, J. Voortman, D. R. Wise, E. Calvo, J. M. Piulats, E. Gonzalez-Billalabeitia, I. Ortego, U. Swami, J. Picus, M. Karlik, *et al.*, "Phase i/ii trial of lava-1207, a novel bispecific gamma-delta t-cell engager alone, or with low dose il-2 or pembrolizumab, in metastatic castration resistant prostate cancer (mcrpc).," 2024.

[160] T. Cerny, B. Borisch, M. Introna, P. Johnson, and A. L. Rose, "Mechanism of action of rituximab," *Anti-cancer drugs*, vol. 13, pp. S3–S10, 2002.

[161] R. Bargou, E. Leo, G. Zugmaier, M. Klinger, M. Goebeler, S. Knop, R. Noppeney, A. Viardot, G. Hess, M. Schuler, *et al.*, "Tumor regression in cancer patients by very low doses of a t cell–engaging antibody," *Science*, vol. 321, no. 5891, pp. 974–977, 2008.

[162] J. Kang, T. Sun, and Y. Zhang, "Immunotherapeutic progress and application of bispecific antibody in cancer," *Frontiers in Immunology*, vol. 13, p. 1020003, 2022.

[163] R. H. Carter, Y. Wang, and S. Brooks, "Role of cd19 signal transduction in b cell biology," *Immunologic research*, vol. 26, pp. 45–54, 2002.

[164] T. F. Tedder, "Cd19: a promising b cell target for rheumatoid arthritis," *Nature reviews Rheumatology*, vol. 5, no. 10, pp. 572–577, 2009.

[165] M. S. Topp, N. Gökbuget, A. S. Stein, G. Zugmaier, S. O'Brien, R. C. Bargou, H. Dombret, A. K. Fielding, L. Heffner, R. A. Larson, and S. Neumann, "Safety and activity of blinatumomab for adult patients with relapsed or refractory b-precursor acute lymphoblastic leukaemia: a multicentre, single-arm, phase 2 study," *The Lancet Oncology*, vol. 16, pp. 57–66, Jan 2015.

[166] J. Bartkowiak, D. Kulczyck-Wojdala, J. Blonski, and T. Robak, "Molecular diversity of gammadelta t cells in peripheral blood from patients with b-cell chronic lymphocytic leukaemia.," *Neoplasma*, vol. 49, no. 2, pp. 86–90, 2002.

[167] D. C. Deniger, K. Switzer, T. Mi, S. Maiti, L. Hurton, H. Singh, H. Huls, S. Olivares, D. A. Lee, R. E. Champlin, *et al.*, "Bispecific t-cells expressing polyclonal repertoire of endogenous $\gamma\delta$ t-cell receptors and introduced cd19-specific chimeric antigen receptor," *Molecular therapy*, vol. 21, no. 3, pp. 638–647, 2013.

[168] M. Peipp, D. Wesch, H.-H. Oberg, S. Lutz, A. Muskulus, J. Van De Winkel, P. Parren, R. Burger, A. Humpe, D. Kabelitz, *et al.*, "Cd20-specific immunoligands engaging nkg2d enhance $\gamma\delta$ t cell-mediated lysis of lymphoma cells," *Scandinavian Journal of Immunology*, vol. 86, no. 4, pp. 196–206, 2017.

[169] M. D. Swanson, S. Rios, S. Mittal, G. Soder, and V. Jawa, "Immunogenicity risk assessment of spontaneously occurring therapeutic monoclonal antibody aggregates," *Frontiers in Immunology*, vol. 13, p. 915412, 2022.

[170] E. San José, A. Borroto, F. Niedergang, A. Alcover, and B. Alarcón, "Triggering the tcr complex causes the downregulation of nonengaged receptors by a signal transduction-dependent mechanism," *Immunity*, vol. 12, no. 2, pp. 161–170, 2000.

[171] S.-F. Cho, L. Lin, L. Xing, J. Liu, T. Yu, K. Wen, P. Hsieh, N. Munshi, K. Anderson, and Y.-T. Tai, "Anti-bcma bite® amg 701 potently induces specific t cell lysis of human multiple myeloma (mm) cells and immunomodulation in the bone marrow microenvironment," *Blood*, vol. 132, p. 592, 2018.

[172] C. Krupka, P. Kufer, R. Kischel, G. Zugmaier, J. Bögeholz, T. Köhnke, F. S. Lichtenegger, S. Schneider, K. H. Metzeler, M. Fiegl, *et al.*, "Cd33 target validation and sustained depletion of aml blasts in long-term cultures by the bispecific t-cell–engaging antibody

amg 330," *Blood, The Journal of the American Society of Hematology*, vol. 123, no. 3, pp. 356–365, 2014.

[173] M. Al-Hussaini, M. P. Rettig, J. K. Ritchey, D. Karpova, G. L. Uy, L. G. Eissenberg, F. Gao, W. C. Eades, E. Bonvini, G. R. Chichili, *et al.*, "Targeting cd123 in acute myeloid leukemia using a t-cell–directed dual-affinity retargeting platform," *Blood, The Journal of the American Society of Hematology*, vol. 127, no. 1, pp. 122–131, 2016.

[174] S. L. Enoksson, P. Bergman, J. Klingström, F. Boström, R. D. S. Rodrigues, M. E. Winerdal, and P. Marits, "A flow cytometry-based proliferation assay for clinical evaluation of t-cell memory against sars-cov-2," *Journal of Immunological Methods*, vol. 499, p. 113159, 2021.

[175] G. M. Siegers, M. Swamy, E. Fernández-Malavé, S. Minguet, S. Rathmann, A. C. Guardo, V. Pérez-Flores, J. R. Regueiro, B. Alarcón, P. Fisch, *et al.*, "Different composition of the human and the mouse $\gamma\delta$ t cell receptor explains different phenotypes of cd3γ and cd3δ immunodeficiencies," *The Journal of experimental medicine*, vol. 204, no. 11, pp. 2537–2544, 2007.

[176] H. M. Horton, M. J. Bernett, E. Pong, M. Peipp, S. Karki, S. Y. Chu, J. O. Richards, I. Vostiar, P. F. Joyce, R. Repp, *et al.*, "Potent in vitro and in vivo activity of an fc-engineered anti-cd19 monoclonal antibody against lymphoma and leukemia," *Cancer research*, vol. 68, no. 19, pp. 8049–8057, 2008.

[177] S. Mensurado, R. Blanco-Domínguez, and B. Silva-Santos, "The emerging roles of $\gamma\delta$ t cells in cancer immunotherapy," *Nature Reviews Clinical Oncology*, vol. 20, no. 3, pp. 178–191, 2023.

[178] A. Paiva, G. V. Alves, L. S. Silveira Jr, E. A. Gil, R. D. Soares, D. G. Silva, R. V. Freitas, F. Bahia, M. R. Barbosa, and G. B. Cavalcanti Jr, "Expression of the cd5 molecule in chronic lymphocytic leukemia," 2017.

[179] Y. Zhang, Q. Liu, S. Yang, and Q. Liao, "Cd58 immunobiology at a glance," *Frontiers in immunology*, vol. 12, p. 705260, 2021.

[180] G. Voisinne, A. Gonzalez de Peredo, and R. Roncagalli, "Cd5, an undercover regulator of tcr signaling," *Frontiers in immunology*, vol. 9, p. 2900, 2018.

[181] A. Hayday, J. Dechanet-Merville, J. Rossjohn, and B. Silva-Santos, "Cancer immunotherapy by $\gamma\delta$ t cells," *Science*, vol. 386, no. 6717, p. eabq7248, 2024.

[182] K. Beckermann, B. Rini, B. T. Aftab, H. Budworth, F. Galimi, S. Green, N. Jahchan, J. Kennedy-Wilde, K. P. Nishimoto, G. S. Vosganian, *et al.*, "640 a phase 1/2 first in human study of adi-270, an armored allogeneic anti-cd70 chimeric antigen receptor $\gamma\delta$ t cell therapy, in patients with relapsed or refractory clear cell renal cell carcinoma," 2024.

[183] S. Biradar, Y. Agarwal, M. T. Lotze, M. T. Bility, and R. B. Mailliard, "The blt humanized mouse model as a tool for studying human gamma delta t cell-hiv interactions in vivo," *Frontiers in Immunology*, vol. 13, p. 881607, 2022.

[184] S. Offner, R. Hofmeister, A. Romaniuk, P. Kufer, and P. A. Baeuerle, "Induction of regular cytolytic t cell synapses by bispecific single-chain antibody constructs on mhc class i-negative tumor cells," *Molecular immunology*, vol. 43, no. 6, pp. 763–771, 2006.

[185] B. Purtic, L. A. Pitcher, N. S. Van Oers, and C. Wülfing, "T cell receptor (tcr) clustering in the immunological synapse integrates tcr and costimulatory signaling in selected t cells," *Proceedings of the National Academy of Sciences*, vol. 102, no. 8, pp. 2904–2909, 2005.

[186] T. J. Crites, K. Padhan, J. Muller, M. Krogsgaard, P. R. Gudla, S. J. Lockett, and R. Varma, "Tcr microclusters pre-exist and contain molecules necessary for tcr signal transduction," *The Journal of Immunology*, vol. 193, no. 1, pp. 56–67, 2014.

[187] A. Tapia-Galisteo, I. Sanchez Rodriguez, O. Aguilar-Sopeña, S. L. Harwood, J. Narbona, M. Ferreras Gutierrez, R. Navarro, L. Martín-García, C. Corbacho, M. Compte, *et al.*, "Trispecific t-cell engagers for dual tumor-targeting of colorectal cancer," *Oncoimmunology*, vol. 11, no. 1, p. 2034355, 2022.

[188] D. Ellerman, "Bispecific t-cell engagers: towards understanding variables influencing the in vitro potency and tumor selectivity and their modulation to enhance their efficacy and safety," *Methods*, vol. 154, pp. 102–117, 2019.

[189] B. Santich, J. Park, H. Tran, *et al.*, "Interdomain spacing and spatial configuration drive the potency of igg-[l]-scfv t cell bispecific antibodies.," 2020.

[190] F. Le Gall, S. M. Kipriyanov, G. Moldenhauer, and M. Little, "Di-, tri-and tetrameric single chain fv antibody fragments against human cd19: effect of valency on cell binding," *FEBS letters*, vol. 453, no. 1-2, pp. 164–168, 1999.

[191] P. J. Hudson and A. A. Kortt, "High avidity scfv multimers; diabodies and triabodies," *Journal of immunological methods*, vol. 231, no. 1-2, pp. 177–189, 1999.

[192] J. S. Klein, S. Jiang, R. P. Galimidi, J. R. Keeffe, and P. J. Bjorkman, "Design and characterization of structured protein linkers with differing flexibilities," *Protein Engineering, Design & Selection*, vol. 27, no. 10, pp. 325–330, 2014.

[193] L. L. Sun, D. Ellerman, M. Mathieu, M. Hristopoulos, X. Chen, Y. Li, X. Yan, R. Clark, A. Reyes, E. Stefanich, *et al.*, "Anti-cd20/cd3 t cell–dependent bispecific antibody for the treatment of b cell malignancies," *Science translational medicine*, vol. 7, no. 287, pp. 287ra70–287ra70, 2015.

[194] Z. Tian, M. Liu, Y. Zhang, and X. Wang, "Bispecific t cell engagers: an emerging therapy for management of hematologic malignancies," *Journal of hematology & oncology*, vol. 14, no. 1, p. 75, 2021.

[195] M. Bacac, T. Fauti, J. Sam, S. Colombetti, T. Weinzierl, D. Ouaret, W. Bodmer, S. Lehmann, T. Hofer, R. J. Hosse, *et al.*, "A novel carcinoembryonic antigen t-cell bispecific antibody (cea tcb) for the treatment of solid tumors," *Clinical Cancer Research*, vol. 22, no. 13, pp. 3286–3297, 2016.

[196] L. Hviid, A. Felsing, and T. G. Theander, "Kinetics of human t-cell expression of lfa-1, il-2 receptor, and icam-1 following antigenic stimulation in vitro.," *Journal of clinical & laboratory immunology*, vol. 40, no. 4, pp. 163–171, 1993.

[197] C. Carrasco-Padilla, A. Hernaiz-Esteban, L. Álvarez-Vallina, O. Aguilar-Sopeña, and P. Roda-Navarro, "Bispecific antibody format and the organization of immunological synapses in t cell-redirecting strategies for cancer immunotherapy," *Pharmaceutics*, vol. 15, no. 1, p. 132, 2022.

[198] N. Föger, R. Marhaba, and M. Zöller, "Involvement of cd44 in cytoskeleton rearrangement and raft reorganization in t cells," *Journal of cell science*, vol. 114, no. 6, pp. 1169–1178, 2001.

[199] T. R. Mempel and F. Marangoni, "Cd44 keeps tumor killers polarized," *Immunity*, vol. 29, no. 6, pp. 843–845, 2008.

[200] I. Kareva, A. Zutshi, J. Rhoden, and S. Kabilan, "Practical guide to calculating impact of avidity in models of bispecific antibodies with two membrane-bound targets," *bioRxiv*, pp. 2022–09, 2022.

[201] S. A. Hammond, R. Lutterbuese, S. Roff, P. Lutterbuese, B. Schlereth, E. Bruckheimer, M. S. Kinch, S. Coats, P. A. Baeuerle, P. Kufer, *et al.*, "Selective targeting and potent

control of tumor growth using an epha2/cd3-bispecific single-chain antibody construct," *Cancer research*, vol. 67, no. 8, pp. 3927–3935, 2007.

[202] T. T. Junttila, J. Li, J. Johnston, M. Hristopoulos, R. Clark, D. Ellerman, B.-E. Wang, Y. Li, M. Mathieu, G. Li, *et al.*, "Antitumor efficacy of a bispecific antibody that targets her2 and activates t cells," *Cancer research*, vol. 74, no. 19, pp. 5561–5571, 2014.

[203] J. Li, N. J. Stagg, J. Johnston, M. J. Harris, S. A. Menzies, D. DiCara, V. Clark, M. Hristopoulos, R. Cook, D. Slaga, *et al.*, "Membrane-proximal epitope facilitates efficient t cell synapse formation by anti-fcrh5/cd3 and is a requirement for myeloma cell killing," *Cancer cell*, vol. 31, no. 3, pp. 383–395, 2017.

[204] J. Spiegel, J. S. Oak, A. Goyal, S. Bornheimer, A. Irvine, R. R. Shen, K. A. Kong, S. Bharadwaj, W.-K. Weng, M. Smith, *et al.*, "Cd19 antigen density down-regulation at time of progression in large b-cell lymphoma patients treated with axicabtagene ciloleucel," *Transplantation and Cellular Therapy, Official Publication of the American Society for Transplantation and Cellular Therapy*, vol. 30, no. 2, p. S204, 2024.

[205] F. Braig, A. Brandt, M. Goebeler, H.-P. Tony, A.-K. Kurze, P. Nollau, T. Bumm, S. Böttcher, R. C. Bargou, and M. Binder, "Resistance to anti-cd19/cd3 bite in acute lymphoblastic leukemia may be mediated by disrupted cd19 membrane trafficking," *Blood, The Journal of the American Society of Hematology*, vol. 129, no. 1, pp. 100–104, 2017.

[206] X. Zhang, H. Wang, and C. Sun, "Bispec pairwise ai: guiding the selection of bispecific antibody target combinations with pairwise learning and gpt augmentation," *Journal of Cancer Research and Clinical Oncology*, vol. 150, no. 5, p. 237, 2024.

[207] P. Ouyang, L. Wang, J. Wu, Y. Tian, C. Chen, D. Li, Z. Yao, R. Chen, G. Xiang, J. Gong, *et al.*, "Overcoming cold tumors: a combination strategy of immune checkpoint inhibitors," *Frontiers in Immunology*, vol. 15, p. 1344272, 2024.

[208] C. Gerard, J. Delyon, A. Wicky, K. Homicsko, M. A. Cuendet, and O. Michielin, "Turning tumors from cold to inflamed to improve immunotherapy response," *Cancer treatment reviews*, vol. 101, p. 102227, 2021.

[209] S. Chan, B. Morgan, M. K. Yong, M. Margetts, A. J. Farchione, E. C. Lucas, J. Godsell, N. A. Giang, C. A. Slade, A. von Borstel, *et al.*, "Cytomegalovirus drives vδ1+ $\gamma\delta$ t cell expansion and clonality in common variable immunodeficiency," *Nature Communications*, vol. 15, no. 1, p. 4286, 2024.

[210] H. Wurzer, C. Hoffmann, A. Al Absi, and C. Thomas, "Actin cytoskeleton straddling the immunological synapse between cytotoxic lymphocytes and cancer cells," *Cells*, vol. 8, no. 5, p. 463, 2019.

[211] D. Fenoglio, A. Poggi, S. Catellani, F. Battaglia, A. Ferrera, M. Setti, G. Murdaca, and M. R. Zocchi, "Vδ1 t lymphocytes producing ifn-γ and il-17 are expanded in hiv-1–infected patients and respond to candida albicans," *Blood, The Journal of the American Society of Hematology*, vol. 113, no. 26, pp. 6611–6618, 2009.

[212] P. J. Dunne, C. O. Maher, M. Freeley, K. Dunne, A. Petrasca, J. Orikiiriza, M. R. Dunne, D. Reidy, S. O'Dea, A. Loy, *et al.*, "Cd3ε expression defines functionally distinct subsets of vδ1 t cells in patients with human immunodeficiency virus infection," *Frontiers in immunology*, vol. 9, p. 940, 2018.

[213] T. R. W. Salinas, A. Gosselin, L. R. Marchand, E. M. Gabriel, O. Tastet, J.-P. Goulet, Y. Zhang, D. Vlad, H. Touil, J.-P. Routy, *et al.*, "Il-17a reprograms intestinal epithelial cells to facilitate hiv-1 replication and outgrowth in cd4+ t cells," *Iscience*, vol. 24, no. 11, 2021.

Chapter 8

Appendices

8.1 Appendix 1

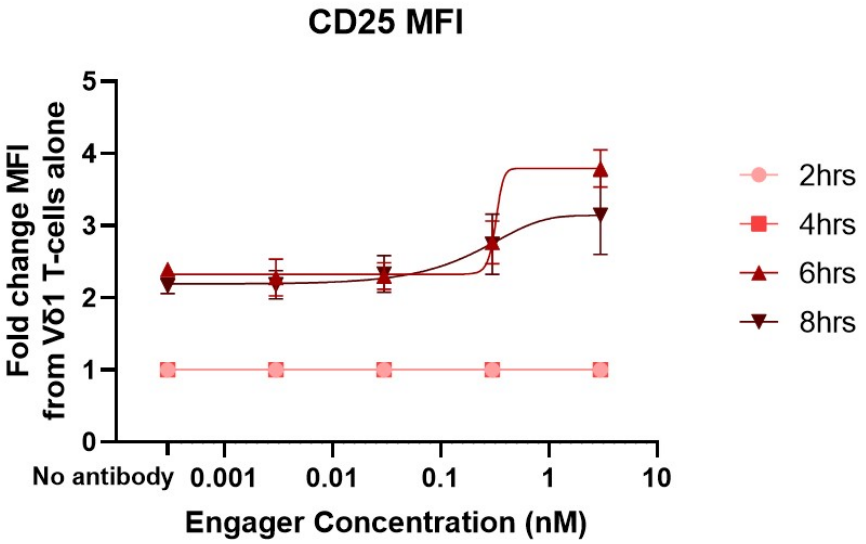


Figure 8.1: ***Antibody-mediated CD25 upregulation on skin-derived Vδ1 T-cells over time*** *CD25 expression on skin expanded (n=1) Vδ1 T-cells was assessed using flow cytometry following treatment with a Vδ1/CD19 BiTE with Nal-6 cells. The Vδ1/CD19 BiTE used here utilised a different, though similar, proprietary Vδ1 binding sequence. Data showing fold change MFI where raw MFI values were normalised to Vδ1 T-cells alone treatment. Error bars represent SEM.*

8.2 Appendix 2

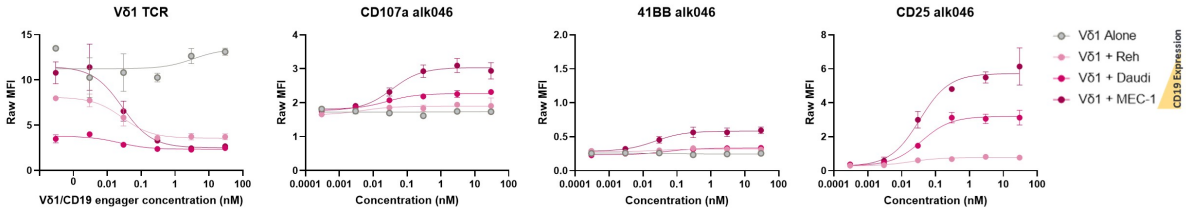


Figure 8.2: ***Cell line type affects baseline TCR downregulation but not activation of Vδ1 T-cells***

Vδ1 activation and cytotoxicity from blood expanded Vδ1 T-cells (representative donor from n=2) cultured alone and with Reh, Daudi or MEC-1 cells with Vδ1/CD19 BiTE treatment where Vδ1 TCR, CD107a and 41BB expression was assessed using flow cytometry after 4 hours of culture and CD25 expression and remaining live target cells were assessed after 24 hours of culture. Expression data presented as raw MFI values.

8.3 Appendix 3

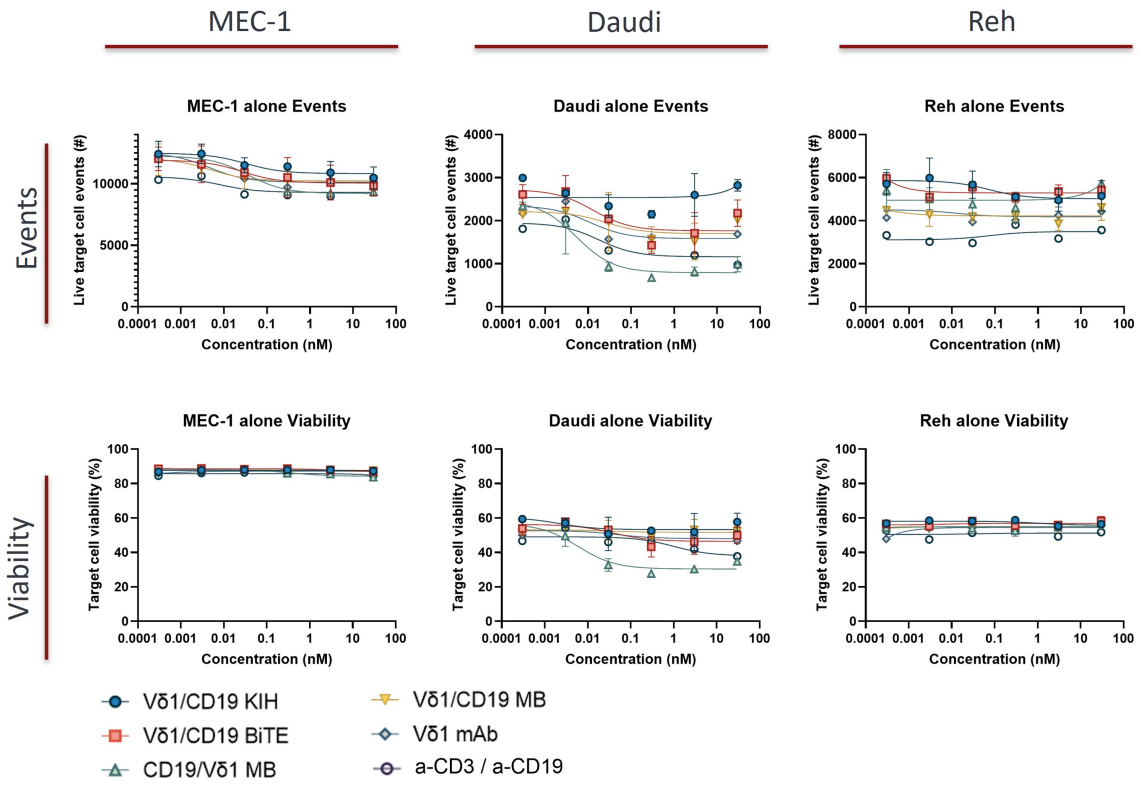


Figure 8.3: ***Vδ1/CD19 antibody-mediated effects on CD19+ cell lines.***

Remaining live CD19+ cells assessed by flow cytometry after culture alone with specified engager treatment for 24 hours. Bars indicated SD from treatment replicates. Top, Live target events. Bottom, % Live target cells identified using the dead cell dye efluor780.

8.4 Appendix 4

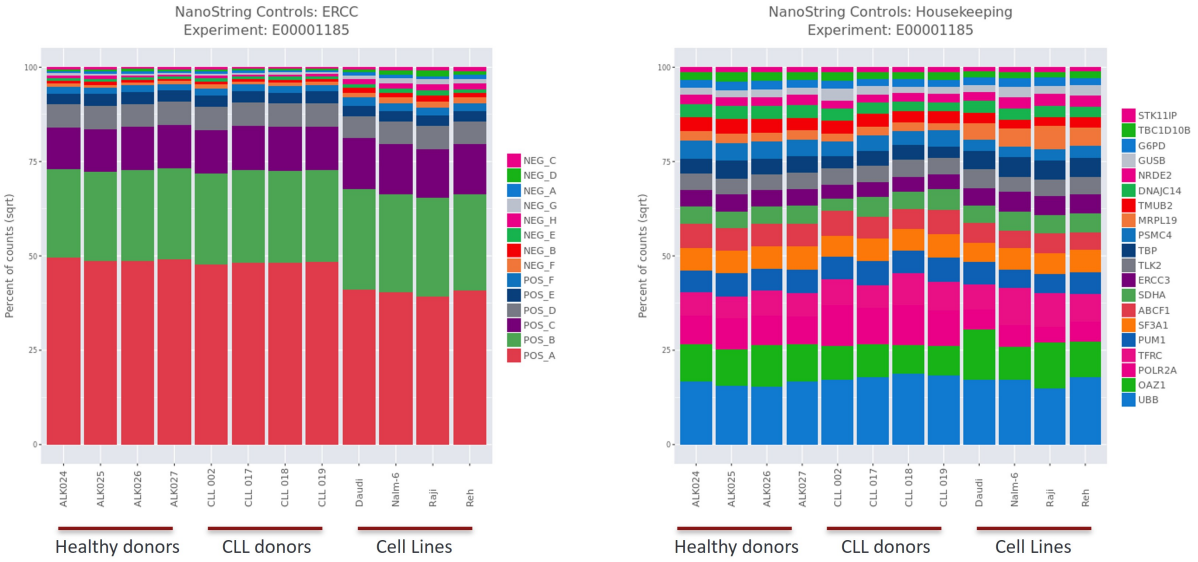


Figure 8.4: ***Nanostring control gene transcripts are comparable between cell samples.*** *RNA levels of engineered (left) and housekeeping gene controls from primary healthy (n=4) and primary CLL B cells (n=4) and CD19$^+$ cell lines, presented as percentage of counts, assessed using Nanostring Technologies.*

8.5 Appendix 5

	Cell Lines			Healthy B-cells				CLL B-cells			
	Daudi	Nalm-6	Reh	Donor 1	Donor 2	Donor 3	Donor 4	Donor 1	Donor 2	Donor 3	Donor 4
Cell Viability (%)	12.9	88.4	74.2	86.5	77.8	84.7	89.6	38.4	80.4	81.4	77.2

Figure 8.5: ***Target cell viability in cytotoxicity assay with blood-derived cytokine-expanded Vδ1 T-cells.***

Cell viability of target cells cultured in the same conditions as figure 4.27, without Vδ1 T-cells. Cell viability was calculated as the percentage of CTV+ cells from flow cytometry that were negative for the viability efluor780 dye.

8.6 Appendix 6

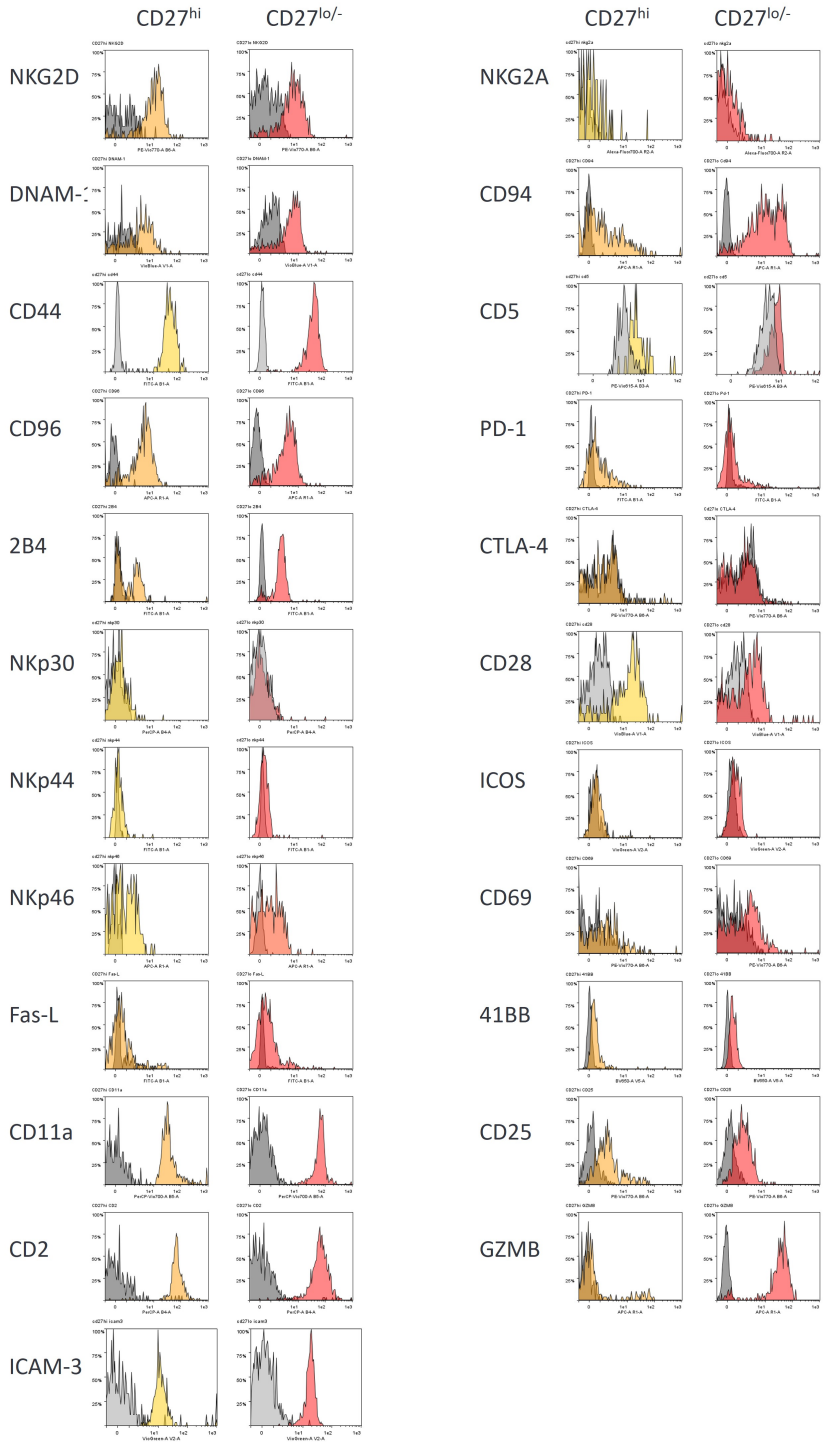


Figure 8.6: ***Representative histogram plots of co-receptor expression from Vδ1 T-cells from untreated PBMCs***

Vδ1 T-cell co-receptor expression from freshly thawed untreated PBMCs (representative donor from n=8) displayed as $CD27^{high}$ (yellow) and $CD27^{low/-}$ (red) subpopulations. FMO staining for indicated marker is highlighted in grey.

8.7 Appendix 7

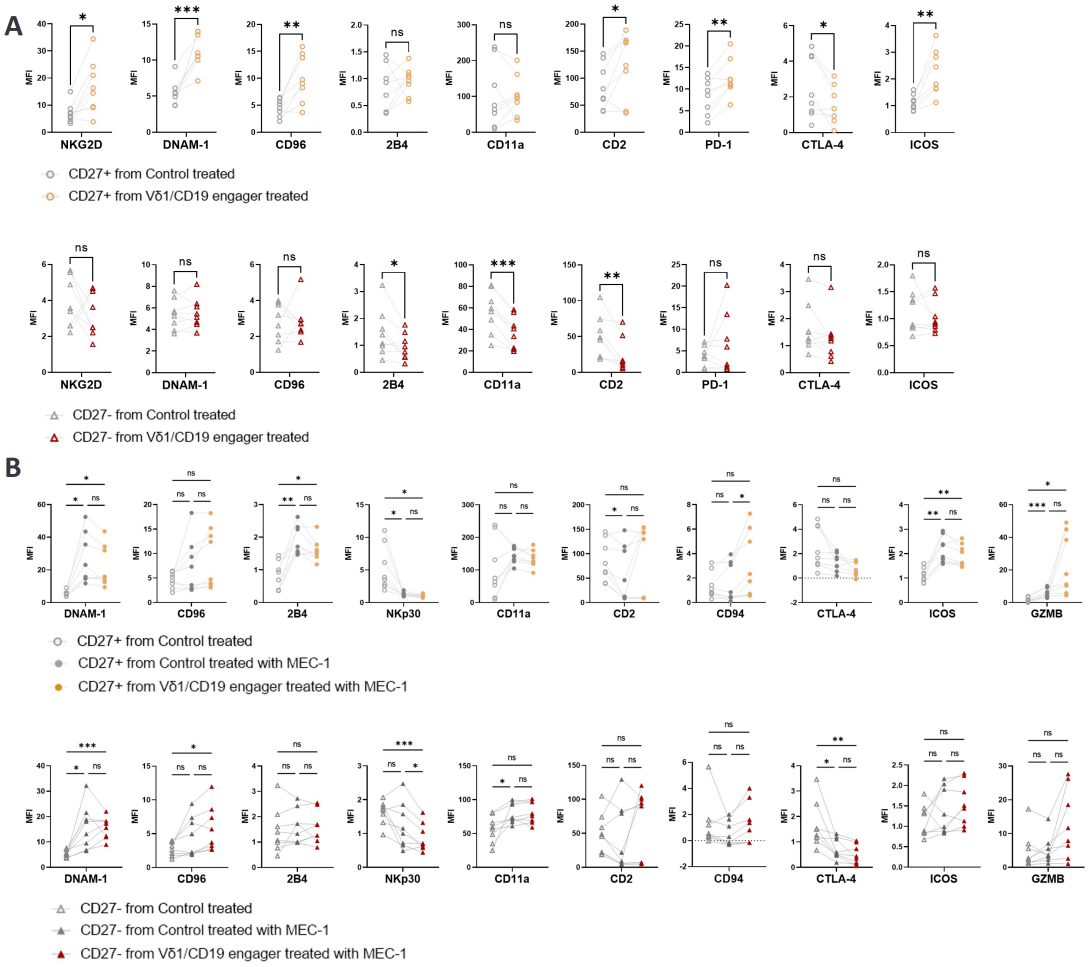


Figure 8.7: ***Vδ1/CD19 engager treatment affects Vδ1 T-cell phenotype***

$CD27^+$ and $CD27^-$ Vδ1 T-cell phenotype after 7 days in whole-PBMC culture (n=8) without (A) and with (B) MEC-1 cells treated with control (RSV BiTEs) and Vδ1/CD19 engagers assessed by flow cytometry. Expression of each surface marker presented as averaged MFI values per donor. A paired student's t test was performed to calculate significance p-values when comparing expression levels to those of control treated PBMCs. Each asterisk (*) denotes a level of significance: $p < 0.05$, $p < 0.01$, $p < 0.001$, and $p < 0.0001$.

8.8 Appendix 8

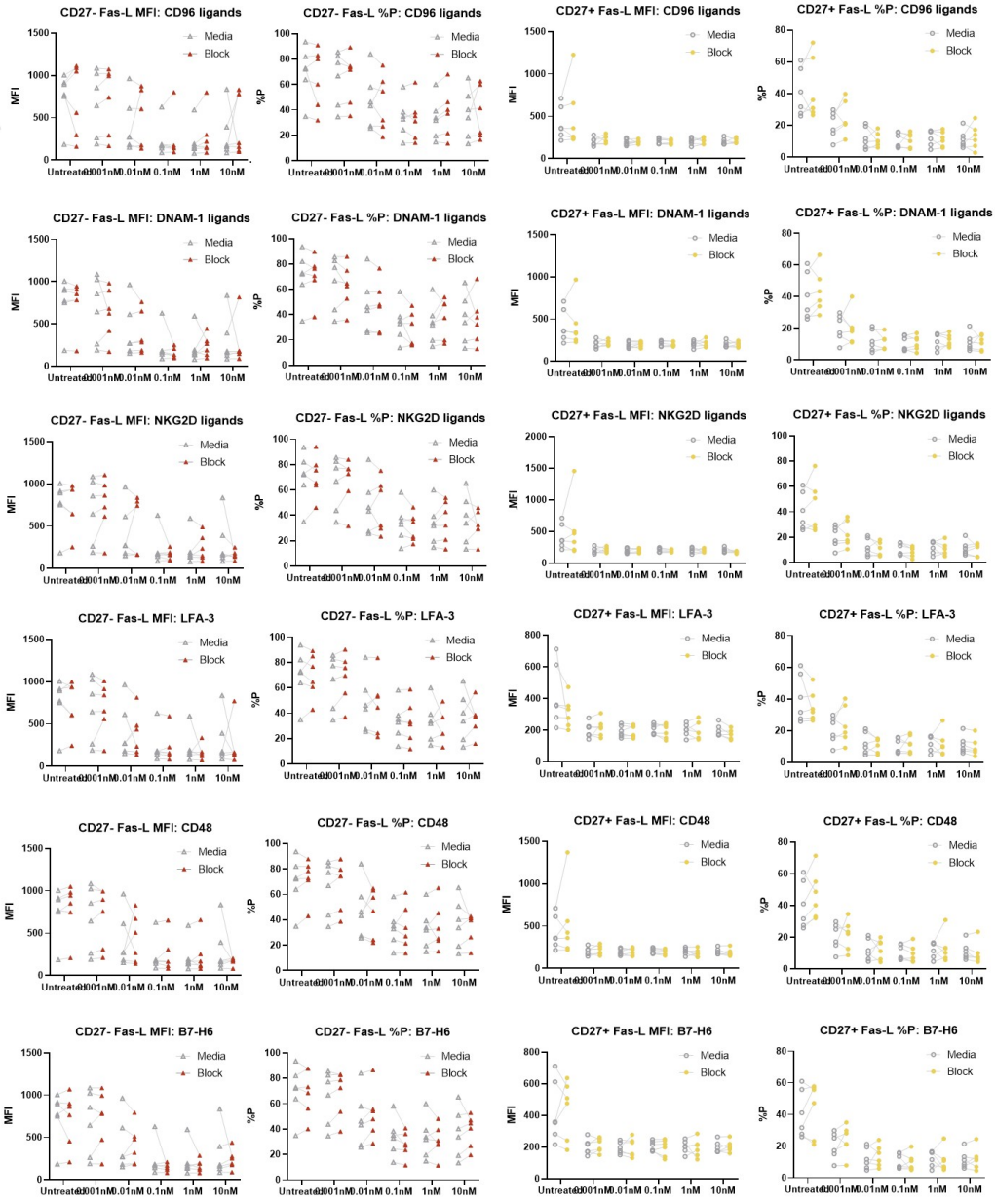


Figure 8.8: ***Engager-treated Vδ1 T-cell Fas-L expression does not change with individual blockade of MEC-1 ligands.***

Fas-L expression on $CD27^-$ (red triangles) and $CD27^+$ (yellow circles) Vδ1 T-cells from individual ligand block (indicated in graph title) in figure 4.43 compared to non-blocked conditions (grey data points), assessed by flow cytometry. Data expressed in raw MFI values and percentage of Vδ1 T-cells expressing Fas-L.

8.9 Appendix 9

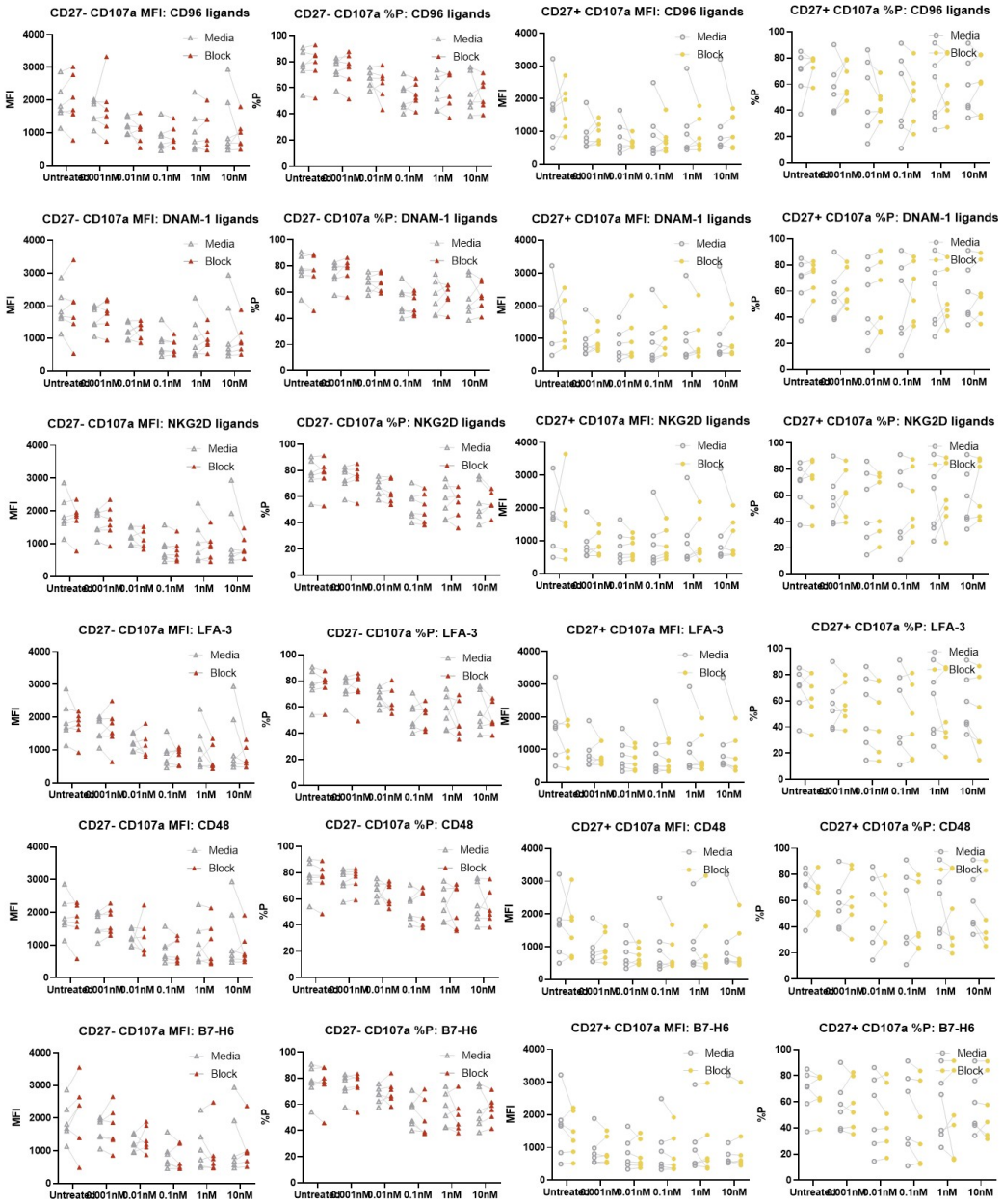


Figure 8.9: ***Engager-treated Vδ1 T-cell CD107a expression does not change with individual blockade of MEC-1 ligands.***

CD107a expression on CD27$^-$ (red triangles) and CD27$^+$ (yellow circles) Vδ1 T-cells from individual ligand block (indicated in graph title) in figure 4.43 compared to non-blocked conditions (grey data points), assessed by flow cytometry. Data expressed in raw MFI values and percentage of Vδ1 T-cells expressing CD107a.

8.10 Appendix 10

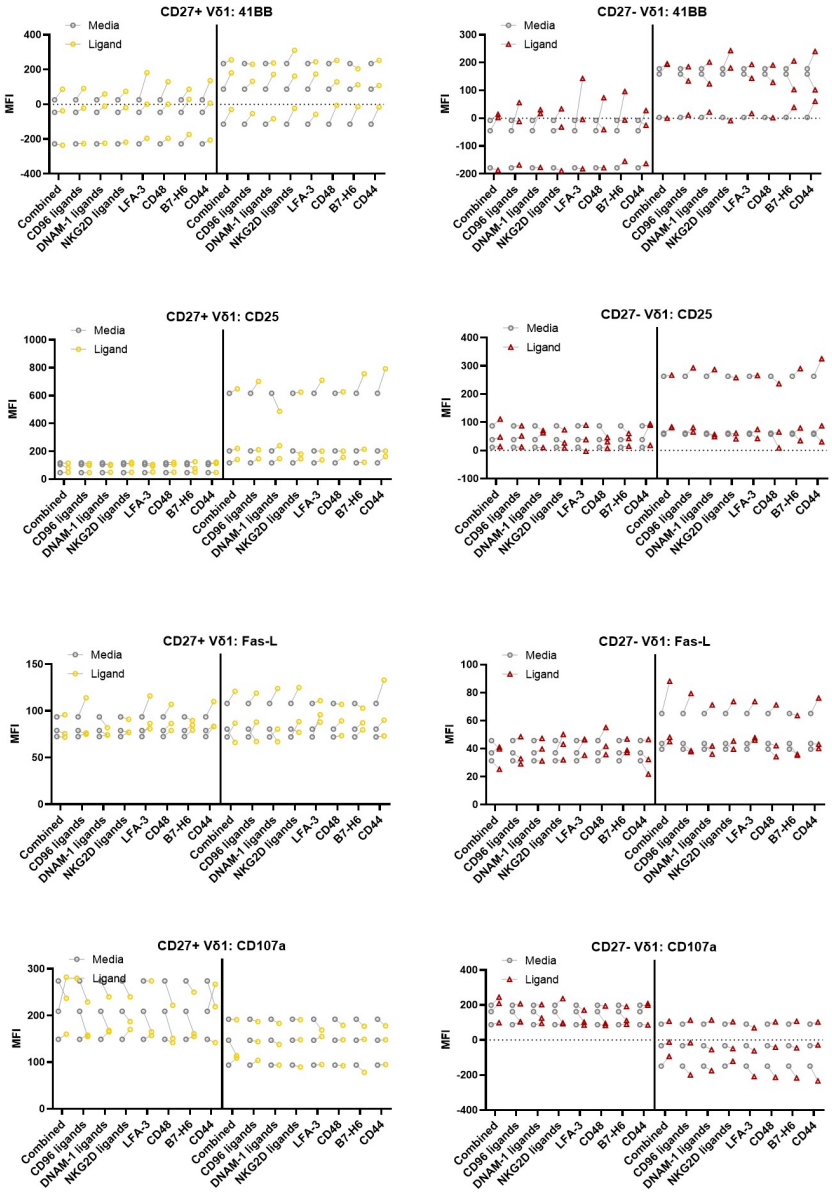


Figure 8.10: ***Engager-treated Vδ1 T-cells activate in response to combination of plate-bound ligands.***

MFI expression of activation markers on isolated Vδ1 T-cells following activation with plate bound recombinant ligands assessed by flow cytometry. Activation of FACS-sorted Vδ1 T-cells (n=3), prestimulated for 7 days with 0pM or 100pM Vδ1/CD19 engager, after culture with recombinant plate-bound stress ligands for 24 hours. 41BB, CD25, Fas-L and CD107a phenotype of Vδ1 T-cells following stimulation from a combination of or individual recombinant plate bound ligands (NKG2D ligands, DNAM-1 ligands, CD96 ligands, LFA-3, B7-H6), compared to a media-control condition containing no plate bound ligands (grey data points). Left panels on each graph represent the unstimulated Vδ1 T-cells, and the right panels represent the Vδ1/CD19 engager prestimulated Vδ1 T-cells, as shown in figure 4.46

8.11 Appendix 11

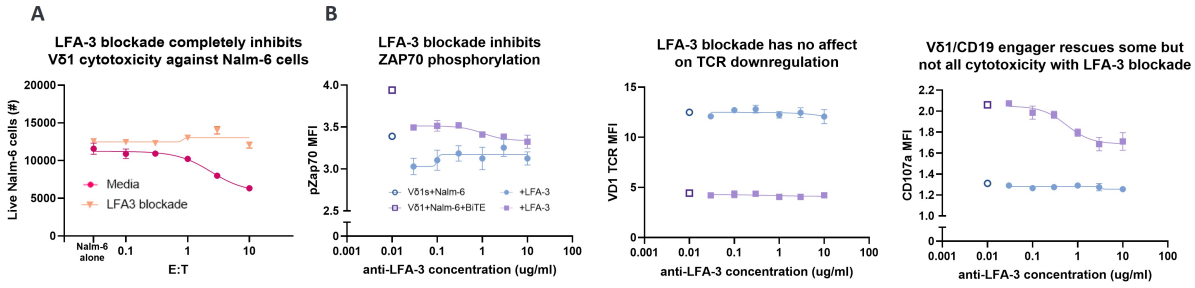


Figure 8.11: ***Skin derived-Vδ1 T-cell cytotoxicity may be dependent on target cell associated LFA-3.***

Skin derived Vδ1 T-cells were assessed for cytotoxicity and activation using flow cytometry following a culture with Nalm-6 cells that were incubated with an LFA-3 blocking antibody for an hour prior to culture. ***A*** *Remaining live Nalm-6 cells after 4 hours culture with cytokine-expanded skin-derived Vδ1 T-cells (n=1). E:T (effector : target) represents the ratio of Vδ1 T-cells to target LFA-3-blocked Nalm-6 cells in each culture.* ***B*** *Intracellular phosphorylated Zap70, surface TCR and CD107a expression was assessed on cytokine-expanded skin-derived Vδ1 T-cells (n=1) after 2 hours of culture with LFA-3-blocked Nalm-6 cells. Vδ1 cytotoxicity was inhibited after LFA-3 was blocked on Nalm-6 cells prior to the addition of skin derived Vδ1 T-cells. This inhibition was associated with reduced CD107a expression and lower levels of intracellular phosphorylated Zap70. Zap70, a protein kinase phosphorylated after TCR stimulation in canonical T-cells, is activated through TCR engagement and CD2 clustering. CD2 can cluster at the immunological synapse by binding to LFA-3 on target cells. In this case, TCR downregulation was unaffected by LFA-3 blockade, suggesting that the reduction in phosphorylated Zap70 may indicate CD2 clustering's role in skin-derived Vδ1 T-cell cytotoxicity. This effect became more pronounced following engager treatment, implying that LFA-3 may play a more significant role in engager-mediated cytotoxicity. Future work is required to verify this role.*